NEW STRATEGIC METHOD TO TUNE EQUATION-OF-STATE TO MATCH EXPERIMENTAL DATA FOR COMPOSITIONAL SIMULATION

A Dissertation

by

ALI ABDALLAH AL-MESHARI

Submitted to the Office of Graduate Studies of
Texas A&M University
in partial fulfillment of the requirements for the degree of

DOCTOR OF PHILOSOPHY

December 2004

Major Subject: Petroleum Engineering

NEW STRATEGIC METHOD TO TUNE EQUATION-OF-STATE TO MATCH EXPERIMENTAL DATA FOR COMPOSITIONAL SIMULATION

A Dissertation

by

ALI ABDALLAH AL-MESHARI

Submitted to Texas A&M University
in partial fulfillment of the requirements
for the degree of

DOCTOR OF PHILOSOPHY

Approved as to style and content by:

William D. McCain , Jr. (Chair of Committee)	Peter P. Valkó (Member)
Daulat D. Mamora (Member)	Kenneth R. Hall (Member)
Steve A. Holditch (Head of Department)	

December 2004

Major Subject: Petroleum Engineering

ABSTRACT

New Strategic Method to Tune Equation-of-State to Match Experimental Data for Compositional Simulation. (December 2004)

Ali Abdallah Al-Meshari, B.S., King Fahd University of Petroleum and Minerals;
M.S., The University of Texas at Austin

Chair of Advisory Committee: Dr. William D. McCain, Jr.

Since the plus fraction of reservoir fluids has some uncertainty in its molecular weight and critical properties, equation-of-state, EOS, are generally not predictive without tuning its parameters to match experimental data. Tuning of the EOS is found to be the best method for improving the predictions of compositional reservoir simulators.

The proposed strategy for tuning EOS consists of seven steps: (1) split the laboratory plus fraction to single carbon number groups, SCN, usually up to SCN 44; the last component will be C_{45}^{+}, (2) use set of correlations to calculate the critical properties and acentric factor for each SCN group, (3) match the saturation pressure at reservoir temperature by altering the measured value of the molecular weight of the plus fraction using the extended composition, (4) group SCN groups to multiple carbon number groups, MCN, (5) assign critical properties and acentric factor for each MCN group, (6) rematch the saturation pressure at reservoir temperature using the grouped composition, and (7) match the volumetric data by regressing on volume shift parameters of all components in grouped composition.

This research shows an accurate method to split the plus fraction to SCN groups. The most accurate set of correlations to calculate the critical properties and acentric factor for each SCN group that will result in a small adjustment for the molecular weight of the plus fraction when saturation pressure is matched using the extended composition. The proposed strategy groups the extended composition to eight pseudocomponents. The binary interaction coefficients between hydrocarbons and between hydrocarbons and non-hydrocarbons are set to zero which dramatically reduces the simulation time.

The strategy proposed in this research for tuning EOS to match experimental data has been tested for a wide range of C_7^+ mole% (4 – 25) which covers gas condensate and volatile oil samples. Also, using this strategy to tune EOS at reservoir temperature will accurately predict the fluid properties at separator conditions and saturation pressures at different temperatures.

The scope of this research is to come up with an accurate and systematic technique for tuning an EOS for use in compositional simulation.

DEDICATION

To my wife, Bassmah Al-Falih, for her patience and support…to my mother and my father for their love, encouragement, and support….for my brothers and sisters for their encouragement.

ACKNOWLEDGMENTS

I am so indebted to Dr. William D. McCain, my research advisor, for his guidance and supervision.

I would like to thank Dr. Peter P. Valkó, Daulat D. Mamora, and Dr. Kenneth R. Hall for their interest in my research and serving as members of my graduate advisory committee.

Finally, I would like to thank the Saudi Aramco Company for sponsoring my PhD studies in Petroleum Engineering at Texas A&M University.

TABLE OF CONTENTS

CHAPTER Page

CHAPTER Page

LIST OF FIGURES

FIGURE Page

FIGURE Page

LIST OF TABLES

TABLE Page

CHAPTER I

INTRODUCTION

Reservoir fluids are composed of a lot of different hydrocarbon and non-hydrocarbon components. These components can be classified as follows:

(a) Defined components which have a well known critical properties and acentric factor.
(b) True boiling point (TBP) or SCN components which have measured or estimated molecular weight and specific gravity, and whose critical properties are difficult to obtain experimentally.
(c) Heavy ends (residue), (i.e. the "plus fraction") which has a measured mole fraction, molecular weight and specific gravity.

In order to describe the phase behavior of a reservoir fluid and calculate its volumetric properties, an EOS requires the values of critical pressure, critical temperature, and acentric factor for each component. There are several correlations in the literature for calculating critical properties and acentric factor for each SCN group. Together with the molecular weight, these properties are sufficient for simpler property prediction models. The liquid density information represented by specific gravity can also be considered a physical constant for many models.

For heavy ends, accurate properties can be predicted with accurate representation of the critical properties and acentric factor. Direct measurement of the critical properties for heavy ends is not practical. So, characterization of the heavy ends is required and it consists of three main steps:

This dissertation follows the style and format of the *JPT*.

(a) Splitting the plus fraction to SCN groups.

(b) Assigning critical properties and acentric factor for each SCN group.

(c) Grouping SCN into multiple carbon number groups, MCN.

Since the heavy ends of reservoir fluids have some uncertainty in molecular weight and critical properties, EOS are generally not predictive without tuning some parameters to experimental data. Tuning of the EOS is found to be the best method for improving the predictions of compositional reservoir simulators.

Tuned EOS is used by petroleum engineers to predict the volumetric and phase behavior of reservoir fluids especially during the evaluation of newly discovered reservoirs and design and management of oil recovery projects during various stages of reservoir exploitation. Several approaches are proposed in the literature for tuning EOS, the types and the numbers of EOS parameters to be altered are different from approach to approach.

Aguilar and McCain[1] proposed a new strategy for tuning an EOS, this strategy is very important to predict accurate compositional simulation of the thermodynamic behavior of the petroleum mixtures. Tuning an EOS is very important when compositional simulators deal with near critical fluids (gas condensates and volatile oils) where the compositions of these fluids change as the reservoir is depleted.

The proposed strategy starts with extending the plus fraction up to C_{45}^{+} using the three-parameter gamma probability distribution function. The molecular weight and boiling point temperature that were proposed by Katz and Firoozabadi[2] are assigned for each SCN group extended from the plus fraction. The specific gravity are calculated for each component by assuming a constant Watson characterization factor. Then critical temperature, critical pressure and acentric factor are assigned for each SCN group using the most accurate correlations. The molecular weight of the plus fraction is adjusted to reproduce the experimental saturation pressure of the fluid. The next step is grouping the SCN to MCN, and assigning critical properties and acentric factor for each MCN group. The final step is matching volumetric data.

CHAPTER II

LITERATURE REVIEW

The main steps for tuning EOS are as follows:

1. Split the laboratory plus fraction to SCN groups, usually up to SCN 44; the last component will be C_{45}^{+}.
2. Use correlations which are usually functions of normal boiling point temperature and specific gravity, to estimate the critical properties and acentric factor for each SCN group.
3. Match the saturation pressure at reservoir temperature using the extended composition.
4. Group SCN groups to MCN groups.
5. Assign critical properties and acentric factor for each MCN group.
6. Match the saturation pressure at reservoir temperature using the grouped composition.
7. Match the volumetric data by regression of the EOS parameters.

Splitting the Plus Fraction

The hydrocarbon plus fraction contains a large number of hydrocarbon components. The experimental data provided in laboratory fluid properties report describing the plus fraction are molecular weight and specific gravity. The measured molecular weight for the plus fraction can have an error of as much as 20%. To better describe the plus fraction, the first step in tuning EOS parameters is splitting the plus fraction into a number of SCN groups.

Phase behavior for volatile oils and gas condensates is very sensitive to the composition and the physical properties of the plus fraction. It is important to have accurate values for the physical properties of the plus fractions to effectively predict the

behavior of complex hydrocarbon mixtures by EOS. Usually these plus fractions are grouped as heptanes-plus or undecanes-plus, C_7^+ or C_{11}^+ respectively. These plus fractions are difficult to characterize without an extended composition[3].

Several authors[3, 4, 5, 6, 7, 8, 9, 10] have shown that erroneous predictions and calculations can result if the plus fraction is used directly as one component in calculations of EOS. One of the errors that can occur when using the plus fraction as one component is that for a gas condensate sample the EOS calculation will sometimes predict a bubble point pressure instead of a dew point pressure at reservoir temperature.

Katz and Firoozabadi[2] verified that the use of the extended composition of C_7^+ with Peng-Robinson EOS, PREOS, will give more accurate PVT predictions for crude oil and gas condensate mixtures.

There are several methods proposed for splitting the plus fraction[3, 4, 7, 9, 11, 12] into SCN groups. Three requirements must be satisfied fro any splitting method. These requirements are as follows: (assuming that the plus fraction is C_7^+)

1. $\sum_{i=7}^{n_e} z_i = z_{C_7+}$

2. $\sum_{i=7}^{n_e} z_i M_i = z_{C_7+} \cdot M_{C_7+}$

3. $\sum_{i=7}^{n_e} \frac{z_i M_i}{\gamma i} = \frac{z_{C_7+} \cdot M_{C_7+}}{\gamma_{C_7+}}$

Behrens and Sandler[4] proposed a semi-continuous thermodynamic description which is used to model the C_7^+ fraction for EOS calculations. This method models the C_7^+ fraction with as few as two pseudo-components, the choice of pseudo-components is rigorous, and does not require iteration or comparison runs. This description is achieved in a discrete component EOS treatment by applying the following four steps: (1) choose a distribution function, (2) fit the parameter of the distribution function to the oil fraction being modeled, (3) assign pseudo component corresponding to the Gaussian quadrature

points, and (4) perform EOS calculations as if the system were composed of only discrete components.

Whitson[11] proposed a three parameter gamma probability distribution function to describe the relation between mole fraction and molecular weight of SCN components of the plus fraction. This proposed model is used as a method to split the plus fraction in some recent papers for tuning EOS[1, 13]. The molar fraction, z_i, for each SCN group is calculated as:

$$z_i = z_{plus} \cdot \int_{M_{i-1}}^{M_i} P(M)dM \quad \text{.....} \quad (1)$$

Where P(M) is

$$P(M) = \frac{(M-\eta)^{\alpha-1} \exp\left[-(M-\eta)/\beta\right]}{\beta^{\alpha} \cdot \Gamma(\alpha)} \quad \text{.....} \quad (2)$$

Where α, η, and β are parameters defining the distribution and determined from the available analytical information. Γ is the gamma function.

Pedersen et al.[7] proposed a logarithmic relationship between the mole fraction and the carbon number as follows:

$$\ln z_i = A + B \cdot CN_i \quad \text{.....} \quad (3)$$

Where A & B are mixture dependent constants, which can be determined from the measured weight fraction of the plus fraction. Molecular weight for a given carbon number, CN, can be calculated as:

$$M_i = 14 \cdot CN_i - 4 \quad \text{.....} \quad (4)$$

Guo and Du[12] proposed a distribution method as:

$$z_i = [M_i^{0.5} / A] \cdot \exp[-M_i / B], \quad \text{(5)}$$

Where A & B are constants, and can be determined by minimizing the following function:

$$\sum_i (z_i - [M_i^{0.5} / A] \cdot \exp[-M_i / B])^2 = 0, \quad \text{(6)}$$

Ahmed, et al.[3, 9] proposed a method for extending the molar distribution of C_7^+ which is shown below:

1. use the experimental specific gravity of the plus fraction to calculate the slope, S:

$$S = 688.0563583 \cdot \exp((-11.46167654)(\gamma_{C_{7+}})), \quad \text{(7)}$$

2. calculate the molecular weight of octanes plus fraction, M_8^+ as:

$$M_{c_{n^+}} = M_{c_{7^+}} \cdot (1 + S(n-7)), \quad \text{(8)}$$

3. solve the two equations below for z_{C7} and z_{C8+}:

$$\begin{aligned} z_n + z_{(n+1)^+} &= z_{n^+} \\ M_n \cdot z_n + M_{(n+1)^+} \cdot z_{n^+} &= M_{n^+} \cdot z_{n^+} \end{aligned}, \quad \text{(9)}$$

4. repeat step 2 & 3 until the sum of the calculated mole fractions is equal to the mole fraction of C_7^+.

Katz[14] proposed the simplest method for splitting the plus fraction. The proposed method uses exponential function which requires only the mole fraction of C_7^+. This equation is as follows:

$$z_n = 1.38205 \cdot z_{c_7^+} \cdot e^{-0.25903 \cdot n} \quad ,\ldots\ldots \quad (10)$$

Assigning Critical Properties and Acentric Factors for SCN Groups

The critical point for a pure component is the point of pressure and temperature where the liquid phase has same properties as the equilibrium vapor phase. An EOS requires this critical point (T_c and P_c) and acentric factor for each individual component in a mixture in order to describe the phase behavior of a given mixture. Also, molecular weights are needed to translate molar volumes to densities[6].

Many correlations for calculating critical properties of SCN groups have been proposed. Most of these correlations are functions of normal boiling point temperature and specific gravity. Ahmed[15] reported most of these correlations. Whitson[6] reviewed some of the most common correlations used by petroleum and chemical engineers. This research will point to some of the most common correlations. Also, Pedersen et al.[7] gave examples of these correlations.

Katz and Firoozabadi[2] introduced generalized properties of SCN fractions, including molecular weights, specific gravities, and normal boiling points. These properties will be used in the absence of measured values. They suggested using Cavett[16] correlation for calculating critical properties. They probably calculated acentric factors using the Edmister[17] correlation, though they did not stated this explicitly[6].

The generalized properties reported by Katz and Firoozabadi[2] are the most well known in the industry. Whitson[11] found that tabulated molecular weights in the Katz and Firoozabadi table were inconsistent with the plotted data in the same paper for SCN

groups 22 – 45. Reviewing the sources from which the data were collected indicated that the graphical data is more correct (the tabulated data showed addition of 14 to the previous molecular weight for SCN 22 – 45)[11].

Kesler and Lee[18] introduced correlations for molecular weight, critical pressure, critical temperature, and acentric factor to improve enthalpy predictions. They mentioned that critical pressures and critical temperatures predicted using their proposed correlations are nearly identical with those from API Data Book up to temperature of 1200 ºF. They modified these correlations for critical properties to extend beyond 1200 ºF; these modifications are not based on experimental evidence. For acentric factor they proposed two correlations for heavy and lighter petroleum fractions.

Whitson[5, 6, 11] proposed a technique for characterizing the plus fraction that will estimate specific gravities for petroleum fractions using molecular weights and a correlation for the Watson characterization factor, K_w. K_w is calculated for each SCN group using a correlation between molecular weight, specific gravity, and boiling point. By assuming a constant K_w for each SCN group, specific gravity can be calculated as follows:

$$\gamma_i = 6.0108 \cdot M_i^{0.17947} \cdot K_w^{-1.18241}, \quad \text{(11)}$$

Whitson suggested calculating critical properties using Riazi-Daubert[19] correlations, and acentric factor using Edmister[17] correlation. He gave modified critical pressure constants for the Riazi-Daubert correlation for SCN heavier than SCN 30 group. This revision causes a discontinuity, which is also reflected in the acentric factor[6]. The most common correlations used for EOS calculations were reviewed by Whitson[6], he concluded that there is no one existing correlation that could give consistently better PVT prediction.

Riazi and Daubert[19] proposed simple correlations to calculate the physical properties for pure compounds and petroleum fractions. These correlations have the same form for all properties; it is a function of normal boiling point and specific gravity.

They claimed that these correlations perform better (though only slightly) than other methods. For compounds not heavier than SCN 25, Riazi and Daubert correlations for estimating physical properties are probably the most accurate and easiest to use[6].

Cavett[16] presented correlations for physical properties of petroleum fractions, which are based on polynomials of second degree in normal boiling point temperature and °API of each component.

Twu[20] proposed a correlation which is based on the principle of corresponding states. The author used all types of hydrocarbon in deriving his correlation with carbon number of 5 to 20 including paraffins, olefins, naphthenes and aromatic compounds.

Riazi and Al-Sahhaf[21] provided equations for calculating boiling point, density, critical properties, acentric factor, and other properties for SCN groups such as molecular weight, specific gravity, critical density, surface tension and liquid phase solubility. They reported a set of data for various basic physical properties of SCN groups from SCN 6 – SCN 50. To show the performance of the proposed equations, they mentioned that these data should be compared to some extensive analysis of PVT calculations for reservoir fluids.

Edmister[17] proposed a simple but accurate equation for calculating the acentric factor of pure compounds. This equation is a function of critical pressure and critical temperature and normal boiling point. This equation has been applied successfully to petroleum fractions.

Avaullee et al.[22] proposed very simple correlations as functions of carbon number for estimating critical temperature, acentric factors and critical volume. They tested the performance of the proposed correlations by using experimental true boiling point. Critical temperatures were correlated with 0.6% average deviation on a set of 268 data, and critical pressure with 2.6 % deviation on a 222 data set. Using estimated true boiling points, the acentric factor of 160 compounds were correlated with 6.5% deviation.

Arbabi and Firoozabadi[23] compared the performance of four correlations: Cavett[16], Kesler-Lee[18], Twu[20], and Riazi-Daubert[21]. The inputs to all of these four

correlations are normal boiling point and specific gravity. Calculated values of critical pressure and critical temperature of normal alkanes from SCN 7 to 40 from these correlations are compared. They claimed that Cavett[16] correlation is preferred over the other three correlations as it does well for estimation of both critical pressure and critical temperature in the range of available data.

Pedersen et al.[24] proposed a correlation for critical properties and acentric factor as a function of density and molecular weight of the plus fraction. They recommended the use of their correlation be with SRK-EOS.

Guo and Du[12] compared four sets of T_c-P_c-ω correlations, these sets are as follows:

- set 1: T_c-P_c, Sim-Daubert (1980); ω-Edmister (1958)
- set 2: T_c-P_c, Cavett (1964); ω-Edmister (1958)
- set 3: T_c-P_c, Kesler-Lee (1976); ω-Edmister (1958)
- set 4: T_c-P_c-ω, Kesler-Lee (1976)
- set 5: T_c-P_c, Cavett (1964); ω-Kesle-Lee (1976)

They recommended the Cavett-Edmister (set 2) and Sim-Daubert (set 1) for crude oil samples because they require smaller adjustment of the plus fraction molecular weight.

Also, Guo and Du[25] compared four sets of T_c-P_c-ω correlations, these sets are as follows:

- set 1: T_c-P_c-ω, Pedersen et al. (1988)
- set 2: T_c-P_c, Sim-Daubert (1980); ω-Edmister (1958)
- set 3: T_c-P_c, Cavett (1964); ω-Edmister (1958)
- set 4: T_c-P_c-ω, Kesler-Lee (1976)

They recommended the set 1 correlations for evaluating critical properties and acentric factor because it requires smaller adjustment of the plus fraction molecular weight and easier to converge in dew point pressure matching.

Matching the Saturation Pressure at Reservoir Temperature Using the Extended Composition

The next step after assigning critical properties for each SCN group is to match the saturation pressure at reservoir temperature using the extended composition by adjusting the molecular weight of the plus fraction. So the criterion for choosing critical properties correlations will be the correlation that results in the least adjustment of the plus fraction molecular weight in saturation point matching[1].

Grouping SCN Groups to MCN Groups

Grouping or Pesudoization is lumping a large number of SCN groups to a few pseudocomponents. In compositional models, the computing time and cost increase as the number of components increases. As the number of the components increases, the number of the iterative phase equilibrium calculations increases; this will increase the simulation time. The main objective of grouping SCN groups to MCN groups is to reduce the simulation time by reducing the number of components, and to have the fluid properties of the grouped system close to those from original system.

There are three key points in grouping SCN components to MCN groups[10]:

- The number of MCN groups required, and the distribution of components within each MCN group.
- The estimation of physical properties for each MCN group that are required in phase behavior calculations.
- The retrieval of fluid description in terms of the original components when needed.

In the literature, there are many recommendations on selecting the number of pseudocomponents. Two to ten pseudocomponents have been considered sufficient for simulation purposes[26].

Aguilar and McCain[1] recommended that the extended C_7^+ fraction be grouped into two MCN groups (MCN1 & MCN2). They presented a correlation that determines the correct fraction to be assigned to MCN2 in mole percent as function of the mole percent of C_7^+ in order to get a good match of volumetric data. This correlation is shown below:

$$z_{MCN2} = \frac{0.028686608}{1 + 335.91986 \cdot e^{-0.56345274 \cdot z_{C_7^+}}}, \quad \text{(12)}$$

$$z_{MCN1} = z_{C_7^+} - z_{MCN2}, \quad \text{(13)}$$

Whitson[11] proposed a method to find the number of MCN groups, and as well as which SCN groups belong to the MCN group. This method representing C_7^+ plus fraction of a fluid mixture by N_p pseudocomponents, this method is as follows:

$$N_p = Integer\left[1 + 3.3\log(N - 7)\right], \quad \text{(14)}$$

Where N is the last SCN group. Also, he showed the molecular weights separating each MCN group as:

$$M_I = M_n \left\{\exp((1/N_p) \cdot \ln(M_N / M_n))\right\}, \quad \text{(15)}$$

Where M_N is the molecular weight of the last SCN group, and I = 1, 2, 3, …..N_p. Molecular weights of SCN groups falling within the boundaries of these values are included in the MCN group I.

Pedersen et al.[27] suggested grouping the components on the basis of each group containing approximately the same weight fraction (equal weight criterion), which will give all hydrocarbon segments of the C_7^+ fractions equal importance. This method utilizes the Redlich-Kwong-Soave EOS. The C_7^+ fraction is divided into three or more groups that, by weight, are of approximately equal size. The weight for each pseudocomponent, W_j, can be calculated as:

$$W_j = \sum_{i=1}^{n_c} z_i \cdot MW_i \,, \qquad (16)$$

Danesh et al.[26] proposed a grouping method based on the concentration and molecular weight of compounds in a mixture. This grouping method arranged the original components in the order of their normal boiling point temperatures and grouped together in ascending order to form N_p groups so that the values of $\Sigma(z_i \ln M_i)$ for all the groups become nearly equal, (Quasi-equal-weight criterion). That is:

$$\left[\sum_{i=1}^{l} z_i \cdot \ln M_i - (I/N_p) \cdot \sum_{i=1}^{n} z_i \cdot \ln M_i\right] \le 0 \,, \qquad (17)$$

and

$$\left[\sum_{i=1}^{l+1} z_i \cdot \ln M_i - (I/N_p) \cdot \sum_{i=1}^{n} z_i \cdot \ln M_i\right] \ge 0 \,, \qquad (18)$$

$$i = 1,2,.....n,\ I = 1,2.....N_p$$

Where z_i and M_i are molar composition and molecular weight respectively, for component i in the mixture fully described by n components and *l* or *l*+1 is the last component in group I, depending on whether above two equations is smaller. The first component in group I+1 is the next to the last component in group I.

Neau et al.[28] developed a method for predicting PVT properties of heavy oils with a restrictive number of components or pseudocomponents (between four and nine). They claim that when the proposed method used with C_{20}^{+} characterization and nine pseudocomponents yields comparable results as those obtained with Pedersen's method that estimates properties of cuts using empirical correlations. Predictions obtained with C_{11}^{+} characterization and only four pseudocomponents are the same accuracy as with Pedersen's method but using eight components.

Assigning Critical Properties and Acentric Factors for MCN Groups

Several methods[1, 11, 29, 30, 31, 32] have been proposed to calculate the critical properties and acentric factor for MCN groups. Mixing rules are used for determining the gross properties of a grouped fraction from its component properties. There are many ways for mixing the properties; different methods will give different mixture properties. The most common method to calculate the properties of MCN groups is the molar averaging:

$$\Theta_k = \left(\sum_{i=1}^{m} z_i \Theta_i \right) / z_k , \qquad z_k = \sum_{i=1}^{m} z_i \ , \ldots\ldots\ldots\ldots\ldots\ldots\ldots\ldots\ldots\ldots \quad (19)$$

Θ is the MCN group property, such as the critical pressure, critical temperature, molecular weight, or acentric factor….etc. Pedersen et al.[27] recommended using the mass fraction instead of the mole fraction for the above two equations.

Hong[29] evaluated six different mixing rules for characterizing the grouped C_7^{+} fraction from its constituent component properties. He used three different reservoir fluids in this study. The mixing rules evaluated were: molar average, surface fraction average, weight fraction average, P_c-weighted average for T_c, V_c-weighted average for T_c, and $V_c^{2/3}$ weighted average. He claimed that weight fraction average is the best mixing rule to characterize the grouped C_7^{+} fraction.

Aguilar and McCain[1] used Leibovici[30, 31] equations for calculating T_{cm} and P_{cm} of MCN groups, these equations are as follows:

$$\frac{T_{cm}^{\ 2}}{P_{cm}} = \sum_{i=1}^{n_g}\sum_{j=1}^{n_g} z_i z_j \frac{T_{ci}T_{cj}}{\sqrt{P_{ci}P_{cj}}}\sqrt{\alpha_i(T_{cm})\alpha_j(T_{cm})}(1-k_{ij}), \quad \text{(20)}$$

$$\frac{T_{cm}}{P_{cm}} = \sum_{i=1}^{n_g} z_i \frac{T_{ci}}{P_{ci}}, \quad \text{(21)}$$

The above two equations can not be used directly to find the pseudocomponents or MCN critical temperature and critical pressure, because T_{cm} appear in both sides of **Eq. 20**. The above two equations can be solved for the critical pressure and temperature of each MCN iteratively with the following starting value[32]:

$$T_{cm} = \frac{\sum_{i=1}^{n_g}\sum_{j=1}^{n_g} z_i \cdot z_j \cdot \frac{T_{ci}T_{cj}}{\sqrt{P_{ci}P_{cj}}}}{\sum_{i=1}^{n_g} z_i \cdot \frac{T_{ci}}{P_{ci}}}, \quad \text{(22)}$$

Once T_{cm} is calculated, P_{cm} can be calculated using **Eq. 21** as follows:

$$P_{cm} = \frac{T_{cm}}{\sum_{i=1}^{n_g} z_i \cdot \frac{T_{ci}}{P_{ci}}}, \quad \text{(23)}$$

Whitson[11] compared two methods for calculating critical properties of MCN groups, these methods were: using Kay's mixing rule, and using average boiling point. The average boiling point method is based on a relation developed between molal-,

weight-, mean-average boiling points, and pseudocritical and critical properties. He concluded that the two different mixing rules did not alter predictions appreciably.

Twu and Coon[32] proposed a consistent way for calculating the acentric factor of pseudo components. They showed an equation for calculating the dimensionless temperature-dependent term for mixture, $\alpha_{m,}$ in the same manner as Leibovici[30, 31]. The acentric factor for each pseudocomponent is calculated as:

$$0.26992 \cdot \omega_m{}^2 - 1.54226 \cdot \omega_m - (0.37464 - m_m) = 0 \quad \text{,……..…} \quad (24)$$

$$m_m = \frac{\sqrt{\alpha_m(T_m)} - 1}{1 - \sqrt{0.7}} \quad \text{, Where} \quad T_m = 0.7 \cdot T_{cm} \quad \text{…….} \quad (25)$$

$$\alpha_m(T_m) = \frac{\sum_{i=1}^{m}\sum_{i=1}^{m} z_i \cdot z_j \cdot \frac{T_{ci}T_{cj}}{\sqrt{P_{ci}P_{cj}}} \cdot \sqrt{\alpha_i(T_m)\alpha_j(T_m)} \cdot (1 - k_{ij})}{\frac{T^2{}_{cm}}{P_{cm}}} \quad \text{,…..…….....} \quad (26)$$

$$\alpha_i(T_m) = \left[1 + m_i\left(1 - \left(\frac{T_m}{T_{ci}}\right)^{0.5}\right)\right]^2 \text{,……..…….....} \quad (27)$$

$$m_i = 0.37464 + 1.54226 \cdot \omega_i - 0.26992 \cdot \omega^2{}_i \quad \text{(PREOS only[33])} \text{…....……} \quad (28)$$

Matching the Saturation Pressure at Reservoir Temperature Using the Grouped Composition

After grouping, the match of calculated and experimental saturation pressure is usually altered slightly. Agiular and McCain[1] defined an adjustment factor, Ψ_b, for T_{cm} and P_{cm} of the heaviest MCN, MCN_2

$$\left(\frac{T_{cmMCN_2}}{P_{cmMCN_2}}\right)_{adjusted} = \Psi_b \left(\frac{T_{cmMCN_2}}{P_{cmMCN_2}}\right)_{grouped} \quad \text{,……..…...…} \quad (29)$$

The value of Ψ_b is determined by iteration to cause the calculated saturation pressure to equal the experimental saturation pressure.

Now, after the values of $\left(\frac{T_{cmMCN_2}}{P_{cmMCN_2}}\right)_{adjusted}$ are obtained a value of constant C can be calculated as:

$$C = \frac{z_{MCN_2}}{\sum_{i=1}^{n_s} z_i . \frac{T_{ci}}{P_{ci}} - \sum_{i=1}^{N-1} z_i . \frac{T_{ci}}{P_{ci}}} \text{,…….……...……...} \quad (30)$$

N is number of components after grouping, (N=8: H_2S, CO_2, N_2, C_1, C_2-C_3, C_4-C_6, MCN_1, and MCN_2), and n_s is total number of components after splitting, (splitting to C_{45}^{+}, $n_s = 50$)

Critical temperature for the heaviest multiple carbon number, MCN_2 then:

$$T_{c_{MCN_2}} = \left[\frac{Z_{MCN_2} \cdot \sqrt{\Psi_b \cdot C}}{z_{MCN_2} \cdot \sqrt{\alpha_{MCN_2}}}\right]^2 \text{,……..…...……..} \quad (31)$$

Where

$$Z_{MCN_2} = z_{MCN_2} \cdot \frac{T_{c_{MCN_2}}}{P_{c_{MCN_2}}^{1/2}} \cdot \sqrt{\alpha_{MCN_2}} \quad \text{,……...……..…} \quad (32)$$

Substitute **Eq. 32** into **Eq. 31**:

$$(T_{c_{MCN_2}})_{adjusted} = \frac{T_{c_{MCN_2}}^{2} \cdot \Psi_b \cdot C}{P_{cMCN2}}, \quad \text{(33)}$$

$$(P_{c_{MCN_2}})_{adjused} = \Psi_b \cdot C \cdot (T_{c_{MCN_2}})_{adjusted}, \quad \text{(34)}$$

Derivation of **Eqs. 33** and **34** are shown in Agiular and McCain paper[1].

Matching Volumetric Data

Failing of cubic EOS to reproduce experimental data for a petroleum system is due to[34]: (1) experimental errors in the compositional and other test data to which EOS parameters are tuned and (2) model imperfection. Tuning EOS parameters can reduce these deficiencies. EOS parameters to be tuned include Ω_a, Ω_b, T_c, P_c, ω, volume shift parameter, molecular weight of the plus fraction, and binary interaction coefficients.

The experimental data to be matched may include the following: saturation pressure, separator test, constant composition expansion (CCE), constant volume depletion (CVD), differential liberation (DL), and swelling test. Each one of these tests may be run at different temperatures for different fluid samples[35].

There is no theory available in the literature to select or alter EOS parameters, the type and the number of regression variables differs from engineer to engineer. Manual regression for EOS parameters proves to be tedious, requires experience and is expensive. Regressing too many variables may lead to good matching, but it may lead to inconsistency. Tuning an EOS to one specific property is found to yield unreliable predictions of other thermodynamic properties[34].

Molecular weight of the plus fraction can be used as a tuning variable for matching saturation pressure using the extended composition, [1, 25, 36, 37, 38]. The measured composition in weight fraction must be maintained constant thus the composition in mole fraction changes with changing the molecular weight of the plus fraction. After the extended composition is grouped to pseudocomponents, saturation pressure may need to rematches again. Agiular and McCain[1] presented a method that allows preservation of

EOS parameters, a & b, of the extended composition that previously matched the saturation pressure considering that the *m* components of the extended composition have been grouped to into *N* pseudocomponents, this is called Equal Property Constraint, and is mathematically expressed as:

$$a_{extended} = a_{grouped}$$

$$b_{extended} = b_{grouped} \qquad \text{,……..…….....} \quad (35)$$

This methodology modifies only one variable, the ratio of critical temperature to critical pressure of the heaviest pseudocomponent for matching saturation pressure.

Agiular and McCain[1] proposed a strategy for tuning EOS; after characterizing the plus fraction they used volume shift parameters[39, 40] as the only parameters for matching volumetric data. They used binary interaction coefficients between hydrocarbon components as zero, and nonzero for hydrocarbon to non-hydrocarbon interactions, as shown in **Table 1**. These are the same values for binary interaction coefficient proposed by Wang[38].

Table 1- Binary interaction parameters used by Aguilar and McCain[1]

Component	N_2	H_2S	CO_2	Hydrocarbon
N_2	0	0.176	-0.012	0.1
H_2S	0.176	0	0.096	0.05
CO_2	-0.012	0.096	0	0.1
Hydrocarbon	0.1	0.05	0.1	0

Abrishami and Hatamian[41] found that the predicted saturation pressures with binary interaction coefficients equal to zero were 1% deviated from the measured saturation pressure. The deviation was 9% with non-zero binary interaction coefficients included. However, the compositions of the liquid phase in CCE tests were better predicted using non-zero binary interaction coefficients.

CHAPTER III

OBJECTIVES

The objectives of this research are based on the work done by reference 1, these objectives are as follows:

1. Validate the work done by Aguilar and McCain[1] "*An Efficient Tuning Strategy to Calibrate Cubic EOS for Compositional Simulation*".
2. Improve the method of splitting the hydrocarbon plus fraction using experimental extended fluid composition for ten reservoir fluids, covering three different types of reservoir fluids; gas condensates, volatile oils and black oils.
3. Use 22 full PVT reports that cover range of 4 – 25 mole% of C_7^+ to test the proposed method of tuning EOS.
4. Find the best correlations for critical properties and acentric factor for SCN that will result the least adjustment of the molecular weight of the plus fraction when the saturation pressure is matched using the extended fluid composition.
5. Confirm and extend the relationship between C_7^+ mole% and the mole% of the heaviest pseudocomponent MCN2 that was proposed by Aguilar and McCain[1].
6. Test the tuned EOS to determine if it can predict fluid properties at separator conditions.
7. Determine if this procedure will match swelling test data.
8. Determine if EOS tuned to reservoir temperature using this procedure will match data at other temperatures.

CHAPTER IV

SPLITTING THE PLUS FRACTION

The first step in tuning an EOS is extending the plus fraction; the procedure is summarized below:

Calculate the apparent molecular weight and weight fraction for all components of the original composition using the following equations:

$$M_a = \sum_{i=1}^{n_o} z_i \cdot M_i \,, \qquad (36)$$

$$w_i = \frac{z_i \cdot M_i}{M_a} \,, \qquad (37)$$

This weight fraction will be maintained constant throughout the following procedures since composition in weight fraction (not mole fraction) is measured during the laboratory procedures.

Use the three-parameter gamma probability distribution function to describe molar distribution; the probability density function is as follows[11, 42]:

$$P(M) = \frac{(M-\eta)^{\alpha-1} \exp\left[-(M-\eta)/\beta\right]}{\beta^{\alpha} \cdot \Gamma(\alpha)} \,, \qquad (38)$$

Where

$$\beta = \frac{M_{c_{n^+}} - \eta}{\alpha} \,, \qquad (39)$$

η calculated as molecular weight of the normal paraffin component smaller than the plus fraction, and will be constant (mathematically η should be the smallest number in the data set).

It is believed in the petroleum industry that the distribution of the mole fraction for the components heavier than heptane is exponential. When α = 1 the distribution of the probability density function is exponential, and **Eqs. 38** and **39** become:

$$P(M) = \frac{\exp\left[-(M-\eta)/\beta\right]}{\beta}, \quad \text{(40)}$$

$$\beta = M_{c_{n+}} - \eta, \quad \text{(41)}$$

β here is fixed for the whole extension, this is important because this honors the molecular weight of the plus fraction.

Rearrangement gives

$$P(M) = \frac{\exp(\eta/\beta)}{\beta} \cdot \exp(-M/\beta), \quad \text{(42)}$$

The cumulative frequency of occurrence, f_i, for SCN group having molecular weight boundaries between M_{i-1} and M_i is simply[11]:

$$f_i = \int_{M_{i-1}}^{M_i} P(M)dM = P(M_i) - P(M_{i-1}), \quad \text{(43)}$$

Integration results is

$$f_i = -\exp(\eta/\beta) \cdot [\exp(-\frac{M_i}{\beta}) - \exp(-\frac{M_{i-1}}{\beta})], \quad \text{(44)}$$

Now the mole fraction, z_i, for each SCN group is calculated by multiplying the cumulative frequency of occurrence of the SCN times mole fraction of the plus fraction.

$$z_i = z_{plus} \cdot f_i \,, \qquad (45)$$

If the plus fraction is extended to SCN 44, the mole fraction for each SCN group is calculated, and the mole fraction of the residue or heaviest fraction z_{C45+}, is calculated as follows:

$$z_{C_{45}^+} = z_{plus} - \sum_{i=1}^{n_e-1} z_i \,, \qquad (46)$$

Molecular weight and boiling point temperature for each SCN group are assigned using the tabular correlation proposed by Katz and Firoozabadi[2] as shown in **Table 2**.

The molecular weight of the heavy fraction is calculated as:

$$M_{C_{45}^+} = \frac{z_{plus} \cdot M_{plus} - \sum_{i=1}^{n_e-1} z_i \cdot M_i}{z_{C_{45}^+}} \,, \qquad (47)$$

Boiling point temperature in ºF for C_{45}^+ will be calculated as recommended by Pedersen et al.[7]:

$$T_{bC_{45}^+} = 1.8 \cdot (97.58 \cdot M_{C_{45}^+}{}^{0.3323} \cdot \gamma_{C_{45}^+}{}^{0.04609}) - 459.67 \,, \qquad (48)$$

Table 2- Molecular weight and boiling point temperature for SCN groups proposed by Whitson[11] and Katz and Firoozabadi[2]			
SCN	**Molecular weight, lb/lb-mol**		**Boiling Temperature, ºR**
	Whitson	**Katz & Firoozabadi**	
6	84	84	607
7	96	96	658
8	107	107	702
9	121	121	748
10	134	134	791
11	147	147	829
12	161	161	867
13	175	175	901
14	190	190	936
15	206	206	971
16	222	222	1002
17	237	237	1032
18	251	251	1055
19	263	263	1077
20	275	275	1101
21	**291**	**291**	1124
22	300	305	1146
23	312	318	1167
24	324	331	1187
25	337	345	1207
26	349	359	1226
27	360	374	1244
28	372	388	1262
29	382	402	1277
30	394	416	1294
31	404	430	1310
32	415	444	1326
33	426	458	1341
34	437	472	1355
35	445	486	1368
36	456	500	1382
37	464	514	1394
38	475	528	1407
39	484	542	1419
40	495	556	1432
41	502	570	1442
42	512	584	1453
43	521	598	1464
44	531	612	1477
45	539	626	1487

Methodology for Splitting the Plus Fraction

In order to find an accurate method to split the hydrocarbon plus fraction a detailed study has been conducted. The objective of that study was to find an accurate method in the literature to split the hydrocarbon plus fraction, improve it, validate the proposed method with experimental data and then compare it with other methods published in the literature.

Ten experimental fluid compositions were used in order to validate the method that will be used for splitting the plus fraction; the data are shown in **Tables 3 and 4** in the data section.

The first step is to group the experimental extended fluid composition to C_7^+ and C_{11}^+ plus fractions. The reason for grouping the experimental extended composition to C_7^+ and C_{11}^+ is that it is believed in the industry that the distribution of the mole fraction of components heavier than C_7 is exponential. But, it is clear from the distribution of mole fraction for non-waxy naturally occurring reservoir fluids that the exponential distribution starts for components heavier than C_{11}. **Figs. 1 and 2** show the distribution of the mole fraction for fluid G. It can be seen that having exponential distribution for the mole fractions of components heavier than C_{11} is more accurate than having exponential distribution for mole fractions of components heavier than C_7. This relationship was true in all ten fluids studied.

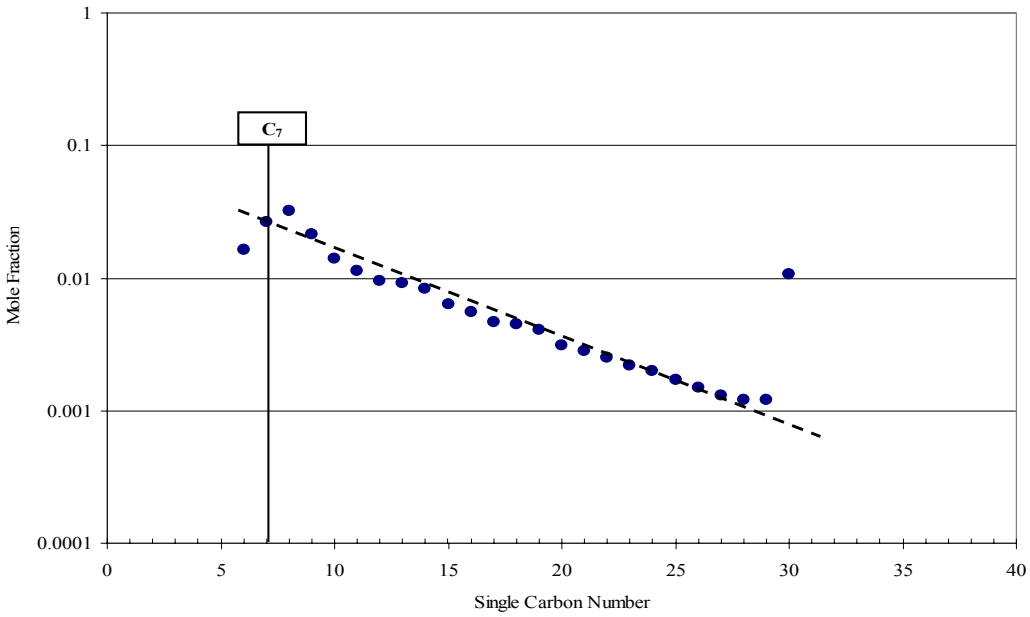

Fig. 1- The effect of having exponential distribution for mole fractions of components heavier than C_7, (Composition of fluid G).

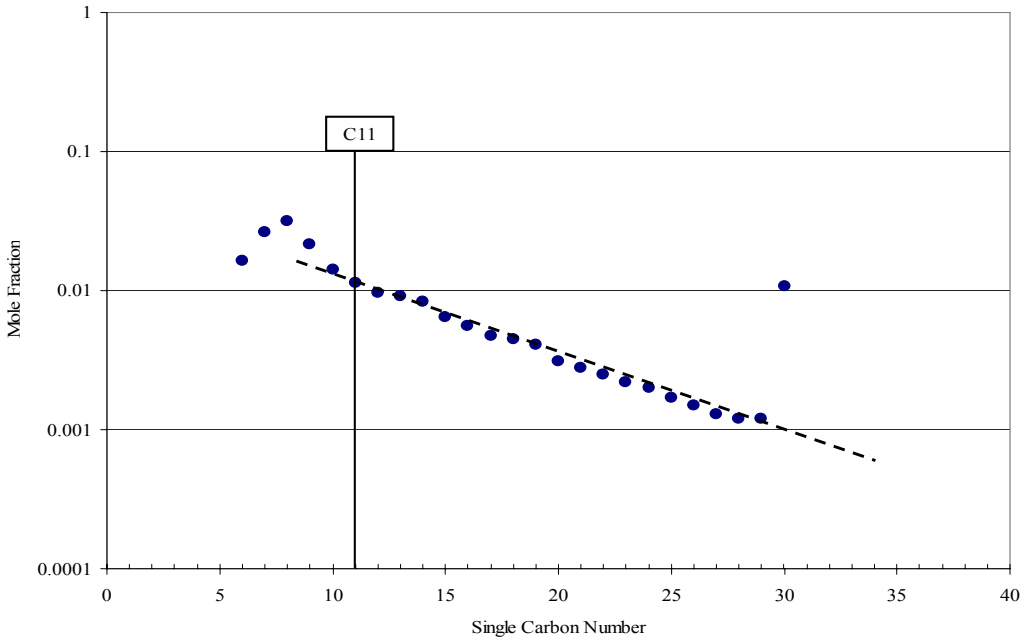

Fig. 2- The effect of having exponential distribution for mole fractions of components heavier than C_{11}, (Composition of fluid G).

The procedures for grouping the experimental extended composition to a plus fraction of C_7^+ or C_{11}^+ are exactly the same; grouping to C_7^+ will be as follows:

- Group the experimental extended fluid composition to C_7^+, the mole fraction of C_7^+ will be calculated as:

$$\sum_{i=7}^{n_e} z_i = z_{C_7+} \text{,} \quad \text{(49)}$$

- Calculate the molecular weight and specific gravity of the new plus fraction, which can be calculated for C_7^+ as follows:

$$M_{C_7^+} = \frac{\sum_{C_7}^{n_e} z_i \cdot M_i}{\sum_{C_7}^{n_e} z_i} \text{,} \quad \text{(50)}$$

$$\gamma_{C_7^+} = \frac{\sum_{C_7}^{n_e} z_i \cdot M_i}{\sum_{C_7}^{n_e} \frac{z_i \cdot M_i}{\gamma_i}} \text{,} \quad \text{(51)}$$

The second step is to split the new plus fraction (C_7^+ or C_{11}^+) to the original experimental extended plus fraction using each proposed method. Also, each grouped composition will be extended to C_{45}^+ in order to observe the values of molecular weight of C_{45}^+ since in tuning EOS most of the proposed methods split the plus fraction to C_{45}^+. The molecular weight of C_{45}^+ must be greater than the molecular weigh of SCN 44.

The last step is to compare the experimental and calculated mole fractions. Experimental mole fraction will be compared with the calculated with an average relative error, ARE:

$$ARE = \frac{\left(\sum_{C_7}^{n_e} \frac{z_{icalc.} - z_{i\exp.}}{z_{i\exp.}} \right)}{N} \quad ,\ldots\ldots (52)$$

Where $z_{iexp.}$ and $z_{icalc.}$ are the experimental and calculated mole fractions for component i respectively, and N is total number of components extended from the plus fraction.

The method used in this study for splitting the hydrocarbon plus fraction is proposed by Whitson[11]. This method used three-parameter gamma distribution function:

$$P(M) = \frac{(M - \eta)^{\alpha - 1} \exp\left[-(M - \eta)/\beta \right]}{\beta^{\alpha} \cdot \Gamma(\alpha)} ,\ldots\ldots (53)$$

$$\beta = \frac{M_{c_{n^+}} - \eta}{\alpha} ,\ldots\ldots (54)$$

η will be used as adjustable variable; different values will be used for η to see which value of η will increase the agreement between the experimental and calculated mole fractions. Mathematically η should be the smallest number in the data set.

Since it is believed in the oil industry that the distribution of the mole fractions for hydrocarbon components heavier than C_7 or C_{11} is an exponential distribution α should equal 1. By setting α = 1, the distribution of the three-parameter gamma distribution function becomes exponential, and **Eqs. 53 and 54** will become:

$$P(M) = \frac{\exp\left[-(M - \eta)/\beta \right]}{\beta} ,\ldots\ldots (55)$$

$$\beta = M_{c_{n+}} - \eta \ ,\ldots\ldots (56)$$

Simplifying **Eq. 55**:

$$P(M) = \frac{\exp(\eta/\beta)}{\beta} \cdot \exp(-M/\beta), \quad \text{(57)}$$

The integration the probability function, **Eq. 57**, will produce the cumulative frequency of occurrence, f_i, for each SCN group having molecular weight boundaries between M_{i-1} and M_i, f_i is simply:

$$f_i = \int_{M_{i-1}}^{M_i} P(M)dM = P(M_i) - P(M_{i-1}), \quad \text{(58)}$$

The question is what molecular weight boundaries should be used in the integration.

In this study two different methods have been used to calculate f_i, the first method is called ***Mid Point Average Method*** and the second method is called ***Normal Cut Method***.

Mid Point Average Method calculates the cumulative frequency of occurrence for component i by integrating the distribution function, **Eq. 58**. The midpoints between SCN molecular weights given in **Table 2** are used as the lower and upper limits for the calculation of the frequency of occurrence of each SCN group. In this method two different molecular weighs of SCN groups that proposed by Katz and Firoozabadi[2] and Whitson[11] have been used.

The result of the integration will be as follows:

$$f_i = -e^{(\eta/\beta)} \cdot \left(e^{-\frac{M_{i+\frac{1}{2}}}{\beta}} - e^{-\frac{M_{i-\frac{1}{2}}}{\beta}}\right), \quad \text{(59)}$$

For example, the cumulative frequency of occurrence for SCN 7 will be calculated using **Eq. 59**, $M_{i+\frac{1}{2}}$ will be midpoint between the molecular weights SCN 7 and 8 and $M_{i-\frac{1}{2}}$ will be midpoint between the molecular weights of SCN 6 and 7.

Normal Cut Method calculates the cumulative frequency of occurrence for component i by integrating the gamma probability distribution function, **Eq. 58**, where the integral end points are as shown in **Eq. 58**.

$$f_i = -e^{(\eta/\beta)} \cdot (e^{-\frac{M_i}{\beta}} - e^{-\frac{M_{i-1}}{\beta}}) \quad \text{..... (60)}$$

Where M_i is the molecular weight of component i and M_{i-1} is the molecular weight of the previous component (i-1). In this method, the molecular weights of the normal paraffins are used to evaluate the integral. However, the molecular weights that are assigned to each SCN group for other splitting calculations such as calculating the molecular weight of the plus fraction were the average molecular weights that proposed by Whitson[11]. In addition, the average molecular weights proposed by Katz and Firoozabadi[2] for each SCN group were used.

η in **Eqs. 59 and 60** is calculated in this study by using five different methods; these methods are as follows (**assuming the plus fraction is C_7^+**):

a) Midpoint between SCN molecular weights of lighter component in the plus fraction and the previous component.

   $\eta = (MWC_6+MWC_7)/2 = 90$

   This method will use the average molecular weights for SCN groups that were proposed by Whitson[11] and Katz and Firoozabadi[2].

b) This method is like method **a** except that the molecular weights used are normal paraffin molecular weights.

$\eta = (MWC_6+MWC_7)/2 = 93.2$

c) Molecular weight of the component smaller than the plus fraction.

η = MW SCN6 = 86.2

Molecular weights used in this method are normal paraffin molecular weights.

d) Molecular weight of the component smaller than the plus fraction.

η = MW SCN6 = 84

This method will use the average molecular weights for SCN groups that were proposed by Whitson[11] and Katz and Firoozabadi[2].

e) η calculated as recommended by Whitson[11]

η =14*n-6 = 92

Where n is the plus fraction number, for C_7^+, n = 7.

Now, with each of the two equations that calculate f_i (**Eqs. 59 and 60**), five different values of η will be used; this will generate ten different values for f_i. **Fig. 3** shows these ten different methods. As shown in the figure ten values for f_i, will be calculated, i.e. f_{1a} means using method 1 to calculate f_i (mid point average method), and (method a) to calculate the value of η.

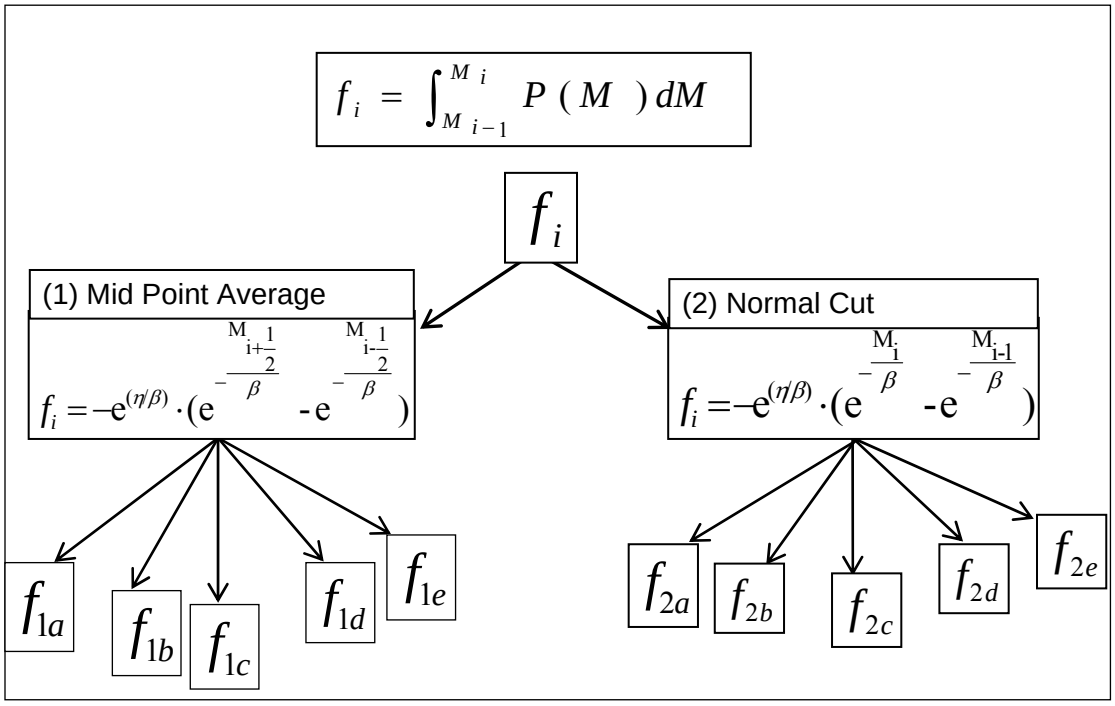

Fig. 3- Different methods to calculate cumulative frequency of occurrence f_i.

The mole fraction for SCN_i, z_i, is calculated by multiplying the cumulative frequency of occurrence of component i, f_i, times the mole fraction of the plus fraction.

$$z_i = z_{plus} \cdot f_i \,, \qquad (61)$$

The ten different values calculated for f_i, are used in **Eq. 61** to calculate 10 different sets of mole fractions for each SCN group. The average relative errors between calculated and measured mole fractions are calculated using **Eq. 52**.

If the hydrocarbon plus fraction is extended to SCN 44, the mole fraction for each SCN group is calculated using **Eq. 61**, and the mole fraction of the final group, z_{C45+}, is calculated as follows:

$$z_{C_{45}^+} = z_{plus} - \sum_{i=1}^{n_e-1} z_i \,, \qquad (62)$$

The molecular weight of the heavy fraction is calculated as:

$$M_{C_{45^+}} = \frac{z_{plus} \cdot M_{plus} - \sum_{i=1}^{n_S-1} z_i \cdot M_i}{z_{C_{45^+}}}, \quad \text{(63)}$$

The molecular weight of C_{45}^{+} must be greater than the molecular weight of the SCN 44 group.

Data

Tables 3 and 4 show the data used in the splitting of plus fraction study. The data used were the experimental extended fluid compositions for the ten reservoir fluids.

Table 3- Summary for the reservoir fluids used in the splitting study

Fluid	Saturation Pressure Type	C_n^+	Grouped composition mole %	
			C_7^+	C_{11}^+
A	Dew	C_{36}^+	5.45	2.32
B	Dew	C_{30}^+	6.12	3.55
C	Dew	C_{20}^+	6.53	2.37
D	Dew	C_{20}^+	10.87	4.71
E	Bubble	C_{20}^+	14.8	10.58
F	Bubble	C_{20}^+	15.66	9.99
G	Bubble	C_{30}^+	18.77	9.4
H	Bubble	C_{36}^+	23.12	15.92
I	Bubble	C_{45}^+	28.96	24.322
J	Bubble	C_{36}^+	34.85	22.85

Table 4- Experimental extended fluid compositions of ten reservoir fluids used to validate splitting the plus fraction method

Component	Fluid #									
	A	**B**	**C**	**D**	**E**	**F**	**G**	**H**	**I**	**J**
H_2S	0	0	0	0	0	0	0	0	0	0
N_2	0.0029	0.0111	0.0047	0.003	0	0.0016	0.0065	0.0019	0.0013	0.008
CO_2	0.002	0	0.0242	0.0435	0.0034	0.001	0.0529	0.0017	0.0004	0.012
C_1	0.8466	0.7903	0.6822	0.6255	0.7247	0.6984	0.5713	0.665	0.6175	0.443
C_2	0.0404	0.0796	0.118	0.0999	0.0457	0.0537	0.0692	0.0358	0.0221	0.055
C_3	0.0223	0.0335	0.0546	0.05	0.0279	0.0322	0.0467	0.0245	0.0263	0.053
IC_4	0.0051	0.0092	0.0083	0.0131	0.0067	0.0087	0.0089	0.0052	0.004	0.009
NC_4	0.0099	0.0083	0.0174	0.022	0.0133	0.017	0.021	0.0119	0.0147	0.025
IC_5	0.0046	0.0026	0.0072	0.0103	0.0069	0.0079	0.0082	0.0058	0.0046	0.011
NC_5	0.0049	0.0019	0.0074	0.0093	0.0082	0.0088	0.0113	0.0067	0.0042	0.015
C_6	0.0068	0.0023	0.0107	0.0147	0.0152	0.0141	0.0163	0.0103	0.0153	0.021
C_7	0.0099	0.0059	0.0109	0.017	0.016	0.015	0.0263	0.0193	0.0163	0.034
C_8	0.0051	0.0092	0.0147	0.0195	0.0131	0.0165	0.0319	0.0219	0.0168	0.035
C_9	0.0112	0.0062	0.0095	0.0146	0.0131	0.0136	0.0214	0.0165	0.0133	0.029
C_{10}	0.0051	0.0044	0.0065	0.0105	0.0112	0.0116	0.0141	0.0143	0.0119	0.022
C_{11}	0.0038	0.0032	0.0044	0.0074	0.0086	0.0091	0.0113	0.0119	0.0129	0.0193
C_{12}	0.003	0.0024	0.0033	0.0057	0.007	0.0075	0.0096	0.011	0.0125	0.017
C_{13}	0.0028	0.0026	0.0031	0.0057	0.0063	0.007	0.0092	0.0113	0.0141	0.0162
C_{14}	0.0022	0.0024	0.0024	0.0045	0.0057	0.0061	0.0083	0.0099	0.0153	0.0144
C_{15}	0.002	0.0024	0.002	0.0038	0.0051	0.0059	0.0064	0.01	0.0148	0.0134
C_{16}	0.0015	0.0017	0.0014	0.003	0.0043	0.0048	0.0056	0.0082	0.0196	0.0115
C_{17}	0.0012	0.0016	0.0012	0.0026	0.0038	0.0043	0.0047	0.0077	0.0104	0.0096
C_{18}	0.0012	0.0018	0.0011	0.0024	0.0035	0.0041	0.0045	0.0078	0.0124	0.0096
C_{19}	0.001	0.0015	0.0009	0.0021	0.0032	0.0037	0.0041	0.0075	0.0082	0.0091
C_{20}	0.0007	0.0019	**0.0039**	**0.0099**	**0.0471**	**0.0474**	0.0031	0.0057	0.0075	0.0072
C_{21}	0.0006	0.0015					0.0028	0.0057	0.0074	0.0065
C_{22}	0.0005	0.0015					0.0025	0.0049	0.0058	0.006
C_{23}	0.0004	0.0015					0.0022	0.0046	0.0057	0.0055
C_{24}	0.0003	0.0014					0.002	0.0043	0.0052	0.0051
C_{25}	0.0003	0.0012					0.0017	0.0038	0.0061	0.0048

Table 4-Continued

Component	Fluid #									
	A	**B**	**C**	**D**	**E**	**F**	**G**	**H**	**I**	**J**
C_{26}	0.0002	0.0011					0.0015	0.0036	0.004	0.0042
C_{27}	0.0002	0.001					0.0013	0.0035	0.0053	0.004
C_{28}	0.0002	0.0009					0.0012	0.0031	0.0044	0.0038
C_{29}	0.0002	0.0008					0.0012	0.0032	0.0044	0.0038
C_{30}	0.0001	**0.0031**					**0.0108**	0.0033	0.004	0.0034
C_{31}	0.0001							0.0032	0.004	0.0033
C_{32}	0.0001							0.0029	0.0033	0.0028
C_{33}	0.0001							0.0024	0.0023	0.0027
C_{34}	0.0001							0.0018	0.0039	0.0024
C_{35}	0.0001							0.002	0.0025	0.0022
C_{36}	**0.0003**							**0.0159**	0.0025	**0.0407**
C_{37}									0.0024	
C_{38}									0.0018	
C_{39}									0.0023	
C_{40}									0.0019	
C_{41}									0.0022	
C_{42}									0.0019	
C_{43}									0.0014	
C_{44}									0.0015	
C_{45}^{+}									**0.0175**	
C_n^{+}	C_{36}^{+}	C_{30}^{+}	C_{20}^{+}	C_{20}^{+}	C_{20}^{+}	C_{20}^{+}	C_{30}^{+}	C_{36}^{+}	C_{45}^{+}	C_{36}^{+}
γ_{Cn+}	0.9313	0.8076	0.889	0.8866	0.9286	0.9238	1.005	1.0113	1.155	1.01
MW_{Cn+}	578	519.3	337	490	478.8	415	588	887	2607.3	593
γ_{C7+}	0.7964	0.825	0.793	0.8095	0.8719	0.8601	0.8368	0.8723	0.928	0.8728
MW_{C7+}	158	204	148	173	255	232	189	261	346.6	245.2
z_{C7+} (mole fraction)	0.0545	0.0612	0.0653	0.1087	0.148	0.1566	0.1877	0.2312	0.2896	0.3485
γ_{C11+}	0.8403	0.8493	0.8422	0.8478	0.8939*	0.8875	0.8789	0.8972	0.942*	0.9026
MW_{C11+}	220	270	271	253	317.6*	300	266	327	392.2*	315
z_{C11+}(mole fraction)	0.0232	0.0355	0.0237	0.0471	0.1058*	0.0999	0.094	0.1592	0.24322*	0.2285

*C_{10}^{+} measured properties not C_{11}^{+} calculated properties.

Results

Two methods were used to calculate the cumulative frequency of occurrence (**Eq. 59 and 60**); the results for each method are presented below:

***Midpoint Average Method*, Table 5** shows the average relative errors that were calculated using **Eq. 52**, for all fluids when the experimental extended composition was grouped to either C_7^+ or C_{11}^+ and then extended to the original plus fraction. These results were generated when the midpoint average method was used and with η calculated using five different methods (a, b, c, d and e). **Tables 6 and 7** show the molecular weights of C_{45}^+ calculated using **Eq. 63** when the experimental extended fluid composition was grouped to either C_7^+ or C_{11}^+ respectively and then extended to C_{45}^+. The molecular weight of C_{45}^+ should be higher than the molecular weight of the SCN 44 group.

As shown in **Tables 5, 6 and 7**, when the mid point average method is used to calculate the cumulative frequency of occurrence the experimental fluid composition should be grouped to C_{11}^+ and η should be calculated with **method a**. This will result a reasonable molecular weight for C_{45}^+ and low average relative error (-0.1 – 0.05). . The molecular weight of C_{45}^+ in this case must be greater than 531 (molecular weigh of SCN 44 as proposed by Whitson[11]).

Table 5- Calculation results when using mid point average method to calculate f_i

Fluid #	C_n^+	Average Relative Error				
		a	**b**	**c**	**d**	**e**
A	C_7^+	-0.07	-0.09	0.28	0.46	-0.57
	C_{11}^+	0.00	-0.42	-0.08	0.23	-0.35
B	C_7^+	-0.03	-0.03	-0.02	-0.02	-0.03
	C_{11}^+	-0.10	-0.08	-0.10	-0.12	-0.08
C	C_7^+	0.07	0.07	0.12	0.14	0.04
	C_{11}^+	-0.02	0.01	-0.01	-0.04	0.01
D	C_7^+	0.12	0.12	0.12	0.11	0.12
	C_{11}^+	-0.05	0.00	-0.04	-0.08	0.00
E	C_7^+	0.10	0.13	0.08	0.06	0.12
	C_{11}^+	0.02	0.07	0.02	0.90	0.06
F	C_7^+	0.11	0.13	0.08	0.06	0.12
	C_{11}^+	0.05	0.13	0.07	0.00	0.12
G	C_7^+	0.10	0.09	0.12	0.12	0.10
	C_{11}^+	0.02	0.05	0.03	0.00	0.05
H	C_7^+	-0.03	-0.03	-0.04	-0.04	-0.03
	C_{11}^+	-0.09	-0.06	-0.08	-0.10	-0.06
I	C_7^+	0.02	0.02	0.01	0.01	0.02
	C_{11}^+	0.00	0.02	0.01	-0.01	0.02
J	C_7^+	0.08	0.09	0.06	0.06	0.08
	C_{11}^+	0.02	0.06	0.03	-0.01	0.05

Table 6- Molecular weight of C_{45}^+ using mid point method- grouping to C_7^+					
	Method used to calculate η				
Fluid #	**a**	**b**	**c**	**d**	**e**
A	495	84	104	100	76
B	644	-863	318	270	9395
C	201	92	91	90	91
D	591	39	148	133	-9
E	699	962	554	504	836
F	675	1413	467	411	974
G	625	-128	228	195	-437
H	705	924	573	525	823
I	791	843	742	718	822
J	689	1062	520	467	872

Table 7- Molecular weight of C_{45}^+ using mid point method- grouping to C_{11}^+					
	Method used to calculate η				
Fluid #	**a**	**b**	**c**	**d**	**e**
A	591	131	-27	191	126
B	662	-455	888	419	-851
C	663	-505	879	423	-962
D	644	-39	1290	339	-107
E	724	1091	745	603	994
F	693	2568	779	531	1671
G	658	-299	930	401	-536
H	721	1166	770	604	1050
I	799	904	808	739	884
J	709	1403	770	574	1187

***Normal Cut Method*, Table 8** shows the average relative errors calculated using **Eq. 52**, for all fluids when the experimental extended composition is grouped to either C_7^+ or C_{11}^+ and then extended to the original plus fraction. These results were generated when the normal cut method was used and when η was calculated using five different methods (a, b, c, d and e). **Tables 9 and 10** show the calculated molecular weights of C_{45}^+ that were calculated using **Eq. 63** when the experimental extended fluid composition was grouped to either C_7^+ or C_{11}^+ respectively and then extended to C_{45}^+.

Tables 8, 9 and 10 show that when the normal cut method was used to calculate the cumulative frequency of occurrence, the experimental fluid composition could be grouped to either C_7^+ or C_{11}^+, and η should be calculated with **method c**. This will result in reasonable molecular weight for C_{45}^+ and low average relative errors (-0.04 – 0.13 when grouped to C_7^+ and -0.08 – 0.11 when grouped to C_{11}^+).

Tables 9 and 10 show that the molecular weight of C_{45}^+ for each fluid, when η was calculated using **method c**, has large values. Such large values will require adjustment for the molecular weight of the plus fraction to exceed ±20 %, when the saturation pressure is matched using the extended composition. *All of the above results were generated with the average molecular weights proposed by Whitson[11] assigned for each SCN group.*

However, assigning average molecular weights proposed by Katz and Firoozabadi[2] for each SCN group extended from the plus fraction result in a more reasonable molecular weight for C_{45}^+ for all of the fluids used in this study as shown in **Table 11**. The molecular weight of C_{45}^+ in this case must be greater than 612 (molecular weigh of SCN 44 as proposed by Katz and Firoozabadi[2]).

Thus we have concluded that for splitting a fluid composition that has a plus fraction of either C_7^+ or C_{11}^+, the cumulative frequency of occurrence should be calculated using normal cut method, and the value of η should be the molecular weight of the normal alkane smaller than the plus fraction. Also, the average molecular weights for each SCN group extended from the plus fraction should be assigned as proposed by Katz and Firoozabadi[2].

Table 8- Calculation results when using normal cut method to calculate f_i						
Fluid #	**C_n^+**	**Average Relative Error**				
		a	**b**	**c**	**d**	**e**
A	C_7^+	-0.43	-0.79	-0.04	0.15	-0.65
	C_{11}^+	0.04	-0.36	-0.03	0.27	-0.29
B	C_7^+	-0.03	-0.03	-0.03	-0.02	-0.04
	C_{11}^+	-0.08	-0.06	-0.08	-0.10	-0.07
C	C_7^+	0.06	0.18	0.06	0.09	0.13
	C_{11}^+	-0.02	0.02	-0.01	-0.04	0.01
D	C_7^+	0.10	0.09	0.10	0.10	0.09
	C_{11}^+	-0.05	0.00	-0.04	-0.09	-0.01
E	C_7^+	0.11	0.13	0.08	0.07	0.13
	C_{11}^+	0.01	0.07	-0.07	-0.03	0.06
F	C_7^+	0.12	0.14	0.09	0.07	0.13
	C_{11}^+	0.04	0.12	-0.03	-0.01	0.11
G	C_7^+	0.12	0.16	0.13	0.14	0.14
	C_{11}^+	0.07	0.10	0.08	0.05	0.09
H	C_7^+	0.01	0.01	0.00	0.00	0.01
	C_{11}^+	-0.03	-0.01	-0.03	-0.05	-0.01
I	C_7^+	0.11	0.12	0.10	0.10	0.11
	C_{11}^+	0.10	0.12	0.11	0.09	0.12
J	C_7^+	0.13	0.14	0.12	0.12	0.14
	C_{11}^+	0.09	0.13	0.10	0.06	0.12

Table 9- Molecular weight of C_{45}^{+} using normal cut method- grouping to C_7^{+}					
	Method used to calculate η				
Fluid #	**a**	**b**	**c**	**d**	**e**
A	78	86	**1437**	118	84
B	-281	-56	**1009**	443	-104
C	88	91	**954**	93	90
D	43	71	**1248**	189	64
E	2076	-5748	**923**	734	10999
F	-6352	-578	**942**	638	-943
G	-54	29	**1090**	312	10
H	1754	43455	**921**	753	4126
I	1060	1189	**947**	897	1136
J	3520	-1592	**929**	699	-3947

Table 10- molecular weight of C_{45}^{+} normal cut method- grouping to C_{11}^{+}					
	Method used to calculate η				
Fluid #	**a**	**b**	**c**	**d**	**e**
A	291	119	**1749**	186	110
B	684	-304	**990**	406	-531
C	689	-331	**987**	411	-578
D	577	-33	**1072**	316	-100
E	883	1920	**923**	672	1562
F	788	-10209	**934**	553	5457
G	663	-214	**1004**	385	-378
H	836	1939	**922**	654	1562
I	936	1127	**950**	837	1088
J	817	3116	**925**	613	2028

Table 11- Molecular weight of C_{45}^+, using normal cut method to calculate f and η calculated using method –c, grouping to C_7^+ and C_{11}^+, using Katz and Firoozabadi average molecular weights for SCN group		
	Molecular Weight of C_{45}^+	
Fluid #	C_7^+	C_{11}^+
A	643	796
B	703	745
C	621	746
D	619	731
E	780	808
F	752	829
G	654	741
H	787	802
I	878	883
J	769	845

Comparing with Different Methods

The proposed method to split the hydrocarbon plus fraction has been compared with three different methods that used for splitting the hydrocarbon plus fraction. These methods are as follows:

- Pedersen, et. al.[7] method (**Eqs. 3-4**).
- Ahmed, et. al.[3, 9] method (**Eqs. 7-9**).
- Katz[14] method (**Eq. 10**).

Tables 12 and 13 show the results of the comparison between the proposed method and these three methods. **Tables 14 and 15** give summaries of the comparisons. The following can be concluded:

- The proposed method is the most accurate method to split the hydrocarbon plus fraction for different reservoir fluids especially those used in compositional simulations compared to the other three methods used in this study.

- The Pedersen, et al.[7] method is not suitable for multiple sample systems because each sample has its own coefficients A& B. Also, this method does not honor the properties of the plus fraction.
- The Ahmed, et al.[3, 9] method was proposed and tested using gas condensate samples; it does not work for oil samples. The range of C_7^+ mole % for the samples used to develop their correlation was 1.54 – 8.21. For this reason the Ahmed, et al. method did not work for three of the oil samples used in this study.
- The Katz[14] method is the simplest to use and the least accurate compared to the other methods used in this study.

Table 12- Comparison results, ARE, for splitting hydrocarbon plus fraction

		Average Relative Error, ((Calc.-Exp.)/Exp.)			
Fluid #	**C_n^+**	**This Method**	**Pedersen**	**Ahmed**	**Katz**
1	C_{36}^+	-0.0436	-0.1455	-0.2046	-0.3291
2	C_{30}^+	-0.0258	-0.1582	0.0630	-0.3299
3	C_{20}^+	0.0624	0.0002	0.1649	-0.0252
4	C_{20}^+	0.0963	-0.0243	0.2208	-0.1025
5	C_{20}^+	0.0831	-0.0226	0.0806	0.0781
6	C_{20}^+	0.0862	-0.0215	0.1414	0.0563
7	C_{30}^+	0.1303	-0.1711	NA	-0.3454
8	C_{36}^+	0.0039	-0.1081	0.3468	-0.4278
9	C_{45}^+	0.1030	0.0393	NA	-0.4535
10	C_{36}^+	0.1240	-0.1155	NA	-0.4303

Table 13- Comparison results, AARE, for splitting hydrocarbon plus fraction					
		Absolute Average Relative Error, |((Cal-Exp)/Exp)|			
Fluid #	**C_n^+**	**This Method**	**Pedersen**	**Ahmed**	**Katz**
1	C_{36}^+	0.1845	0.2042	0.4217	0.5132
2	C_{30}^+	0.2678	0.5193	0.2593	0.6207
3	C_{20}^+	0.1420	0.1811	0.2991	0.1433
4	C_{20}^+	0.1796	0.1295	0.3424	0.2264
5	C_{20}^+	0.2067	0.0604	0.4000	0.4561
6	C_{20}^+	0.1586	0.0750	0.3705	0.4698
7	C_{30}^+	0.2001	0.3321	NA	0.4893
8	C_{36}^+	0.0938	0.1977	0.5465	0.7576
9	C_{45}^+	0.2276	0.1389	NA	0.9501
10	C_{36}^+	0.1801	0.1672	NA	0.6993

Table 14- Comparison results summary, ARE			
Method used	**Average Relative Error**		
	Minimum	Mean	Maximum
This Method	-0.0436	0.0620	0.1303
Pedersen et. al. Method	-0.1711	-0.0727	0.0393
Ahmed et. Al. Method	-0.2046	0.1161	0.3468
Katz Method	-0.4535	-0.2309	0.0781

Table 15- Comparison results summary, AARE			
Method used	**Absolute Average Relative Error**		
	Minimum	Mean	Maximum
This Method	0.0938	0.1841	0.2678
Pedersen et. al. Method	0.0604	0.2005	0.5193
Ahmed et. al. Method	0.2593	0.3771	0.5465
Katz Method	0.1433	0.5326	0.9501

Figs. 4 to **13** show the comparisons between the experimental and calculated mole fractions for all of the extended components for each fluid compositions used in this

study. These comparisons between experimental and calculated mole fractions are based on the normal cut method and η equal to the molecular weight of the normal alkane smaller than the plus fraction (method-c), for the splits starting with the experimental fluid compositions grouped to C_7^+.

Summary

The following can be summarized:

1. When splitting a fluid composition that has a plus fraction as either C_7^+ or C_{11}^+, calculate the cumulative frequency of occurrence using normal cut method with a value of η equal to the molecular weight of the normal alkane smaller than the plus fraction.
2. When assigning average molecular weights for the SCN groups the correlation proposed by Katz and Firoozabadi gave more accurate molecular weights of C_{45}^+ fraction than the Whitson correlation.

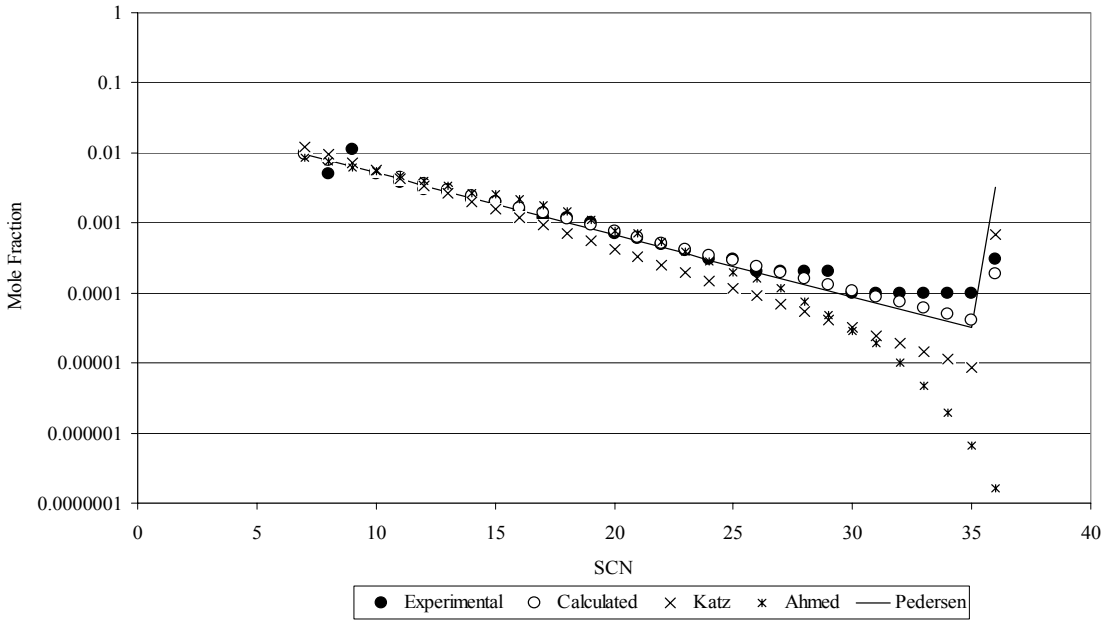

Fig. 4- Comparing the experimental and calculated mole fraction for fluid-A using the proposed method (calculated) and three other methods.

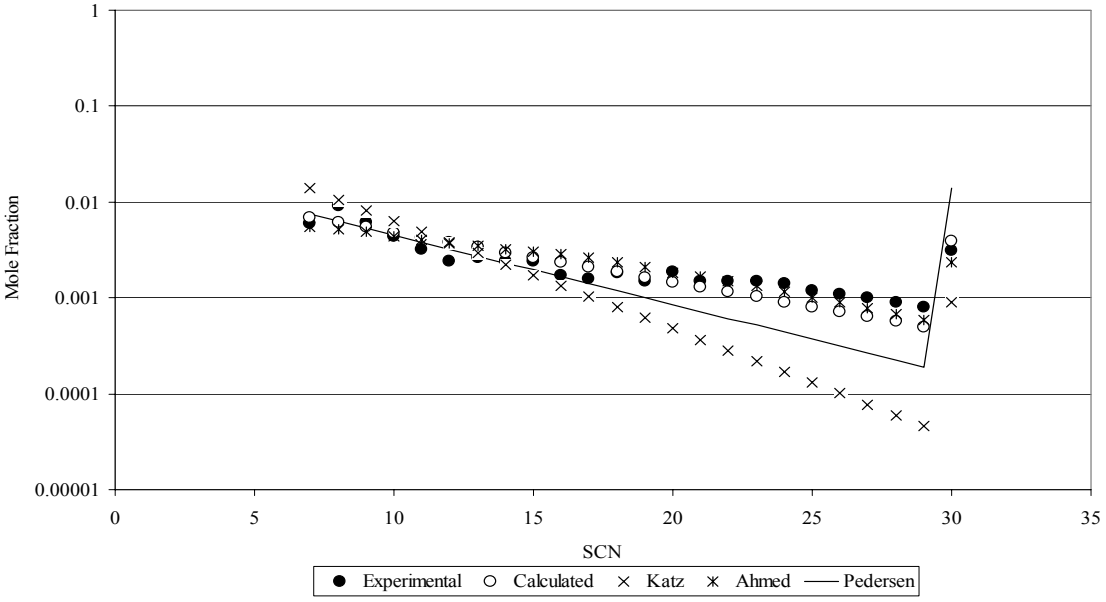

Fig. 5- Comparing the experimental and calculated mole fraction for fluid-B using the proposed method (calculated) and three other methods.

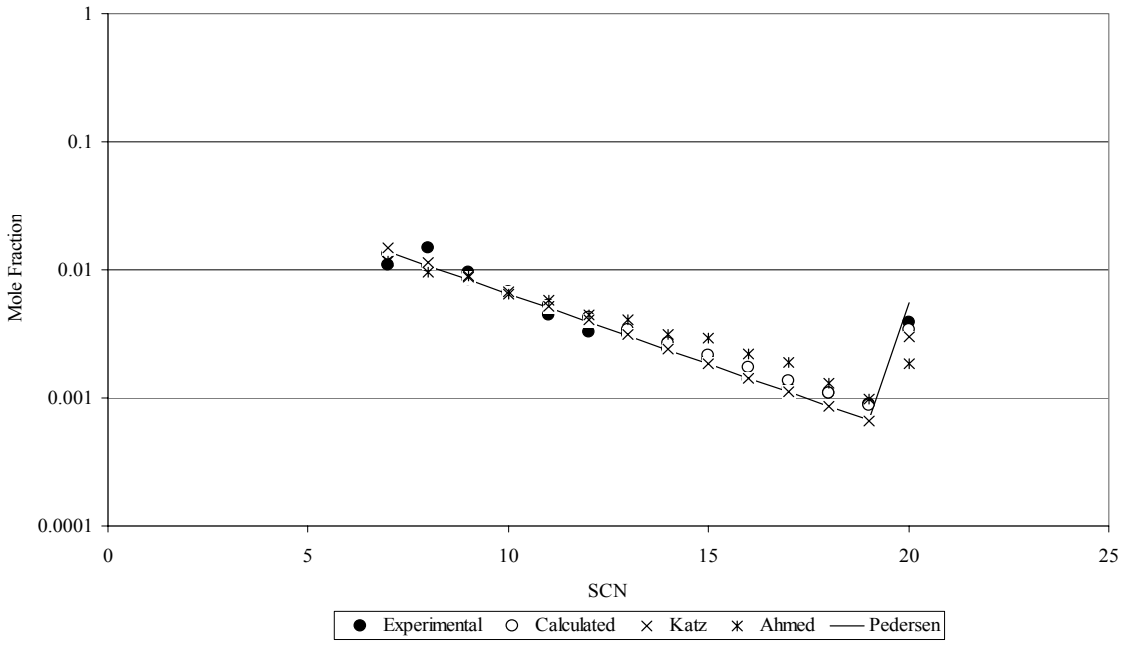

Fig. 6- Comparing the experimental and calculated mole fraction for fluid-C using the proposed method (calculated) and three other methods.

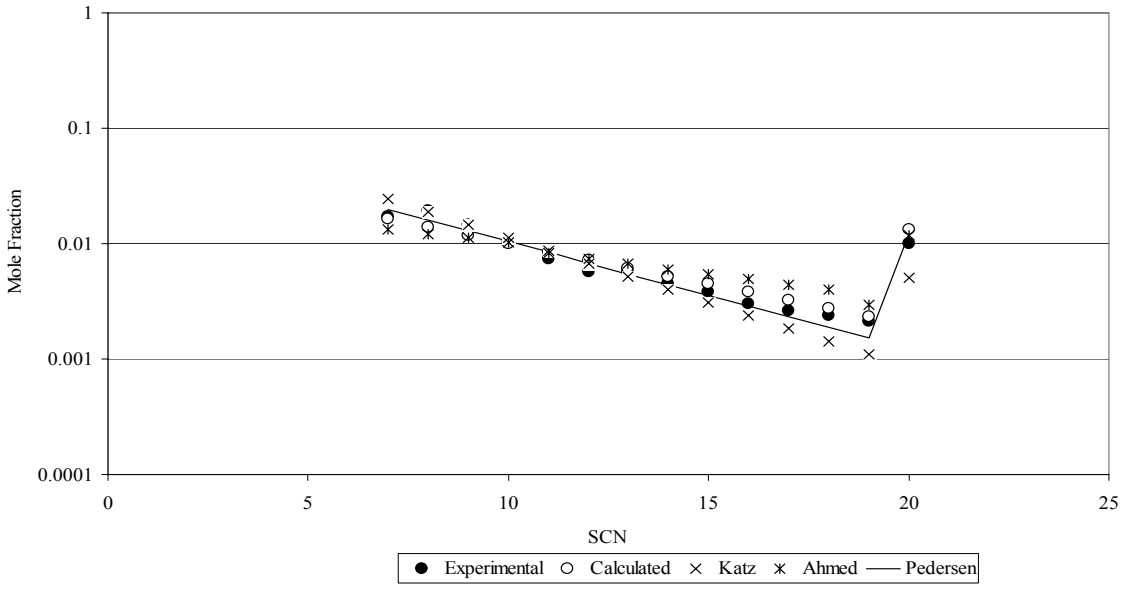

Fig. 7- Comparing the experimental and calculated mole fraction for fluid-D using the proposed method (calculated) and three other methods.

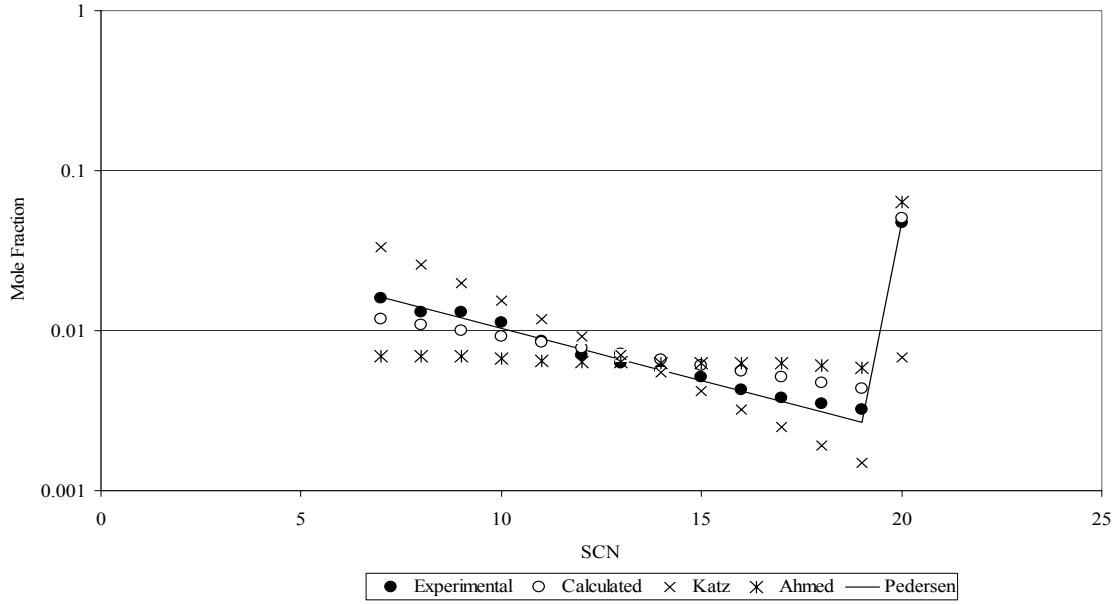

Fig. 8- Comparing the experimental and calculated mole fraction for fluid-E using the proposed method (calculated) and three other methods.

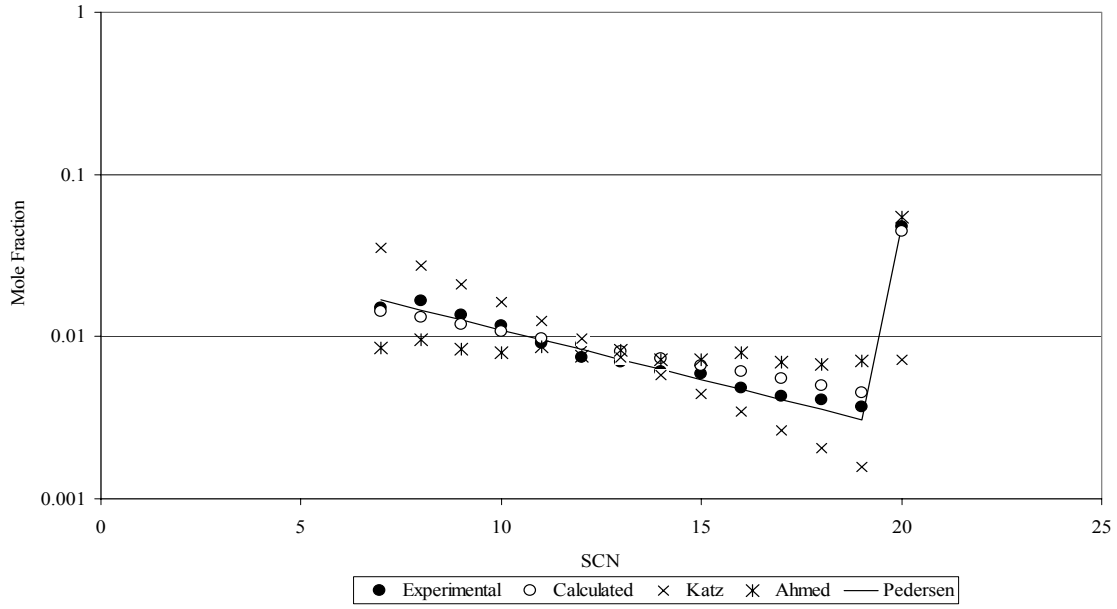

Fig. 9- Comparing the experimental and calculated mole fraction for fluid-F using the proposed method (calculated) and three other methods.

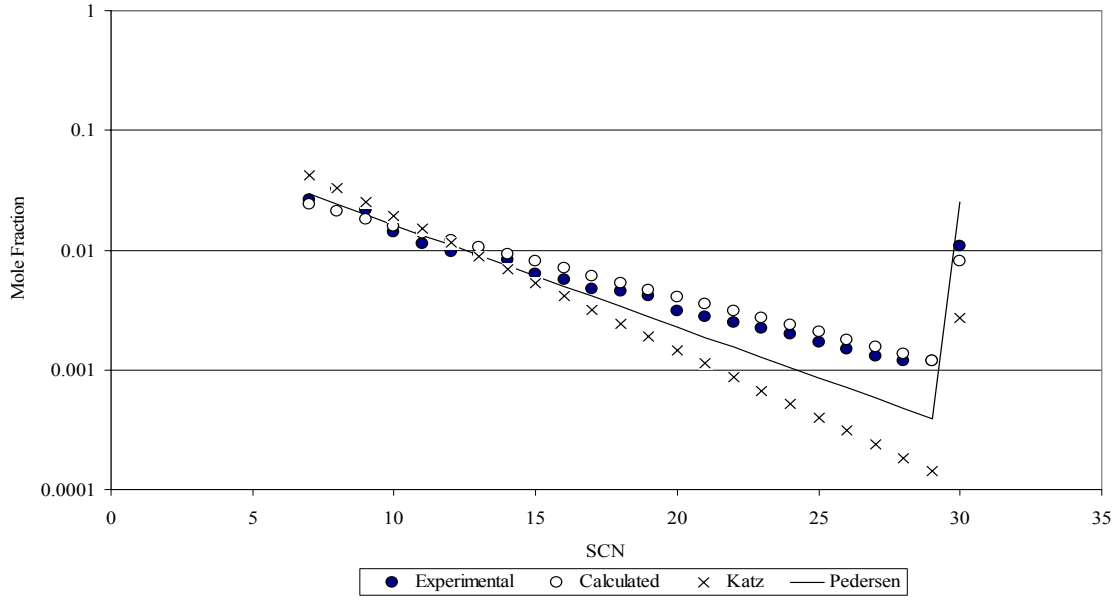

Fig. 10- Comparing the experimental and calculated mole fraction for fluid-G using the proposed method (calculated) and three other methods.

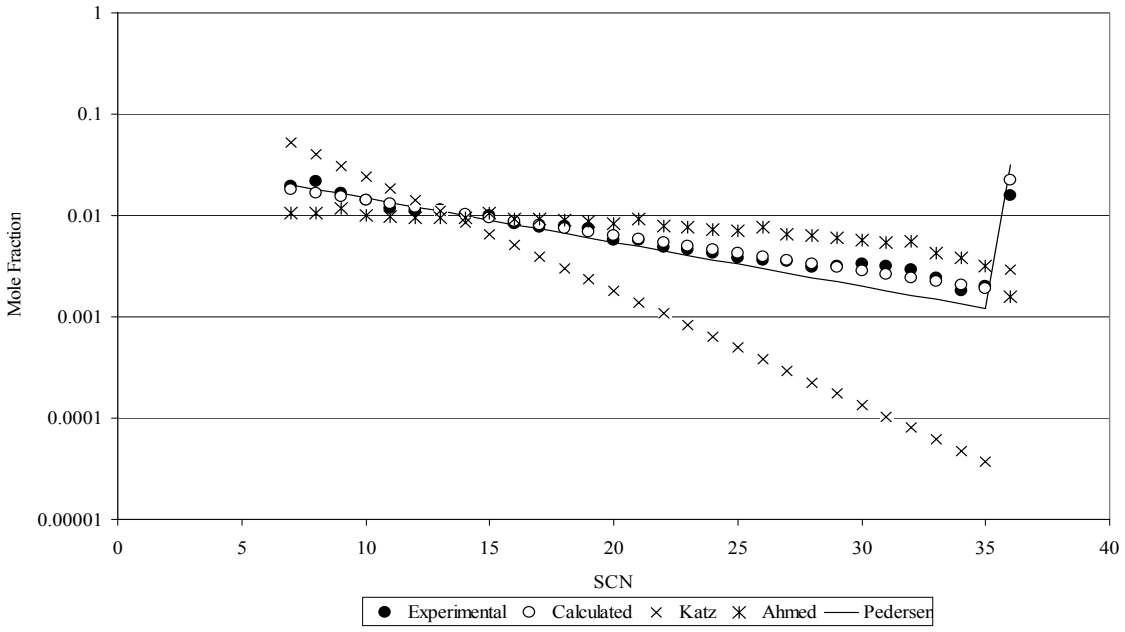

Fig. 11- Comparing the experimental and calculated mole fraction for fluid-H using the proposed method (calculated) and three other methods.

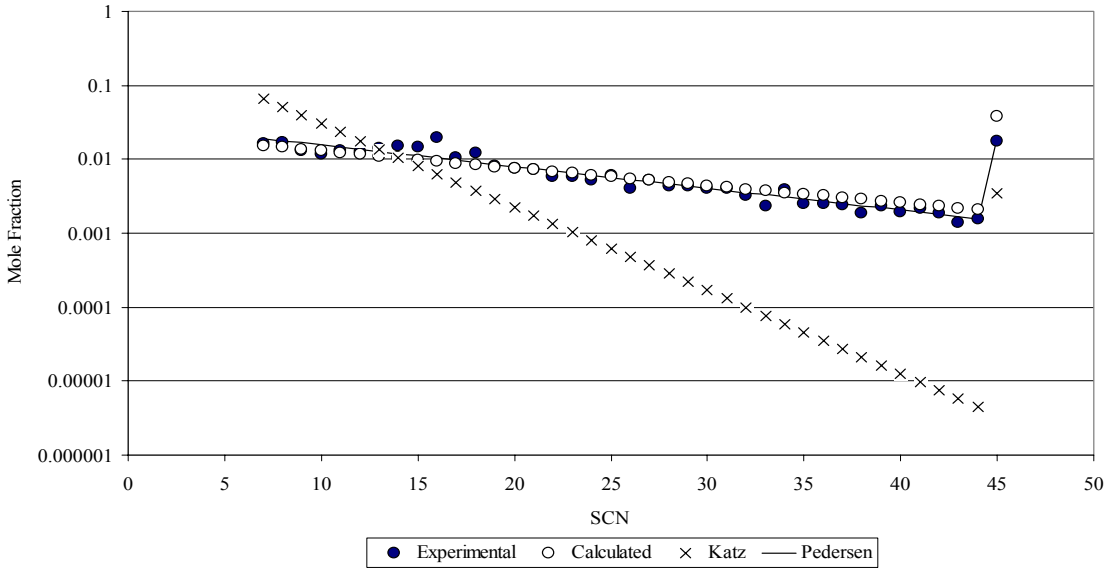

Fig. 12- Comparing the experimental and calculated mole fraction for fluid-I using the proposed method (calculated) and three other methods.

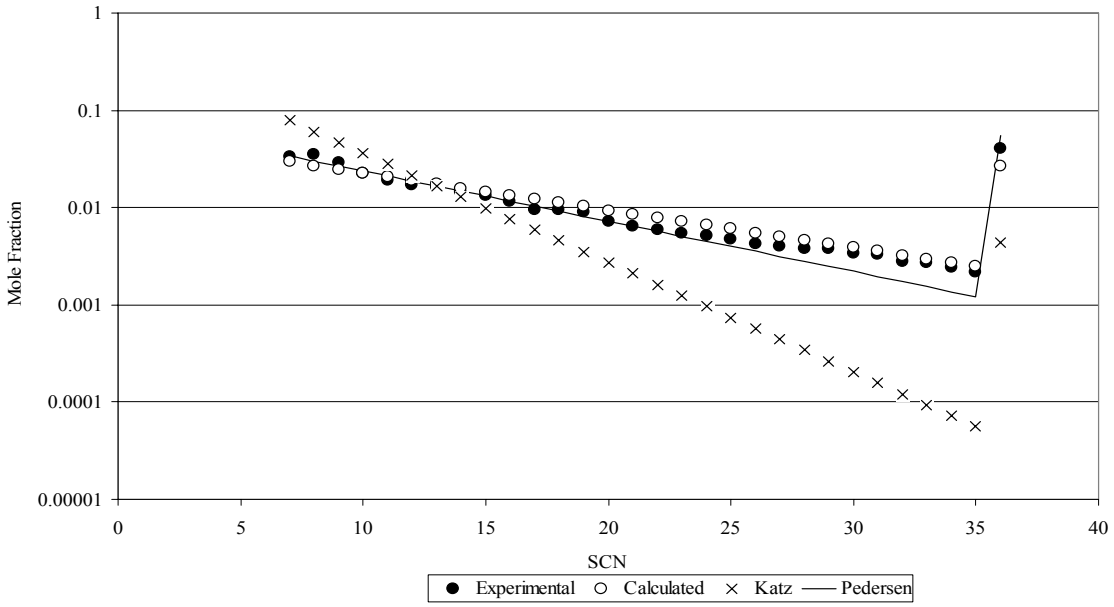

Fig. 13- Comparing the experimental and calculated mole fraction for fluid-J using the proposed method (calculated) and three other methods.

CHAPTER V

ACCURATE SET OF CORRELATIONS FOR CRITICAL PROPERTIES AND ACENTRIC FACTORS OF SCN GROUPS

The specific gravity of each SCN group must be calculated since most of the correlations used to calculate the critical properties are function of boiling point temperature and specific gravity. The specific gravity for each SCN group will be calculated by assuming a constant Watson characterization factor. The Watson characterization factor, K_W, is calculated using the following equation to honor the measured specific gravity and molecular weight of the plus fraction, and will be kept constant for all SCN[1, 11].

$$K_w = \left[\frac{\xi \cdot \gamma_{plus}}{z_{plus} \cdot M_{plus}} \right]^{-0.84573} \quad \text{,.....} \quad (64)$$

Where γ_{plus} and M_{plus} are the measured specific gravity and molecular weight of the plus fraction and ξ is defined as[1]:

$$\xi = \sum_{i=n}^{45} \left[4.5579 \cdot M_i^{\,0.15178} \right]^{\frac{1}{0.84573}} z_i . M_i \text{ ,.....} \quad (65)$$

Where n is the first component of the plus fraction, i.e., for C_7^+, n = 7.

The specific gravity for each component is calculated as[1]:

$$\gamma_i = \left[\frac{K_w}{4.5579 \cdot M_i^{\,0.15178}} \right]^{-\frac{1}{0.84573}} \text{,.....} \quad (66)$$

Aguilar and McCain[1] recommended using Cavett[16] correlations for critical temperature and critical pressure along with Riazi and Al-Sahhaf[21] acentric factor correlation. They claimed that this combination yielded the least adjustment for the molecular weight of the plus fraction when matching saturation pressure using the extended composition. Cavett[16] correlations for critical properties are as follows:

$$\begin{aligned}\log p_{ci} = {} & 2.8290406 + (0.94120109 \cdot 10^{-3}) \cdot T_{bi} \\ & - (0.30474749 \cdot 10^{-5}) \cdot T_{bi}{}^{2} \\ & - (0.20887611 \cdot 10^{-4}) \cdot API_i \cdot T_{bi} \\ & + (0.15184103 \cdot 10^{-8}) \cdot T_{bi}{}^{3} \\ & + (0.11047899 \cdot 10^{-7}) \cdot API_i \cdot T_{bi}{}^{2} \\ & - (0.48271599 \cdot 10^{-7}) \cdot API_i{}^{2} \cdot T_{bi} \\ & + (0.13949619 \cdot 10^{-9}) \cdot API_i{}^{2} \cdot T_{bi}{}^{2}\end{aligned} \quad ,\ldots\ldots\ldots\ldots (67)$$

$$\begin{aligned}T_{ci} = {} & 768.07121 + 1.7133693 \cdot T_{bi} \\ & - (0.10834003 \cdot 10^{-2}) \cdot T_{bi}{}^{2} \\ & - (0.89212579 \cdot 10^{-2}) \cdot API_i \cdot T_{bi} \\ & + (0.38890584 \cdot 10^{-6}) \cdot T_{bi}{}^{3} \\ & + (0.5309492 \cdot 10^{-5}) \cdot API_i \cdot T_{bi}{}^{2} \\ & + (0.327116 \cdot 10^{-7}) \cdot API_i{}^{2} T_{bi}{}^{2}\end{aligned} \quad ,\ldots\ldots\ldots\ldots (68)$$

Riazi and Al-Sahhaf[21] acentric factor correlation is as follows:

$$\omega = -\left[0.3 - \exp\left(-6.252 + 3.64457 \cdot M_i^{0.1}\right)\right], \ldots\ldots\ldots\ldots (69)$$

In **Eqs. 67 and 68** P_c in psia, T_c in (ºR) and T_b in (ºF), and API is calculated as:

$$API_i = \frac{141.5}{\gamma_i} - 131.5, \ldots\ldots\ldots\ldots (70)$$

Methodology for Finding the Accurate Set of Correlations for Critical Properties and Acentric Factors of SCN Groups

EOS calculations require critical properties and acentric factor for each component in order to determine the saturation pressure and volumetric data at a fixed temperature. Seven different sets of correlations were used to calculate the critical properties and acentric factor for the SCN groups in the extended composition. The saturation pressure will be calculated and matched with the experimental saturation pressure by adjusting the molecular weight of the plus fraction using these critical properties and acentric factors.

The results (variation of the molecular weight of the plus fraction) of six sets of correlations will be compared to the base case. The base case here will be the set of correlations selected as best by Aguilar and McCain[1]; these are the Cavett[16] correlations for calculating critical properties and using the Riazia and Al-Sahhaf[21] correlation for acentric factors. The other six sets of correlations are as follows:

First set: Cavett[16]-T_c & P_c (**Eqs. 67** & **68**), ω-Edmister[17] (**Eq. 71**)

$$\omega = \frac{3}{7}\left(\frac{\log\left(\frac{P_c}{14.7}\right)}{\frac{T_c}{T_B}-1}\right)-1, \quad \text{(71)}$$

This set of correlations was recommended by Katz and Firoozabadi[2] and Guo[12].

Second set: Winn[43]-T_c & P_c (**Eqs. 72** & **73**), ω-Riazi & Al-Sahhaf[21] (**Eq. 69**)

$$T_c = (Exp\ (4.2009\ \cdot T_B^{\ 0.08615}\ \cdot \gamma^{\ 0.04614}\ )/1.8) \quad \text{(72)}$$

$$P_c = 6.1483 \cdot 10^{12} \cdot T_B^{-2.3177} \cdot \gamma^{2.4853} \quad \text{..... (73)}$$

T_c & T_B are in ºR, P_c in psia.

Third set: Riazi-Daubert[19]-T_c & P_c (**Eqs. 74** & **75**), ω- Edmister[17] (**Eq. 71**)

$$T_c = 24.2787 \cdot T_B^{0.58848} \cdot \gamma^{0.3596} \quad \text{,..... (74)}$$

$$P_c = 3.12281 \cdot 10^{9} \cdot T_B^{-2.3125} \cdot \gamma^{2.3201} \quad \text{..... (75)}$$

T_c & T_B are in ºR, P_c in psia

This set of correlations has been recommended by Whitson[16].

Fourth set: Lee-Kesler [18]-T_c & P_c (**Eqs. 76** & **77**), ω- Edmister[17] (**Eq. 90**)

$$T_c = 341.7 + 811 \cdot \gamma + (0.4244 + 0.1174 \cdot \gamma) \cdot T_B + (0.4669 - 3.2623 \cdot \gamma) \cdot 10^5 / T_B \text{.....} \quad \text{(76)}$$

$$P_c = Exp(8.3634 - 0.0566/\gamma - (0.24244 + 2.2898/\gamma + 0.11857/\gamma^2) \cdot 10^{-3} \cdot T_B + (1.4685 + 3.648/\gamma + 0.47227/\gamma^2) \cdot 10^{-7} \cdot T_B^2 - (0.42019 + 1.6977/\gamma^2) \cdot 10^{-10} T_B^3) \text{.....} \quad \text{(77)}$$

T_c & T_B are in ºR, P_c in psia

Fifth set: Riazi-Daubert[19]-T_c & P_c (**Eqs. 74** & **75**), ω- Riazi & Al-Sahhaf[21] (**Eq. 69**)

Sixth set: Lee-Kesler[18]-T_c & P_c (**Eqs. 76 & 77**), ω- Riazi & Al-Sahhaf[21] (**Eq. 69**)

The objective of evaluating and comparing these sets of correlations is to find the correlations that will lead to the least adjustment of the molecular weight of the plus fraction when the saturation pressure is matched using the extended composition. The procedures are shown in Chapter VI page 61.

Data

Tables 16 and 17 show a summary of the data used in this research for gas condensate and oil samples respectively.

Table 16- Laboratory data for gas condensate samples

Fluid #	Analysis extent	M_{plus}	P_{sat}, psia	T_{res}, °F	C_7^+ mole%
1	C_{12}^+	226	5668	262	4.3
2	C_{12}^+	226	5732.7	275	5
3	C_{12}^+	252	5987.7	305	6.48
4	C_{12}^+	232	6159.7	266	6.87
5	C_{12}^+	222.83	5040	229	7.23
6	C_{12}^+	228	5636.7	291	8.04
7	C_{12}^+	248.5	6024.7	256	9.99
8	C_{12}^+	273.6	5224.7	305	10.87
9	C_{12}^+	257.8	4464.7	190	11.45
10	C_{12}^+	251	4922.7	301	12.27
11	C_{12}^+	224	4535.7	305	12.39

Table 17- Laboratory data for oil samples					
Fluid #	**Analysis extent**	**M_{plus}**	**P_{sat}, psia**	**T_{Res}, °F**	**C_7^+ mole%**
12	C_7^+	205	6604	179	12.92
13	C_7^+	259	9120	197	14.8
14	C_7^+	232	7451.7	190	15.66
15	C_7^+	173	4460	176	16.92
16	C_7^+	218	4577.7	307	17.2
17	C_7^+	250	6200	287	19
18	C_7^+	188	3981.7	302	20.53
19	C_7^+	168	2666.7	220	21.3
20	C_7^+	177	3150	185	22.73
21	C_7^+	171	2632	185	23.7
22	C_7^+	240	2996	235	24.68

Results

The critical properties and acentric factor for each SCN group extended from the plus fraction were calculated using six different sets of correlations, as discussed above.

The main objective of testing these different sets of correlations is to find the set of correlations that will lead to the least adjustment for the molecular weight of the plus fraction when the measured saturation pressure is matched using the extended composition.

Table 18 shows the variation in the molecular weight of the plus fraction that was required to match the saturation pressure when the extended composition was used. Since the experimental molecular weight has an experimental error of approximately ± 20%, the variation in the molecular weight of the plus fraction was limited to that range of error. Symbol A in **Table 18** means the variation required in the molecular weight of the plus fraction exceeded ± 20%. Also the equation-of-state must calculate same type of saturation pressure (i.e. dew point pressure for gas condensates samples and bubble point pressure for volatile oil and oil samples). Symbol B in **Table 18** indicates that the type of calculated saturation pressure was different than the experimental saturation pressure.

Table 18 shows that the best set of correlations to estimate the critical properties and acentric factor for each SCN group which lead to the least adjustment in the molecular weight of the plus fraction is the base case (Cavett[16] correlation for calculating critical properties and Riazi and Al-Sahhaf[21] correlation for calculating the acentric factor). These results match the recommendation of Aguilar and McCain[1].

The fifth set of correlations works for all gas condensate samples and is slightly more accurate than the base case. But this set of correlations does not work for many of the oil samples used in this study. So the base case is the most accurate method that will give good results for all of the samples used in this study.

Figs. 14, 15 and 16 show the calculated critical properties using Cavett correlation and acentric factor using Riazi-Al-Sahhaf correlation for each SCN group after matching saturation pressures using extended composition for fluid 1, 9 and 18 respectively. These fluids have been picked to show examples of critical properties and acentric factors of SCN groups of gas condensate, near critical and volatile oil samples.

Table 18- The variation of the molecular weight of the plus fraction using six different set of correlations compared to the base case

Fluid #	Base case	First case	Second case	Third case	Fourth case	Fifth case	Sixth case
	% variation, M_{plus}						
1	-1.34	A	A	20.00	20.00	-3.64	-3.64
2	-0.69	A	-4.46	20.79	20.79	-3.23	0
3	-4.56	A	-4.10	A	A	-5.54	-3.3
4	1.16	A	-1.99	A	A	0.66	2.066
5	20.45	A	16.95	A	A	19.56	A
6	2.22	A	-0.06	A	A	1.80	4.859
7	16.14	A	12.55	A	A	12.55	15.32
8	5.17	A	1.92	A	A	5.04	9.923
9	6.60	B	-2.28	A & B	A & B	2.40	8.824
10	-10.59	A & B	-11.00	19.20	A & B	-7.98	-5.22
11	-3.47	A & B	-2.60	B	B	-0.34	0
12	14.22	A	-4.70	A	A	B	B
13	-4.02	A	A & B	A	A	B	B
14	8.71	A	B	A	A	B	B
15	19.83	A	14.32	A	A	B	A
16	-3.68	A	-8.60	A	A	-3.10	4.145
17	1.55	A	-0.26	A	A	0.00	A
18	-7.39	A	-7.39	A	A	-3.82	-5.19
19	-0.38	20.00	3.46	20.07	20.07	8.39	8.394
20	20.11	A	A	A	A	A	A
21	16.46	A	11.79	A	A	19.14	20.01
22	-20.00	A	-20.07	A	A	-18.16	-20.07

A = percentage variation that applied to the molecular weight of the plus fraction was exceeded ± 20%.

B = predicting different saturation pressure type

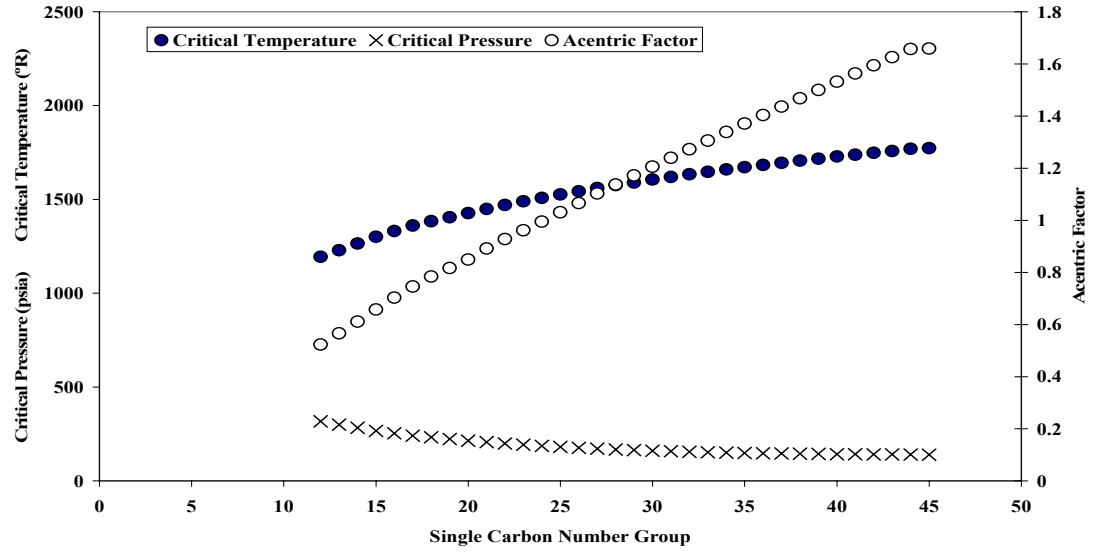

Fig. 14- Calculated critical properties and acentric factor for each SCN group extended from plus fraction of fluid-1.

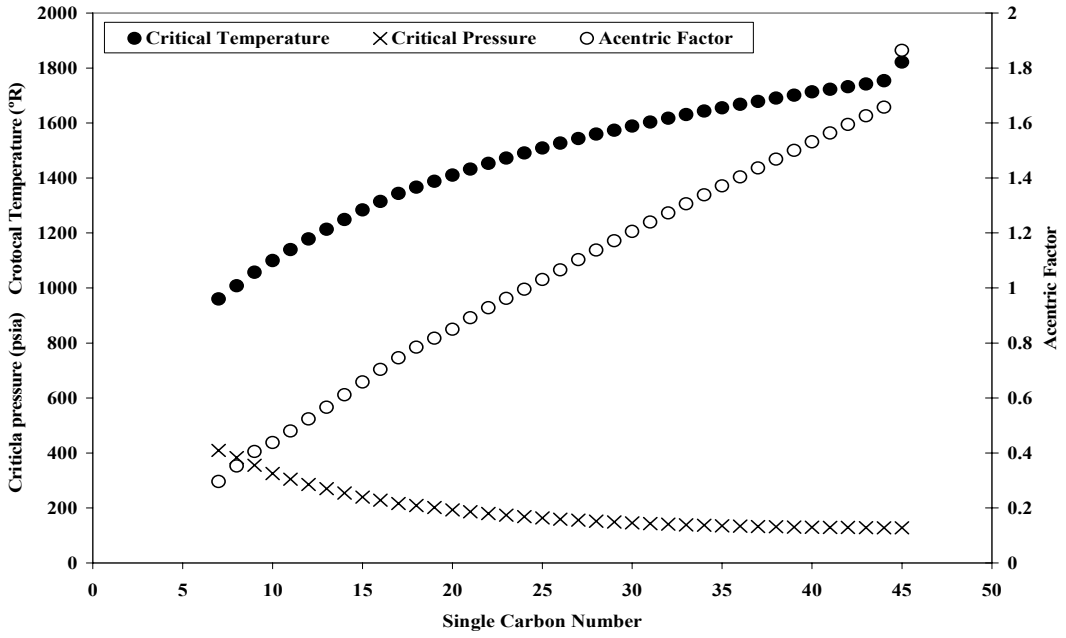

Fig. 15- Calculated critical properties and acentric factor for each SCN group extended from plus fraction of fluid-9.

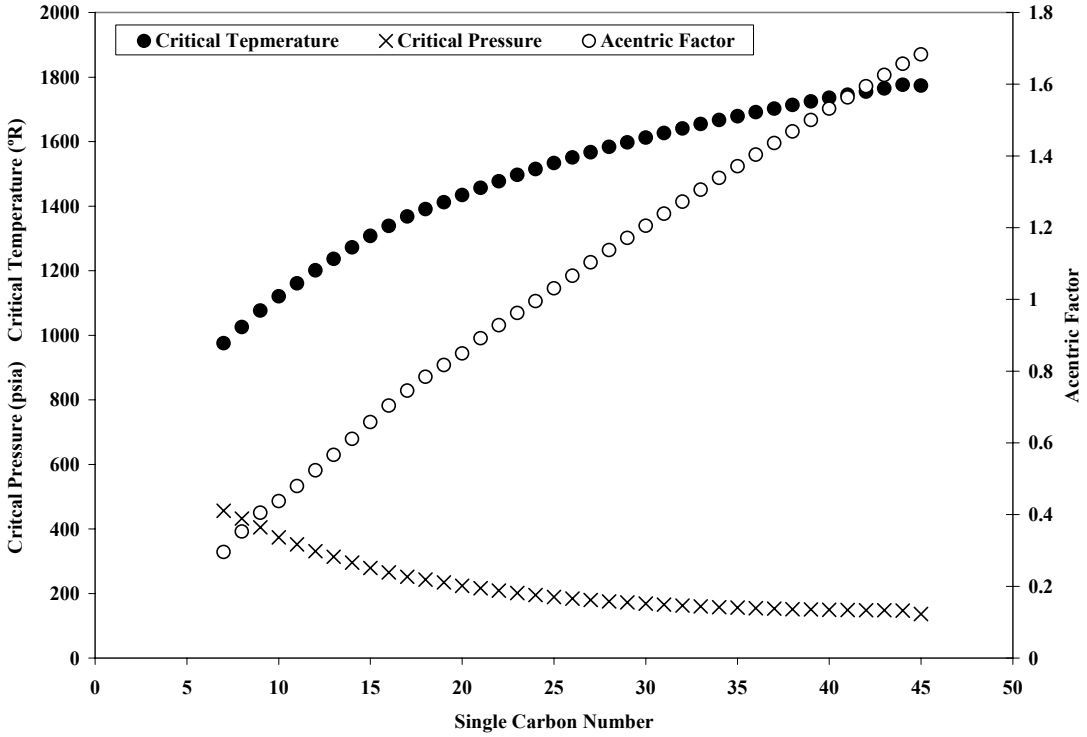

Fig. 16- Calculated critical properties and acentric factor for each SCN group extended from plus fraction of fluid-18.

CHAPTER VI

MATCHING SATURATION PRESSURE USING THE EXTENDED COMPOSITION

The saturation pressure is matched using the extended composition by adjusting the measured molecular weight of the plus fraction.

Since the measurement for molecular weight of the plus fraction has approximately ±20 % experimental error, it is reasonable to use the molecular weight of the plus fraction as the tuning variable for matching saturation pressure with the extended composition. So the molecular weight of the plus fraction will be adjusted within the experimental error to cause the saturation pressure calculated using the EOS with the extended composition match the experimental saturation pressure.

Methodology for Matching Saturation Pressure Using the Extended Composition

Once the molecular weight of the plus fraction is adjusted, the molar composition of the mixture must be recalculated since the laboratory measures composition in weight fraction. The following steps are recommended by Aguilar and McCain[1] to match saturation pressure by adjusting the molecular weight of the plus fraction:

- After the plus fraction is split and molecular weight, critical properties, and acentric factor for each SCN group are assigned and the C_{45}^{+} properties calculated, the saturation pressure is calculated using the EOS.
- If there is not a match, the plus fraction molecular weight is adjusted. **Eq. 37** shows that it is not possible to modify the plus fraction molecular weight directly. But the apparent molecular weight of the mixture can be adjusted; this has the same effect as adjusting the plus fraction molecular weight. Here the weight fraction is constant throughout the calculation. After adjusting the mixture molecular weight, the mole fraction is recalculated as:

$$z_i = \frac{w_i \cdot M_a}{M_i}, \quad \text{(78)}$$

- The mole fraction and molecular weight of the plus fraction are calculated as:

$$z_{plus} = 1 - \sum_{i=1}^{n-1} z_i, \quad \text{(79)}$$

$$M_{plus} = \frac{M_a - \sum_{i=1}^{n-1} z_i M_i}{z_{plus}}, \quad \text{(80)}$$

- The plus fraction is extended to C_{45}^{+} using three-parameter gamma probability distribution function, and critical properties and acentric factors are assigned for extended components.
- The new composition is used to recalculate the saturation pressure with the EOS.
- These steps are repeated until the calculated saturation pressure matches the experimental saturation pressure.

Data

The data used are shown in **Tables 16 and 17** for gas condensate and volatile oil samples.

Results

Tables 19 and 20 give the results of matching saturation pressures using the extended composition for gas condensate samples and oil samples respectively. The plus fraction for all of the gas condensate samples and all of the oil samples was C_{12}^{+} and C_7^{+} respectively.

Table 19- Saturation pressure matching results for the gas condensate samples using the extended composition							
Fluid #	**M_{plus} exp.**	**$P_{sat\ exp}$, psia**	**M_{plus} calc.**	**$P_{sat\ calc.}$, psia**	**% variation, M_{plus}**	**% variation, Ma**	**% match, P_{sat}**
1	226	5668	223.0	5874.7	-1.34	-0.016	3.65
2	226	5732.7	224.4	5839.7	-0.71	-0.013	1.87
3	252	5987.7	240.5	5991.6	-4.56	-0.102	0.065
4	232	6159.7	234.7	6160.0	1.16	0.029	0.00
5	222.83	5040	223.15	5043	0.144	0.003	0.06
6	228	5636.7	233.1	5626.2	2.22	0.057	-0.19
7	248.5	6024.7	253.9	5965.7	2.17	0.1045	-0.98
8	273.6	5224.7	258.24	5208.6	-5.61	-0.2356	-0.308
9	257.8	4464.7	270.19	4463.5	4.81	0.2733	-0.027
10	251	4922.7	224.4	4951.6	-10.59	- 0.432	0.59
11	224	4535.7	216.2	4552.0	-3.47	-0.186	0.36

Table 20- Saturation pressure matching results for the oil samples using the extended composition							
Fluid #	**M_{plus} exp.**	**$P_{sat\ exp}$, psia**	**M_{plus} calc.**	**$P_{sat\ calc.}$, psia**	**% variation, M_{plus}**	**% variation, Ma**	**% match, P_{sat}**
12	205	6604	234.2	6611.2	14.24	1.609	0.11
13	259	9120	264.6	9113.8	2.16	0.3076	-0.07
14	232	7451.7	252.2	7450.7	8.71	1.254	-0.01
15	173	4460	207.3	4269.2	19.83	2.800	-4.28
16	218	4577.7	210	4578.8	-3.68	- 0.647	0.02
17	250	6200	253.9	6215	1.55	0.310	0.24
18	188	3981.7	174.1	4003	-7.39	- 1.638	0.53
19	168	2666.7	167.4	2693.3	-0.36	- 0.0815	1
20	177	3150	212.6	2896.2	20.11	3.806	-8.06
21	171	2632	199.2	2632	16.46	3.231	0
22	240	2996	192	3015	-20	-6.170	0.63

CHAPTER VII

GROUPING AND ESTIMATING THE CRITICAL PROPERTIES AND ACENTRIC FACTORS FOR MCN GROUPS

Once the calculated saturation pressure is matched with the experimental saturation pressure using the extended composition, grouping into MCN groups reduces the number of components. The extended composition is grouped to reduce the total number of components from 50 SCN groups to 8 pseudocomponents, and then the critical properties and acentric factor for each pseudocomponent are calculated.

Methodology for Grouping

- C_1, N_2, CO_2 and H_2S will not be grouped.
- Intermediate components will be grouped as C_2-C_3 and C_4-C_6.
- Components C_7 to C_{45}^{+} are grouped into two multiple carbon number groups: MCN1 and MCN2. The split for MCN1 and MCN2 is as follows:

$$z_{MCN\,2}\,(mole\%) = \frac{0.008521264}{0.00297073 + e^{(-0.563823853 \cdot z_{C_7^+})}}, \quad \text{(81)}$$

$$z_{MCN_1} = z_{C_7^+} - z_{MCN_2}, \quad \text{(82)}$$

Methodology for Estimating Critical Properties and Acentric Factors for the MCN Groups

Critical temperature and critical pressure for each pseudocomponent are calculated as follows in an attempt to preserve constants a and b in the EOS[31, 32]: (*see* ***Appendix A*** *to see how* ***Eqs. 83 and 84*** *were derived*)

$$\frac{T_{cm}^{\ 2}}{P_{cm}} = \sum_{i=1}^{n_g}\sum_{j=1}^{n_g} z_i z_j \frac{T_{ci}T_{cj}}{\sqrt{P_{ci}P_{cj}}}\sqrt{\alpha_i(T_{cm})\alpha_j(T_{cm})}(1-k_{ij}), \quad (83)$$

$$\frac{T_{cm}}{P_{cm}} = \sum_{i=1}^{n_g} z_i \frac{T_{ci}}{P_{ci}}, \quad (84)$$

The number of components in each mixture is n_g; for example in pseudocomponent C_2-C_3 there are only two components, that is n_g=2.

The above two equations (83 & 84) can not be used directly to find the critical temperature and critical pressure of MCN group because T_{cm} appears in both sides of **Eq. 61**. The MCN critical pressure and critical temperature can be solved iteratively by successive substitutions starting with the following value:

$$T_{cm} = \frac{\sum_{i=1}^{n_g}\sum_{j=1}^{n_g} z_i \cdot z_j \cdot \frac{T_{ci}T_{cj}}{\sqrt{P_{ci}P_{cj}}}}{\sum_{i=1}^{n_g} z_i \cdot \frac{T_{ci}}{P_{ci}}}, \quad (85)$$

Once the value of T_{cm} is calculated, P_{cm} can be calculated using the following equation:

$$P_{cm} = \frac{T_{cm}}{\sum_{i=1}^{n_g} z_i \cdot \frac{T_{ci}}{P_{ci}}}, \quad (86)$$

- The acentric factor for each pseudocomponent is calculated as follows[1]:

$$0.26992 \cdot \omega_m^{\ 2} - 1.54226 \cdot \omega_m - (0.37464 - m_m) = 0, \quad (87)$$

$$m_m = \frac{\sqrt{\alpha_m(T_m)} - 1}{1 - \sqrt{0.7}}, \quad \text{(88)}$$

Where $T_m = 0.7 \cdot T_{cm}$

$$\alpha_m(T_m) = \frac{\sum_{i=1}^{m}\sum_{i=1}^{m} z_i \cdot z_j \cdot \frac{T_{ci}T_{cj}}{\sqrt{P_{ci}P_{cj}}} \cdot \sqrt{\alpha_i(T_m)\alpha_j(T_m)} \cdot (1 - k_{ij})}{\frac{T^2{}_{cm}}{P_{cm}}}, \quad \text{(89)}$$

$$\alpha_i(T_m) = \left[1 + m_i\left(1 - \left(\frac{T_m}{T_{ci}}\right)^{0.5}\right)\right]^2, \quad \text{(90)}$$

$$m_i = 0.37464 + 1.54226 \cdot \omega_i - 0.26992 \cdot \omega^2{}_i \quad \text{(PREOS only)} \quad \text{(91)}$$

The smallest positive root from the above quadratic equation will be the acentric factor for the MCN.

Relationship Between Composition of C_7^+ and Composition of MCN2

Agiular and McCain[1] recommended an excellent method to group the extended composition and introduced a new correlation that will calculate the composition of the MCN2 as a function of the composition of C_7^+. They claimed that this correlation will improve the agreement between calculated and experimental PVT data.

The recommended correlation is shown in **Eqs. 12 and 13**. This correlation was based on PVT reports of samples of 10 naturally occurring reservoir fluids. This correlation has been validated and extended with a wider range of fluid compositions. The extended correlation has the same form as the correlation proposed by Aguilar and McCain[1] but with different coefficients. These coefficients were changed for each fluid

during the PVT matching to see which are the best coefficients for this correlation that will improve the agreement between the experimental and calculated PVT data for all of the fluids used in this research. The extended correlation is shown below:

$$z_{MCN2}(mole\%) = \frac{0.008521264}{0.00297073 + e^{(-0.563823853 \cdot z_{C_7^+})}} \quad \text{(81)}$$

$$z_{MCN_1} = z_{C_7^+} - z_{MCN_2} \quad \text{(82)}$$

Table 21 shows the experimental and calculated composition of C_7^+ after adjusting the molecular weight of the plus fraction, when the saturation pressure is matched using the extended composition. Using the calculated composition of C_7^+, the composition of MCN2 and MCN1 can be calculated using the above equations. **Fig. 17** shows the relationship between the composition of C_7^+ and the composition of MCN2. **Fig. 18** shows the results of Agiular and McCain[1] on the same plot.

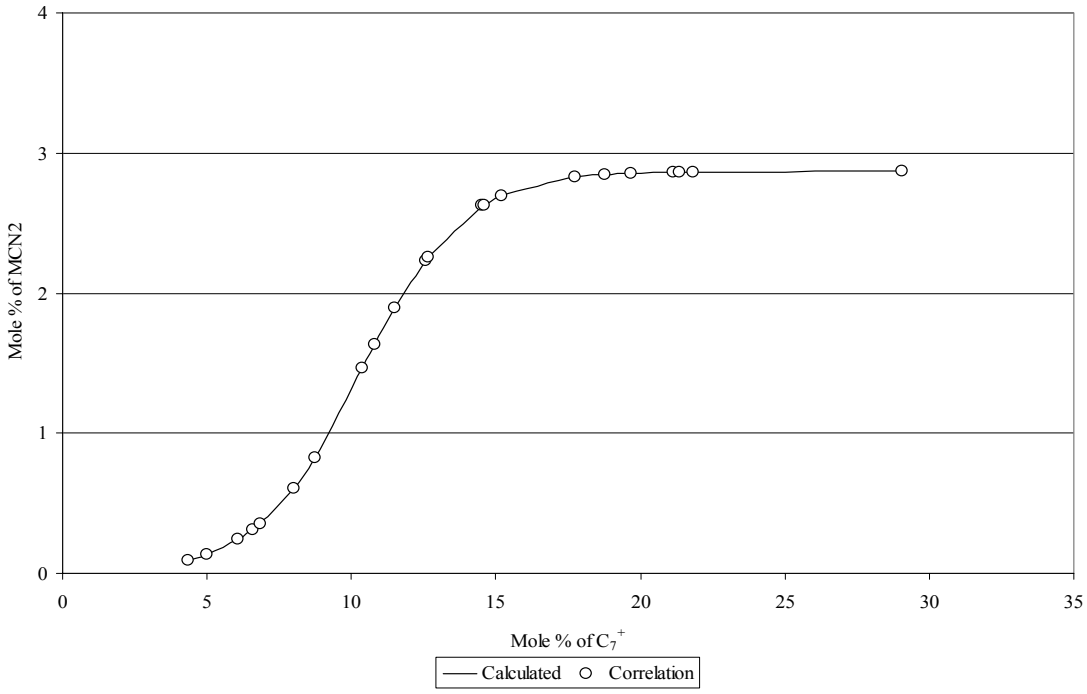

Fig. 17- Relationship between the mole % of MCN2 and C_7^+.

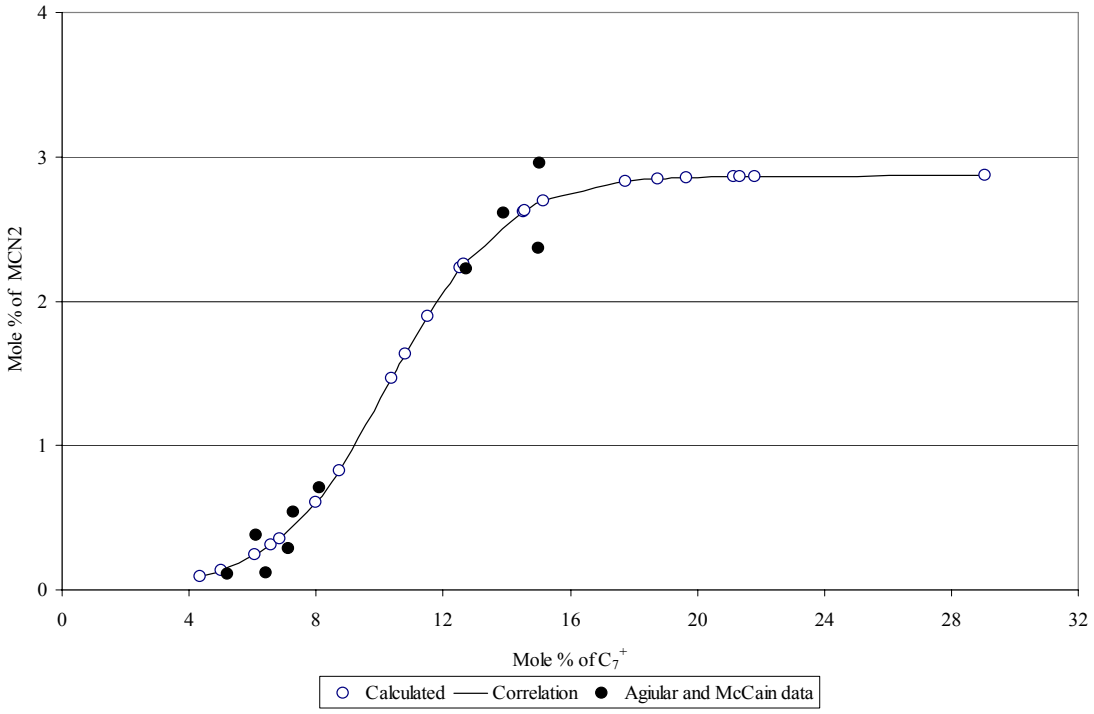

Fig. 18- Relationship between the mole % of MCN2 and C_7^+ of Aguilar and McCain compared with the new correlation.

Table 21- Experimental and calculated composition of C_7^+ and the calculated composition of MCN2			
	C_7^+ mole%		
Fluid #	**Experimental**	**Calculated after adjusting MW of the plus fraction**	**mole % of MCN2**
1	4.3	4.334	0.095
2	5	5.012	0.137
3	6.48	6.575	0.310
4	6.87	6.843	0.354
5	7.23	6.077	0.240
6	8.04	7.988	0.607
7	9.99	8.722	0.828
8	10.87	10.392	1.462
9	11.45	10.818	1.633
10	12.27	12.650	2.260
11	12.39	12.550	2.232
12	12.92	11.496	1.892
13	14.8	15.176	2.694
14	15.66	14.581	2.630
15	16.92	14.527	2.623
16	17.2	17.742	2.825
17	19	18.768	2.844
18	20.53	21.811	2.864
19	21.3	21.364	2.863
20	22.73	19.673	2.854
21	23.56	21.152	2.862
22	24.68	29.057	2.869

CHAPTER VIII
MATCHING SATURATION PRESSURE USING THE GROUPED COMPOSITION

After grouping, the match of calculated and experimental saturation pressure is usually altered slightly. The acentric factor of the heaviest pseudocomponent has been used in this research as tuning variable to match the saturation pressure using the grouped composition. Using the acentric factor as adjustable variable will honor the relationship between critical temperature and critical pressure of MCN1 and MCN2 which will be the same relationship between critical temperature and critical pressure of all SCN groups extended from the plus fraction.

Aguilar and McCain[1] proposed a method to match saturation pressures when the grouped composition is used. Their methodology to match saturation pressure was by modifying only one variable, the ratio of the critical temperature to the critical pressure of the heaviest pseudocomponent. This methodology was reviewed in this study and it works for saturation pressure matching but it does not honor the relationship between critical temperature and critical pressure of MCN2.

Methodology for Matching Saturation Pressure Using the Grouped Composition

The grouped composition is used to match saturation pressure by adjusting the acentric factor of the heaviest pseudocomponent, MCN2.

Results

Tables 22 and 23 show the results of matching saturation pressure using the grouped composition for gas condensate and oil samples, respectively. The third column in each table shows the initial value of acentric factor of the heaviest pseudocomponent that was calculated using **Eq. 87.**

Table 22- Adjusting acentric factor of the heaviest pseudocomponent, MCN2, for matching saturation pressure using the grouped composition for gas condensate samples						
Fluid #	**$P_{sat\ exp}$, psia**	**ω-initial value**	**ω-adjusted**	**$P_{sat\ calc.}$, psia**	**% variation ω**	**% match P_{sat}**
1	5668	1.182	1.3558	5668	14.7	0
2	5732.7	1.2754	1.2245	5732.7	-4.0	0
3	5987.7	1.24998	1.2195	5987.7	-2.4	0
4	6159.7	1.2747	1.311	6159.7	2.8	0
5	5040	1.4612	1.732	5040	18.5	0
6	5636.7	1.134477	0.9485	5636.7	-16.4	0
7	6024.7	1.21887	1.489	6024.7	22.2	0
8	5224.7	1.118241	1.3685	5224.7	22.4	0
9	4464.7	1.233919	1.5393	4464.7	24.7	0
10	4922.7	0.909529	0.9887	4922.7	8.7	0
11	4535.7	0.9257	0.8775	4535.7	-5.2	0

Table 23- Adjusting acentric factor of the heaviest pseudocomponent, MCN2, for matching saturation pressure using the grouped composition for oil samples						
Fluid #	**$P_{sat\ exp}$, psia**	**ω-initial value**	**ω-adjusted**	**$P_{sat\ calc.}$, psia**	**% variation ω**	**% match P_{sat}**
12	6604	1.37915	1.5511	6604	12.5	0
13	9120	1.5407	1.81785	9120	18.0	0
14	7451.7	1.473104	1.6861	7451.7	14.5	0
15	4460	1.25072	1.3955	4460	11.6	0
16	4577.7	1.254532	1.5562	4577.7	24.0	0
17	6200	1.51185	1.9216	6200	27.1	0
18	3981.7	1.115838	1.3653	3981.7	22.4	0
19	2666.7	1.0529	1.335	2666.7	26.8	0
20	3150	1.316335675	1.765	3150	34.1	0
21	2632	1.218905281	1.682	2632	38.0	0
22	2996	1.28876	1.6135	2996	25.2	0

CHAPTER IX
MATCHING VOLUMETRIC DATA

Peneloux et al.[39] developed a method to improve the volumetric capabilities of the SRK EOS by using a molar volume translation as a third parameter in SRK EOS. The third parameter does not change the vapor-liquid equilibrium conditions determined by the unmodified, two-parameter EOS, but modifies the molar volumes of the phases by effecting certain translations along the volume axis. These translations leave the predicted equilibrium conditions unchanged. This third parameter is called molar volume shift parameter.

These translation parameters are correction terms that applied to molar volume calculated by the EOS[40]:

$$v_L = v_L^{EOS} - \sum_{i=1}^{n_S} x_i \cdot c_i \,, \qquad (92)$$

$$v_V = v_V^{EOS} - \sum_{i=1}^{n_S} y_i \cdot c_i \,, \qquad (93)$$

Where v_L^{EOS} and v_v^{EOS} are liquid and gas volume calculated by EOS, and c_i is the molar volume translation parameter for each component i.

When the molar volume shift is introduced to the EOS for mixtures, the fugacity expression for vapor and liquid will be as follows[39, 44]:

$$(f_{gi})_{modified} = (f_{v_i})_{original} \cdot \exp(-c_i \frac{p}{RT}) \,, \qquad (94)$$

$$(f_{L_i})_{modified} = (f_{l_i})_{original} \cdot \exp(-c_i \frac{p}{RT}), \quad (95)$$

When **Eq. 95** is divided by **Eq. 94** it is seen that fugacity ratio is unaltered by the volume shift parameter[39, 44].

Jhaveri and Youngren[40] defined a dimensionless shift parameter by dividing the volume translation parameter, c, by the second PR-EOS parameter, b. These two parameters have the same units, molar volume. Thus dimensionless parameter is defined as:

$$s_i = \frac{c_i}{b_i}, \quad (96)$$

Volumetric data is matched is by regressing on the dimensionless shift parameter of each component of the grouped composition.

In this research binary interaction coefficients between hydrocarbon components and between hydrocarbons to non-hydrocarbon were set to zero in order to decrease the computational time. It was found that it still give good matching of PVT data.

Methodology for Matching Volumetric Data

The volumetric data from three main experiments: constant composition expansion, constant volume depletion and differential liberation are matched by regressing on the molar volume shift parameters of all components in the grouped composition. For all the calculations the EOS used in this research was the three parameter Peng-Robinson EOS. This EOS was selected for its wide use in the industry and also for its improved accuracy in calculating liquid density.

Data

Tables 16 and 17 show a summary of the data used in this research for gas condensate and oil samples respectively. The detailed data for the CCE, CVD and DL are shown in **Appendixes C and D** for gas condensate and oil samples respectively.

Results

An EOS usually fails to reproduce the experimental volumetric data due to its deficiency in estimating liquid density; for this reason this strategy chooses the molar volume shift parameters of all components in the grouped composition to be the only regression variables used to match the experimental volumetric data. Using these variables will not affect the vapor-liquid equilibria calculations and therefore will not affect the original vapor-liquid equilibria calculations of the EOS[39]. Also, these variables were selected as regression variables because it changes the least accurate values calculated by EOS, densities, especially for liquids.

After matching saturation pressure using the grouped composition, the 3-parameter PREOS is ready to simulate the volumetric data. If this EOS does not match the experimental data regressing on volume shift parameters will improve the match of the volumetric data. **Appendix B** shows the matching between the experimental data and calculated results for all of the fluids that used in this study.

Some of the fluids had excellent match of the volumetric data without regressing on the molar volume shift parameters. Examples are fluids 7, 15, 20 and 21.

Using this strategy with MCN1 and MCN2 gave good matching between the experimental and calculated volumetric data. If there is not good agreement between experimental data and calculated results there is most likely bad data. Bad data can usually be matched by splitting MCN1 into two MCNs, MCN1a and MCN1b. MCN1 will be split into MCN1a-MCN1b as 95-5 mole % for gas condensates. Agiular and McCain[1] recommended splitting MCN1 to MCN1a-MCN1b as 60-40 mole % for oil samples if there is not good matching of the volumetric data because of the bad experimental data.

Examples of that for gas condensate fluids are fluid 3, 5 and 6. For these three fluids after regression using two MCNs, the matching for volumetric data was good except for liquid saturation of CVD experiment. After extending MCN1 into MCN1a and MCN1b the agreement between volumetric data was the same as grouping into two MCNs except for liquid saturation that gave better matching. In **Appendix B**, **Figs. B.9 to B.12** show matching of volumetric data for fluid 3, after regression using two MCNs and three MCNs. **Figs. B.16 to B.19** and **Figs. B.20 to B-23** show the same thing for fluid 5 and 6, respectively. In this study, the volumetric data matching for all of the oil samples was good without splitting MCN1 to MCN1a and MCN1b.

For near critical gas condensate fluids such as fluid 10 and 11 that , during the saturation pressure matching using the grouped composition where the intermediate components were grouped as C_2-C_3 and C_4-C_6, the predicted saturation pressure type was incorrectly predicting, i.e. bubble point pressure instead of dew point pressure. We found that for near critical gas condensate fluids to leave the intermediate components C_2 to C_6 as pure components will result in the correct type of saturation pressure. This will make the total number of components after grouping to be 13 (H_2S, CO_2, N_2, C_1, C_2, C_3, i-C_4, n-C_4, i-C_5, n-C_5, C_6, MCN1 and MCN2).

CHAPTER X
TESTING TUNED EOS

The proposed method was tested using twenty-two full PVT reports as shown in the PVT matching chapter. Also, the tuned EOS for some of these fluids was tested to see if it could predict fluid properties at separator conditions, if it could predict saturation pressure at different temperatures other than reservoir temperature, and if it could match swelling test data or phase diagrams.

Fluid Properties at Separator Conditions

The tuned EOS using the proposed strategy has been tested to see if it can predict the fluid properties at separator conditions, such as gas-oil-ratio, formation volume factor, total gas-oil ratio and oil density.

This test has been applied to data at separator conditions from PVT reports of six fluids, these fluids are fluids 14, 18, 20, 21 and 22. The results show that the tuned EOS will predict accurate results for fluid properties at separator conditions. **Tables 24, 25, 26, 27 and 28** show the experimental and the calculated fluid properties for these six fluids respectively.

Table 24- Experimental and calculated fluid properties at separator conditions for fluid 14				
		GOR, Mscf/Sep. Bbl		
Pressure, psia	Temperature, ºF	Experimental	Calculated	% Deviation
584.7	77	1.898	1.5783	-16.8440
14.7	70	0.263	0.2175	-17.3004
		Separator Volume Factor		
Pressure, psia	Temperature, ºF	Experimental	Calculated	% Deviation
584.7	77	1.138	1.112	-2.2847
14.7	70	1.005	1.0023	-0.2687
		Oil phase density (lb/ft^3)		
Pressure, psia	Temperature, ºF	Experimental	Calculated	% Deviation
7451.7	190	35.37	38.08	7.6683
584.7	77	49.86	50.31	0.9026
14.7	70	52.14	52.71	1.0912

Table 25- Experimental and calculated fluid properties at separator conditions for fluid 18				
		GOR, Mscf/Sep. Bbl		
Pressure, psia	Temperature, ºF	Experimental	Calculated	% Deviation
514.7	80.0	1.3860	1.2317	-11.1328
64.7	80.0	0.2930	0.3147	7.4061
14.7	80.0	0.0910	0.0965	6.0440
		Total GOR (Mscf/STB)		
		Experimental	Calculated	% Deviation
		1.8040	1.921	6.4856

Table 26- Experimental and calculated fluid properties at separator conditions for fluid 20				
		GOR, Mscf/Sep. Bbl		
Pressure, psia	Temperature, ºF	Experimental	Calculated	% Deviation
514.7	115.0	0.8800	0.8420	-4.3182
264.7	110.0	0.0871	0.0863	-0.9071
64.7	105.0	0.1530	0.1459	-4.6281
14.7	100	0.139*	0.123*	11.0305
		Separator Volume Factor		
Pressure, psia	Temperature, ºF	Experimental	Calculated	% Deviation
514.7	115.0	1.2500	1.2496	-0.0320
264.7	110.0	1.2040	1.1967	-0.6063
64.7	105.0	1.1138	1.1029	-0.9786
		Total GOR (Mscf/STB)		
		Experimental	Calculated	% Deviation
		1.4900	1.4246	-4.3893

*GOR unit in Mscf/STB

Table 27- Experimental and calculated fluid properties at separator conditions for fluid 21				
		GOR, Mscf/Sep. Bbl		
Pressure, psia	Temperature, ºF	Experimental	Calculated	% Deviation
514.7	115	0.782	0.867	10.8355
264.7	110	0.091	0.103	13.1719
64.7	105	0.164	0.176	7.3192
14.7	100	0.126*	0.1295*	-2.8053
		Separator Volume Factor		
Pressure, psia	Temperature, ºF	Experimental	Calculated	% Deviation
514.7	115	1.300	1.281	-1.4765
264.7	110	1.242	1.217	-1.9572
64.7	105	1.127	1.106	-1.9337
		Total GOR (Mscf/STB)		
		Experimental	Calculated	% Deviation
		1.441	1.542	6.9882

*GOR unit in Mscf/STB

Table 28- Experimental and calculated fluid properties at separator conditions for fluid 22				
		GOR, Mscf/Sep. Bbl		
Pressure, psia	Temperature, ºF	Experimental	Calculated	% Deviation
189.7	115	1.11591	1.01620	-8.9353
59.7	110	0.06435	0.06980	8.4693
34.7	85	0.01041	0.01130	8.5495
14.7	85	0.03340	0.03620	8.3832

Saturation Pressure at Different Temperatures

The tuned EOS using the proposed strategy was tested to see if it can predicts saturation pressures at temperatures other than reservoir temperature. Out of the 22 PVT reports used in this research 6 PVT reports have data that show saturation pressures at different temperature. These PVT reports for the following fluids: fluid 1, 4, 11, 20, 21 and 22.

The results show that the tuned EOS for a reservoir fluid using the proposed strategy at reservoir temperature can predict saturation pressures at different temperatures accurately. **Table 29, 30, 31, 32, 33 and 34** show the results of predicting saturation pressures at different temperatures for these six fluids.

Table 29- Saturation pressures at different temperatures for fluid 1			
	Saturation pressure, psia		
Temperature, ºF	Experimental	Calculated	% Deviation
150	6091	5721.2	-6.07
200	5928	5789.5	-2.34
262	5668	5668.2	0.00

Table 30- Saturation pressures at different temperatures for fluid 4			
	Saturation pressure, psia		
Temperature, ºF	Experimental	Calculated	% Deviation
150	6564.7	5863.1	-10.69
225	6314.7	6140.9	-2.75
266	6159.7	6160.5	0.01

Table 31- Saturation pressures at different temperatures for fluid 11			
	Saturation pressure, psia		
Temperature, ºF	Experimental	Calculated	% Deviation
250	4510.7	4649.0	3.07
275	4532.7	4682.7	3.31
305	4535.7	4685.6	3.30

Table 32- Saturation pressures at different temperatures for fluid 20			
	Saturation pressure, psia		
Temperature, ºF	Experimental	Calculated	% Deviation
110	2815	2532.72	-10.03
185	3150	3149.46	-0.02

Table 33- Saturation pressures at different temperatures for fluid 21			
	Saturation pressure, psia		
Temperature, ºF	Experimental	Calculated	% Deviation
110	2311	2142.3	-7.30
185	2632	2631.9	0.00

Table 34- Saturation pressures at different temperatures for fluid 22			
	Saturation pressure, psia		
Temperature, ºF	Experimental	Calculated	% Deviation
100	2192	2045.4	-6.69
145	2492	2415.3	-3.08
190	2760	2733.4	-0.97
235	2996	2996.6	0.02

Matching Swelling Test Data

No appropriate data have been found to test the proposed method of tuning EOS in matching swelling tests.

Matching Phase Diagram

Usually PVT reports show data of the constant composition expansion experiment, CCE, at reservoir temperature. The data usually are relative volume and liquid saturation at different pressures for a fixed temperature. In order to plot the phase diagram for a reservoir fluid with quality lines, the CCE experiment must be conducted at different temperatures.

The tuned EOS for two fluids have tested to see if they could match the phase diagram. Results show that the tuned EOS of state for these two fluids cannot predicts the phase diagram. These two fluids are fluid 4 and fluid 11. The PVT reports for fluid 4 and 11 show data for the CCE experiment at four and three different temperatures respectively.

In **Appendix B**, for fluid 4 **Figs. B.13, B.14 and B.15** show a good match between experimental and calculated data of relative volume, vapor z-factor and liquid saturation respectively at reservoir temperature, 266 ºF. **Figs. B.91, B.94, and B.97** show a good match between the experimental and calculated relative volume at three different temperatures 225, 150 and 100 ºF. **Figs. B.92, B.95, and B.98** show a good match between the experimental and calculated vapor z-factor at three different temperatures 225, 150 and 100 ºF. **Figs. B.93, B.96, and B.99** show a good match between the experimental and calculated liquid saturation at the temperatures 225 ºF, and a bad match at the other temperatures of 150 and 100 ºF. As shown from these plots that the tuned EOS for fluid 4 can reproduce the experimental data of relative volume and vapor z-factor. For the liquid saturation, as the temperature decreases the agreement between the experimental and calculated data become increasingly worse.

For fluid 11, the CCE experiment has been conducted at three different temperatures 305, 275 and 250 ºF; the reservoir temperature was 305 ºF. **Figs. B.35,**

B.36 and B.37 show a good match between the experimental and calculated relative volume, vapor z-factor and liquid saturation respectively at reservoir temperature, 305 ºF. **Figs. B.100 and B.103** show a good match between the experimental and calculated relative volume at two different temperatures 275 and 250 ºF. **Figs. B101 and B.104** show a good match between the experimental and calculated vapor z-factor at two different temperatures 275 and 250 ºF. **Figs. B.102 and B.105** show a bad match between the experimental and calculated liquid saturation at two different temperatures 275 and 250 ºF. Since fluid 11 is near critical reservoir fluid (C_7^+ mole % = 12.39) the EOS predicted saturation pressure at temperature less than the reservoir temperature incorrectly (i.e. bubble point instead of dew point), see **Figs. B.102 and B.105**.

From above results we can conclude that the tuned EOS using the proposed method cannot match the phase diagram. For near critical reservoir fluid such as fluid 11, the PVT software used in this research predicted a bubble point pressure instead of the dew point for temperatures lower than reservoir temperature.

CHAPTER XI
CONCLUSIONS

The proposed strategy to tune EOS is very accurate, simple, systematic, and can be applied to any naturally occurring reservoir fluid. This research has covered a wide range of C_7^+ mole% (4-25) with a total of 22 PVT reports. The following is concluded:

- Matching saturation pressure using the extended composition can be done by using the molecular weight of the plus fraction as the adjustable variable.
- Matching saturation pressure using the grouped composition can be done by using the acentric factor of the heaviest pseudocomponent as the adjustable variable.
- Matching the volumetric data can be done by regressing on the molar volume shift parameters of all components in the grouped composition.
- Splitting a fluid composition that has a plus fraction as either C_7^+ or C_{11}^+, to calculate the cumulative frequency of occurrence using normal cut method, and the value of η is the molecular weight of the normal alkane smaller than the plus fraction gives good results.
- Assigning average molecular weight for SCN groups using the correlation proposed by Katz and Firoozabadi gave more accurate molecular weight of plus fraction C_{45}^+than the Whitson correlation.
- Calculating critical properties using Cavett correlation and acentric factor using Riazi-Al-Sahhaf correlation will lead to the least adjustment for the molecular weight of the plus fraction to match saturation pressure using the extended composition.
- Setting the binary interaction coefficients between hydrocarbons and between hydrocarbons to non-hydrocarbons as zero does not affect the PVT matching and will reduce the computational time.
- Grouping the extended composition into two MCN groups using **Eq. 81** was confirmed and extended from the correlation that proposed by Aguilar and McCain[1].

- Leaving the intermediate components C_2 to C_6 as pure components is recommended for near critical gas condensate fluids in order to predict the correct type for the saturation pressure.
- Using the proposed strategy can predict accurately the fluid properties at separator conditions.
- Using the proposed strategy the tuned EOS at reservoir temperature can predict the saturation pressure at other different temperatures with reasonable accuracy. However, for near critical reservoir fluids the EOS may predict the incorrect type of saturation pressure.
- Using the proposed strategy to tune EOS cannot match the phase diagram at other temperatures.

CHAPTER XII
SUMMARY OF THE PROPOSED METHOD TO TUNE EOS

1. Calculate the average molecular weight and weight fraction for the entire components of the original composition using the following equations:

$$M_a = \sum_{i=1}^{n_o} z_i \cdot M_i$$

$$w_i = \frac{z_i \cdot M_i}{M_a}$$

2. Calculate the mole fraction, z_i, for each SCN group using the following equations:

$$z_i = z_{plus} \cdot f_i$$

$$f_i = -\exp(\eta/\beta) \cdot [\exp(-\frac{M_i}{\beta}) - \exp(-\frac{M_{i-1}}{\beta})]$$

$$z_{C_{45}^+} = z_{plus} - \sum_{i=1}^{n_e-1} z_i$$

3. Assign molecular weight and mole fraction for each SCN group from **Table 2**, the molecular weight and boiling temperature of C_{45}^+ is calculated using the following equations:

$$M_{C_{45^+}} = \frac{z_{plus} \cdot M_{plus} - \sum_{i=1}^{n_e-1} z_i \cdot M_i}{z_{C_{45^+}}}$$

$$T_{bC_{45^+}} = 1.8 \cdot (97.58 \cdot M_{C_{45^+}}{}^{0.3323} \cdot \gamma_{C_{45^+}}{}^{0.04609}) - 459.67$$

4. Calculate specific gravity for each component by assuming constant Watson Characterization Factor, using the following equations:

$$K = \left[\frac{\xi \cdot \gamma_{plus}}{z_{plus} \cdot M_{plus}} \right]^{-0.84573}$$

$$\xi = \sum_{i=n}^{45} \left[4.5579 \cdot M_i{}^{0.15178} \right]^{\frac{1}{0.84573}} z_i . M_i$$

$$\gamma_i = \left[\frac{K}{4.5579 \cdot M_i{}^{0.15178}} \right]^{\frac{1}{0.84573}}$$

5. Assign critical properties and acentric factor for each components using the following correlations:

$$\begin{aligned} \log p_{ci} = {} & 2.8290406 + (0.94120109 \cdot 10^{-3}) \cdot T_{bi} \\ & - (0.30474749 \cdot 10^{-5}) \cdot T_{bi}{}^2 \\ & - (0.20887611 \cdot 10^{-4}) \cdot API_i \cdot T_{bi} \\ & + (0.15184103 \cdot 10^{-8}) \cdot T_{bi}{}^3 \\ & + (0.11047899 \cdot 10^{-7}) \cdot API \cdot T_{bi}{}^2 \\ & - (0.48271599 \cdot 10^{-7}) \cdot API^2 \cdot T_{bi} \\ & + (0.13949619 \cdot 10^{-9}) \cdot API^2 \cdot T_{bi}{}^2 \end{aligned}$$

$$T_{ci} = 768.07121 + 1.7133693 \cdot T_{bi} - (0.10834003 \cdot 10^{-2}) \cdot T_{bi}^{\,2} - (0.89212579 \cdot 10^{-2}) \cdot API_i \cdot T_{bi} + (0.38890584 \cdot 10^{-6}) \cdot T_{bi}^{\,3} + (0.5309492 \cdot 10^{-5}) \cdot API \cdot T_{bi}^{\,2} + (0.327116 \cdot 10^{-7}) \cdot API^2 T_{bi}^{\,2}$$

$$\omega = -\left[0.3 - \exp\left(-6.252 + 3.64457 \cdot M_i^{\,0.1}\right)\right]$$

6. Calculate saturation pressure using the extended composition with the assigned molecular weight and boiling temperatures and calculated critical properties and acentric factor.
7. Compare calculated saturation pressure with the experimental if there is not a match adjusts the average molecular weight of the fluid composition – which is indirectly adjusting the molecular weight of the plus fraction- until the calculated saturation pressure matched the experimental saturation pressure. The procedure to match saturation pressure is as follows:

    - The weight fraction that was calculated for each component in the original fluid composition in the first step is held constant.
    - The average molecular weight is calculated as shown in first step.
    - The mole fraction is calculated as follows

$$z_i = \frac{w_i \cdot M_a}{M_i}$$

- The mole fraction and molecular weight of the plus fraction is calculated as following:

$$z_{plus} = 1 - \sum_{i=1}^{n-1} z_i$$

$$M_{plus} = \frac{M_a - \sum_{i=1}^{n-1} z_i M_i}{z_{plus}}$$

- Once the molecular weight of the plus fraction is adjusted, the molar composition of the mixture must be recalculated since the laboratory measures composition in weight fraction.
- Repeat step 2-7 until the calculated saturation pressure matches the experimental saturation pressure.

8. Once the calculated saturation pressure is matched with the experimental saturation pressure using the extended composition, the number of components is reduced by grouping into MCN groups using the following method:

- C_1, N_2, CO_2 and H_2S will not be grouped.
- Intermediate components will be grouped as C_2-C_3 and C_4-C_6.
- Group components C_7 to C_{45}^+ into two multiple carbon number groups: MCN1 and MCN2.
- Mole fraction for MCN1 and MCN2

$$z_{MCN2}(mole\%) = \frac{0.008521264}{0.00297073 + Exp(-0.563823853 \cdot z_{C_7^+})}$$

$$z_{MCN_1} = z_{C_7^+} - z_{MCN_2}$$

9. Critical temperature and critical pressure for each pseudocomponent is calculated by solving these two equations iteratively as shown below:

$$\frac{T_{cm}^{\ 2}}{P_{cm}} = \sum_{i=1}^{n_g}\sum_{j=1}^{n_g} z_i z_j \frac{T_{ci}T_{cj}}{\sqrt{P_{ci}P_{cj}}}\sqrt{\alpha_i(T_{cm})\alpha_j(T_{cm})}(1-k_{ij})$$

$$\frac{T_{cm}}{P_{cm}} = \sum_{i=1}^{n_g} z_i \frac{T_{ci}}{P_{ci}}$$

- The starting value can be calculated as follows:

$$T_{cm} = \frac{\sum_{i=1}^{n_g}\sum_{j=1}^{n_g} z_i \cdot z_j \cdot \frac{T_{ci}T_{cj}}{\sqrt{P_{ci}P_{cj}}}}{\sum_{i=1}^{n_g} z_i \cdot \frac{T_{ci}}{P_{ci}}}$$

- Once T_{cm} is calculated, P_{cm} can be calculated as:

$$P_{cm} = \frac{T_{cm}}{\sum_{i=1}^{n_g} z_i \cdot \frac{T_{ci}}{P_{ci}}}$$

10. The acentric factor for each pseudocomponent is calculated as follows:

$$0.26992 \cdot \omega_m{}^2 - 1.54226 \cdot \omega_m - (0.37464 - m_m) = 0$$

$$m_m = \frac{\sqrt{\alpha_m(T_m)} - 1}{1 - \sqrt{0.7}}$$

Where $T_m = 0.7 \cdot T_{cm}$

$$\alpha_m(T_m) = \frac{\sum_{i=1}^{m}\sum_{i=1}^{m} z_i \cdot z_j \cdot \frac{T_{ci}T_{cj}}{\sqrt{P_{ci}P_{cj}}} \cdot \sqrt{\alpha_i(T_m)\alpha_j(T_m)} \cdot (1 - k_{ij})}{\frac{T^2{}_{cm}}{P_{cm}}}$$

$$\alpha_i(T_m) = \left[1 + m_i\left(1 - \left(\frac{T_m}{T_{ci}}\right)^{0.5}\right)\right]^2$$

$$m_i = 0.37464 + 1.54226 \cdot \omega_i - 0.26992 \cdot \omega^2{}_i$$

- Compare calculated saturation pressure with the experimental if there is not a match adjust the acentric factor of the heaviest MCN, MCN2.

11. Match volumetric data by regressing on the molar volume shift parameters of all components in the grouped composition.

NOMENCLATURE

API	=	liquid gravity in ºAPI
b_i	=	coefficient for component i in PREOS
c_i	=	volume shift parameter
C	=	constant defined in **Eq. 30**
CN	=	carbon number
f	=	frequency of occurrence
K	=	Watson characterization factor
m	=	total number of components in multiple carbon number
m	=	constant in PREOS calculated in **Eq. 25 and 28**
M	=	molecular weight
M_i	=	molecular weight for component i
$M_{i+1/2}$	=	average Molecular weight of component i and proceeding component i+1
$M_{i-1/2}$	=	average Molecular weight of component i and previous component i-1
M_{cn+}	=	molecular weight for plus fraction, C_n^+
M_a	=	apparent (average) molecular weight
N	=	total number of components after grouping
n_e	=	total number of extended components
n_g	=	number of components in a pseudocomponent
n_o	=	total number of components of the original fluid composition
n_s	=	total number of components after splitting plus fraction
n	=	first SCN in plus fraction
P( )	=	probability density function
p_c	=	critical pressure
p_{cm}	=	critical pressure for mixture
p_{sat}	=	saturation pressure
s_i	=	dimensionless shift parameter for component i

T_b = normal boiling point temperature

T_c = critical temperature

T_{cm} = critical temperature for mixture

T_m = constant defined in **Eq. 25**

w_i = weight fraction for component i

v_L = liquid volume

v_V = vapor volume

z_i = mole fraction for component i

z_{iexp} = experimental mole fraction for component i

z_{icalc} = calculated mole fraction for component i

Z = constant defined for heaviest MCN **Eq. 32**

Greek

α, β, η = parameters used in gamma distribution function

$\alpha_i( )$ = temperature-dependent EOS parameter for component i

γ = specific gravity @ 60 ºF and 60 psia

$\acute{\Gamma}$ = gamma function

ω = acentric factor

ξ = constant defined in **Eq. 65**

ψ_b = dimensionless correction factor

Subscripts

n^+ = plus fraction starting with SCN C_n

plus = plus (heavy) fraction of the fluid composition

o = original fluid composition

s = splitting composition

b_i = normal boiling point temperature

MCN = multiple carbon number
m = mixture of SCN
sat = saturation
Res = reservoir
calc. = calculated
exp. = experimental

Abbreviation

SCN = single Carbon Number
MCN = multiple carbon number
PREOS= Peng-Robinson Equation-of-state
CCE = constant composition expansion laboratory experiment
CVD = constant volume depletion laboratory experiment
DL = differential liberation experiment
EOS = equation-of-state
PVT = pressure-volume-temperature

REFERENCES

1. Aguilar, R. A. and McCain, W. D., Jr.: "An Efficient Tuning Strategy to Calibrate Cubic EOS for Compositional Simulation," paper SPE 77382, presented at the SPE Annual Technical Conference and Exhibition, San Antonio, 29 September – 2 October 2002.
2. Katz, D. L. and Firoozabadi, A.: "Prediction Phase Behavior of Condensate/Crude-Oil System Using Methane Interaction Coefficients," paper SPE 6721, presented at the SPE-AIME 52nd Annual Fall Technical Conference and Exhibition, Denver, 9-12 October, 1977.
3. Ahmed, T., Cady, G. V., and Story, A. L.: "A Generalized Correlation for Characterizing the Hydrocarbon Heavy Fraction," paper SPE 14266 presented at the 60th Annual Technical Conference and Exhibition of the Society of Petroleum Engineers, Las Vegas, 22-25 September, 1985.
4. Behrens, R. A., and Sandler, S. I.: "The Use of Semicontinuous Description to Model the C_7^+ Fraction in Equation of State Calculations," paper SPE 14925 presented at the SPE /DOE 5th Symposium on Enhance Oil Recovery, Tulsa, 20-23 April, 1986.
5. Whitson, C. H.: "Critical Properties Estimation from an Equation of State," paper SPE 12634 presented at the SPE/DOE 4th Symposium on Enhance Oil Recovery, Tulsa, 15-18 April, 1984.
6. Whitson, C. H.: "Effect of Physical Properties Estimation on Equation-of-State Predictions," paper SPE 11200 presented at the 57th Annual Fall Technical Conference and Exhibition, New Orleans, 26-29 September, 1982.
7. Pedersen, K. S., Thomassen, P., and Fredenslund, A.: *Properties of Oils and Natural Gases, Contributions in Petroleum Geology and Engineering*, Vol. 5, Gulf Publishing Co., Houston (1989).
8. Coats, K. H.: "Simulation of Gas Condensate Reservoir Performance," paper SPE 10512 presented at the 1982 SPE Reservoir Simulation Symposium, New Orleans, 31 January- 3 February.

9. Ahmed, T., Cady, G. V., and Story, A. L.: "An Accurate Method for Extending the Analysis of C_7^+," paper SPE 12916 presented at the 1984 Rocky Mountain Regional Meeting, Casper, Wyoming 21-23 May.
10. Danesh, A.: *PVT and Phase Behavior of Petroleum Reservoir Fluid*, Elsevier, Amsterdam (1998).
11. Whitson, C. H.: "Characterizing Hydrocarbon Plus Fractions," paper SPE 12233 presented at the 1980 European Offshore Petroleum Conference and Exhibition, London, 21-24 October.
12. Guo, T. M., and Du L.: "A New Three Parameter Cubic Equation of State for Reservoir Fluids – Part II. Application to Reservoir Crude Oils," paper SPE 19373 available from SPE, Richardson, TX.
13. Zuo, J. Y. and Zhang D.: "Plus Fraction Characterization and PVT Data Regression for Reservoir Fluids near Critical Conditions," paper SPE 64520 presented at the 2000 SPE Asia Pacific Oil and Gas Conference and Exhibition, Brisbane, Australia, 16-18 October.
14. Katz, D. L., "Overview of Phase Behavior of Oil and Gas Production," *JPT* (June 1983) **228**, 1205-1214.
15. Ahmed, T.: *Hydrocarbon Phase Behavior*, Gulf Publishing Company, Houston (1989).
16. Cavett, R. H.: "Physical Data for Distillation Calculations- Vapor-Liquid Equilibrium," *Proc.* 27th Annual Meeting, American Petroleum Institute, Dallas (1962) 351-66.
17. Edmister, W. C.: "Applied Hydrocarbon Thermodynamics, Part 4: Compressibility Factors and Equations of State," *Pet. Refiner* (1958) **37**, 173-175.
18. Kesler, M. G., and Lee, B. I.: "Improve Prediction of Enthalpy of Fractions," *Hydro. Proc.* (March 1976), **55**, 153-158.
19. Riazi, M. R., and Daubert, T. E.: "Simplify Property Predictions," *Hydro. Proc.* (March 1980) **23**, 115-116.

20. Twu, C. H.: "An Internally Consistent for Predicting the Critical Properties and Molecular Weights of Petroleum and Coal-Tar Liquids," *Fluid Phase Equilibria*, (1984) **16**, 137-150.
21. Riazi, M. R., and Al-Sahhaf, T. A.: "Physical Properties of Heavy Petroleum Fractions and Crude Oils," *Fluid Phase Equilibria* (1996) **117**, 217-224.
22. Avaullee, L., Trassy, E., Neau, E., and Jaubert, J. N.: "Thermodynamic of State and Group Contribution for the Estimation of Thermodynamic Parameters of Heavy Hydrocarbons," *Fluid Phase Equilibria* (1997) **139**, 155-170.
23. Arbabi, S., and Firoozabadi, A.: "Near-Critical Phase Behavior of Reservoir Fluids Using Equation of State," paper SPE 24491, SPE Advanced Technology Series, (1995) **3** No. 1.
24. Pedersen, K. S., Thomassen, P., and Fredenslund, A.: "Characterization of Gas Condensate Mixtures," presented at the 1988 AIChE Spring National Meeting, New Orleans, 6-10 March.
25. Guo, T. M., and Du L.: "A New Three Parameter Cubic Equation of State for Reservoir Fluids – Part III. Application to Gas Condensates," paper SPE 19374 available from SPE, Richardson, TX.
26. Danesh, A., Xu, D., and Todd, A. C.: "A Grouping Method to Optimize Oil Description for Compositional Simulation of Gas-Injection Processes," paper SPE 20745 presented at the 1990 SPE Annual Technical Conference and Exhibition, New Orleans, 23-26 September.
27. Pedersen, K. S., Thomassen, P., and Fredenslund, A.: "Thermodynamics of Petroleum Mixtures Containing Heavy Hydrocarbons. I. Phase Envelope Calculations by Use of the Soave-Redlich-Kwong Equation of Sate," *Ind. Eng. Chem. Process Des. Dev.* (1984) **23**, 163-170.
28. Neau, E., and Jaubert, J. N.: "Characterization of Heavy Oils," *Ind. Eng. Chem. Res.* (1993) **32**, 1196-1203.

29. Hong, K. C.: "Lumped-Component Characterization of Crude Oils Compositional Simulation," paper SPE 10691 presented at the 1982 SPE/DOE Third joint Symposium on EOR, Tulsa, 4-7 April.
30. Leibovici, C. F., Govel. P. L., and Placentino, T.: "A Consistent Procedure for the Estimation of Pseudo-Component," paper SPE 2611 presented at the 68th Annual Technical Conference and Exhibition of the Society of Petroleum Engineers, Houston, 3-6 October, 1993.
31. Leibovici, C. F.: "A Consistent Procedure for the Estimation of Properties Associated to Lumped Systems," *Fluid Phase Equilibria* (1993) **87**, 189-197.
32. Twu, C. H., and Coon, J. E.: "An Internally Consistent Approach for Determining the Properties of Lumped Components Using a Cubic Equation of State," *Fluid Phase Equilibria* (1996) **117**, 233-240.
33. McCain, W. D., Jr.: *The Properties of Petroleum Fluids*, 2nd ed., PennWell Books, Tulsa, (1990).
34. Pedersen, K. S., Thomassen, P., and Fredenslund, A.: "On the Dangers of 'Tuning' Equation of State Parameters," paper SPE 14487, available from SPE, Richardson, TX.
35. Liu, K.: "Fully Automatic Procedure for Efficient Reservoir Fluid Characterization," paper SPE 56744 presented at the 1999 SPE Annual Technical Conference and Exhibition, Houston, 3-6 October.
36. Thomassen, P., Pedersen, K. S., and Fredenslund, A.: "Adjustment of C_7^+ Molecular Weights in the Characterization of Petroleum Mixtures Containing Heavy Hydrocarbons," paper SPE 16036 available from SPE, Richardson, TX.
37. Guo, T. M., and Du L.: "A New Three Parameter Cubic Equation of State for Reservoir Fluids – I. Development of the Thermodynamic Model," paper SPE 19372 available from SPE, Richardson, TX.
38. Wang, P.: "Prediction of Phase Behavior for Gas Condensate," paper SPE 19503 available from SPE, Richardson, TX.

39. Peneloux, A. and Rauzy, E.: "A Consistent Correction for Redlich-Kwong-Sovae Volumes," *Fluid Phase Equilibria*, (1982), **8**, 7-23.
40. Jhaveri, B. S. and Youngren, G. K.: "Three-parameter Modification of the Peng-Robinson Equation of State to Improve Volumetric Predictions," paper SPE 13118 presented at the 1984 SPE Annual Technical Conference and Exhibition, Houston, 16-19 September.
41. Abrishami, Y. and Hatamian, H.: "The Accuracy of Cubic Equations of State for Composition Predictions," paper SPE 36245 presented at the 7th Abu Dhabi International Petroleum Exhibition and Conference, Abu Dhabi, U. A. E. 13-16 October 1996.
42. Chorn, L. G., and Mansoori, G. A.: *Advanced in Thermodynamics Volume 1: C_7^+ Fraction Characterization*, Taylor & Francis, New York (1989).
43. Winn, F. W., "Physical Properties by Nomogram," *Pet. Refiner*, (1957) **36**, 157-159.
44. Whitson, C. H. and Brule, M. R.: *Phase Behavior*, First Edition, Monograph Vol. 20 SPE Henry L. Doherty Series, Richardson, Texas (2000).

Supplemental Resources

Ahmed, T.: "A Practical Equation-of-State," paper SPE 18532 presented at the 1988 Eastern Regional Meeting held in Charleston, NC, 1-4 November.

Coats, K. H. and Smart G. T.: "Application of a Regression-Based EOS PVT Program to Laboratory Data," paper SPE 11197 presented at the 1982 Annual Fall Technical Conference and Exhibition, held in New Orleans, 26-29 September.

Gary, R. D, JR., Heidman, J. L., Springer, R. D. and Tsonopoulos, C.: "Characterization and Property Prediction for Heavy Petroleum and Synthetic Liquids," *Fluid Phase Equilibria* (1989) **53**, 355-376.

Merrill, R. C., Hartman, K. J. and Creek, J. L.: "A Comparison of Equation of State Tuning Method," paper SPE 28586 presented at the 69th Annual Technical Conference and Exhibition, New Orleans, 25-28 September, 1994.

Montel, F., and Gouel, P. L.: "A New Lumping Scheme of Analytical Data for Compositional Studies," paper SPE 13119 presented at the 59th Annual Technical Conference and Exhibition, Houston, 16-19 September, 1984.

Peng, D. Y., and Robinson, D. B.: "A New Two-Constant Equation of State," *Ind. Eng. Chem. Fundam.*, (1976), **15**, No. 1, 59-64.

Shariati, A., Peters, C., and Moshfeghian, M.: "A Systematic Approach to Characterize Gas Condensates and Light Petroleum Fraction," *Fluid Phase Equilibria* (1999) **154**, 165-179.

Slot-Petersen, C.: "A Systematic and Consistent Approach to Determine Binary Interaction Coefficients for the Peng-Robinson Equation of State," paper SPE 16941 presented at the 62nd Annual Technical Conference and Exhibition, Dallas, 27-30 September, 1987.

APPENDIX A

DERIVATION OF EQUATION 83 AND 84

Eqs. 83 and **84** are solved iteratively to calculate the critical properties of mixtures. This method introduced by Leibovici[38] which is based on the mixing rules of the cubic EOS to calculate critical properties of mixtures.

The parameters of a and b for Peng-Robinson EOS are calculated with the following equation:

$$a = \sum_{i=1}^{n}\sum_{j=1}^{n} z_i z_j (a_i a_j)^{\frac{1}{2}}(1-k_{ij}) \quad \text{(A-1)}$$

$$b = \sum_{i=1}^{n} z_i b_i \quad \text{(A-2)}$$

Where

$$a_i = a_{ci} \cdot \alpha_i \quad \text{(A-3)}$$

$$a_{ci} = 0.45724 \frac{R^2 \cdot T_{ci}^2}{P_{ci}} \quad \text{(A-4)}$$

$$\alpha_i(T) = \left[1 + m_i\left(1 - \left(\frac{T}{T_{ci}}\right)\right)\right]^2 \quad \text{(A-5)}$$

$$m_i = 0.37464 + 1.5422 \cdot \omega_i - 0.26992 \cdot \omega_i^2 \quad \text{(A-6)}$$

$$b_i = 0.07780 \frac{R \cdot T_{ci}}{P_{ci}} \quad \text{(A-7)}$$

According to Leibovici[38], a_{cm} is equal to the mixing parameter *a* of the m components present in the mixture. That is mean $a=a_{cm}$, where a_{cm} can be written as follows:

$$a_{cm} = 0.45724 \frac{R^2 T_{cm}^2}{P_{cm}} \quad \text{(A-8)}$$

By equating **Eq. A-8** and **A-1**, we can solve for T_{cm}: as shown below:

$$0.45724 \frac{R^2 T_{cm}^2}{P_{cm}} = \sum_{i=1}^{m} \sum_{j=1}^{m} z_i z_j (a_i a_j)^{\frac{1}{2}} (1 - k_{ij}) \quad \text{(A-9)}$$

Substituting **Eq. A-3** into **Eq. A-9**:

$$0.45724 \frac{R^2 T_{cm}^2}{P_{cm}} = \sum_{i=1}^{m} \sum_{j=1}^{m} z_i z_j \left(a_{ci} a_{cj} \alpha_i(T_{cm}) \alpha_j(T_{cm})\right)^{\frac{1}{2}} (1 - k_{ij}) \quad \text{(A-10)}$$

Substituting **Eq. A-4** into **Eq. A-10**:

$$0.45724 \frac{R^2 T_{cm}^2}{P_{cm}} = \sum_{i=1}^{m} \sum_{j=1}^{m} z_i z_j \left(0.45724 \frac{R^2 \cdot T_{ci}^2}{P_{ci}} 0.45724 \frac{R^2 \cdot T_{cj}^2}{P_{cj}} \alpha_i(T_{cm}) \alpha_j(T_{cm}) \right)^{\frac{1}{2}} (1 - k_{ij}) \quad \text{(A-11)}$$

$$0.45724 \frac{R^2 T_{cm}^2}{P_{cm}} = 0.45724 R^2 \sum_{i=1}^{m} \sum_{j=1}^{m} z_i z_j \frac{T_{ci} T_{cj}}{\sqrt{P_{ci} P_{cj}}} \left(\alpha_i(T_{cm}) \alpha_j(T_{cm})\right)^{\frac{1}{2}} (1 - k_{ij}) \quad \text{(A-12)}$$

Simplifying **Eq. A-12**:

$$\frac{T_{cm}^{2}}{P_{cm}} = \sum_{i=1}^{m}\sum_{j=1}^{m} z_i z_j \frac{T_{ci}T_{cj}}{\sqrt{P_{ci}P_{cj}}}\left(\alpha_i(T_{cm})\alpha_j(T_{cm})\right)^{\frac{1}{2}}(1-k_{ij}) \quad \text{(A-13)}$$

For α (T_{cm}) in **Eq. A-13**

$$\alpha_i(T_{cm}) = \left[1 + m_i\left(1 - \left(\frac{T_{cm}}{T_{ci}}\right)\right)\right]^2 \quad \text{(A-14)}$$

The second parameter in Peng-Robinson EOS for mixture can be written as follows:

$$b_m = 0.07780\frac{R \cdot T_{cm}}{P_{cm}} \quad \text{(A-15)}$$

Equating **Eq. A-2** and **A-15**:

$$0.07780\frac{R \cdot T_{cm}}{P_{cm}} = \sum_{i=1}^{n} z_i b_i \quad \text{(A-16)}$$

Substituting **Eq. A-7** into **Eq. A-16**:

$$0.07780\frac{R \cdot T_{cm}}{P_{cm}} = \sum_{i=1}^{m} z_i\, 0.07780\frac{R \cdot T_{ci}}{P_{ci}} \quad \text{(A-17)}$$

Simplifying **Eq. A-17**:

$$\frac{T_{cm}}{P_{cm}} = \sum_{i=1}^{m} z_i \frac{T_{ci}}{P_{ci}} \quad \text{(A-18)}$$

APPENDIX B

SIMULATION RESULTS

Fluid 1 (T_{res} = 262 °F)

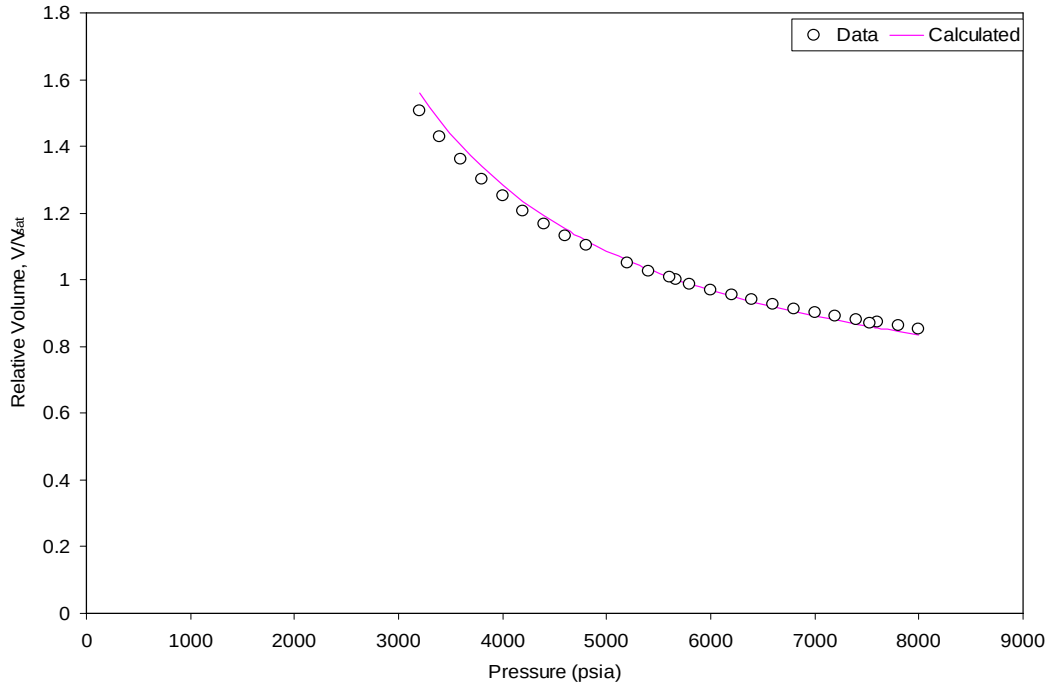

Fig. B.1- Relative volume from CCE experiment for fluid 1.

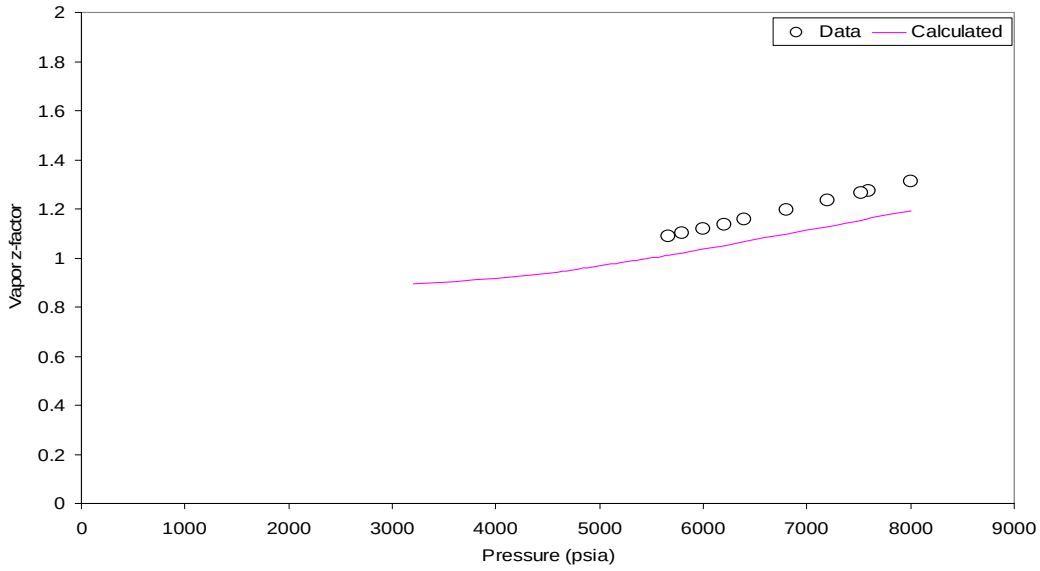

Fig. B.2- Vapor z-factor from CCE experiment for fluid 1.

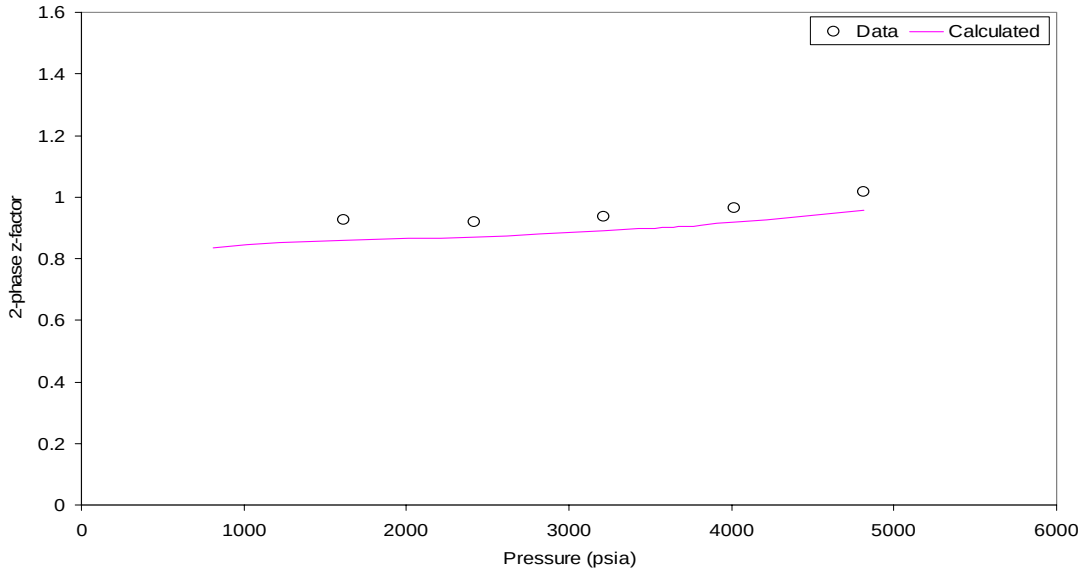

Fig. B.3- 2-phase z-factor from CVD experiment for fluid 1.

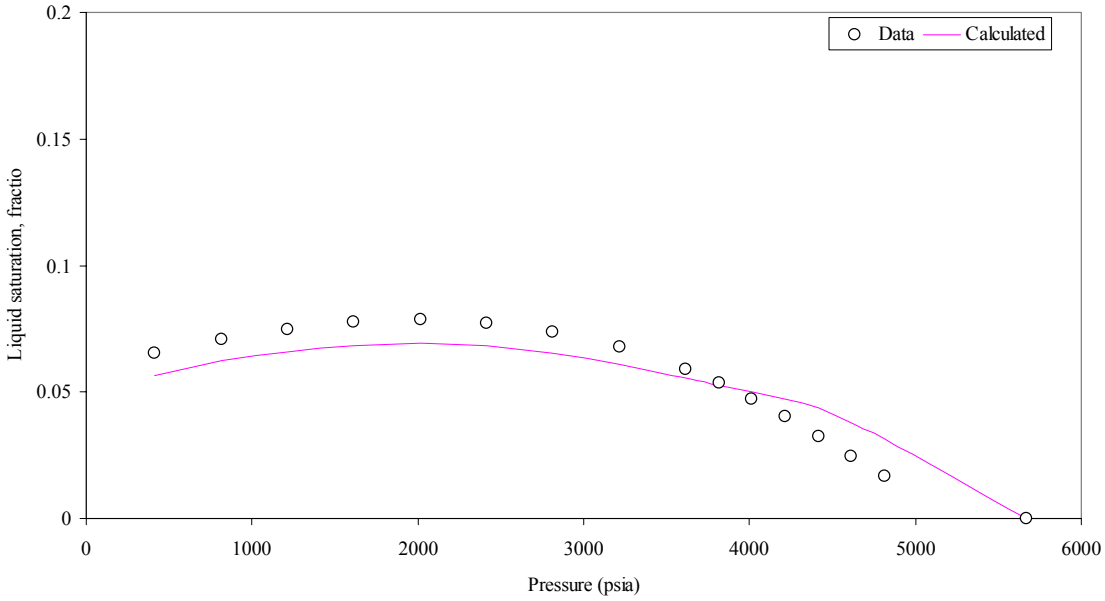

Fig. B.4- Liquid saturation from CVD experiment for fluid 1.

Fluid 2 (T_{res} = 275 °F)

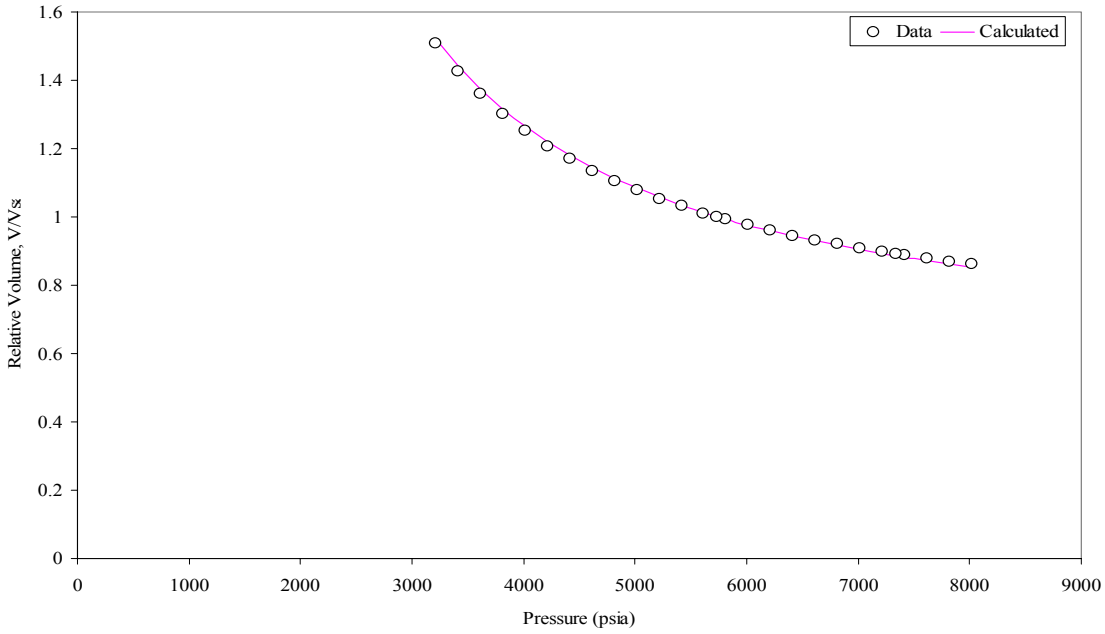

Fig. B.5- Relative volume from CCE experiment for fluid 2.

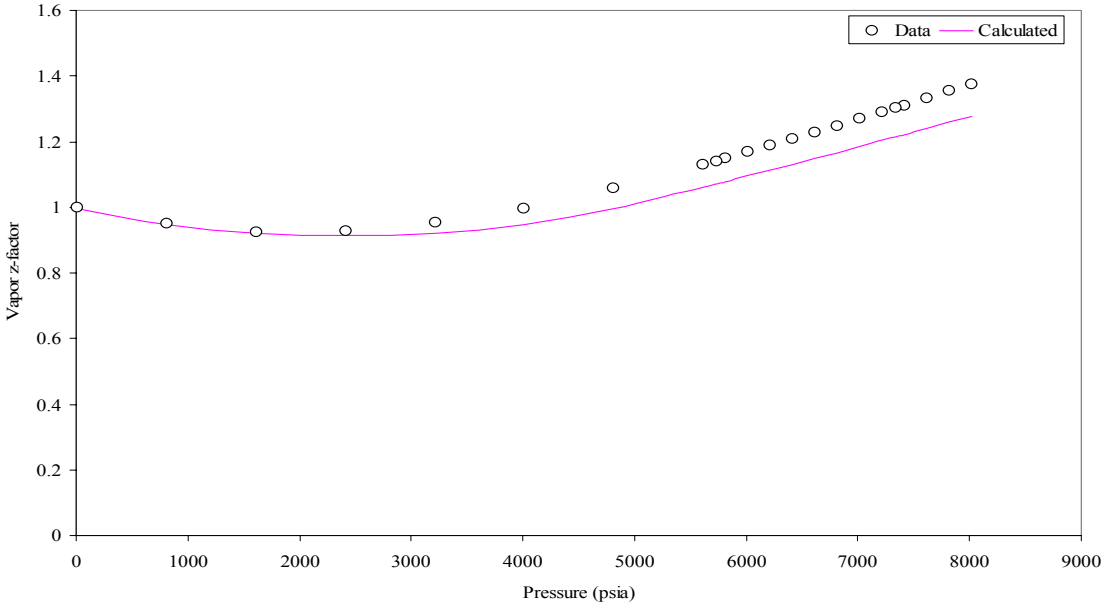

Fig. B.6- Vapor z-factor from CCE experiment for fluid 2.

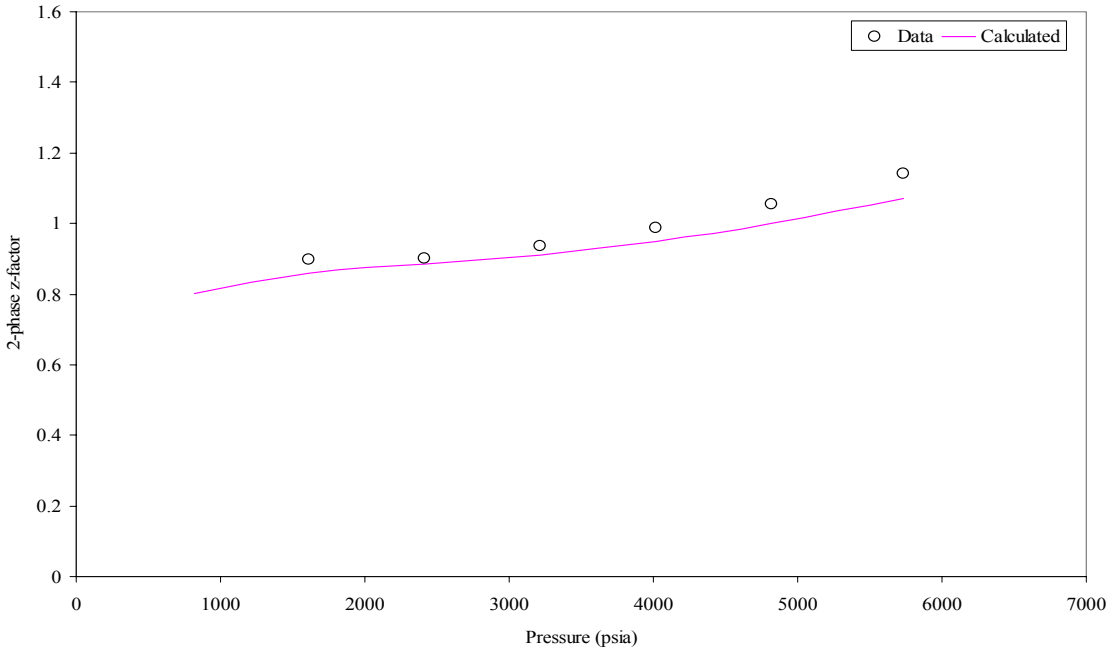

Fig. B.7- 2-phase z-factor from CVD experiment for fluid 2.

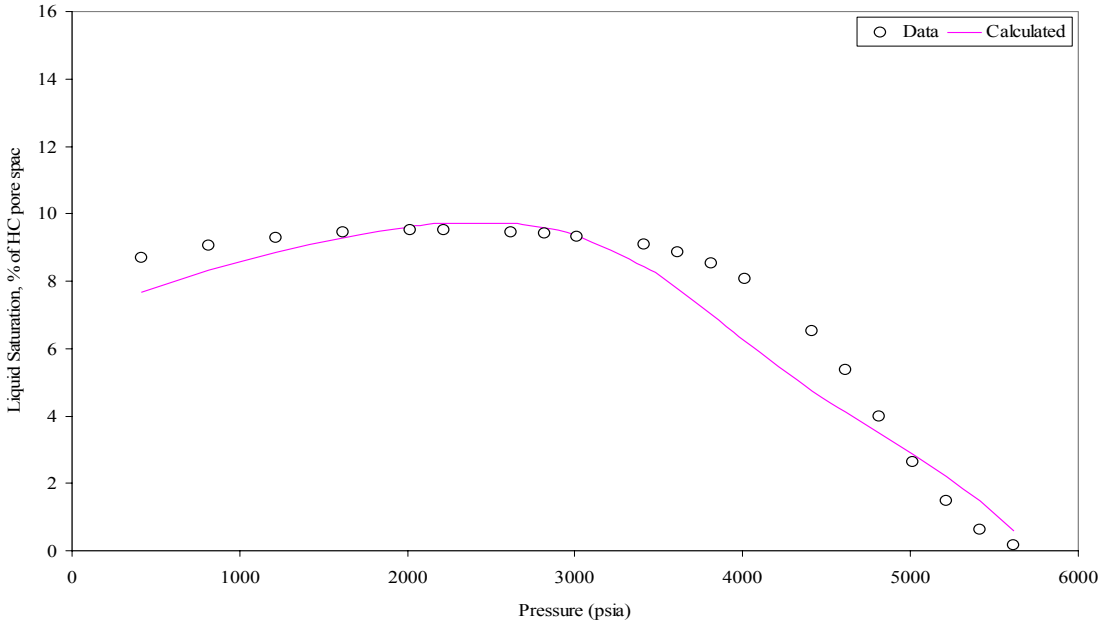

Fig. B.8- Liquid saturation from CVD experiment for fluid 2.

Fluid 3 (T_{res} = 305 °F)

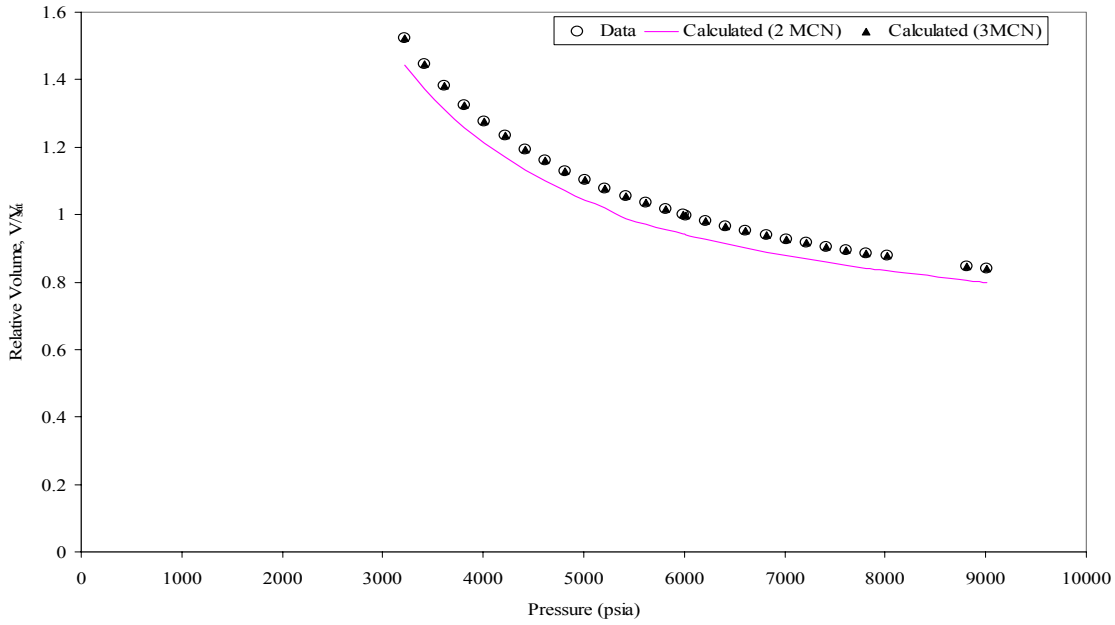

Fig. B.9- Relative volume from CCE experiment for fluid 3, grouping into two and three MCN.

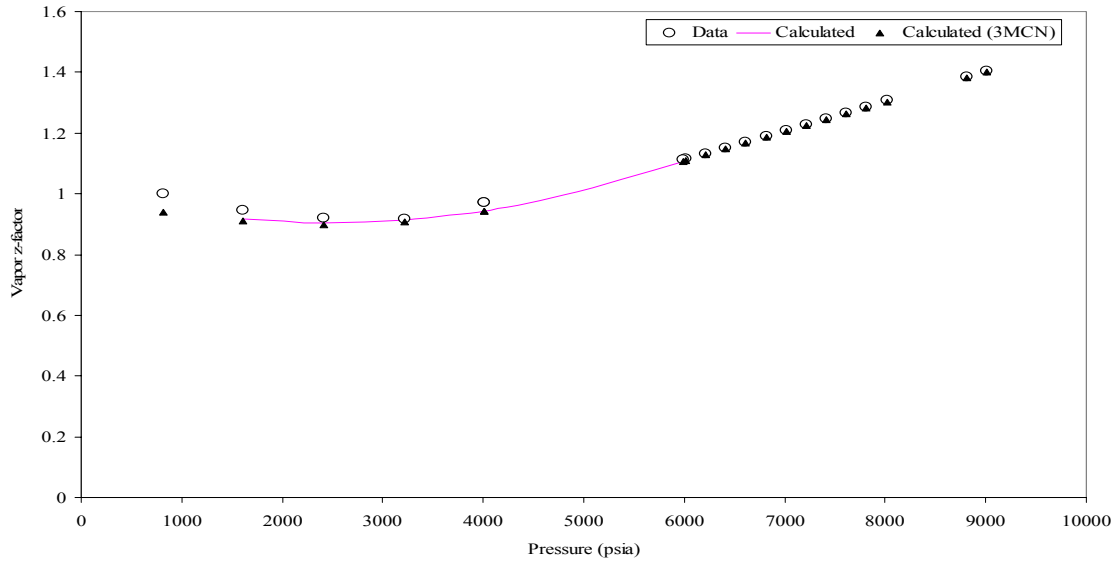

Fig. B.10- Vapor z-factor from CCE experiment for fluid 3, grouping into two and three MCN.

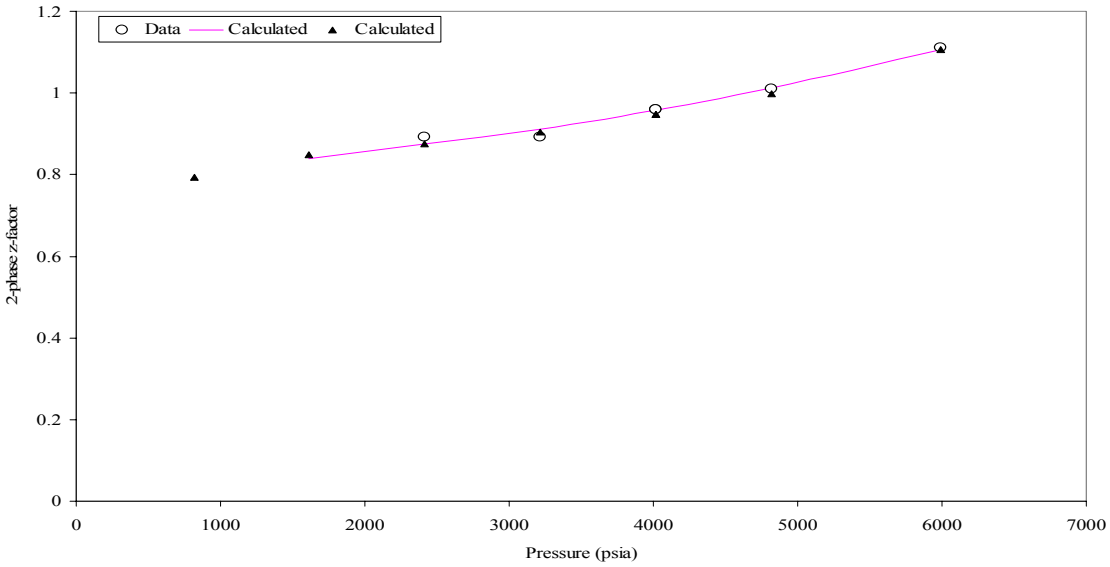

Fig. B.11- 2-phase z-factor from CVD experiment for fluid 3, grouping into two and three MCN.

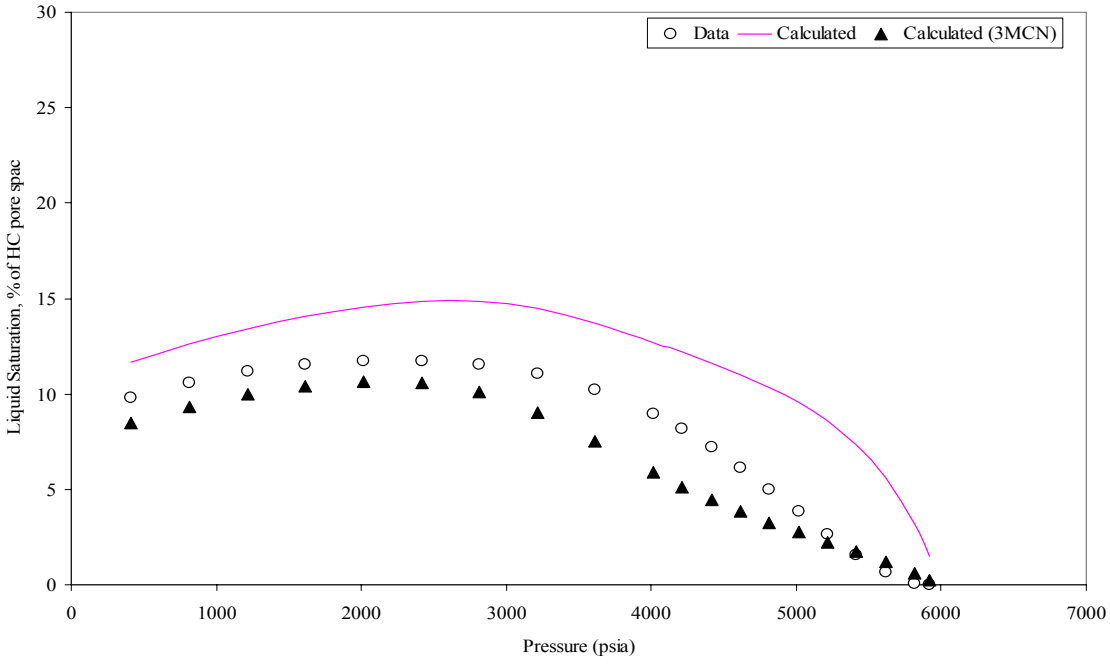

Fig. B.12- Liquid saturation from CVD experiment for fluid 3, grouping into two and three MCN.

Fluid 4 (T_{res} = 266 °F)

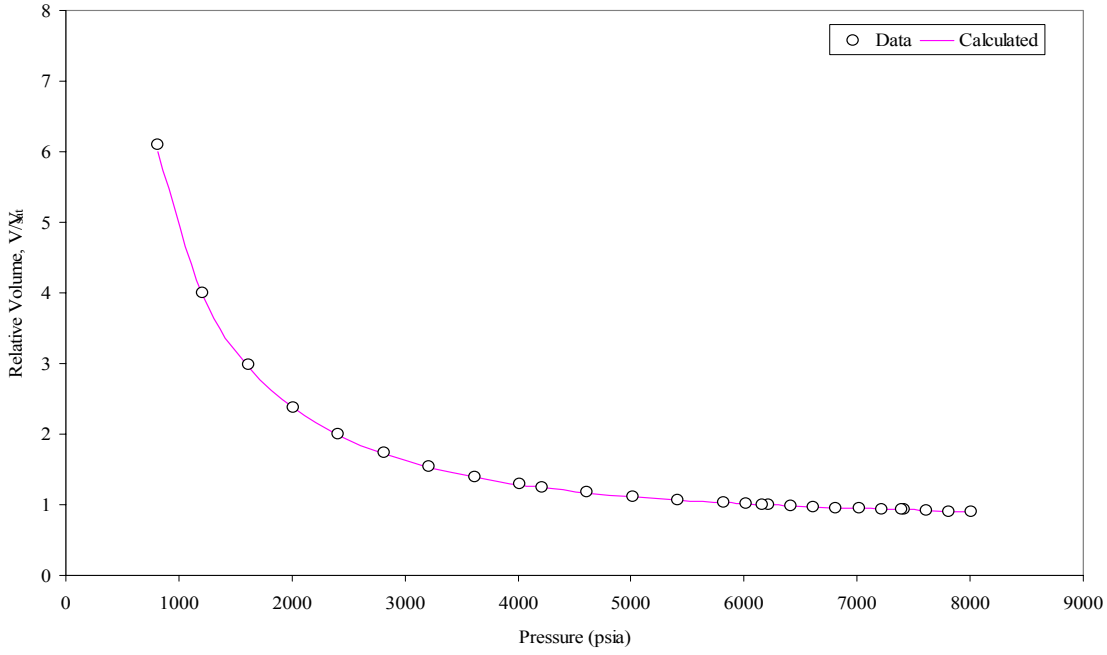

Fig. B.13- Relative volume from CCE experiment for fluid 4 at reservoir temperature.

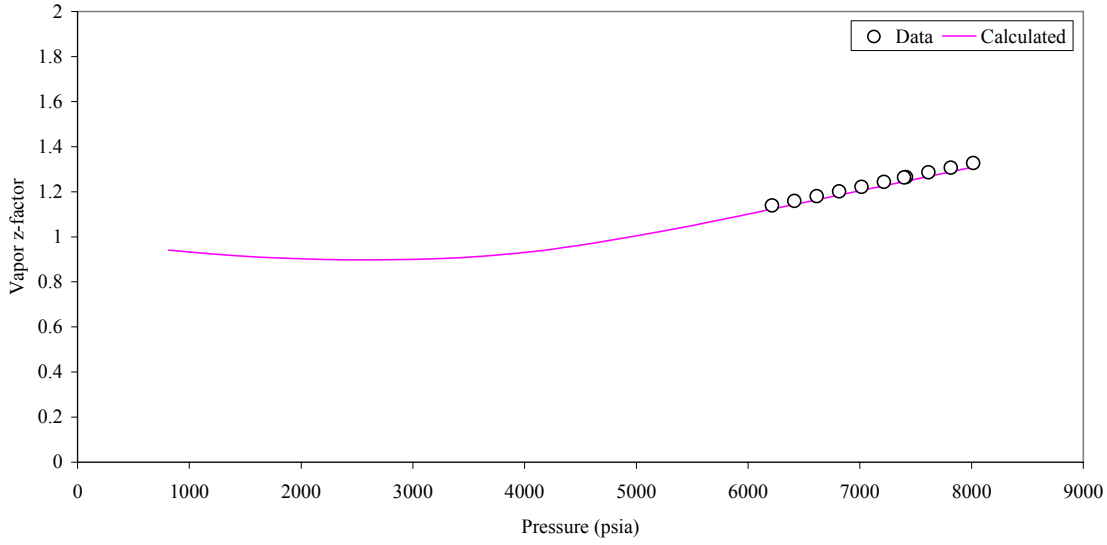

Fig. B.14- Vapor z-factor from CCE experiment for fluid 4 at reservoir temperature.

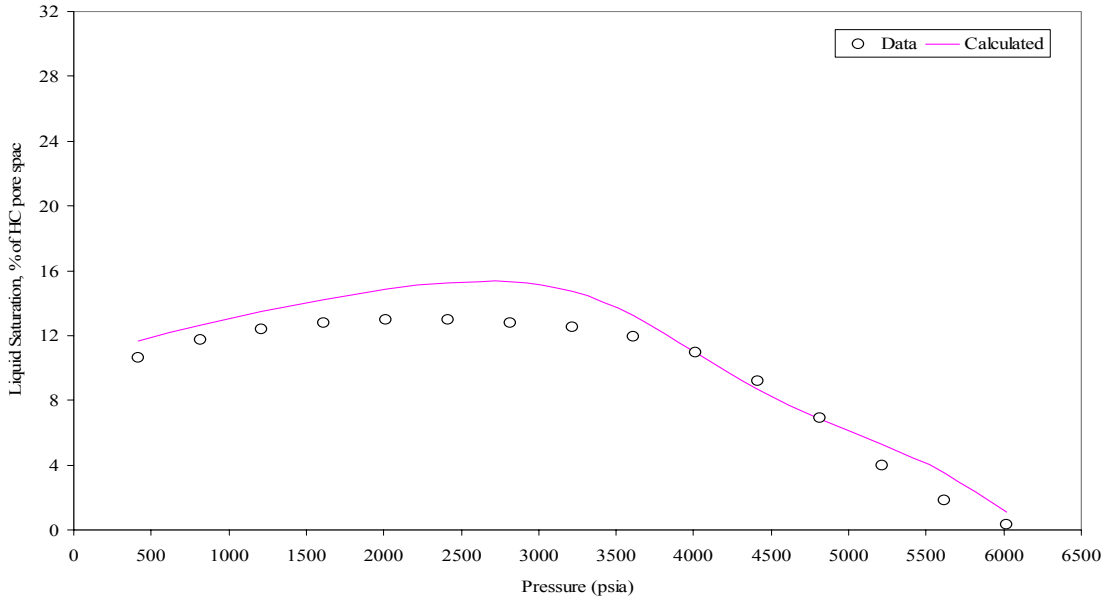

Fig. B.15- Liquid saturation from CVD experiment for fluid 4 at reservoir temperature.

Fluid 5 (T_{res} = 229 °F)

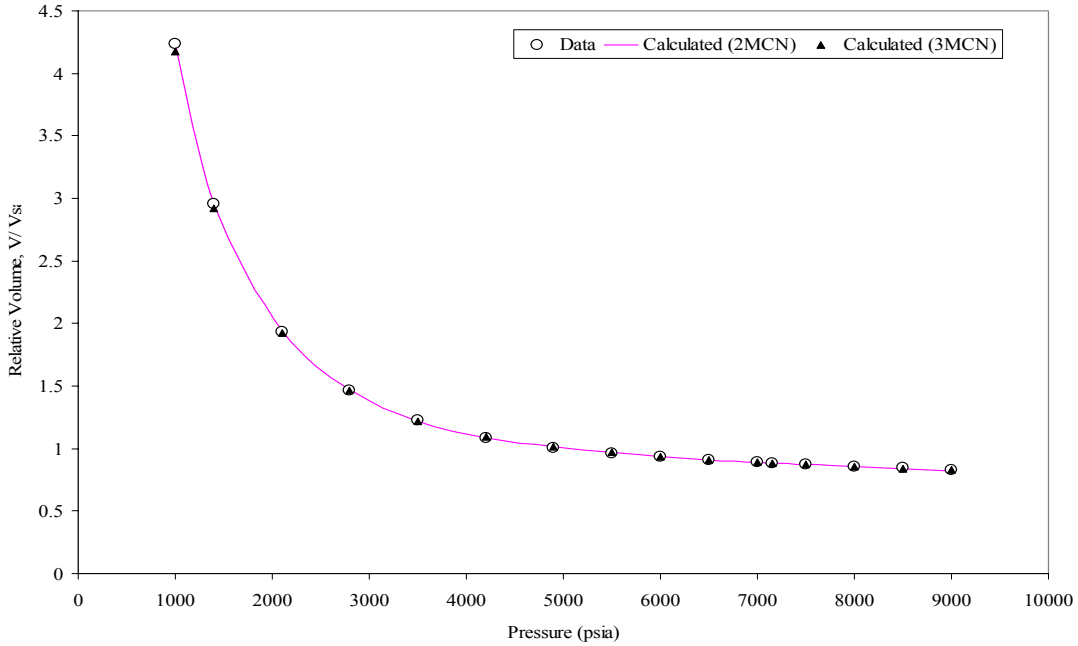

Fig. B.16- Relative volume from CCE experiment for fluid 5, grouping into two and three MCN.

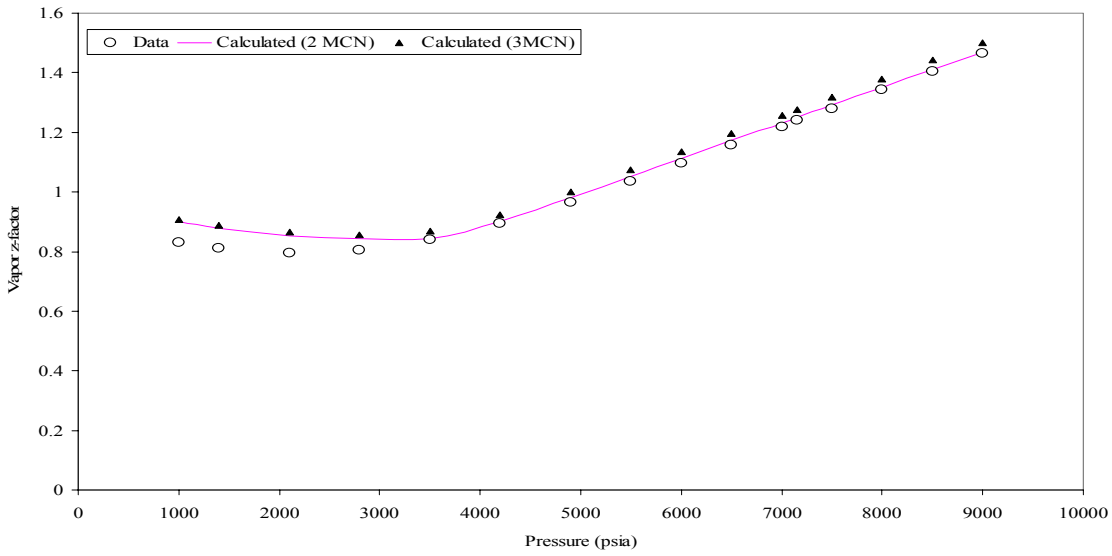

Fig. B.17- Vapor z-factor from CCE experiment for fluid 5, grouping into two and three MCN.

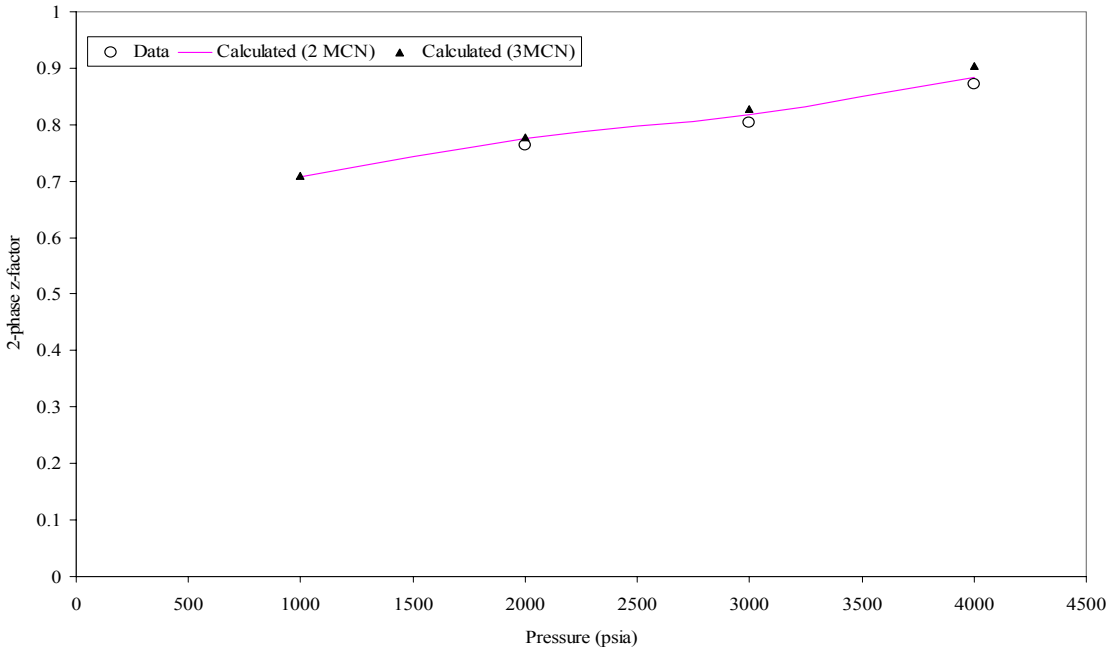

Fig. B.18- 2-phase z-factor from CVD experiment for fluid 5, grouping into two and three MCN.

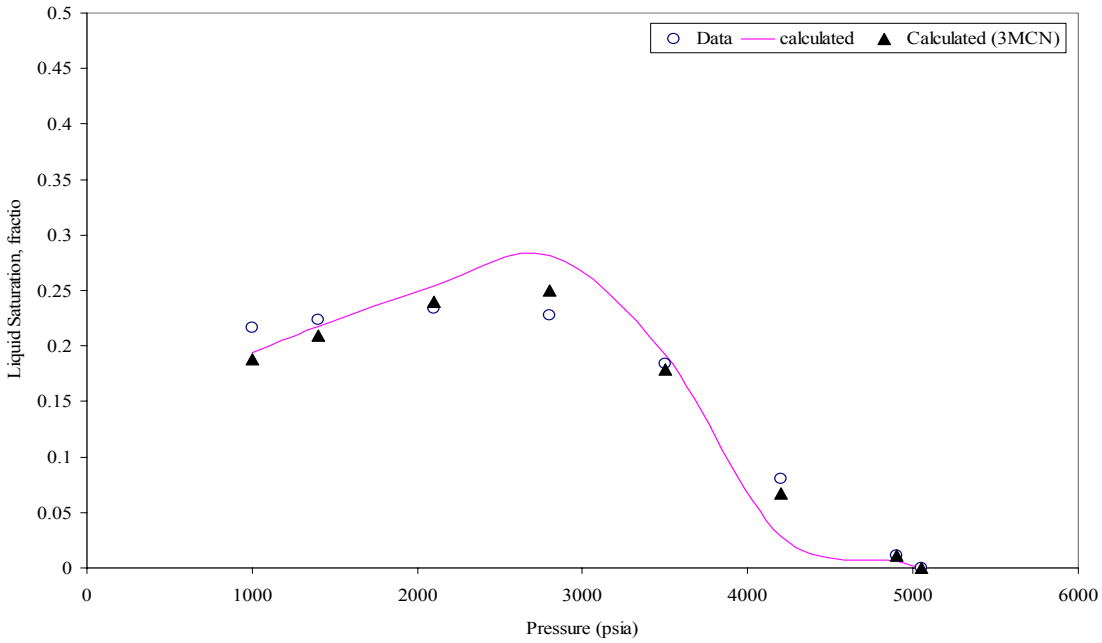

Fig. B.19- Liquid saturation from CVD experiment for fluid 5, grouping into two and three MCN.

Fluid 6 (T_{res} = 291 °F)

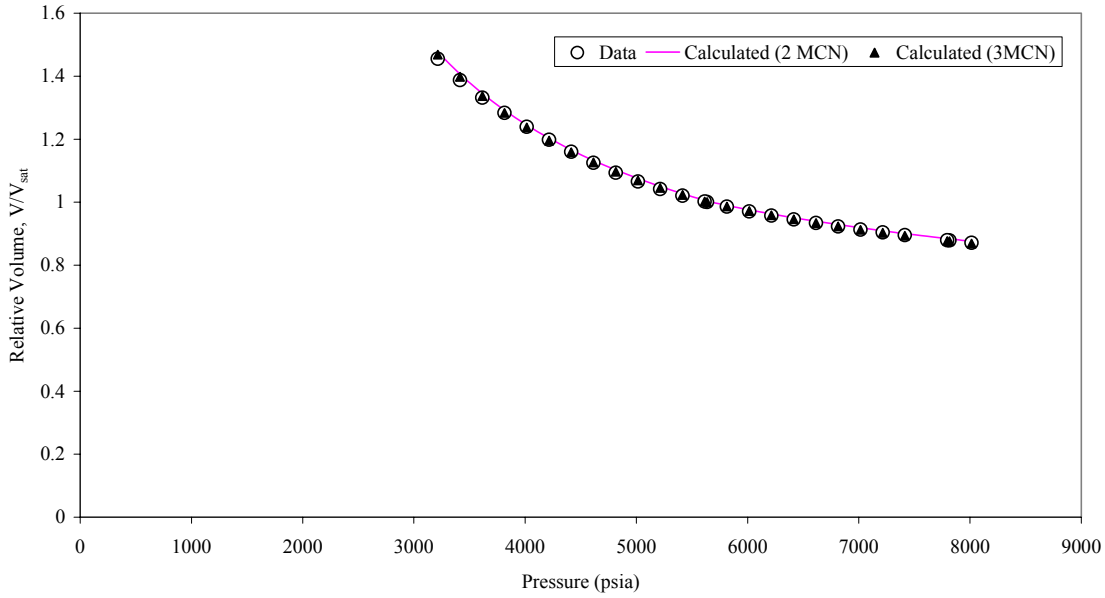

Fig. B.20- Relative volume from CCE experiment for fluid 6, grouping into two and three MCN.

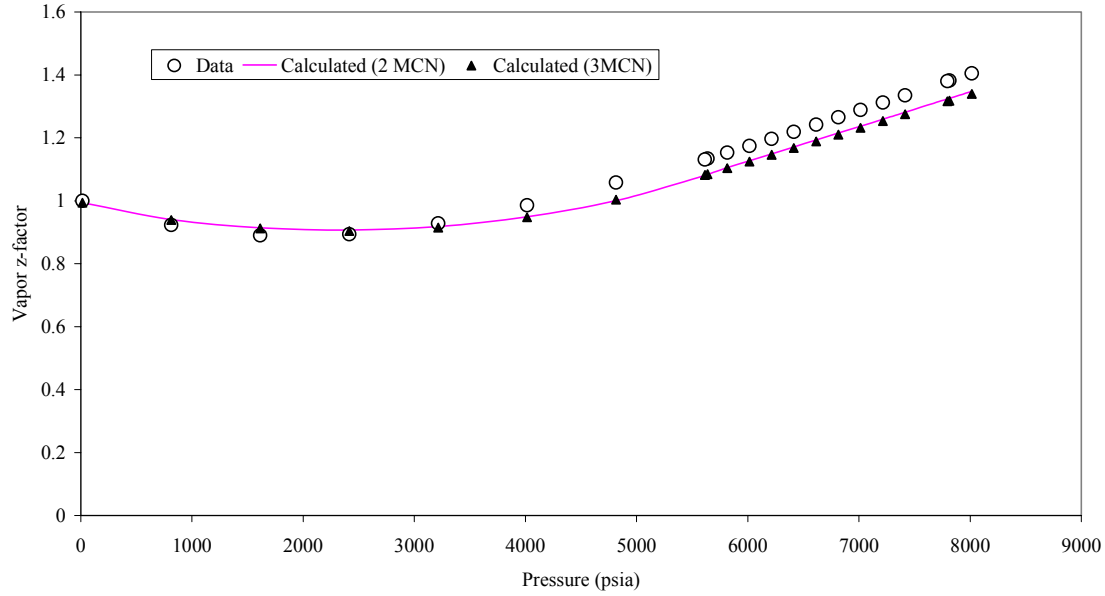

Fig. B.21- Vapor z-factor from CCE experiment for fluid 6, grouping into two and three MCN.

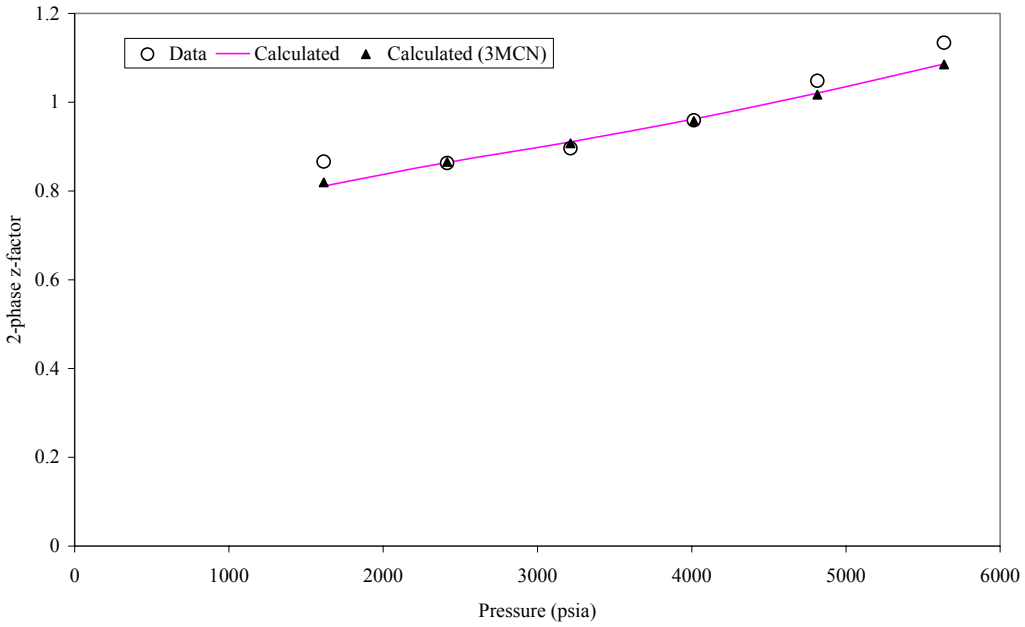

Fig. B.22- 2-phase z-factor from CVD experiment for fluid 6, grouping into two and three MCN.

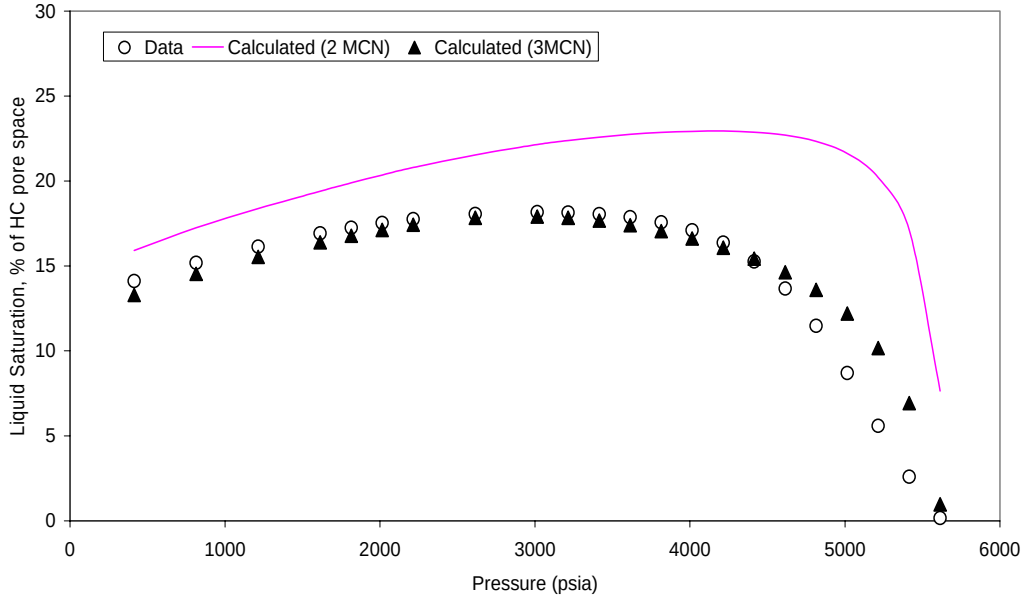

Fig. B.23- Liquid saturation from CVD experiment for fluid 6, grouping into two and three MCN.

Fluid 7 (T_{res} = 256 °F)

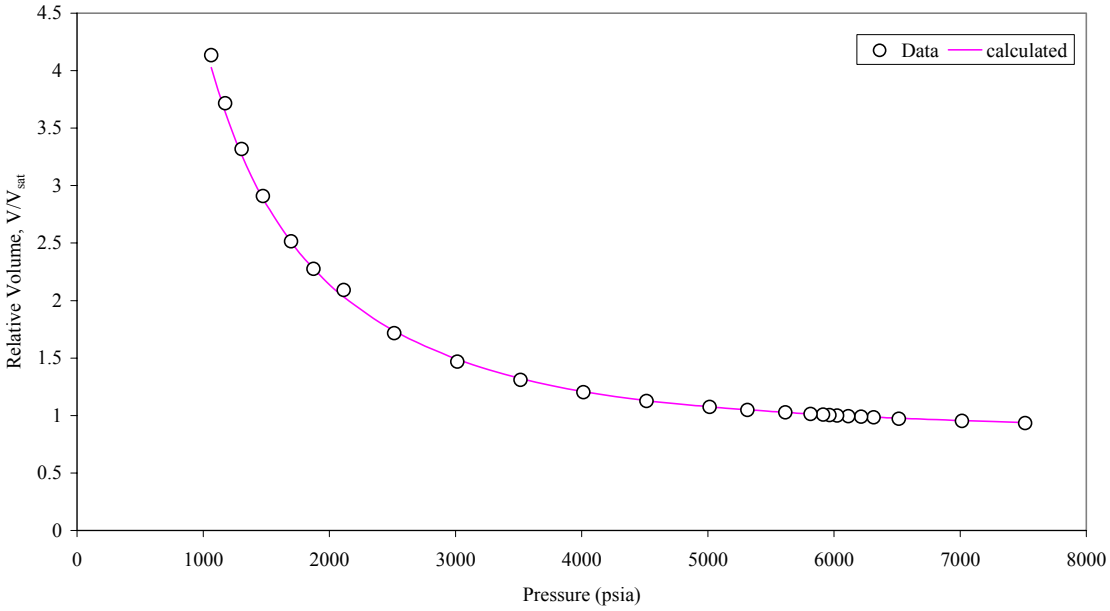

Fig. B.24- Relative volume from CCE experiment for fluid 7.

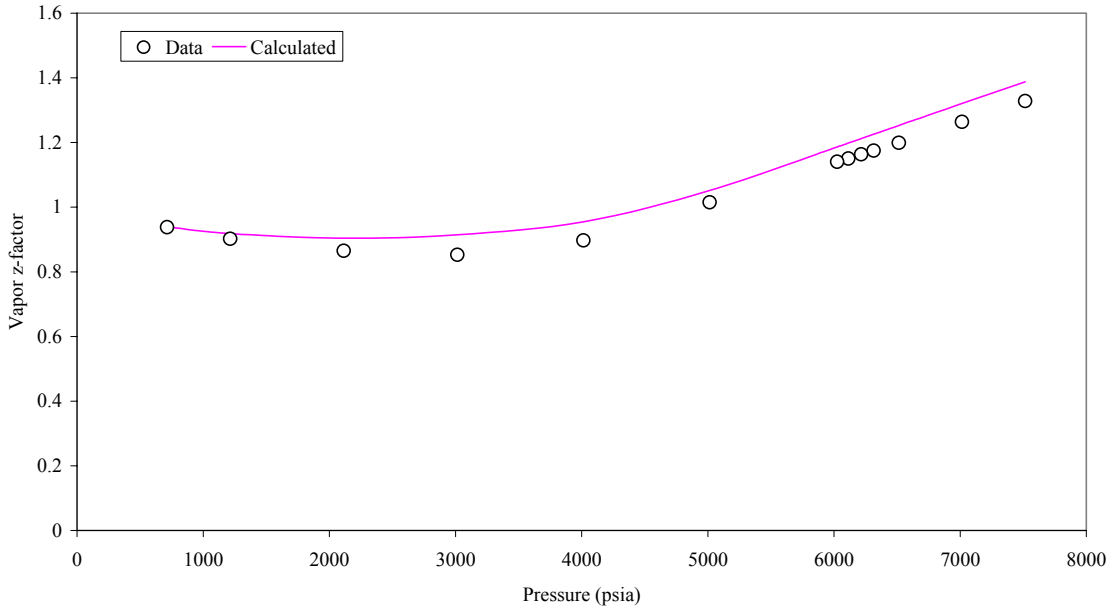

Fig. B.25- Vapor z-factor from CCE experiment for fluid 7.

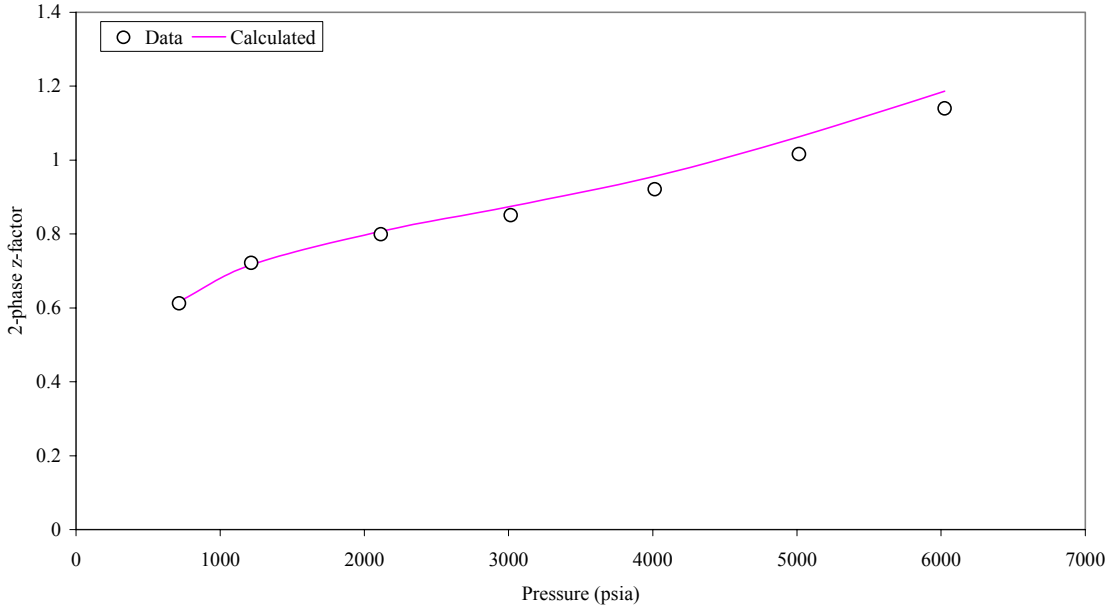

Fig. B.26- 2-phase z-factor from CVD experiment for fluid 7.

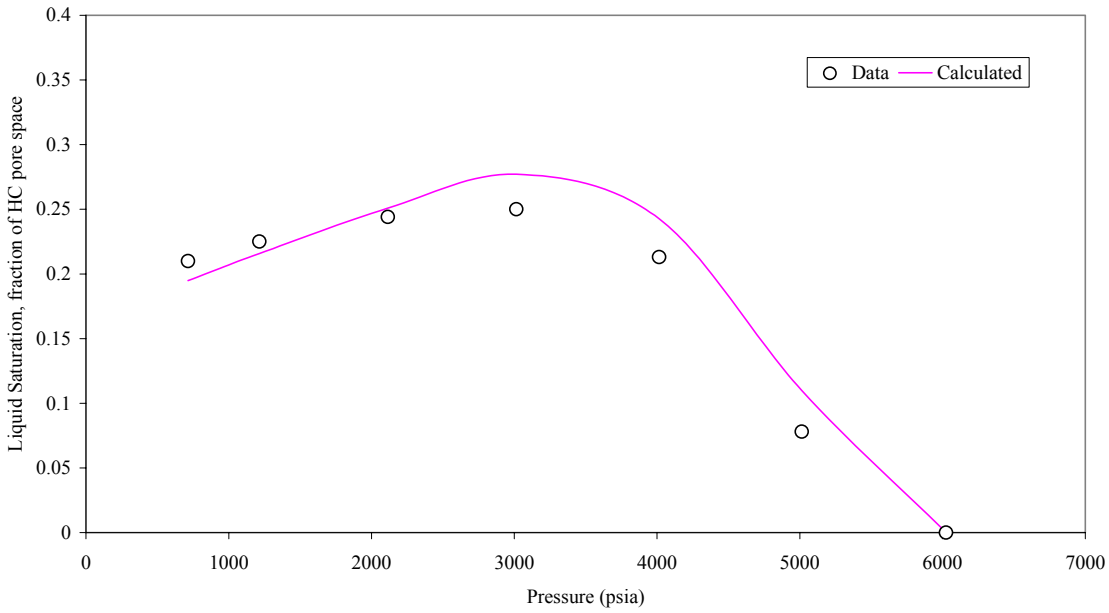

Fig. B.27- Liquid saturation from CVD experiment for fluid 7.

Fluid 8 (T_{res} = 305 °F)

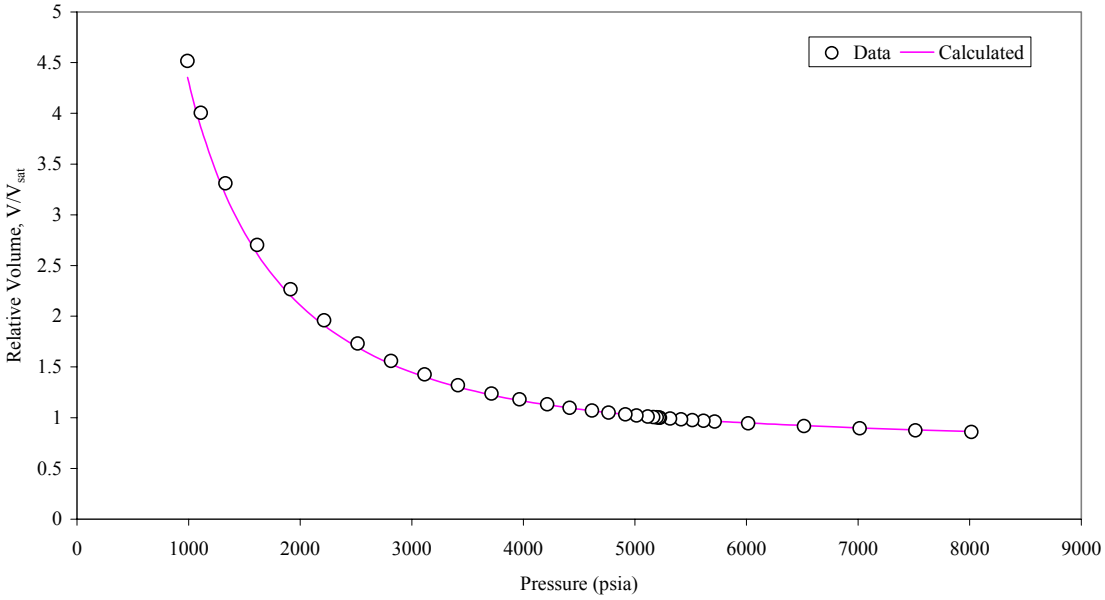

Fig. B.28- Relative volume from CCE experiment for fluid 8.

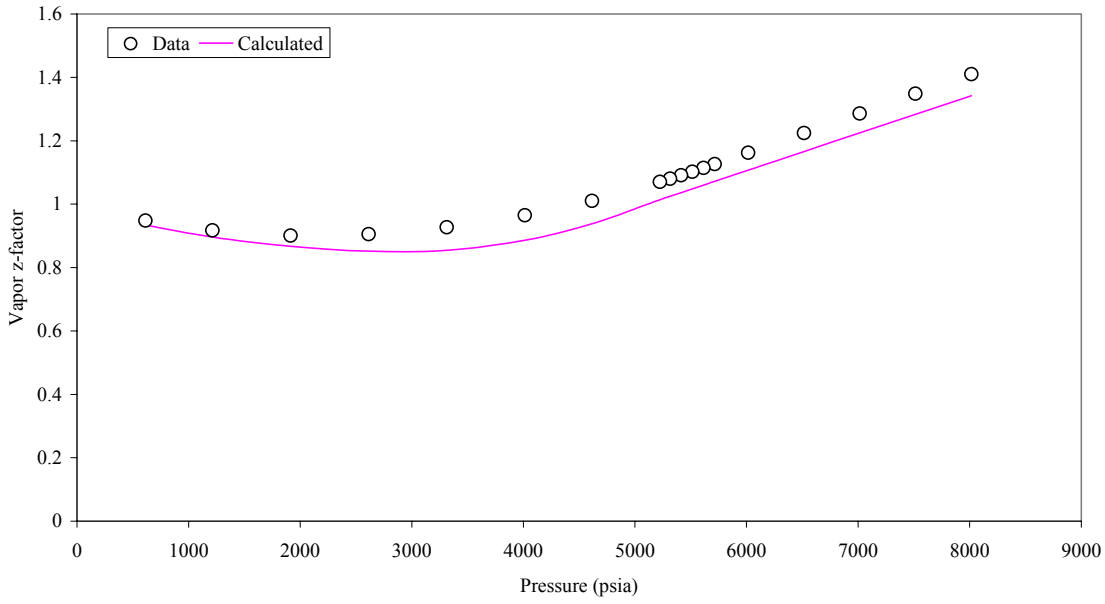

Fig. B.29- Vapor z-factor from CCE experiment for fluid 8.

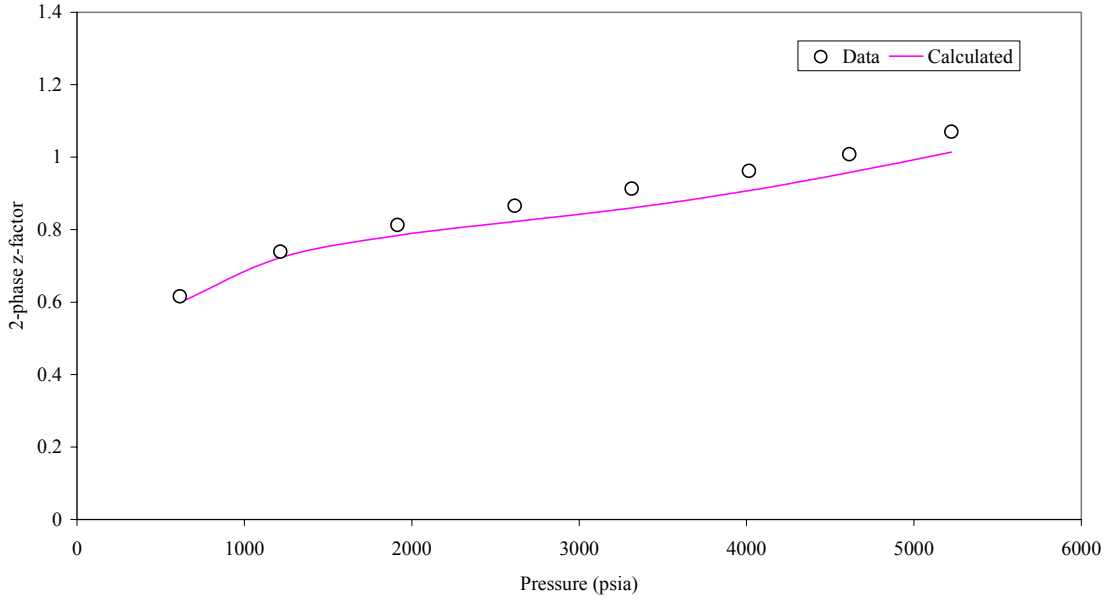

Fig. B.30- 2-phase z-factor from CVD experiment for fluid 8.

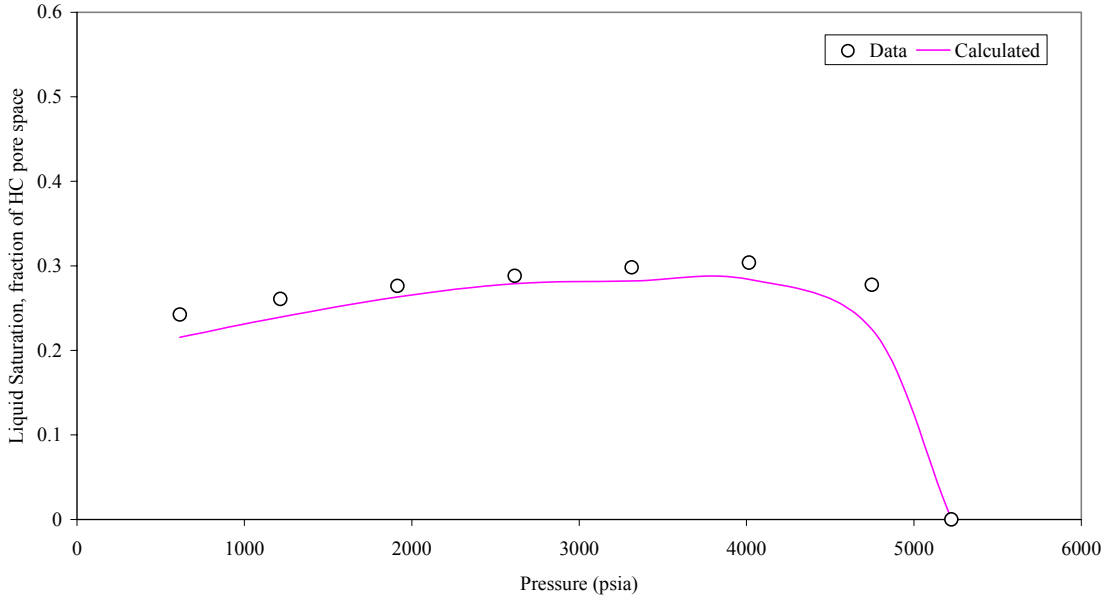

Fig. B.31- Liquid saturation from CVD experiment for fluid 8.

Fluid 9 (T_{res} = 190 °F)

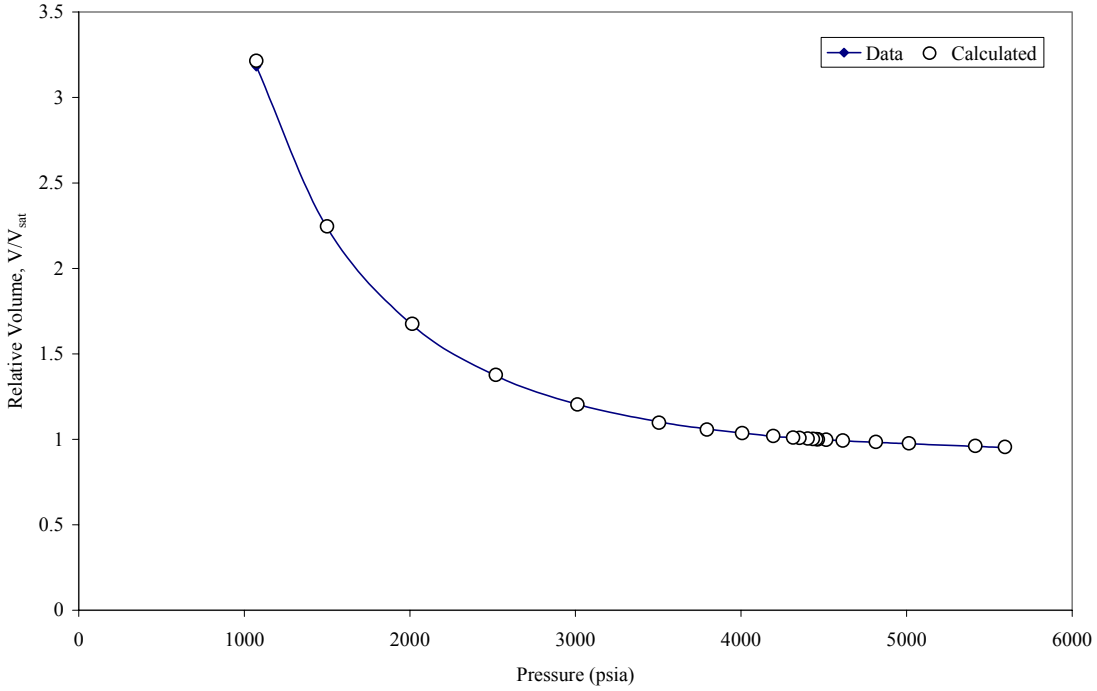

Fig. B.32- Relative volume from CCE experiment for fluid 9.

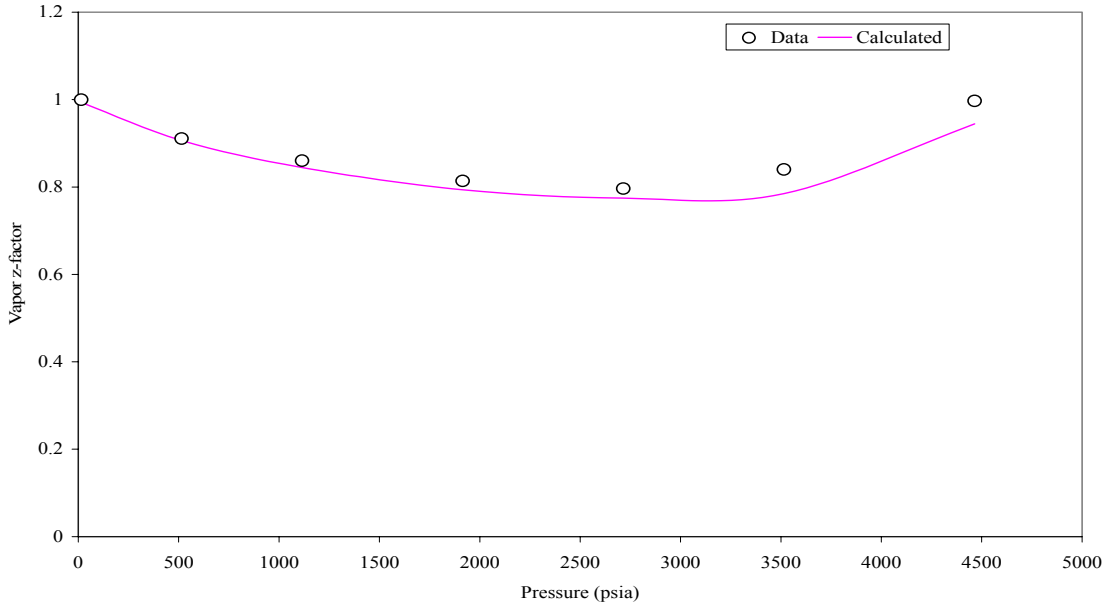

Fig. B.33- Vapor z-factor from CCE experiment for fluid 9.

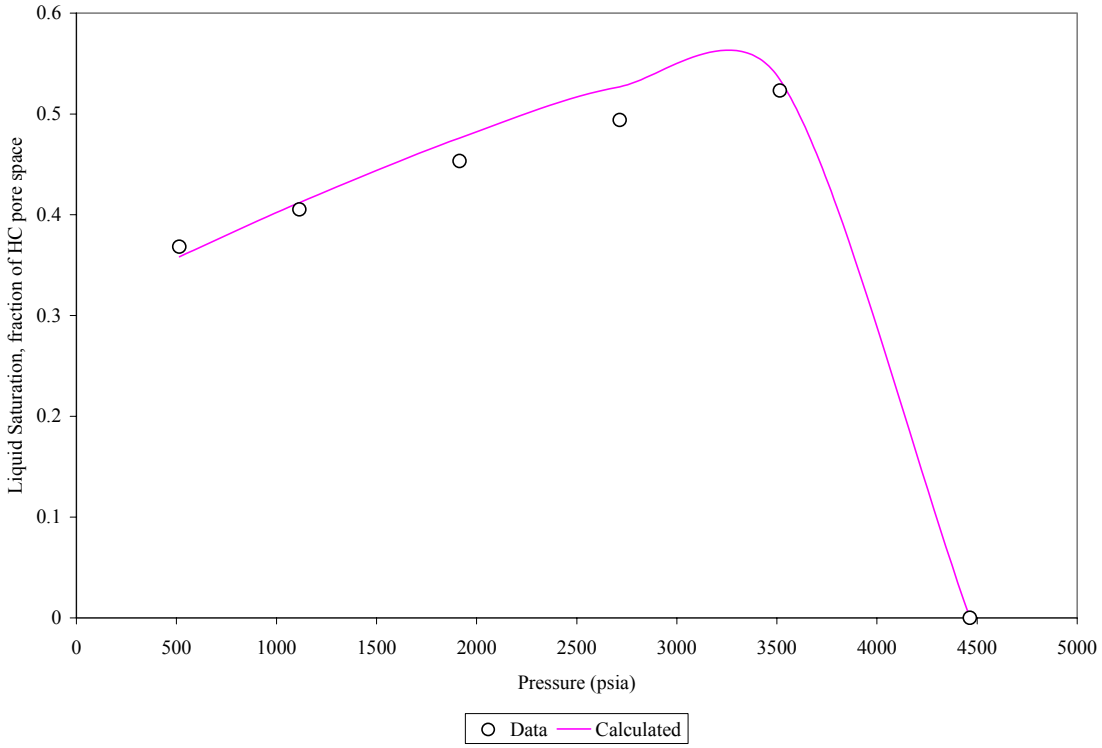

Fig. B.34- Liquid saturation from CVD experiment for fluid 9.

Fluid 10 (T_{res} = 301 °F)

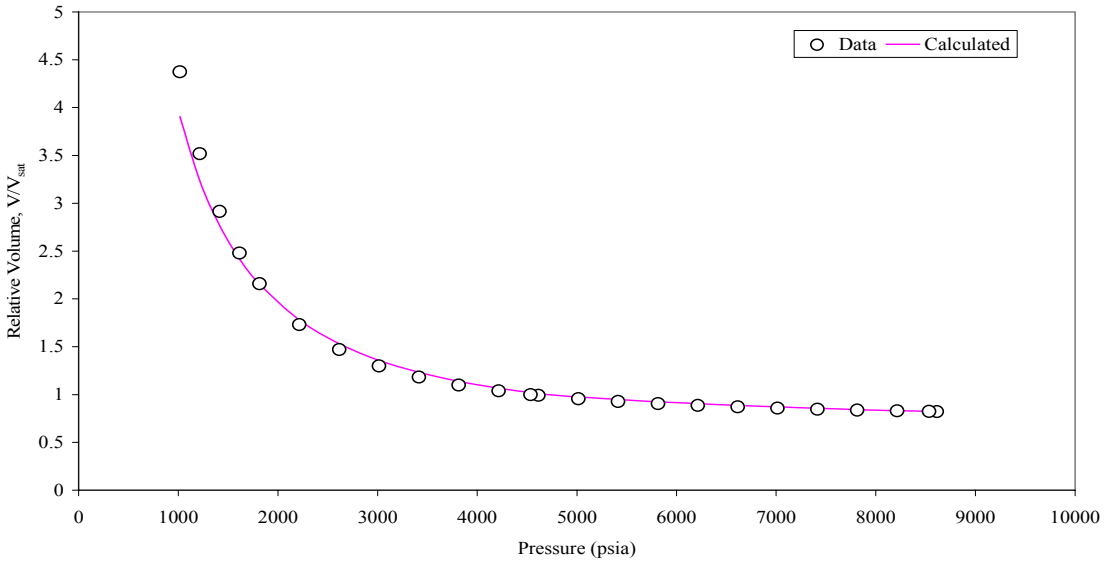

Fig. B.39- Relative volume from CCE experiment for fluid 10.

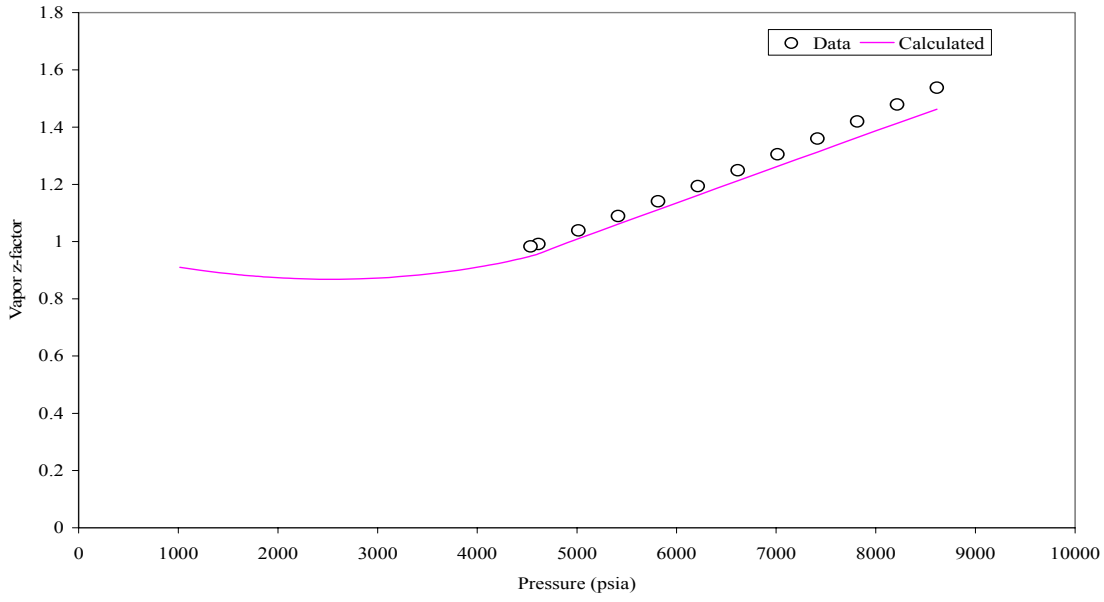

Fig. B.40- Vapor z-factor from CCE experiment for fluid 10.

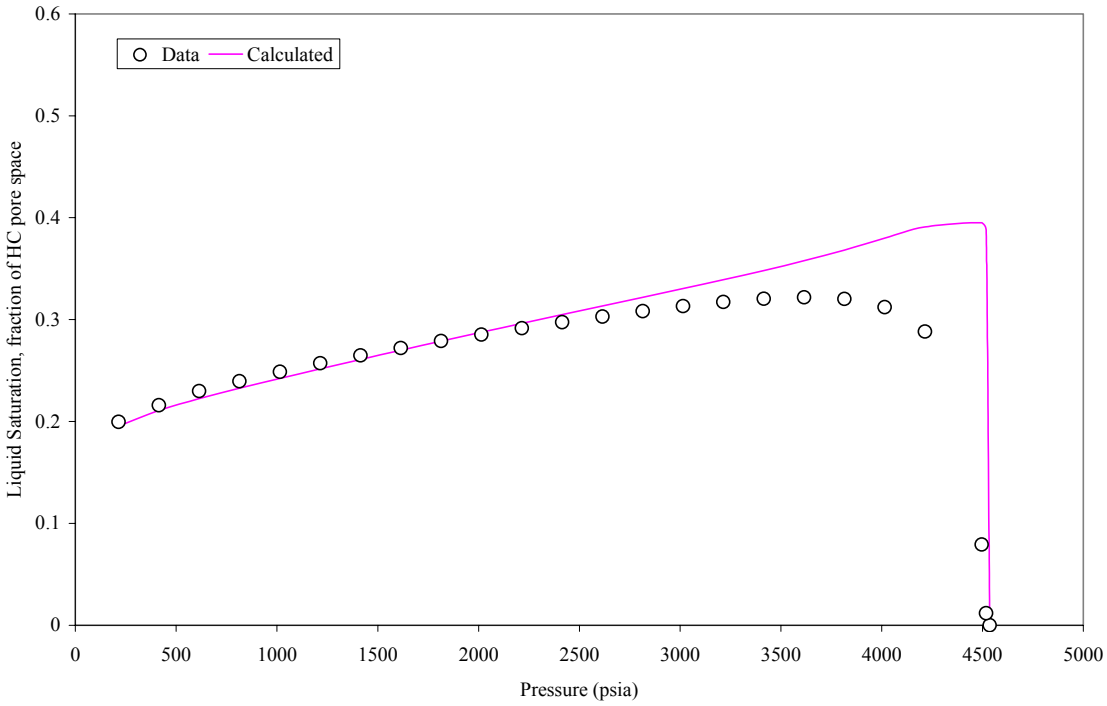

Fig. B.41- Liquid saturation from CVD experiment for fluid 10.

Fluid 11 (Matching at reservoir temperature of 305 ºF)

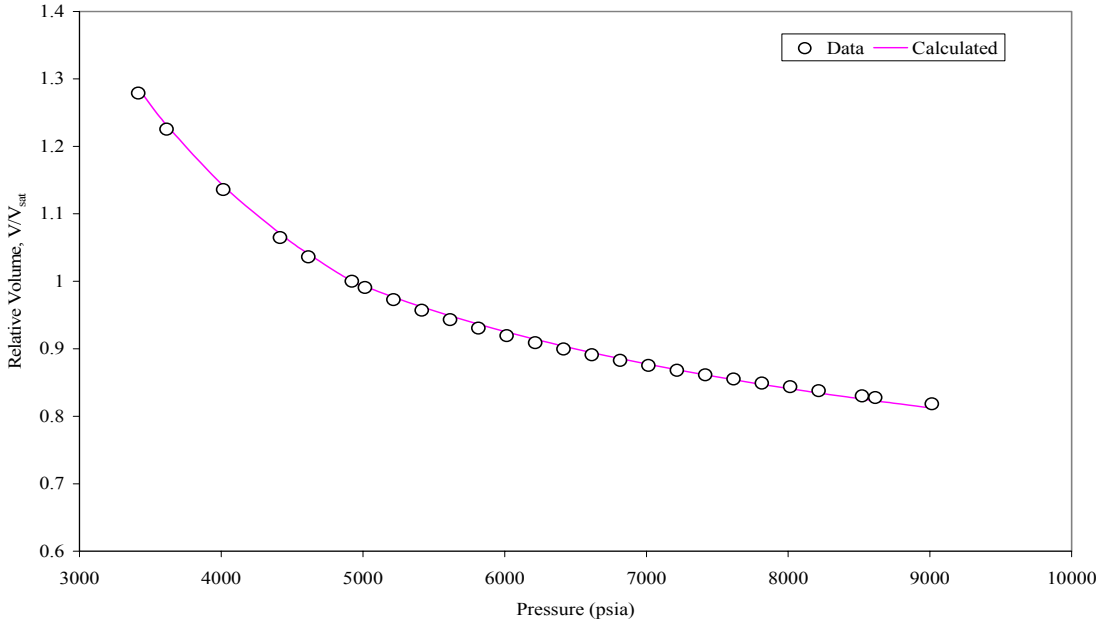

Fig. B.35- Relative volume from CCE experiment for fluid 11 at reservoir temperature.

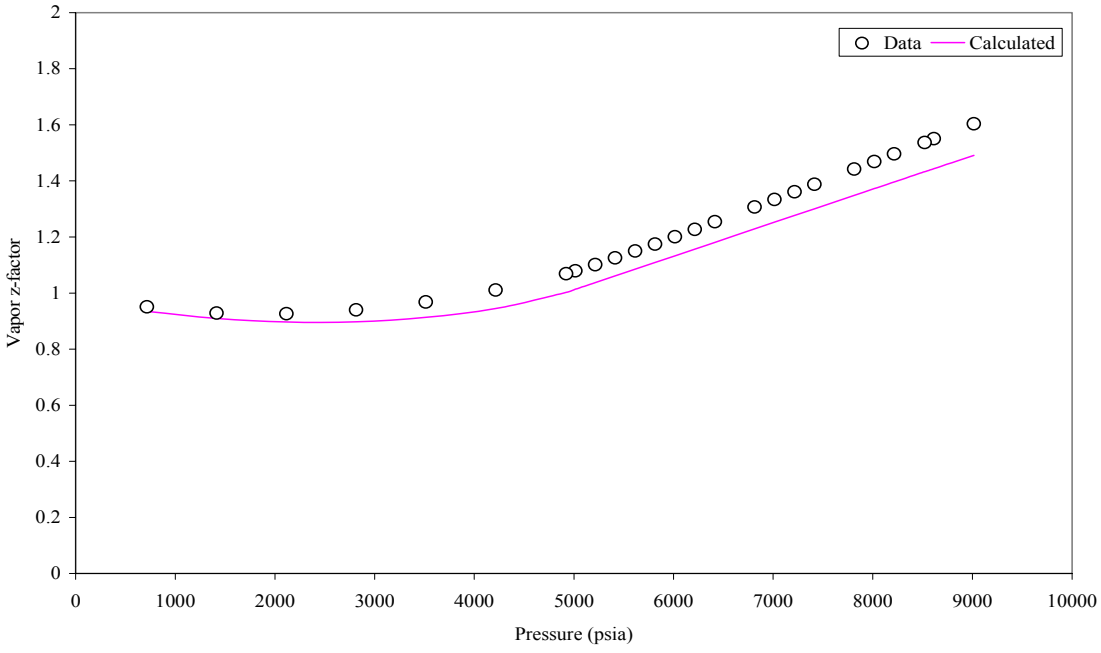

Fig. B.36- Vapor z-factor from CCE experiment for fluid 11 at reservoir temperature.

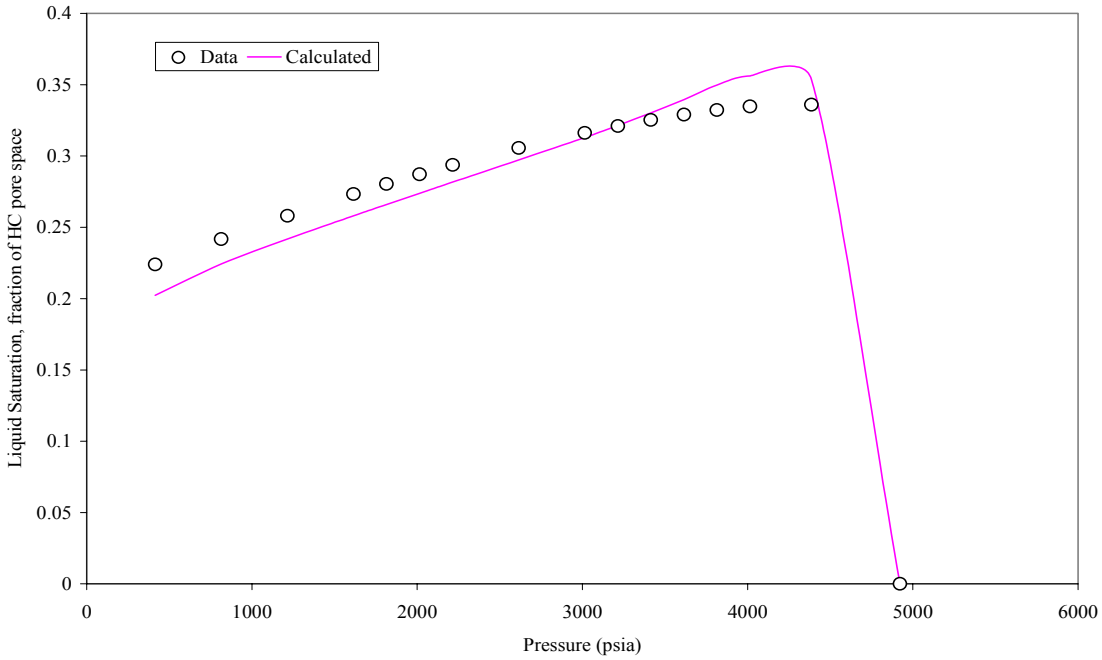

Fig. B.37- Liquid saturation from CVD experiment for fluid 11 at reservoir temperature.

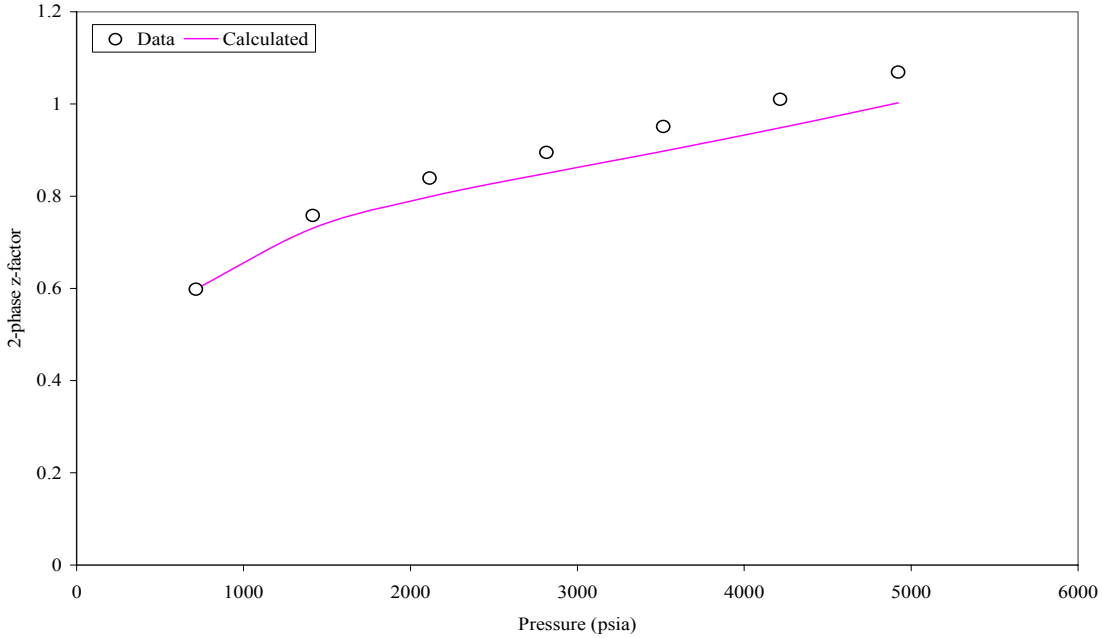

Fig. B.38- 2-phase z-factor from CVD experiment for fluid 11 at reservoir temperature.

Fluid 12 (T_{res} = 179 °F)

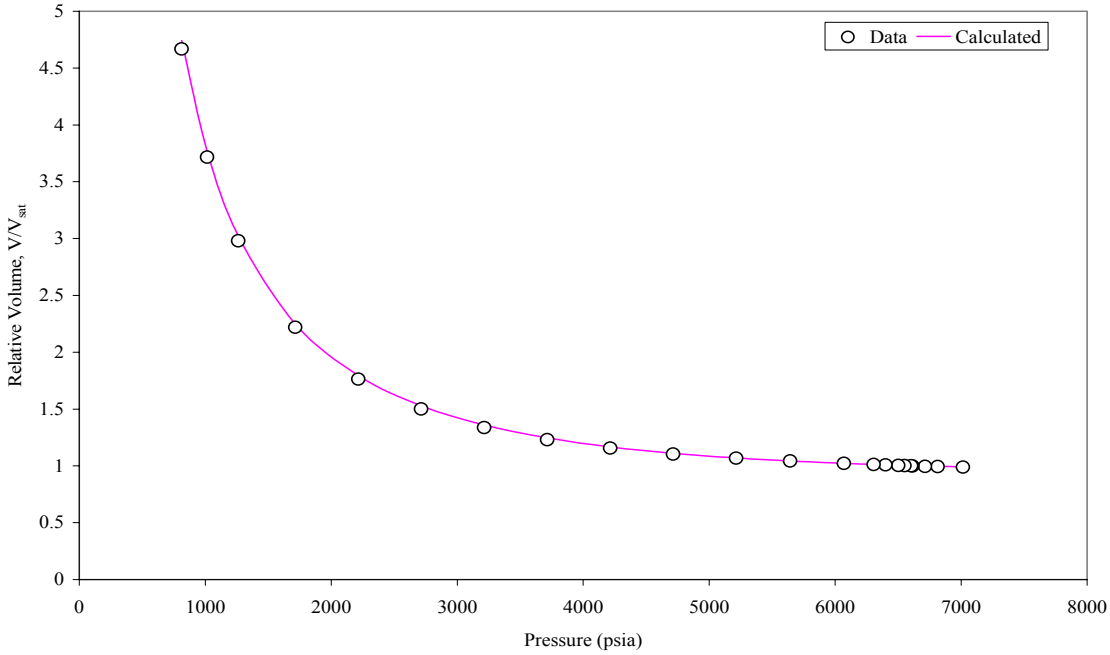

Fig. B.42- Relative volume from CCE experiment for fluid 12.

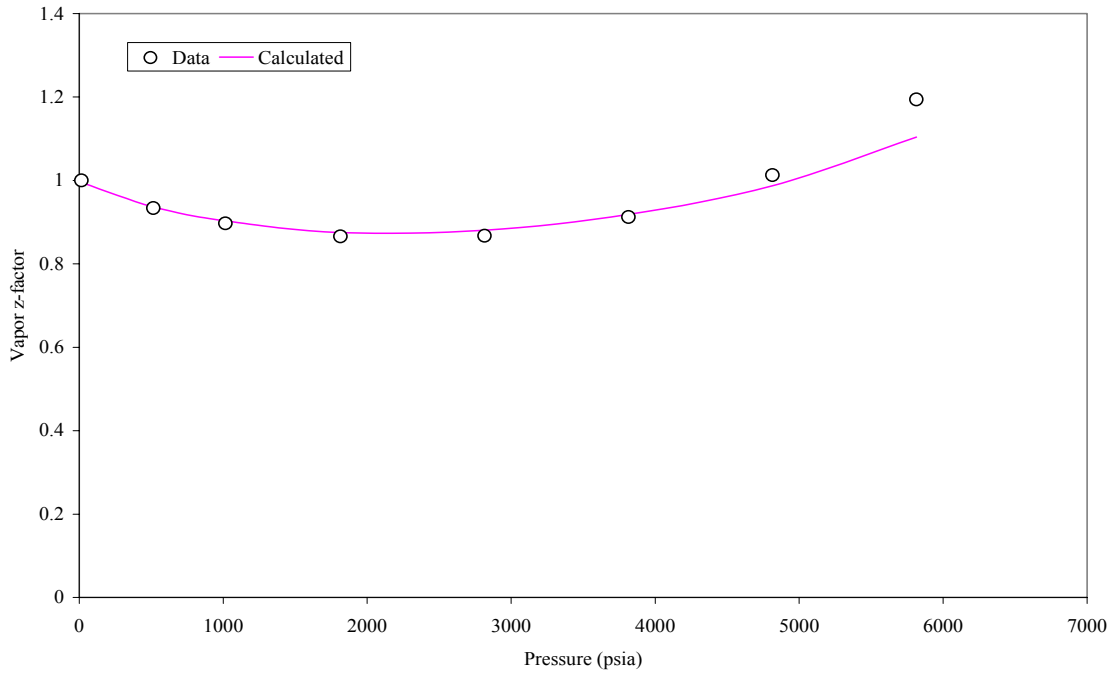

Fig. B.43- Vapor z-factor from CCE experiment for fluid 12.

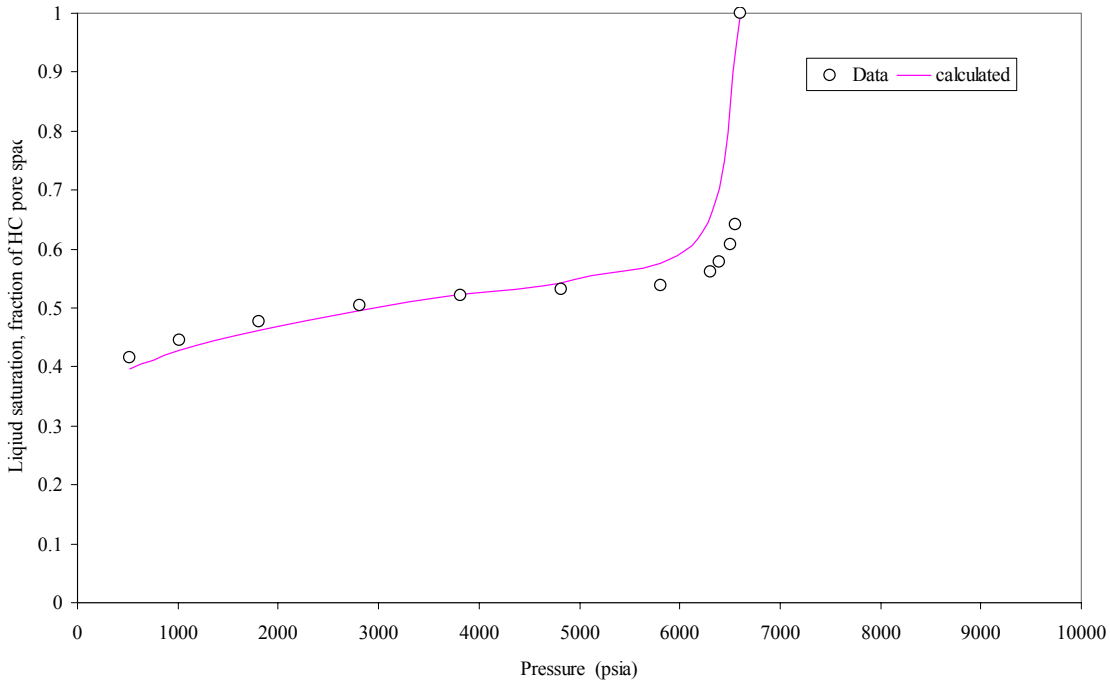

Fig. B.44- Liquid saturation from CVD experiment for fluid 12.

Fluid 13 (T_{res} = 197 °F)

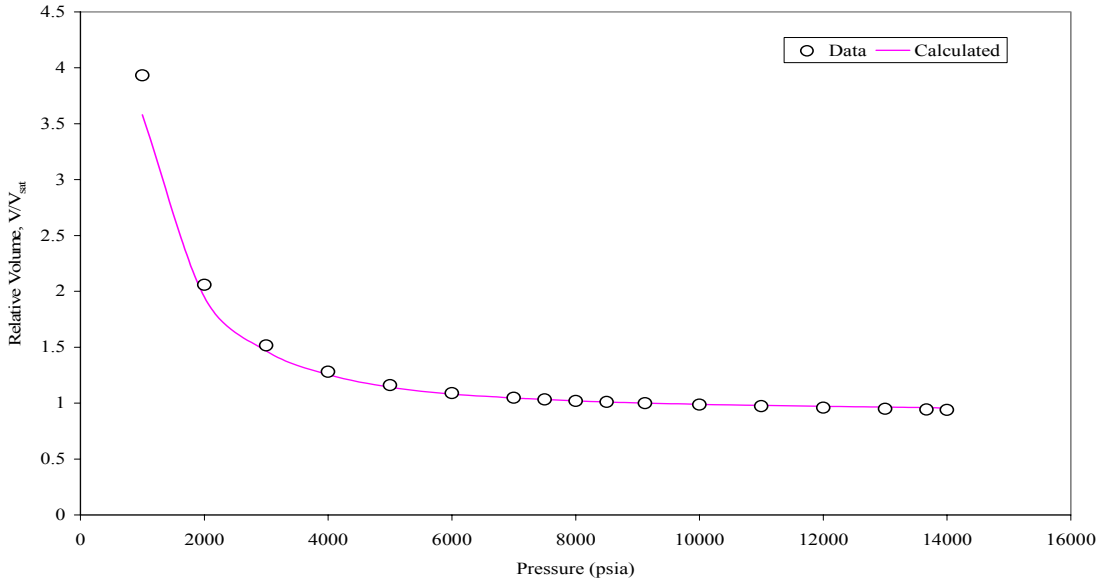

Fig. B.45- Relative volume from CCE experiment for fluid 13.

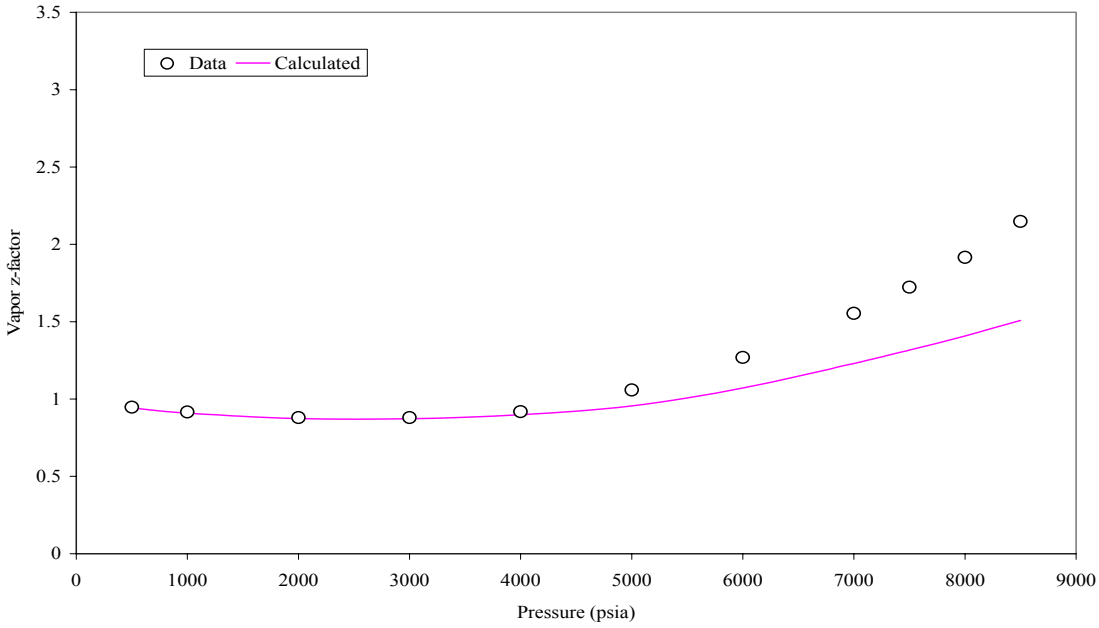

Fig. B.46- Vapor z-factor from CCE experiment for fluid 13.

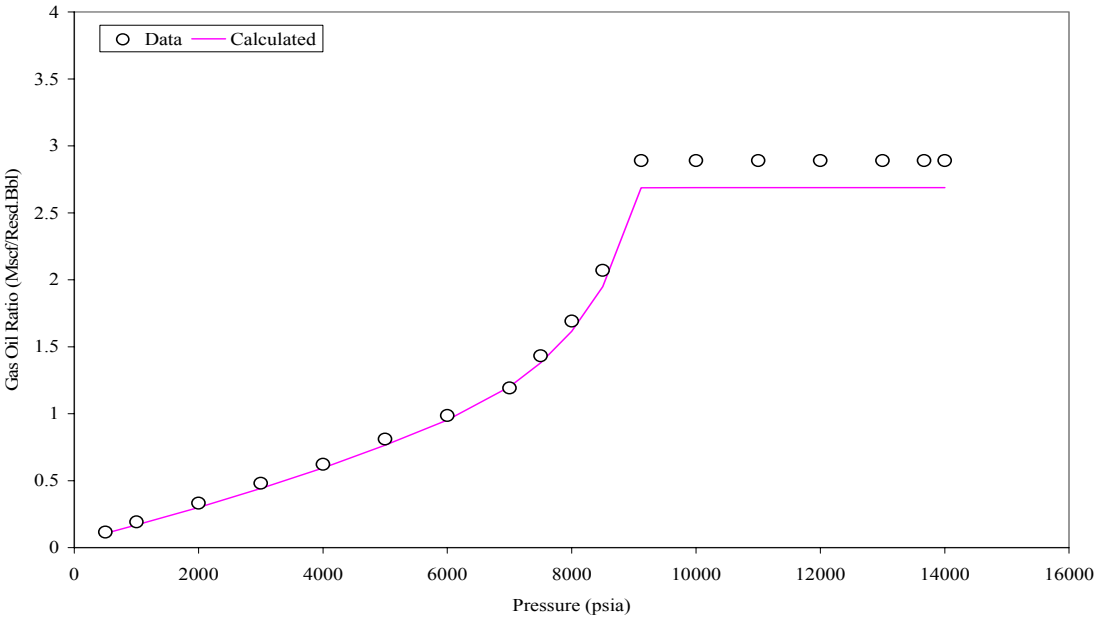

Fig. B.46- Gas oil ratio from DL experiment for fluid 13.

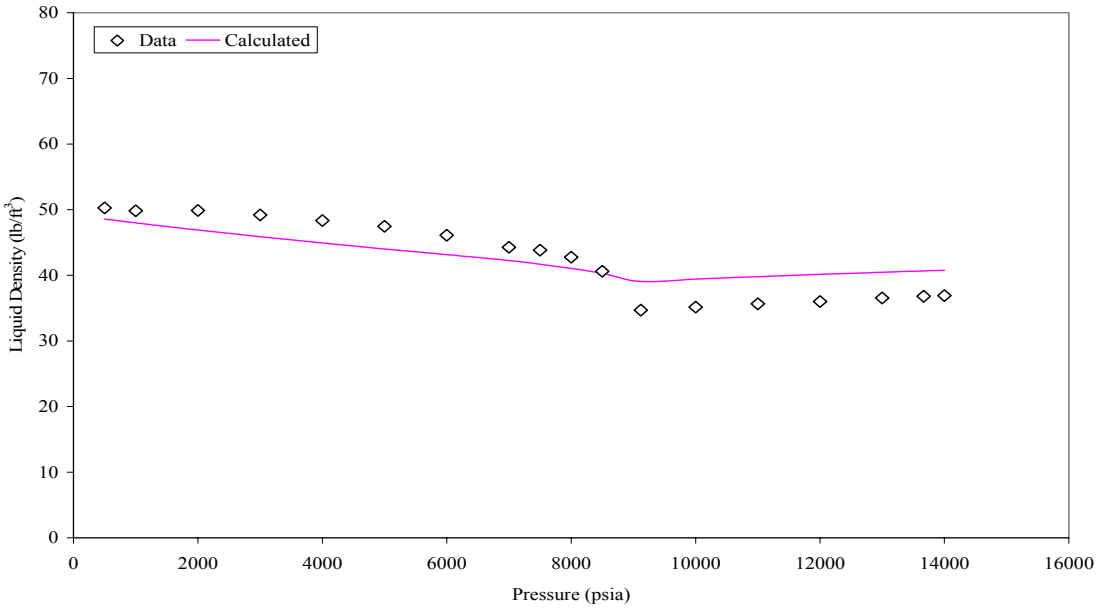

Fig. B.47- Liquid density from DL experiment for fluid 13.

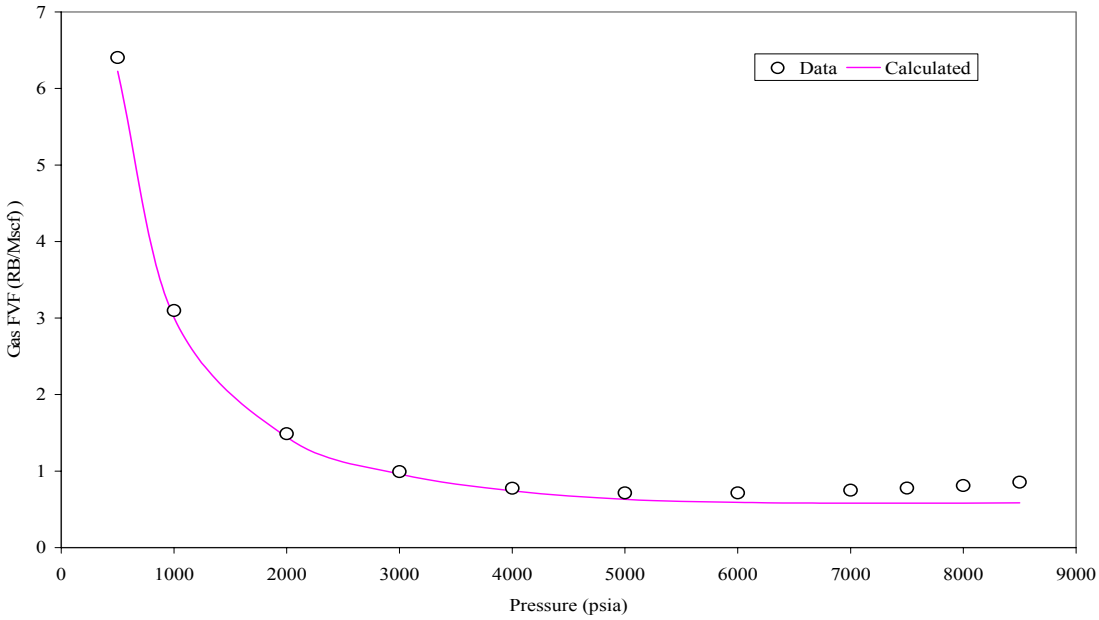

Fig. B.48- Gas FVF from DL experiment for fluid 13.

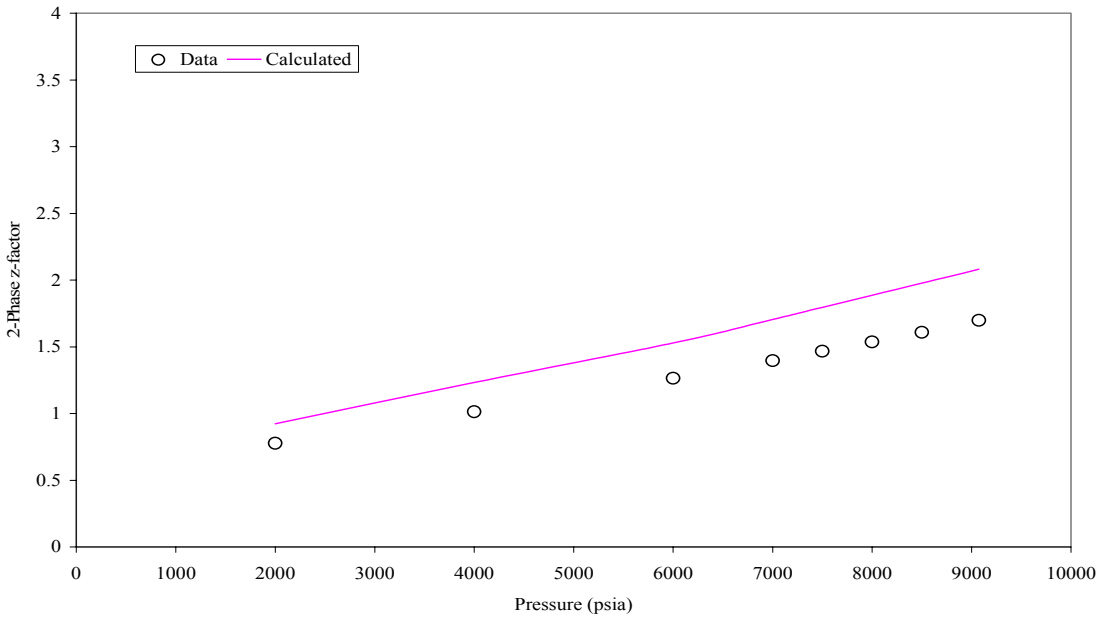

Fig. B.49- 2-phase z-factor from CVD experiment for fluid 13.

Fluid 14 (T_{res} = 190 °F)

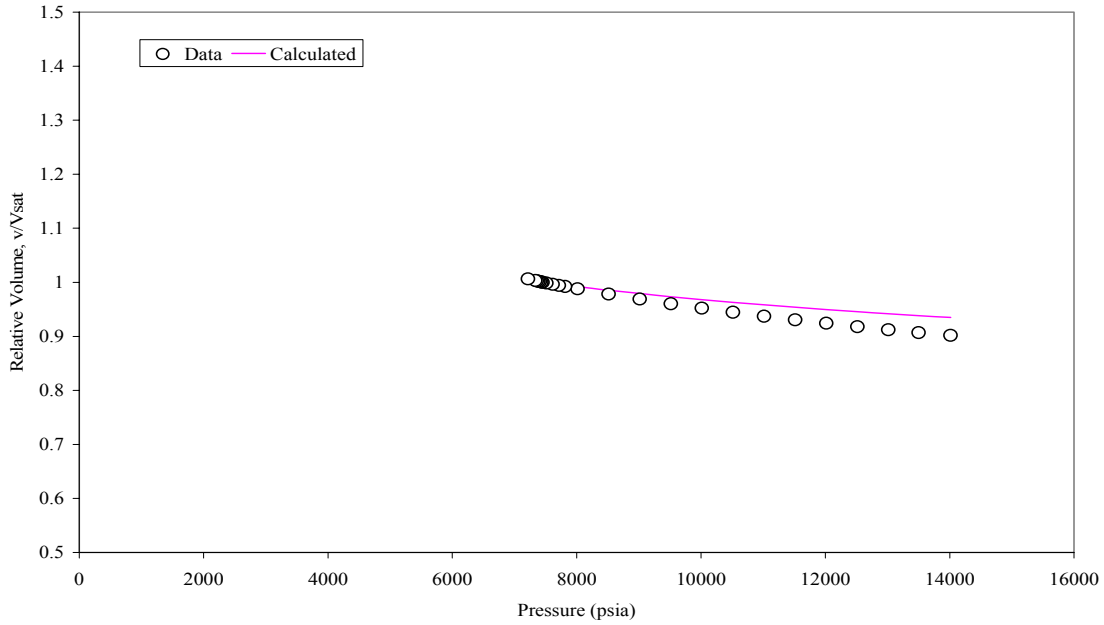

Fig. B.50- Relative volume from CCE experiment for fluid 14.

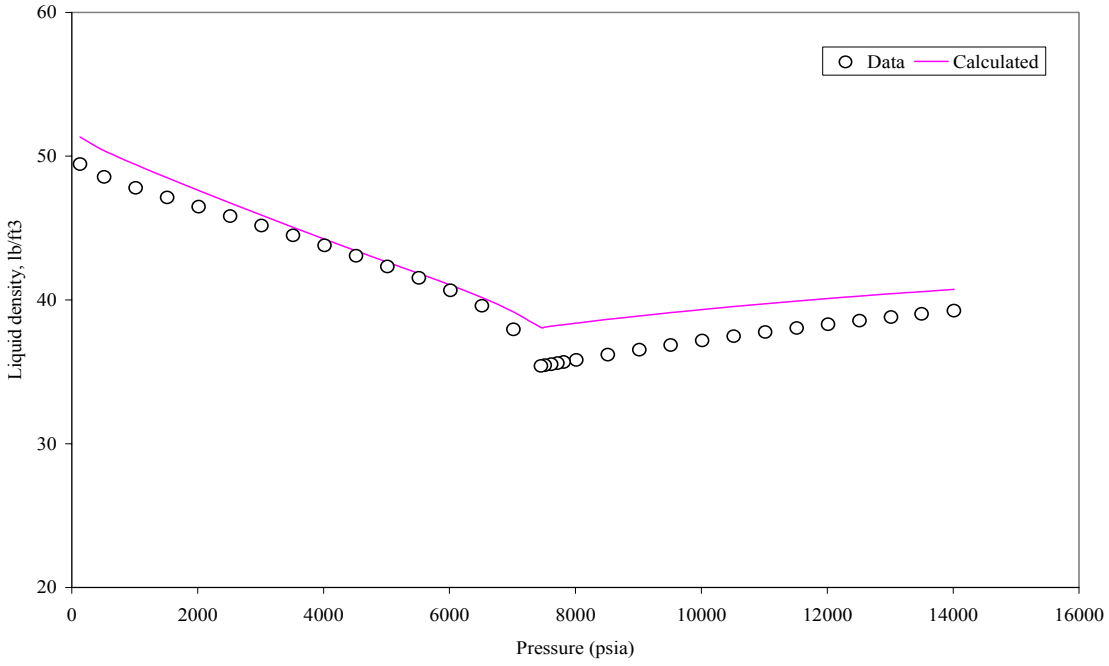

Fig. B.51- Liquid density from CCE experiment for fluid 14.

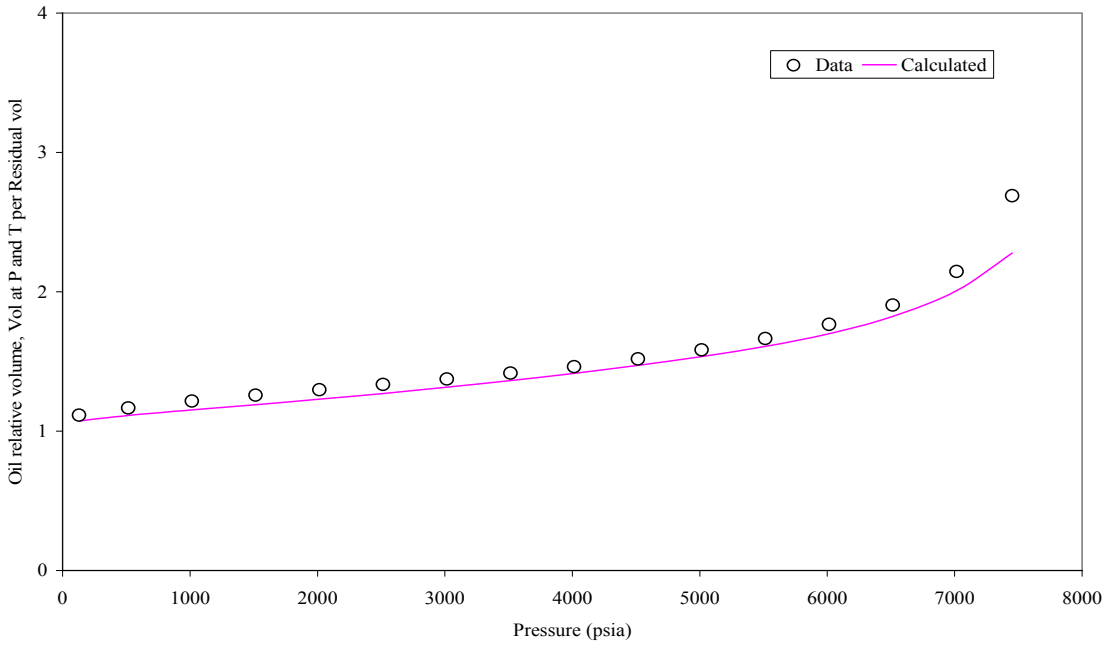

Fig. B.52- Oil relative volume from DL experiment for fluid 14.

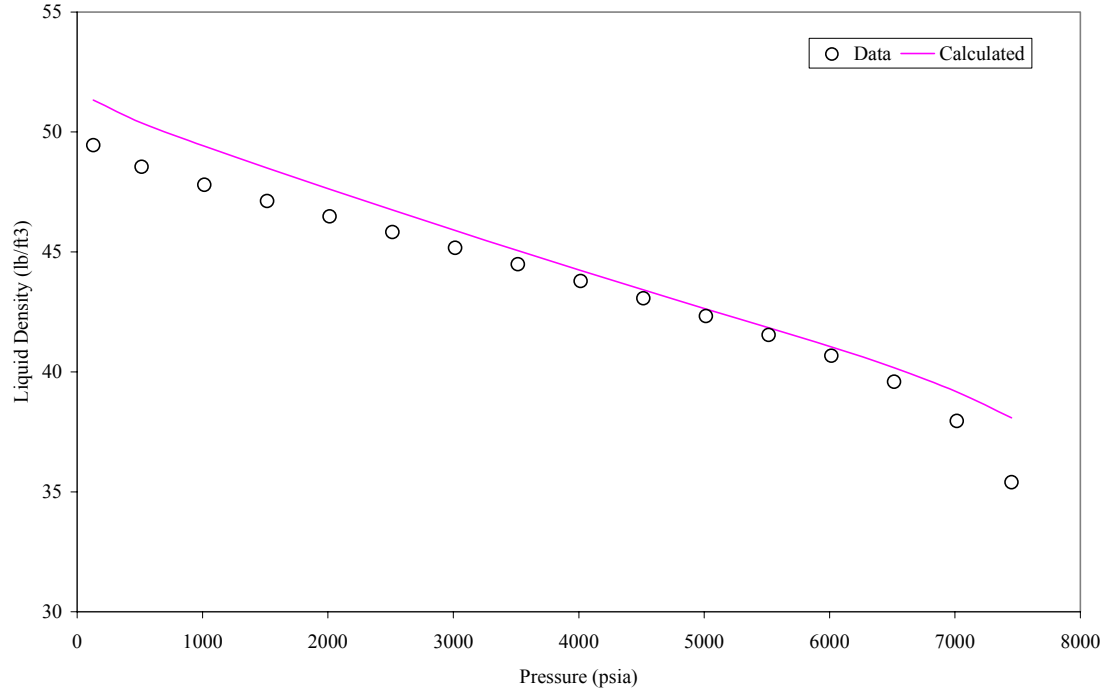

Fig. B.53- Liquid density from DL experiment for fluid 14.

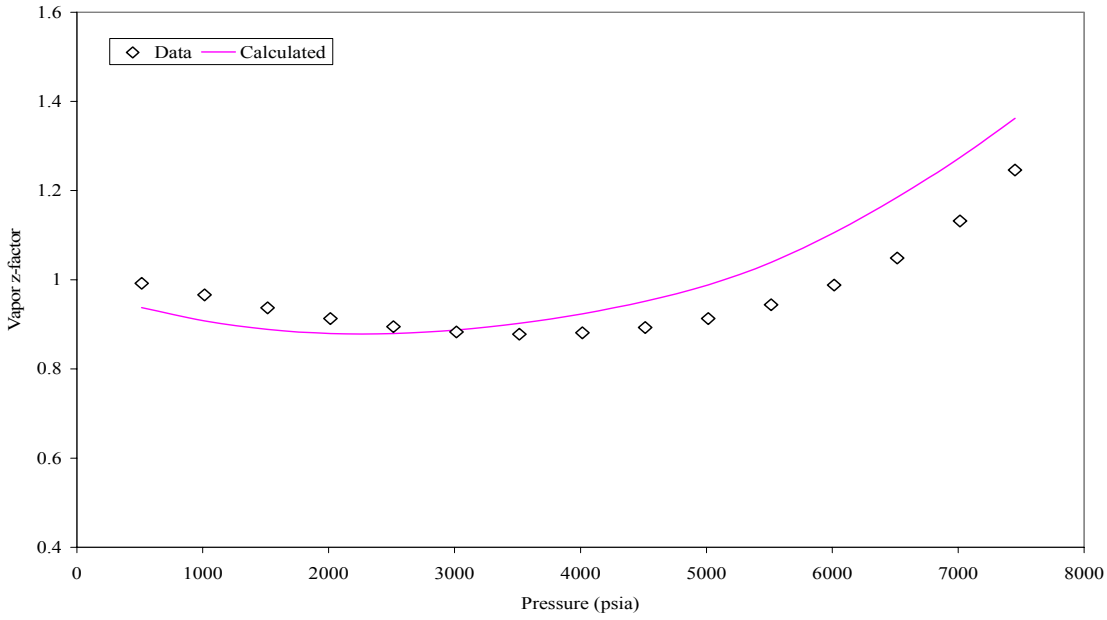

Fig. B.54- Vapor z-factor from DL experiment for fluid 14.

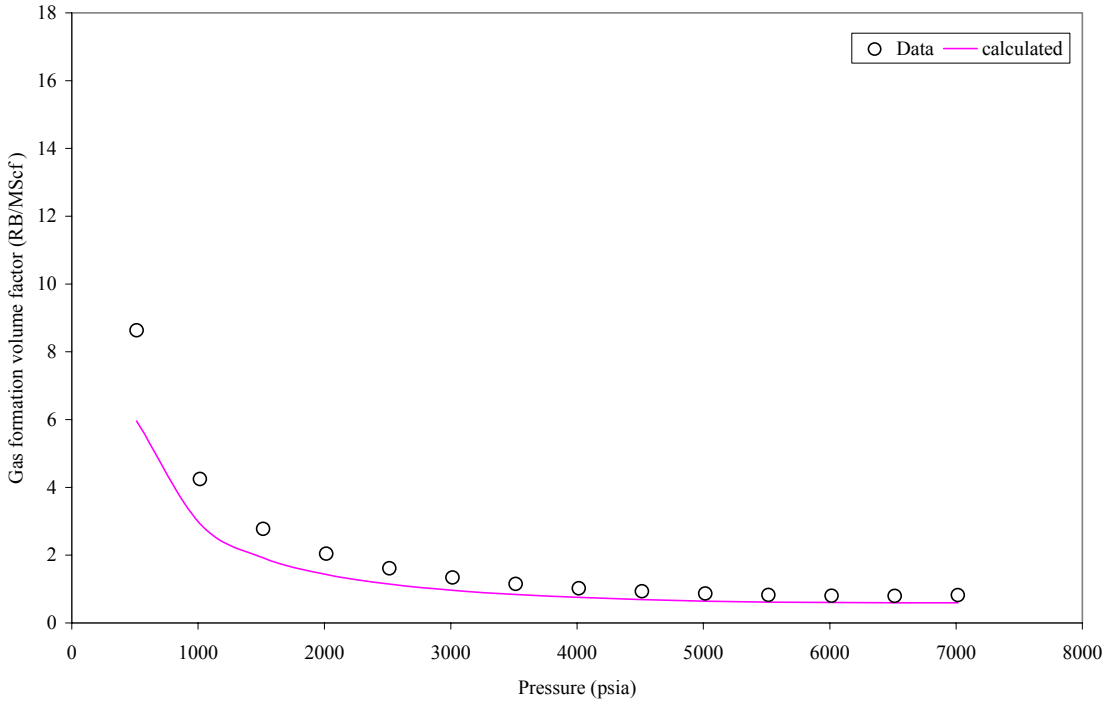

Fig. B.55- Gas formation volume factor from DL experiment for fluid 14.

Fluid 15 (T_{res} = 176 °F)

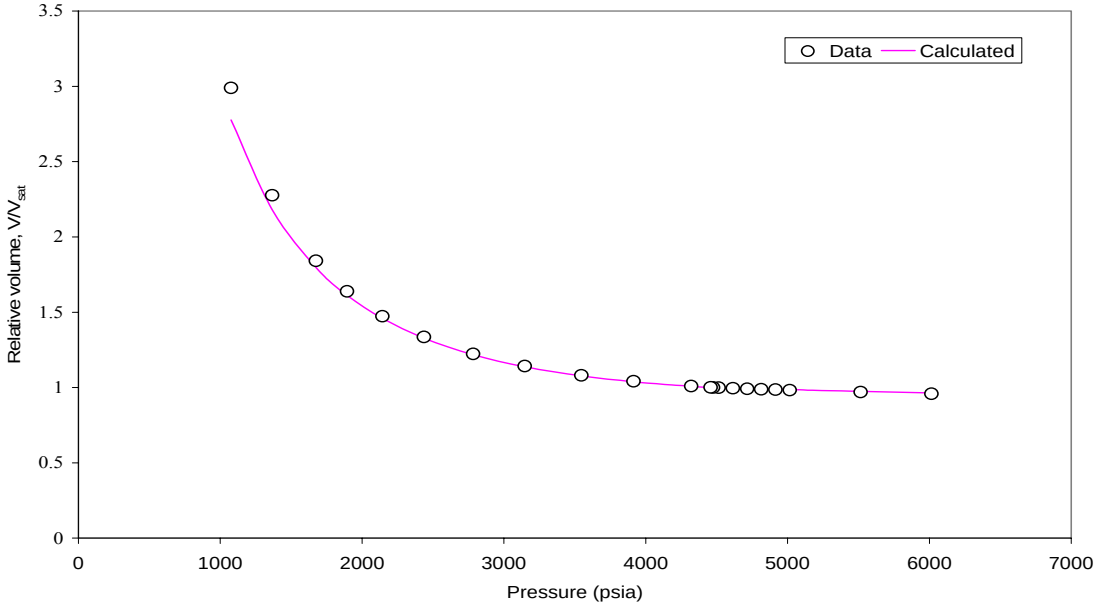

Fig. B.56- Relative volume from CCE experiment for fluid 15.

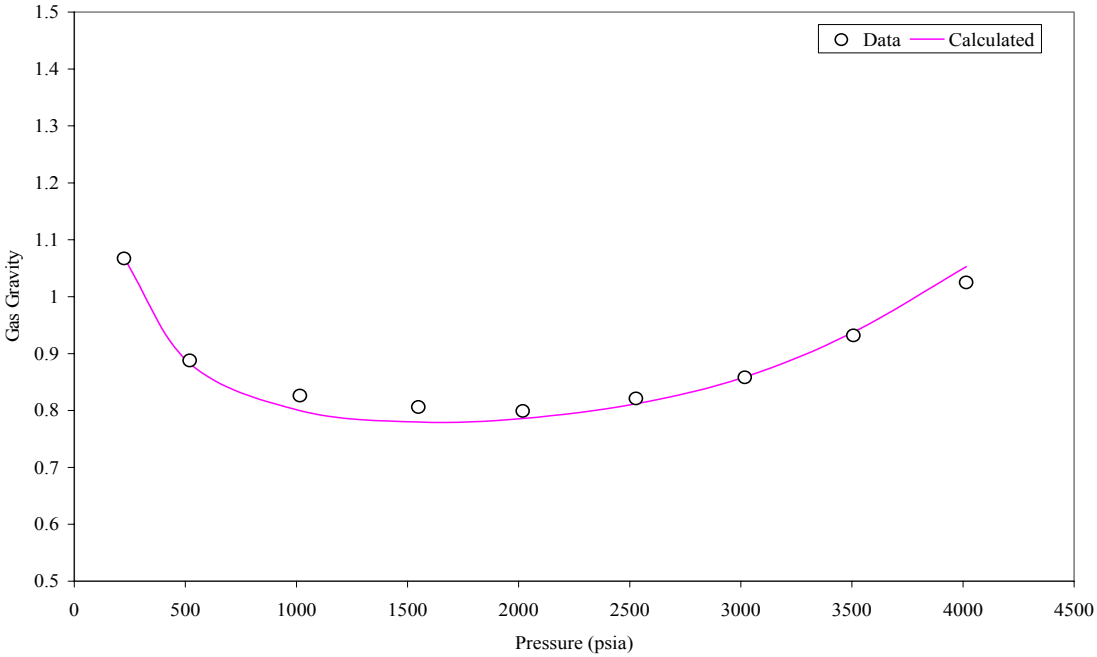

Fig. B.57- Gas gravity from DL experiment for fluid 15.

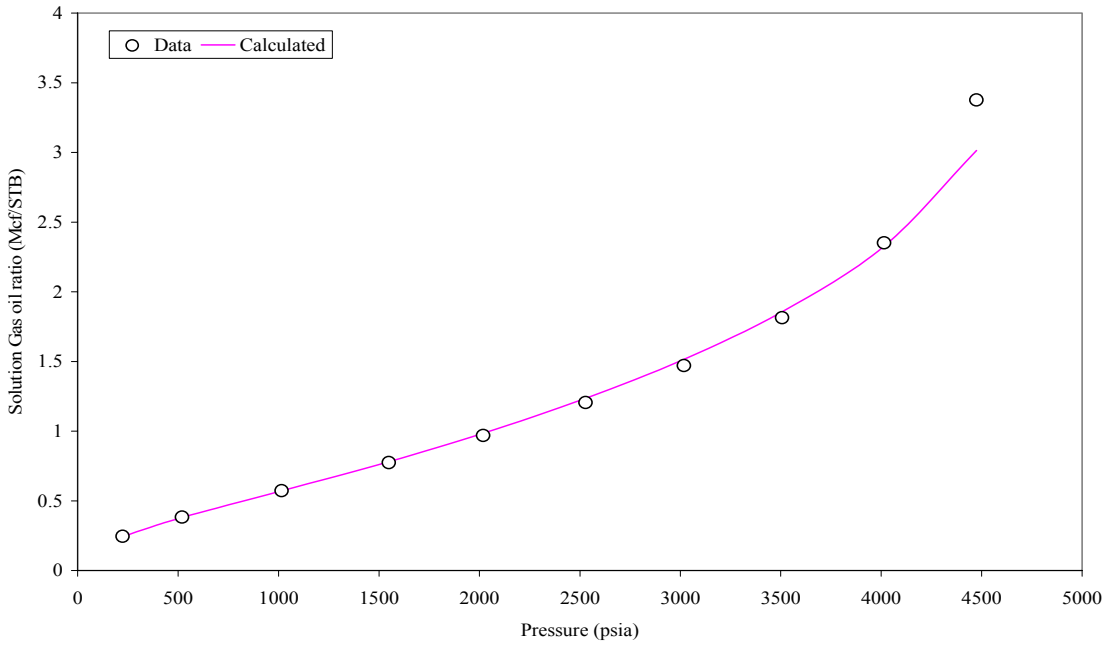

Fig. B.58- Solution gas-oil ratio from DL experiment for fluid 15.

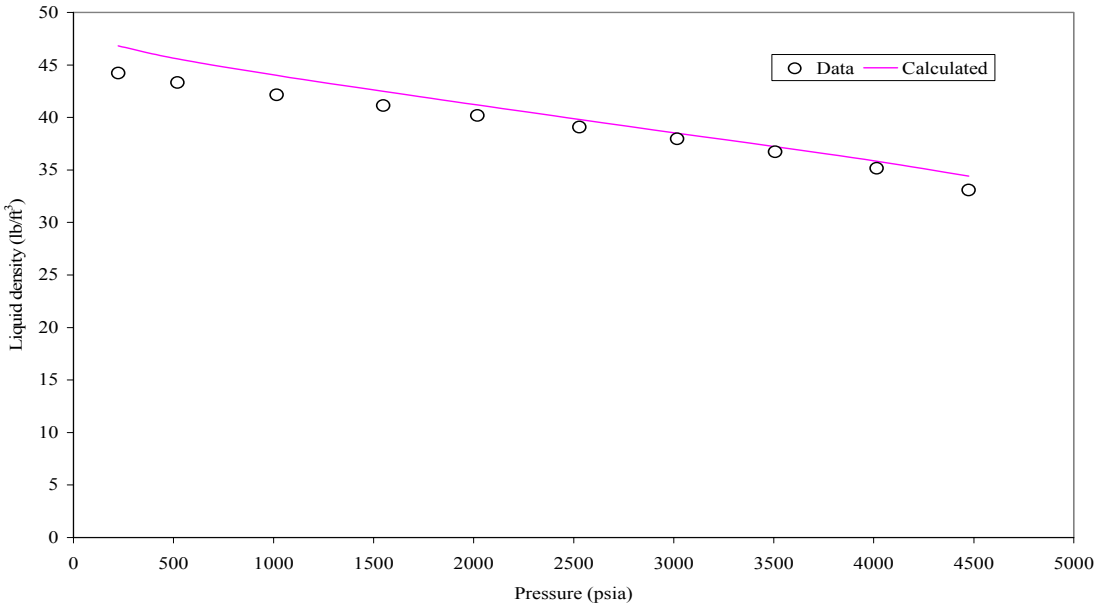

Fig. B.59- Liquid density from DL experiment for fluid 15.

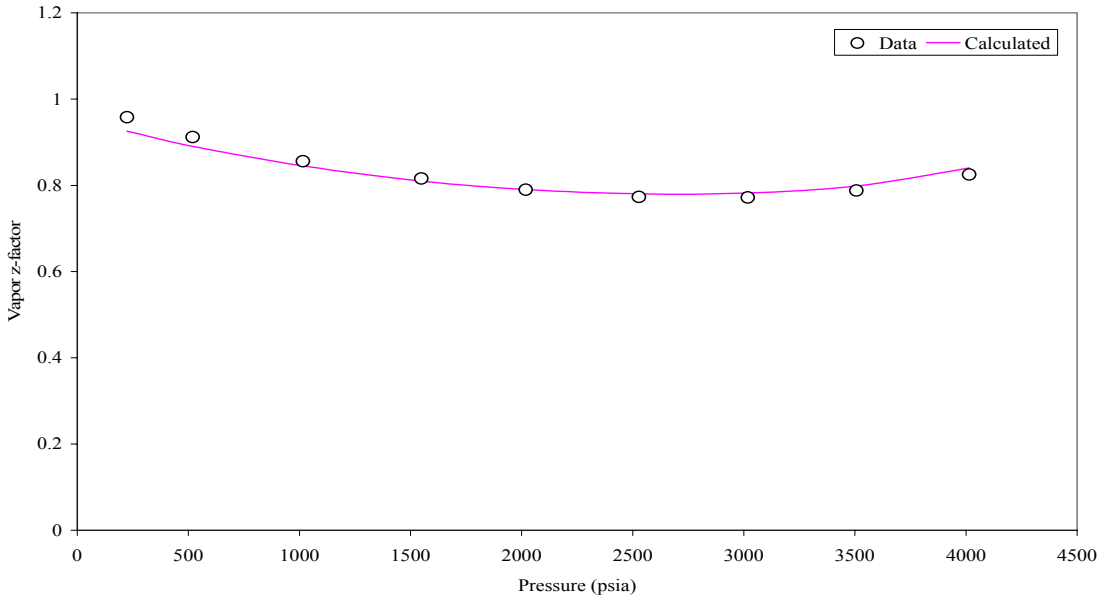

Fig. B.60- Vapor z-factor from DL experiment for fluid 15.

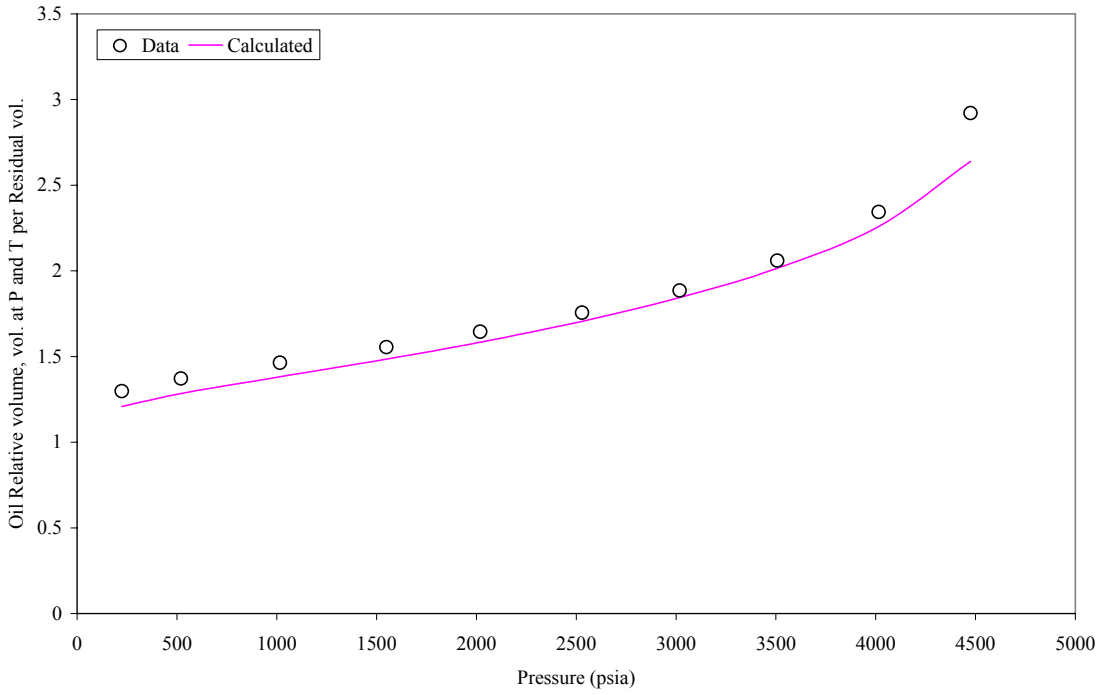

Fig. B.61- Oil relative volume from DL experiment for fluid 15.

Fluid 16 (T_{res} = 307 °F)

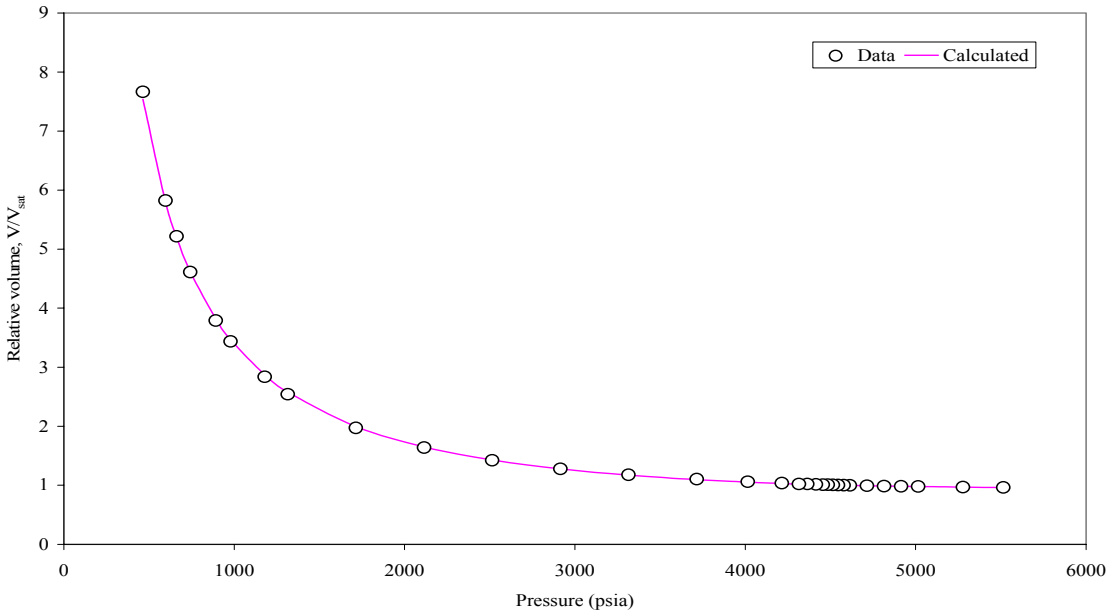

Fig. B.62- Relative volume from CCE experiment for fluid 16.

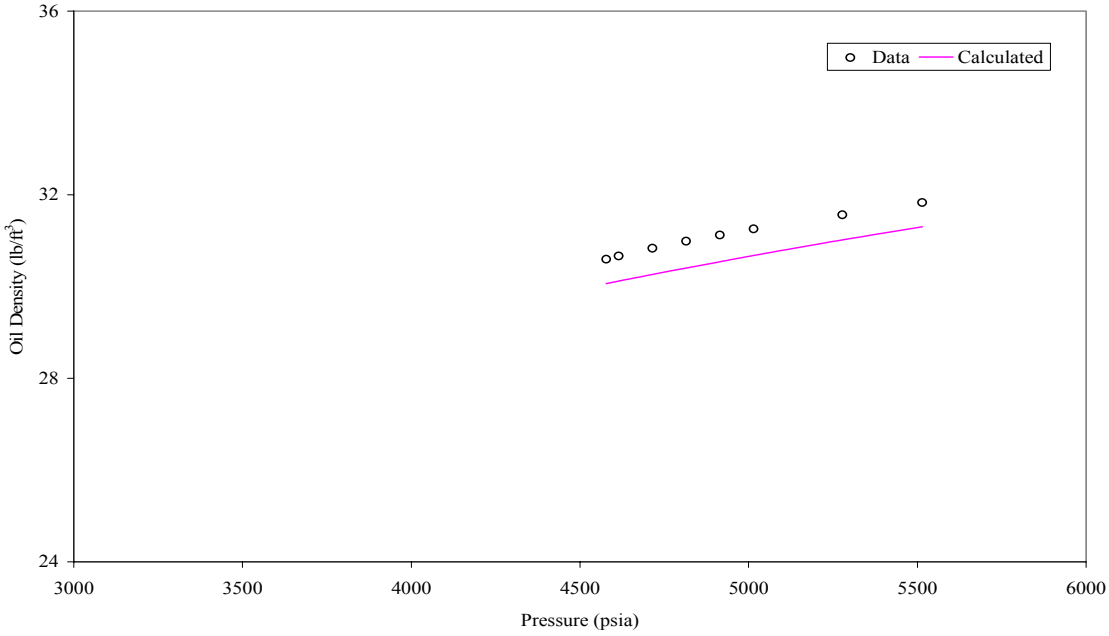

Fig. B.63- Liquid density from CCE experiment for fluid 16.

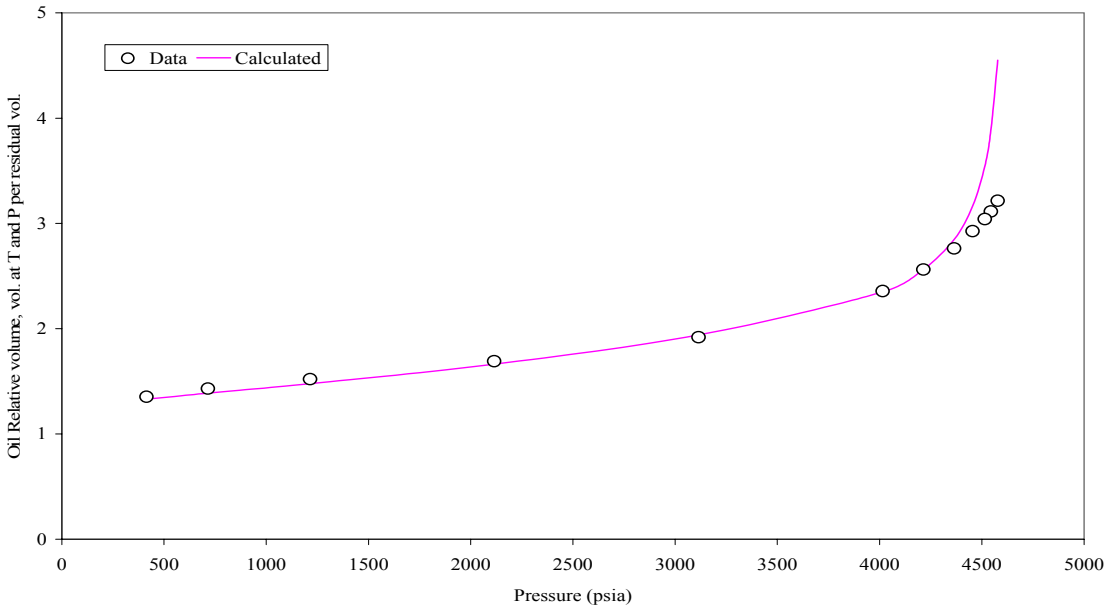

Fig. B.64- Oil relative volume from CVD experiment for fluid 16.

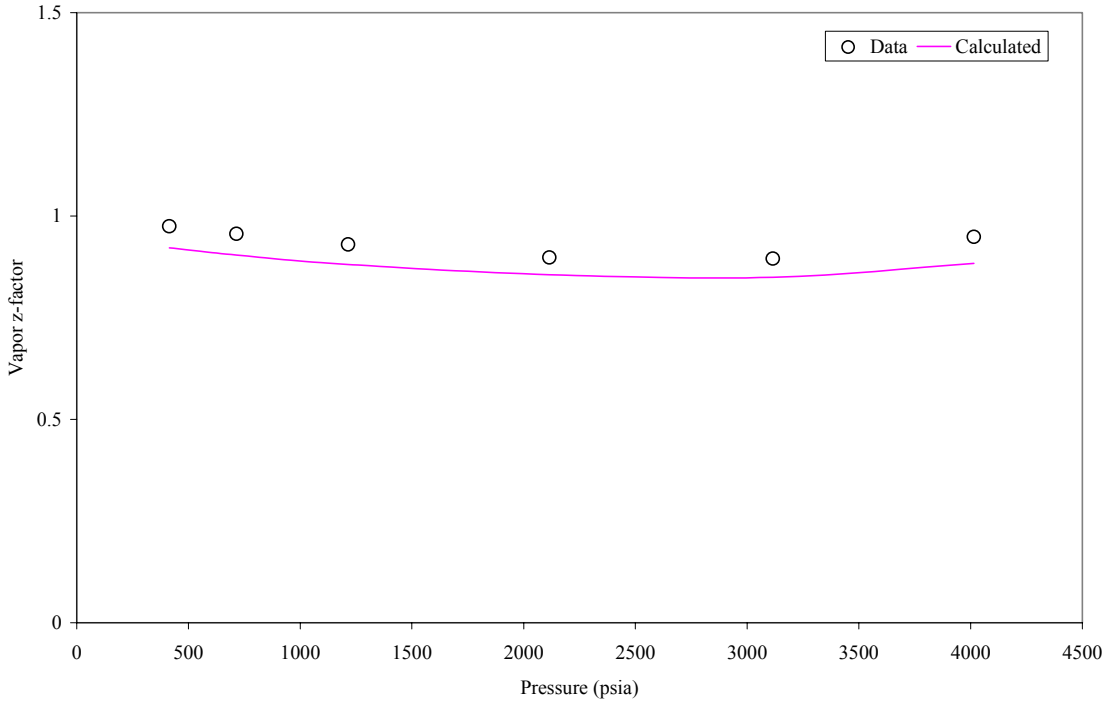

Fig. B.65- Vapor z-factor from CVD experiment for fluid 16.

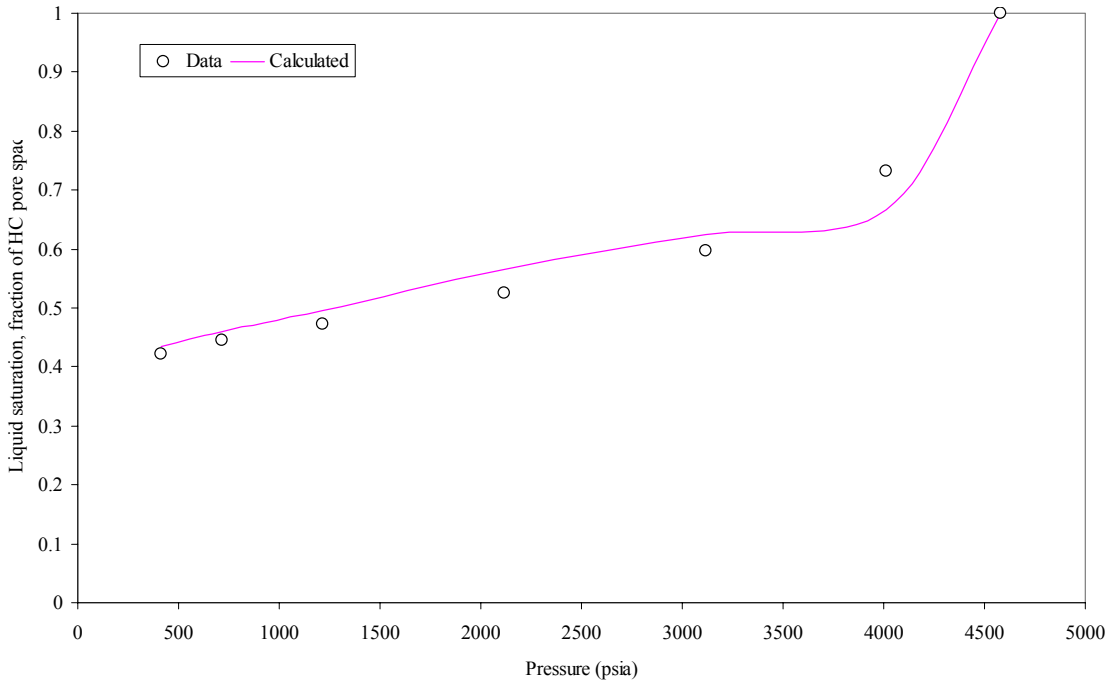

Fig. B.66- Liquid saturation from CVD experiment for fluid 16.

Fluid 17 (T_{res} = 287 °F)

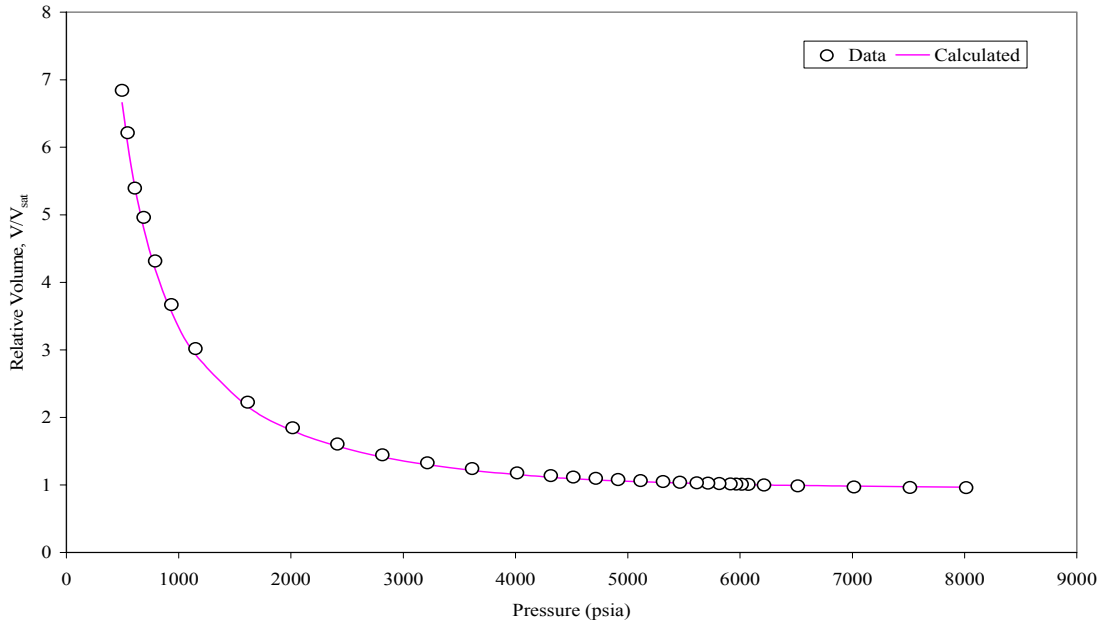

Fig. B.67- Relative volume from CCE experiment for fluid 17.

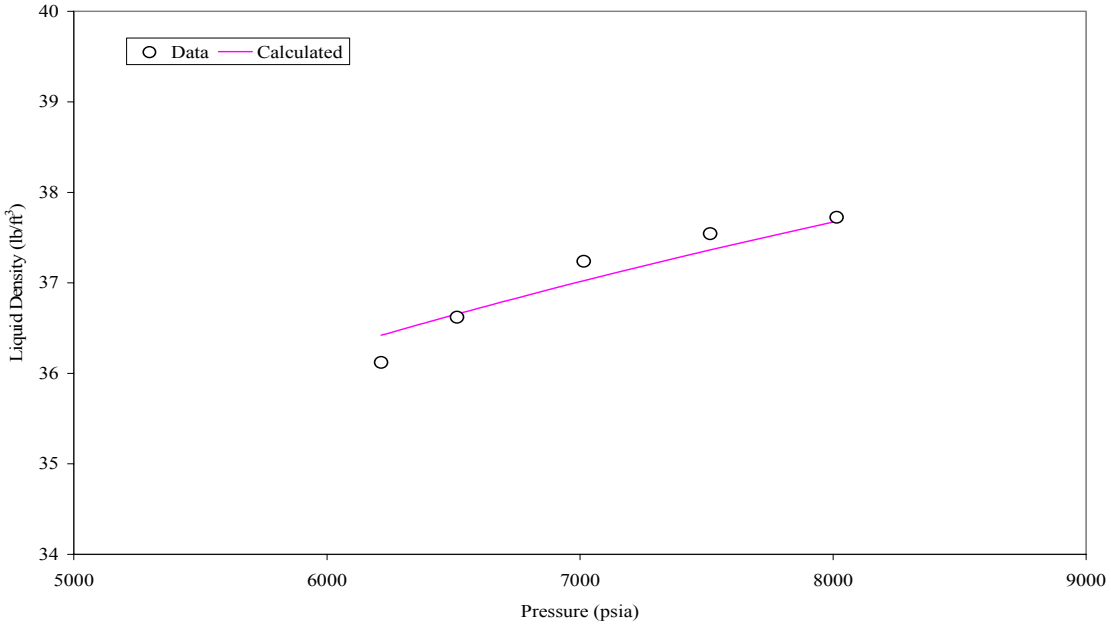

Fig. B.68- Liquid density from CCE experiment for fluid 17.

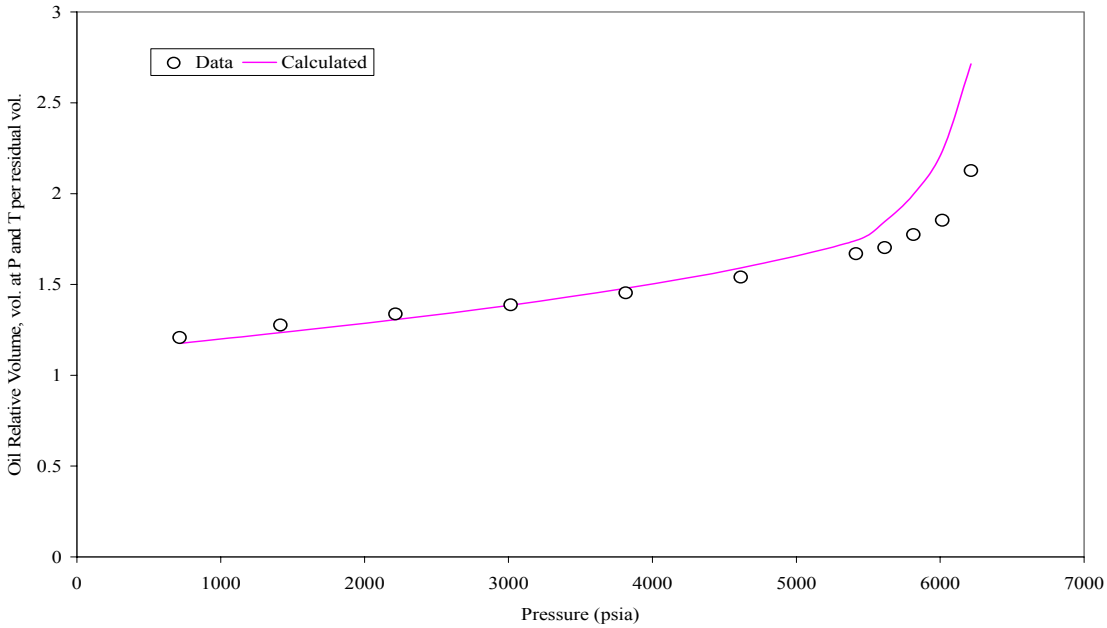

Fig. B.69- Oil relative volume from DL experiment for fluid 17.

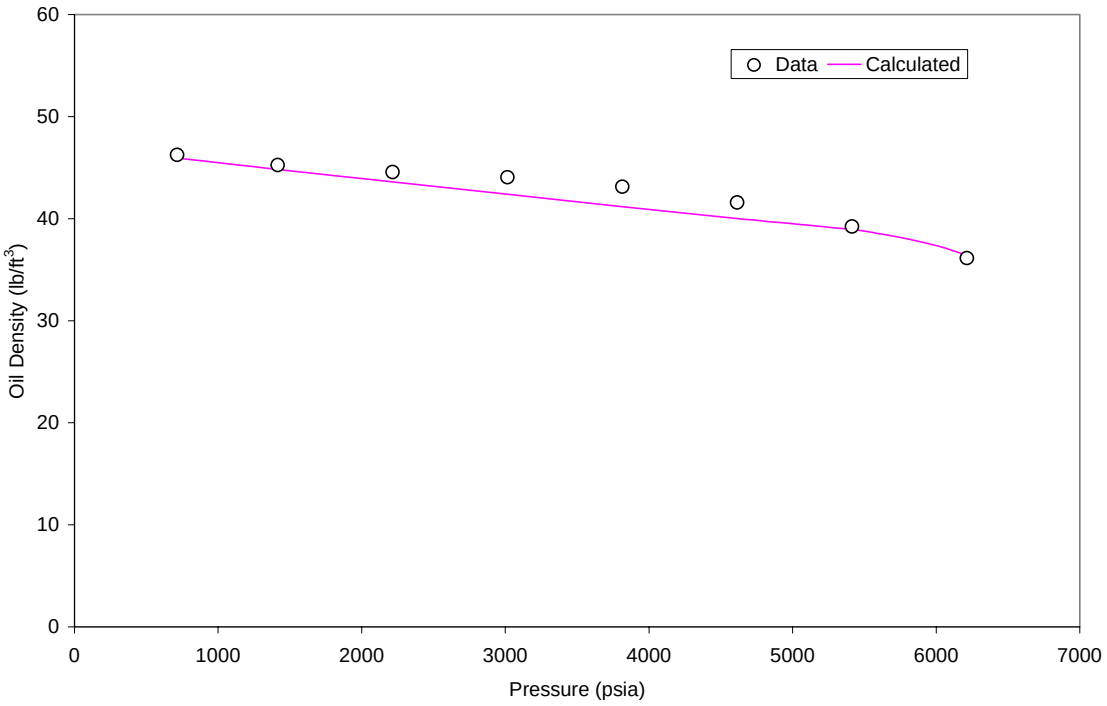

Fig. B.70- Oil density from DL experiment for fluid 17.

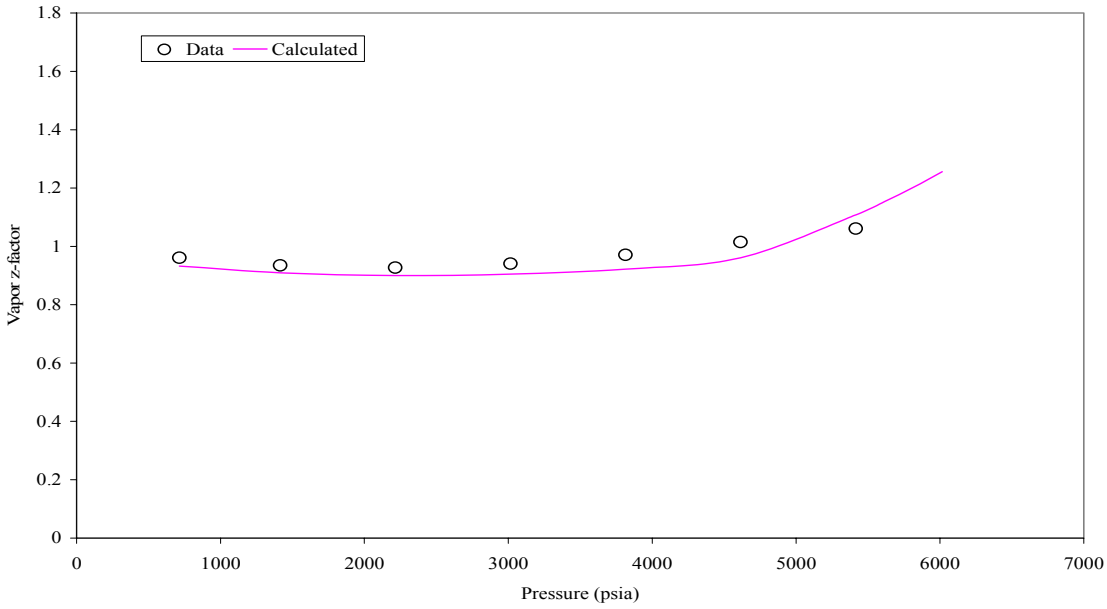

Fig. B.71- Vapor z-factor from DL experiment for fluid 17.

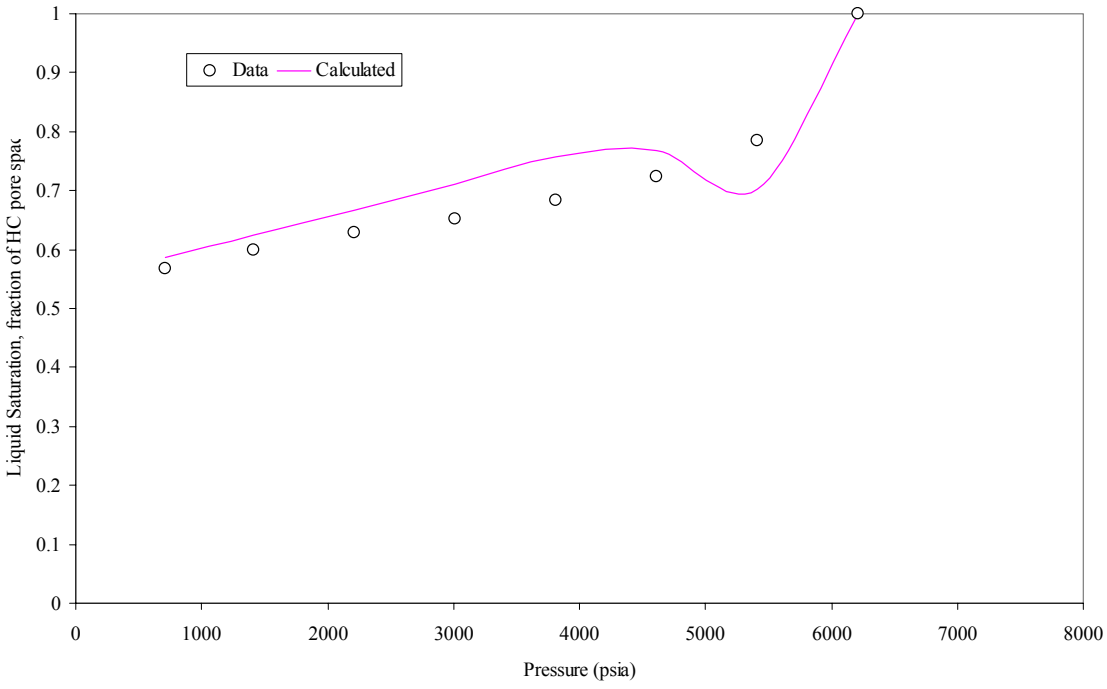

Fig. B.72- Liquid saturation from DL experiment for fluid 17.

Fluid 18 (T_{res} = 302 °F)

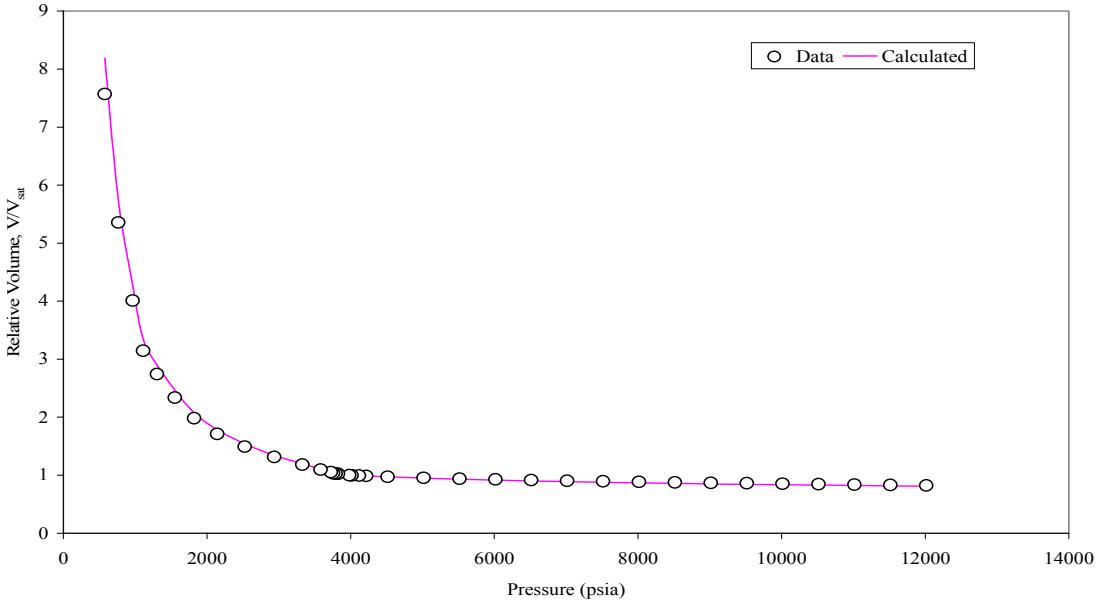

Fig. B.73- Relative volume from CCE experiment for fluid 18.

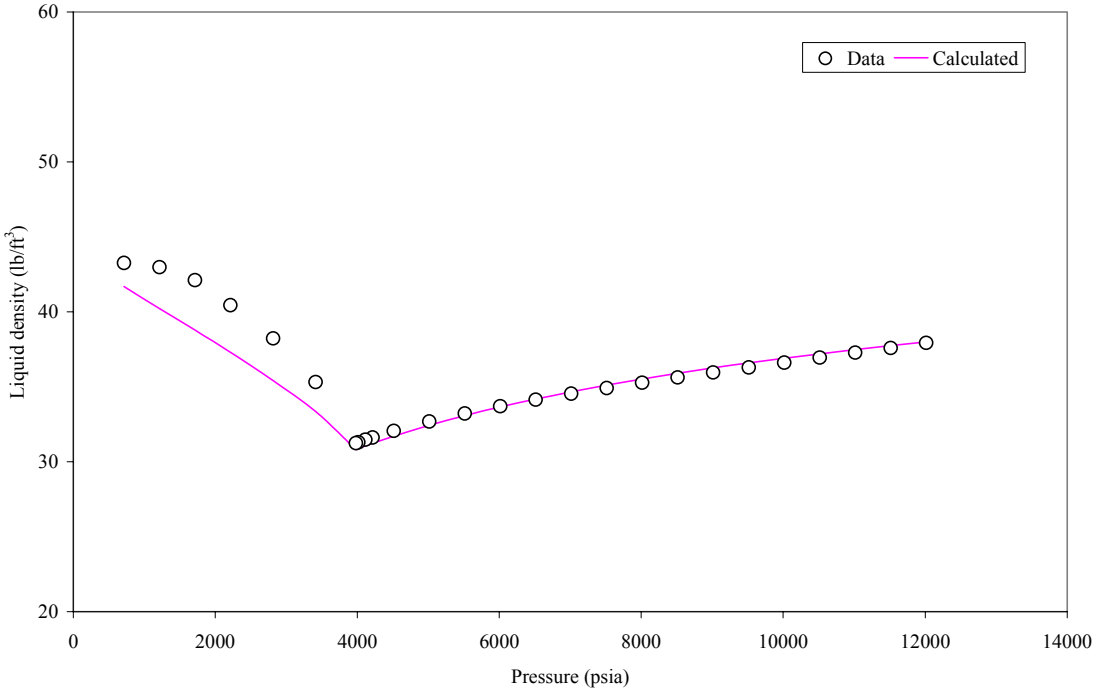

Fig. B.74- Oil density from CCE experiment for fluid 18.

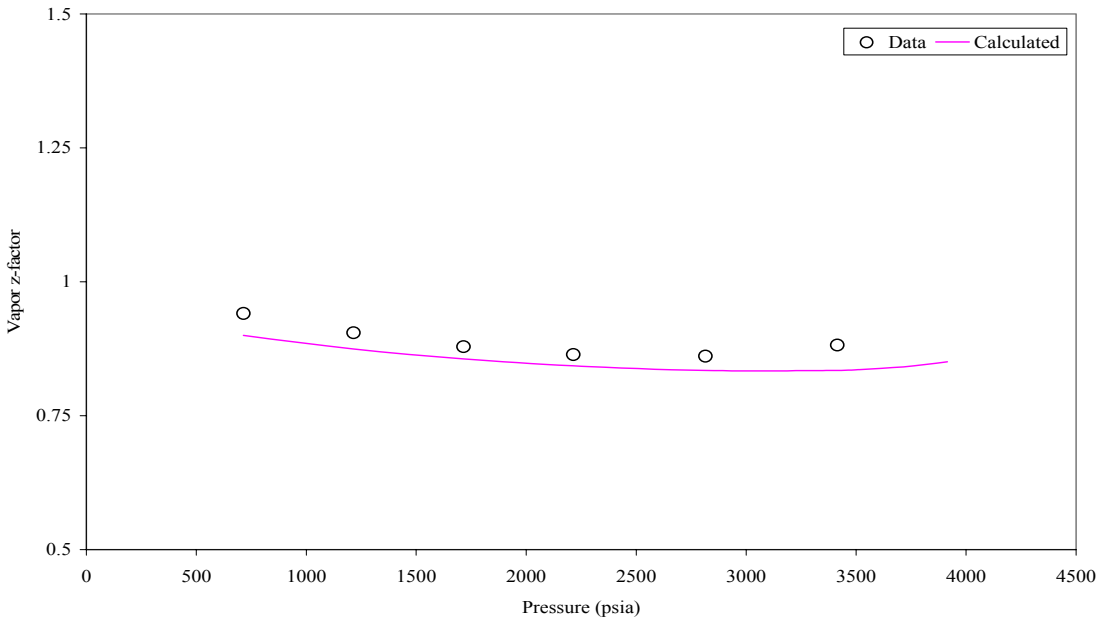

Fig. B.75- Vapor z-factor from DL experiment for fluid 18.

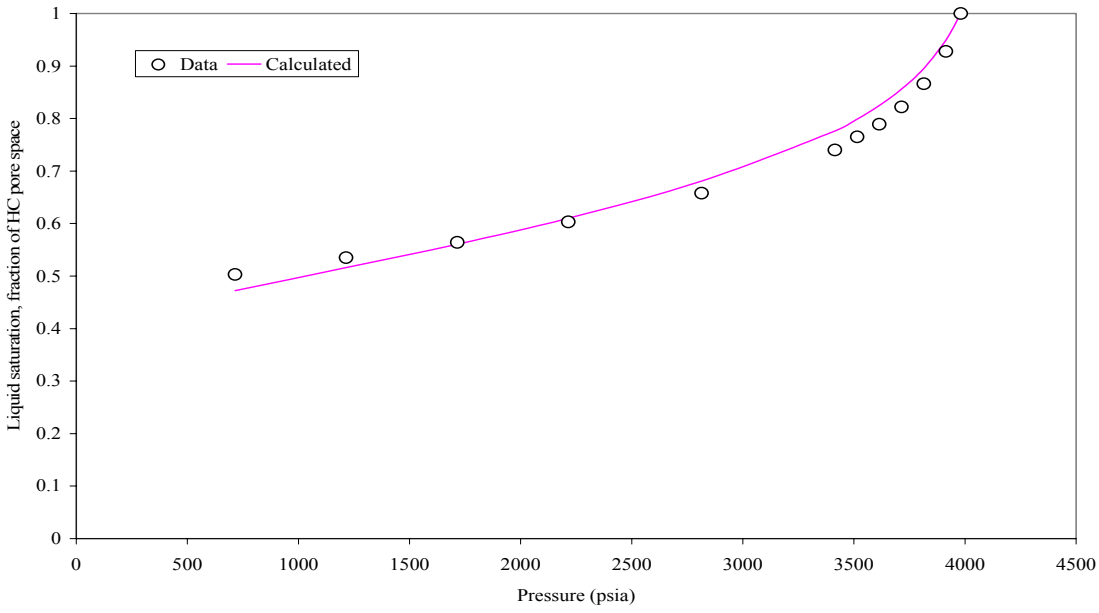

Fig. B.76- Liquid saturation from DL experiment for fluid 18.

Fluid 19 (T_{res} = 220 °F)

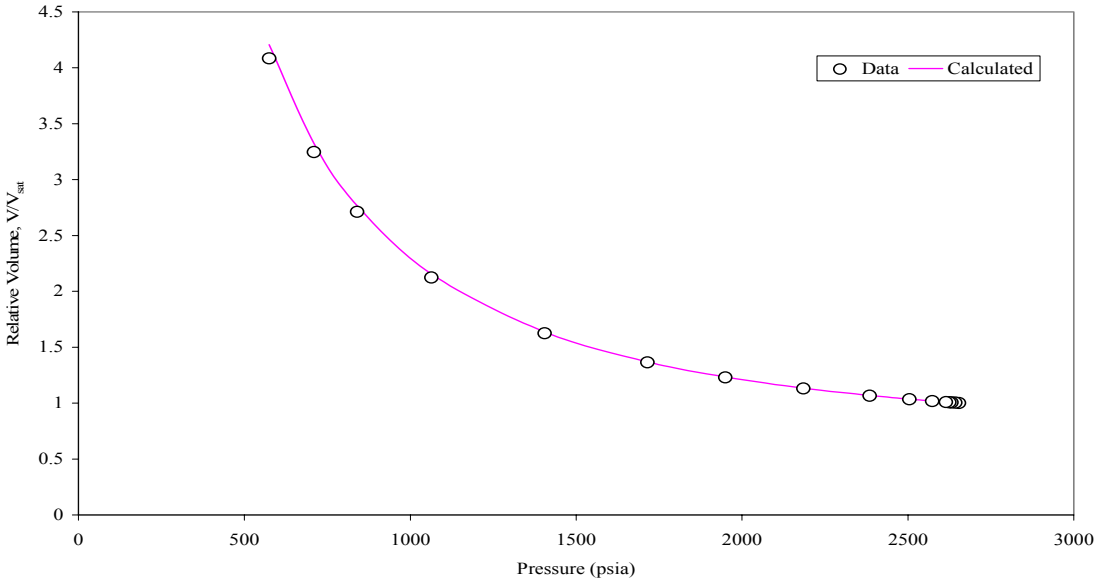

Fig. B.77- Relative volume from CCE experiment for fluid 19.

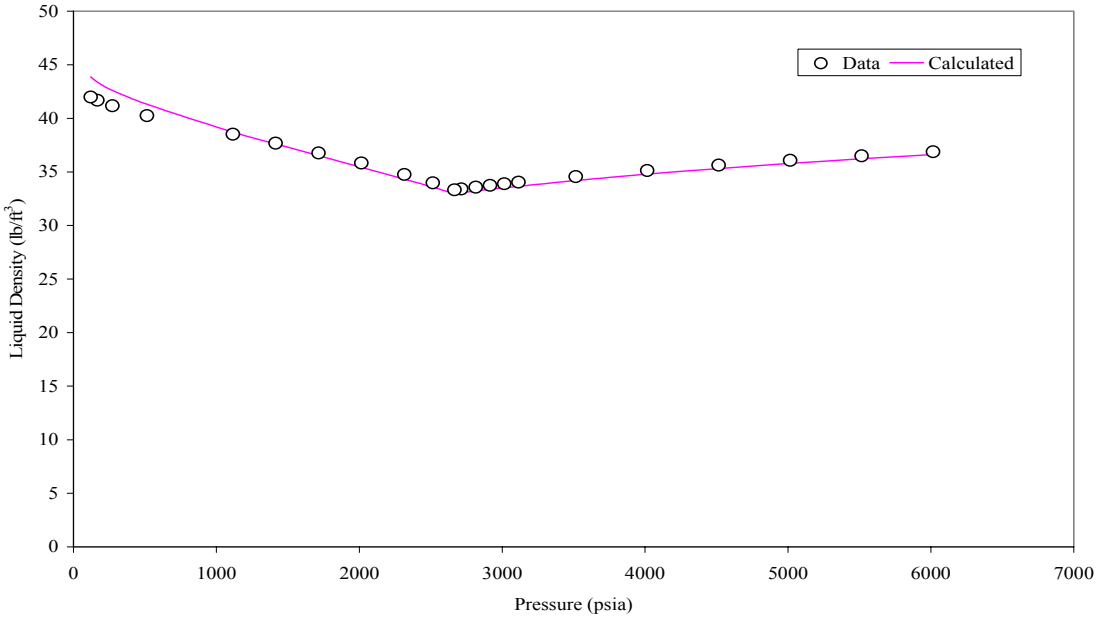

Fig. B.78- Liquid density from CCE experiment for fluid 19.

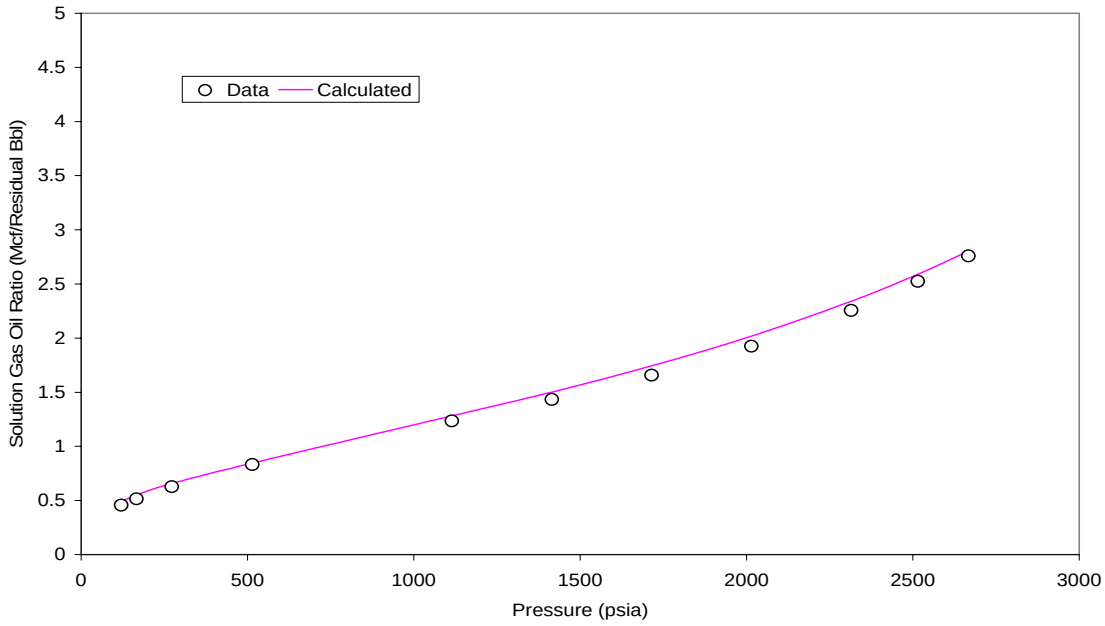

Fig. B.79- Solution gas-oil ratio from DL experiment for fluid 19.

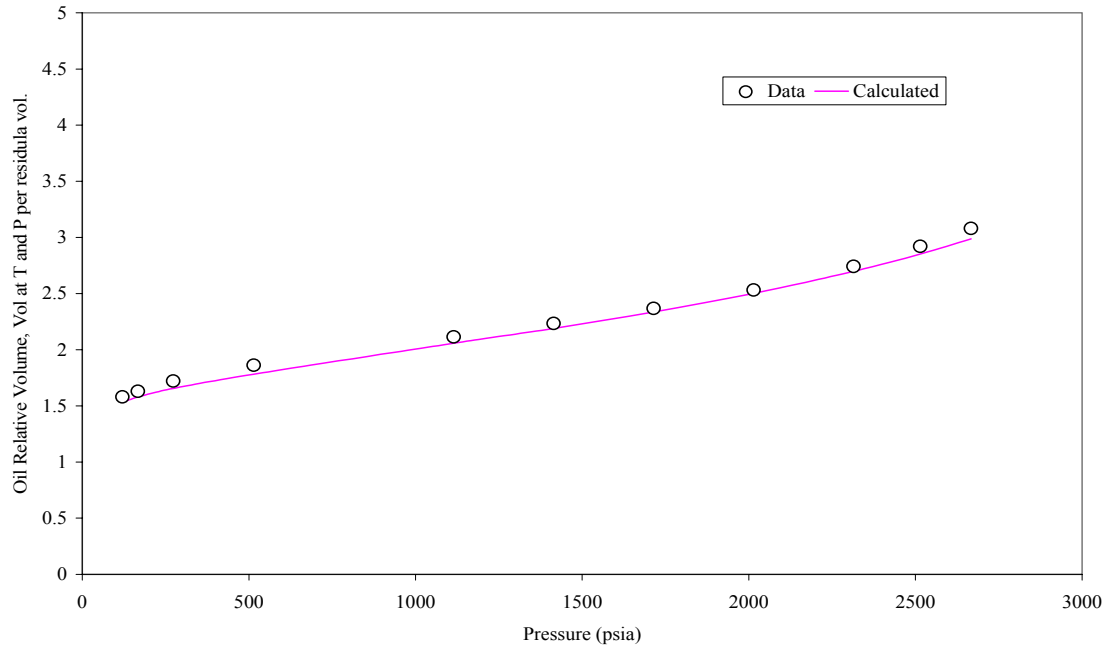

Fig. B.80- Oil relative volume from DL experiment for fluid 19.

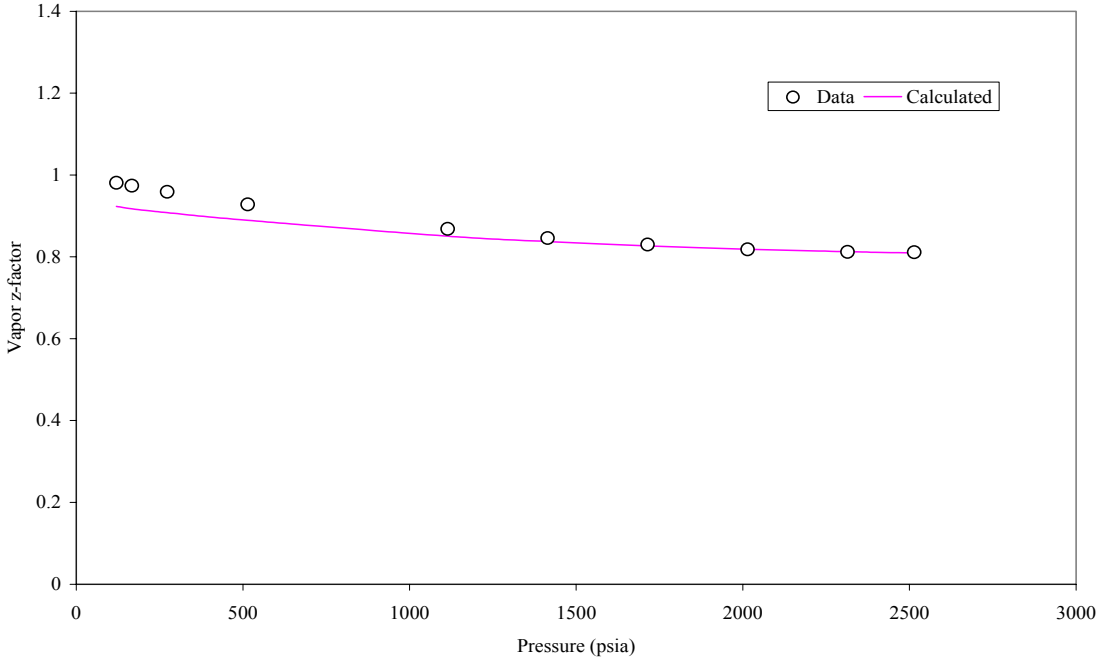

Fig. B.81- Vapor z-factor from DL experiment for fluid 19.

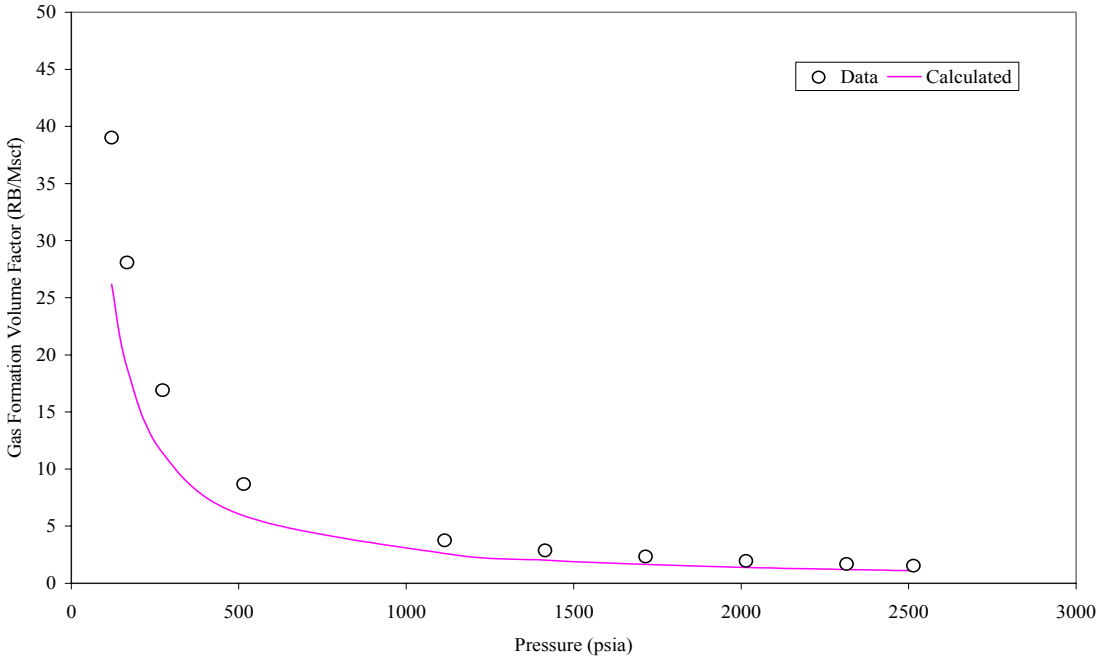

Fig. B.82- Gas formation volume factor from DL experiment for fluid 19.

Fluid 20 (T_{res} = 185 °F)

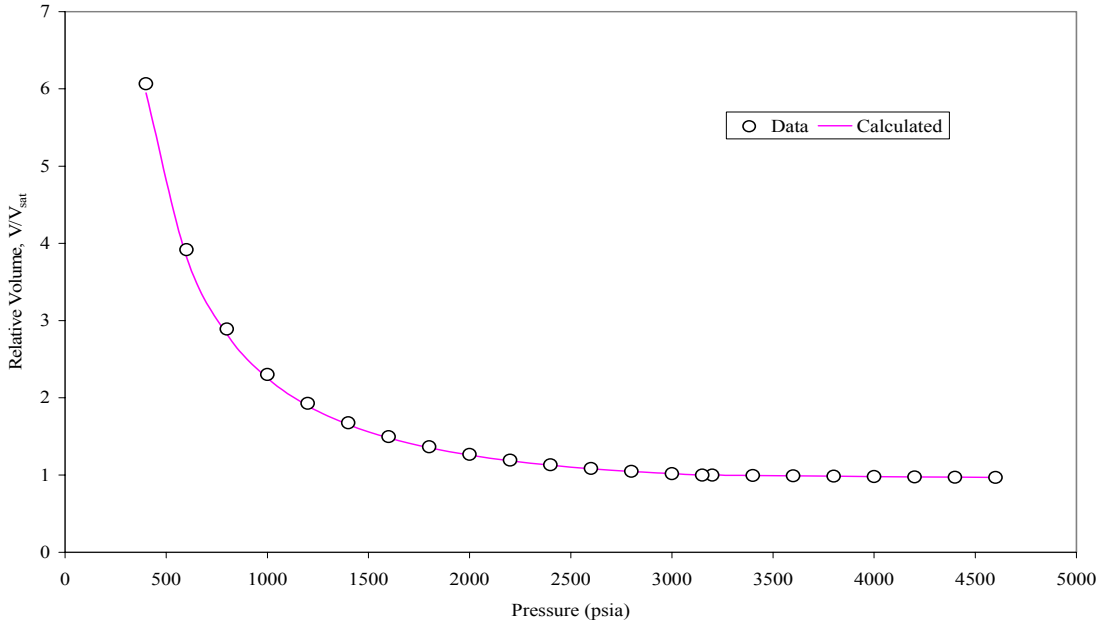

Fig. B.83- Relative volume from CCE experiment for fluid 20.

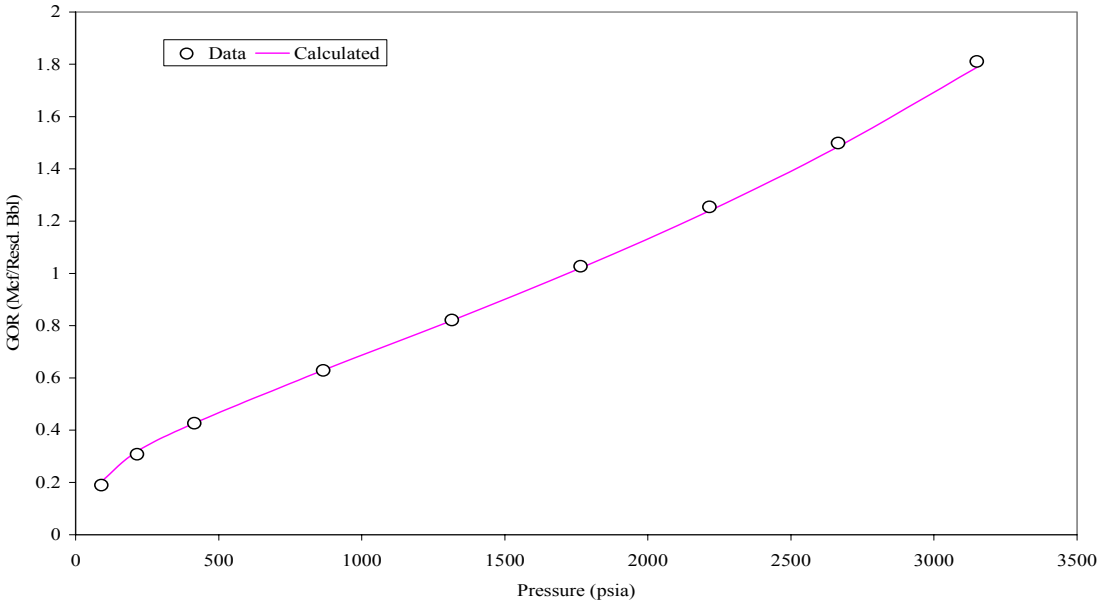

Fig. B.84- Gas oil ratio factor from DL experiment for fluid 20.

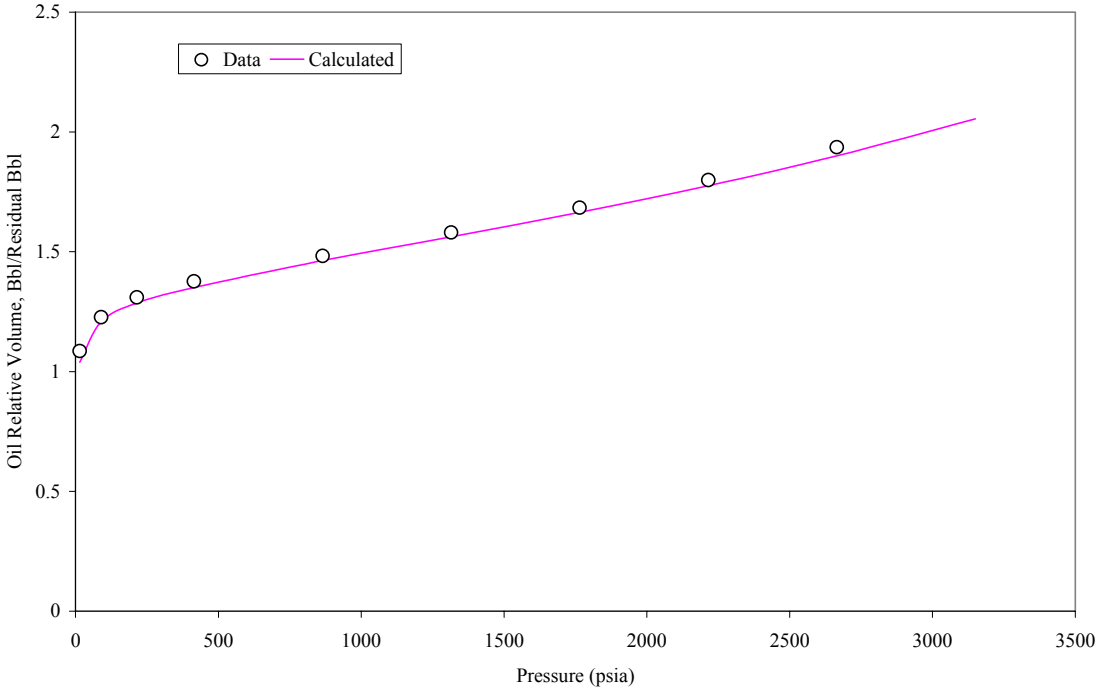

Fig. B.85- Oil relative volume from DL experiment for fluid 20.

Fluid 21 (T_{res} = 300 °F)

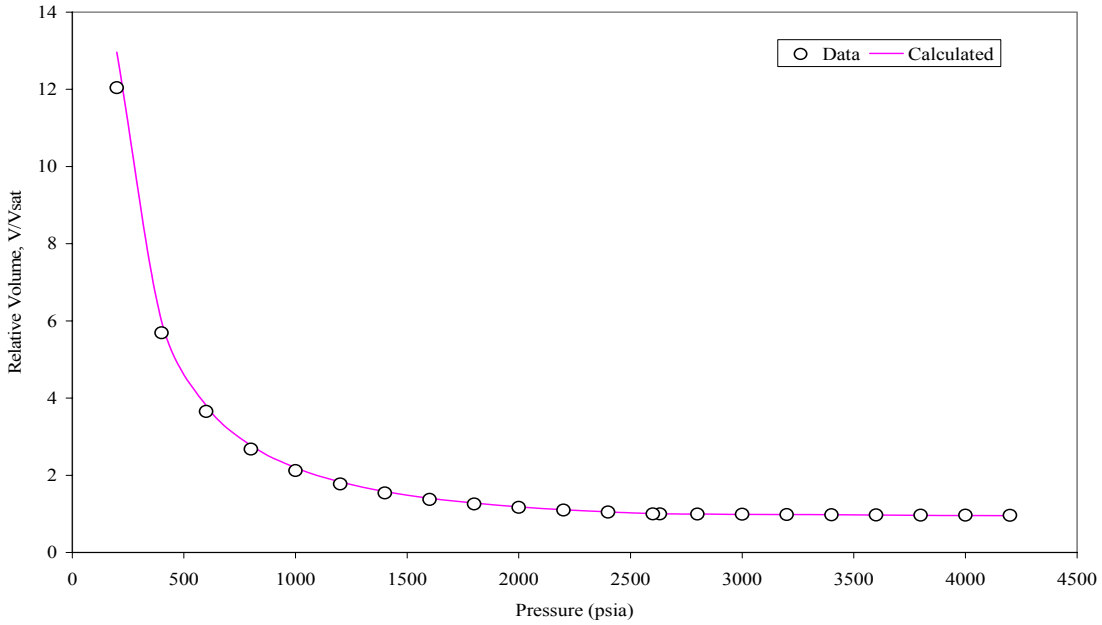

Fig. B.86- Relative volume from CCE experiment for fluid 21.

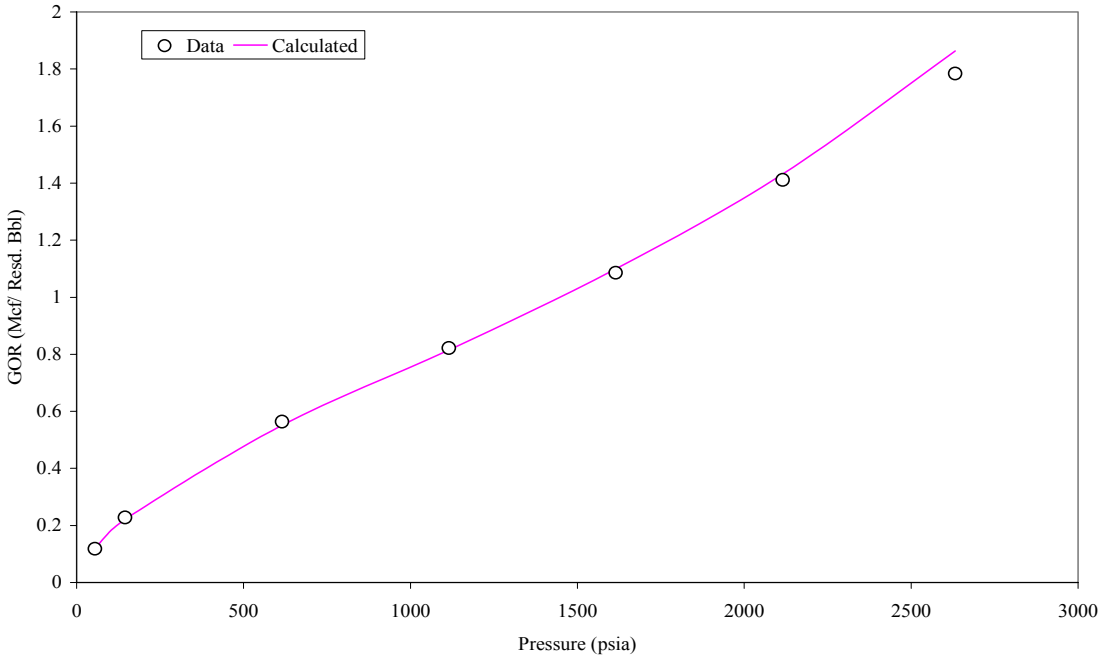

Fig. B.87- Gas oil ratio factor from DL experiment for fluid 21.

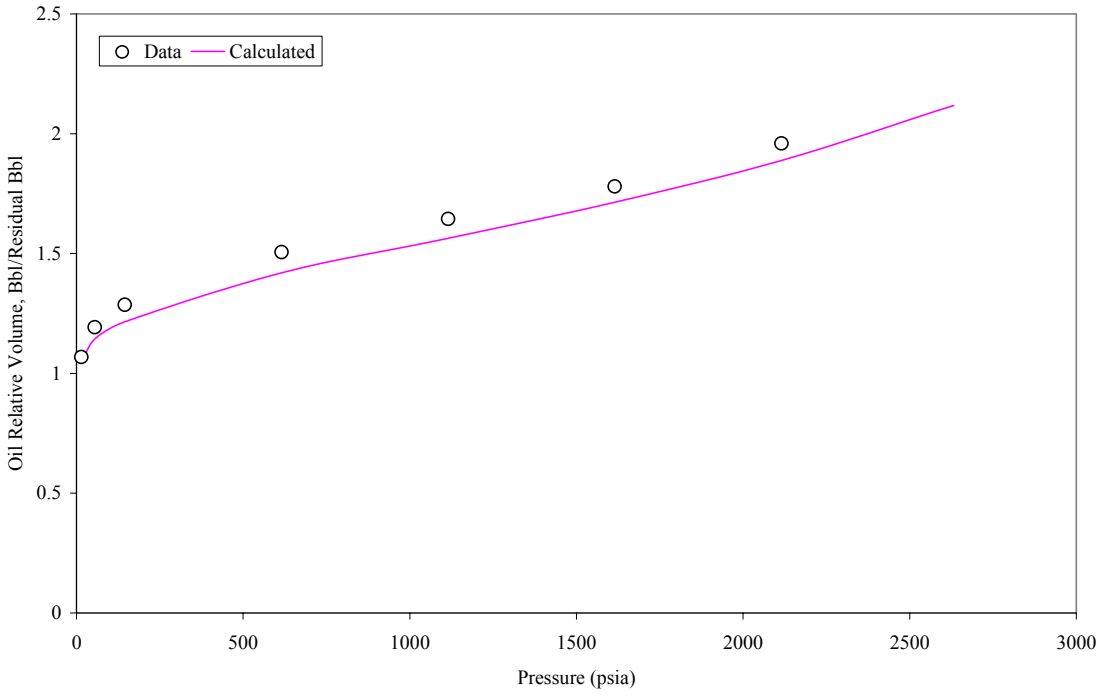

Fig. B.88- Oil relative volume from DL experiment for fluid 21.

Fluid 22 (T_{res} = 235 °F)

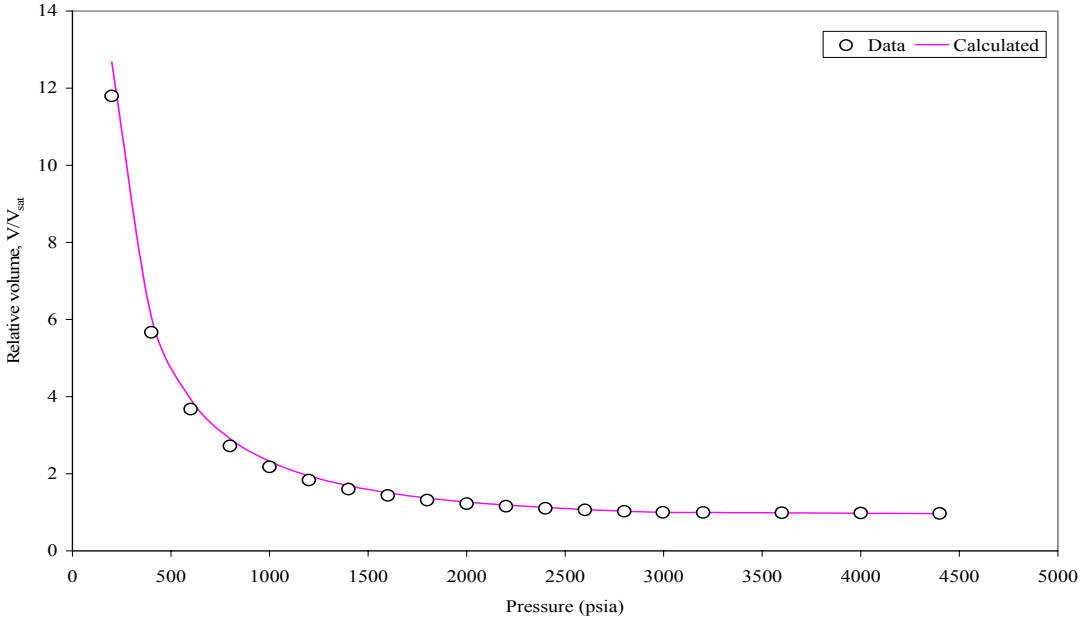

Fig. B.88- Relative volume from CCE experiment for fluid 22.

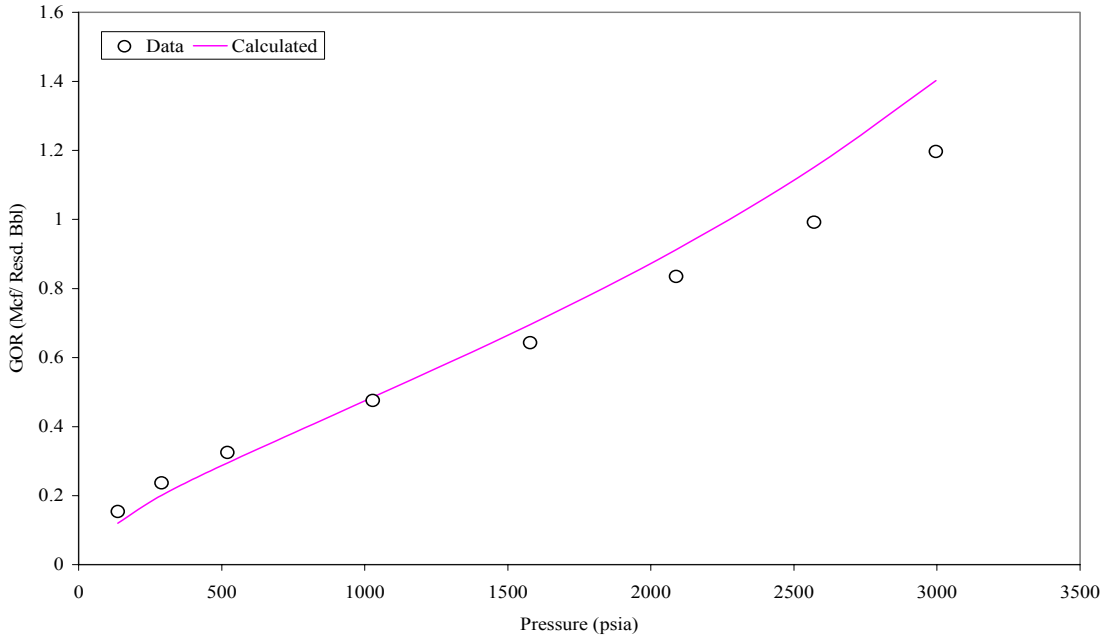

Fig. B.89- Gas oil ratio factor from DL experiment for fluid 22.

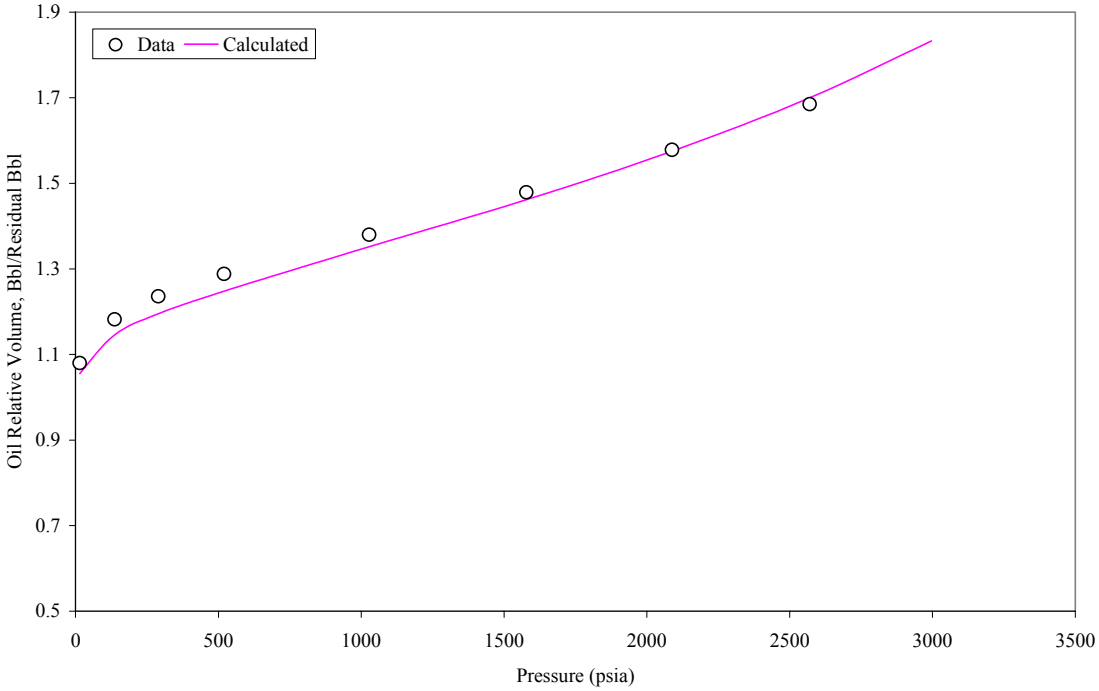

Fig. B.90- Oil relative volume from DL experiment for fluid 22.

Fluid 4 (matching at temperature of 225 ºF)

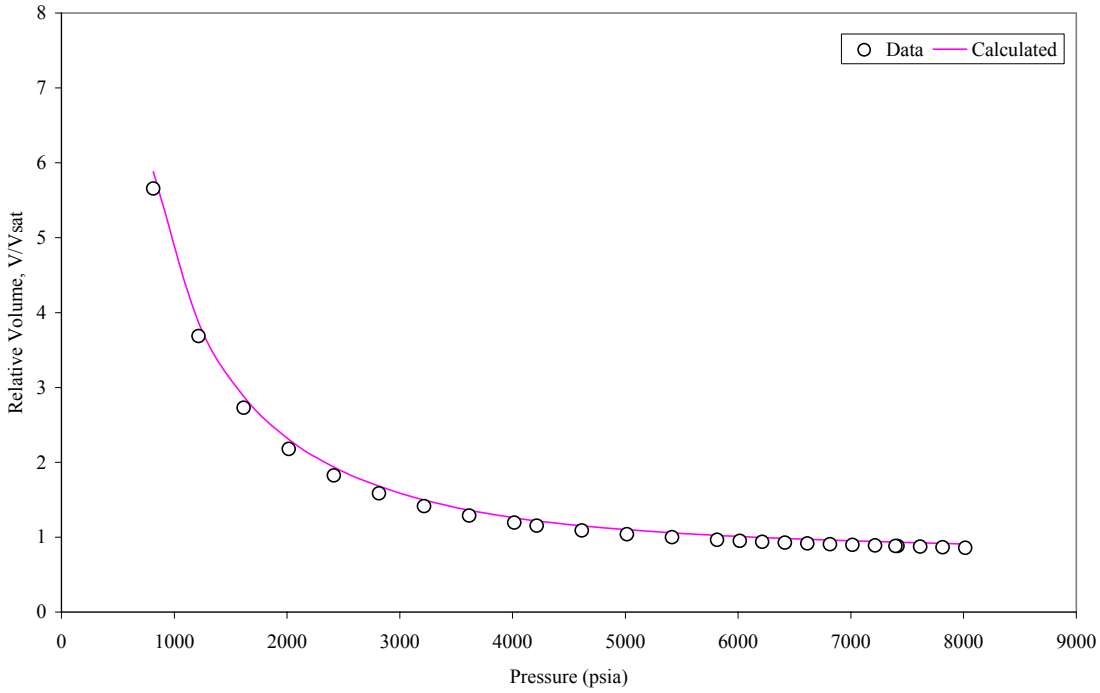

Fig. B.91- Relative volume from CCE experiment for fluid 4 at 225 ºF.

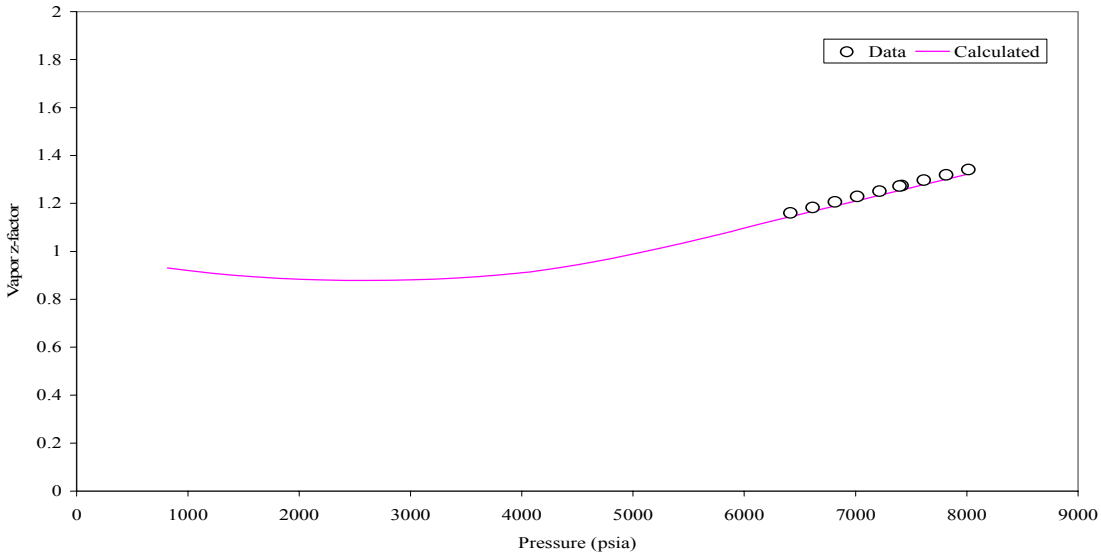

Fig. B.92- Vapor z-factor from CCE experiment for fluid 4 at 225 ºF.

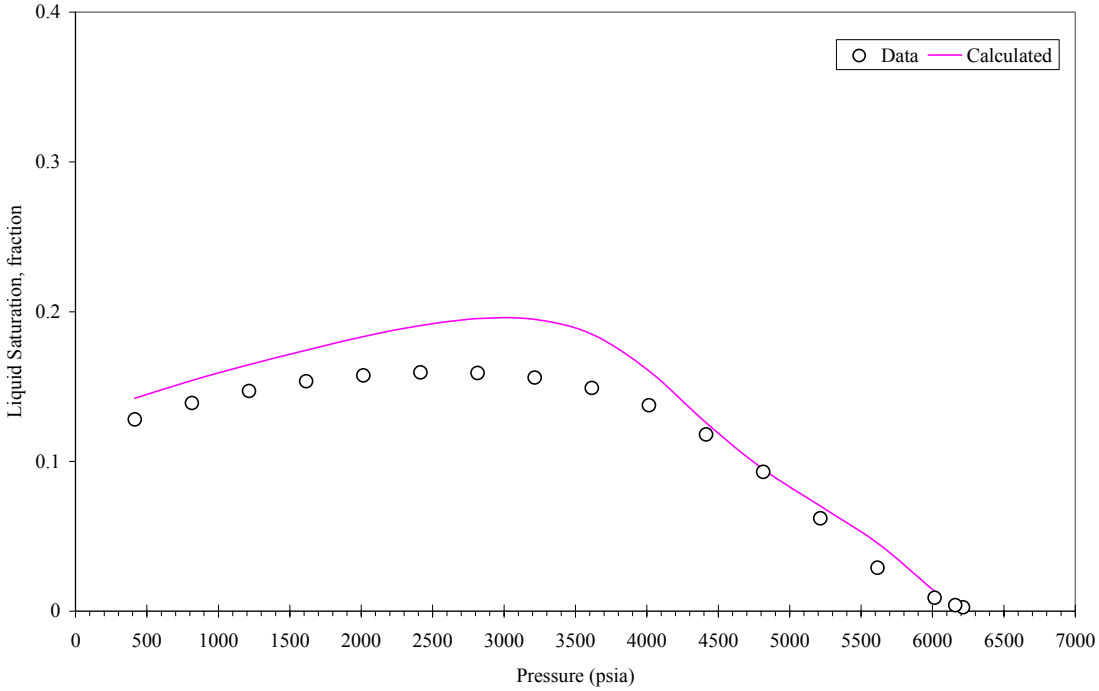

Fig. B.93- Liquid saturation from CVD experiment for fluid 4 at 225 ºF.

Fluid 4 (matching at temperature of 150 ºF)

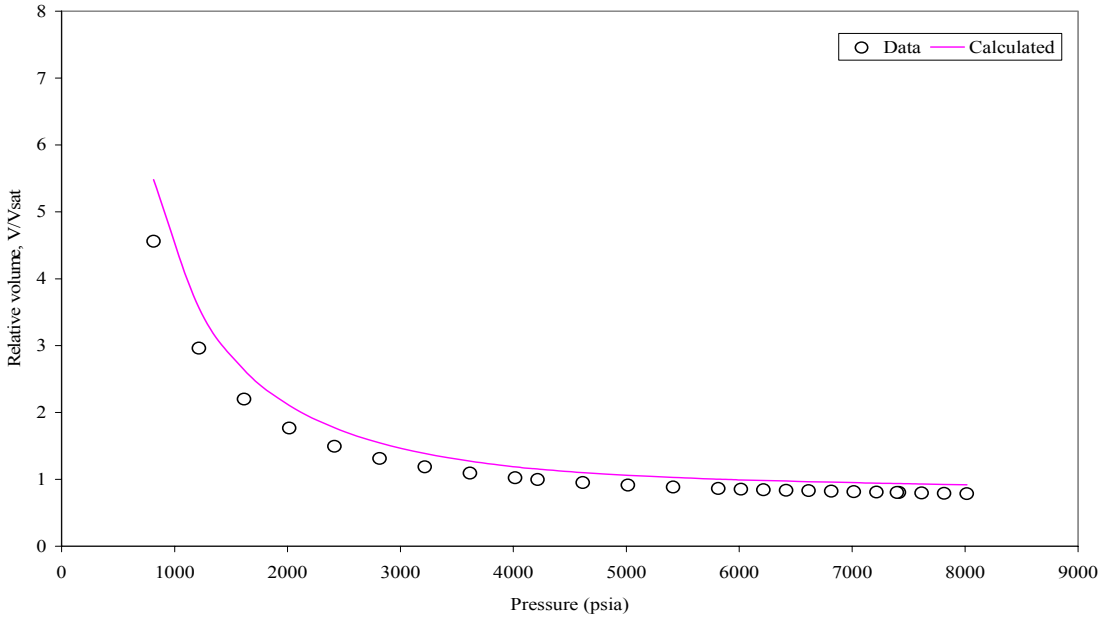

Fig. B.94- Relative volume from CCE experiment for fluid 4 at 150 ºF.

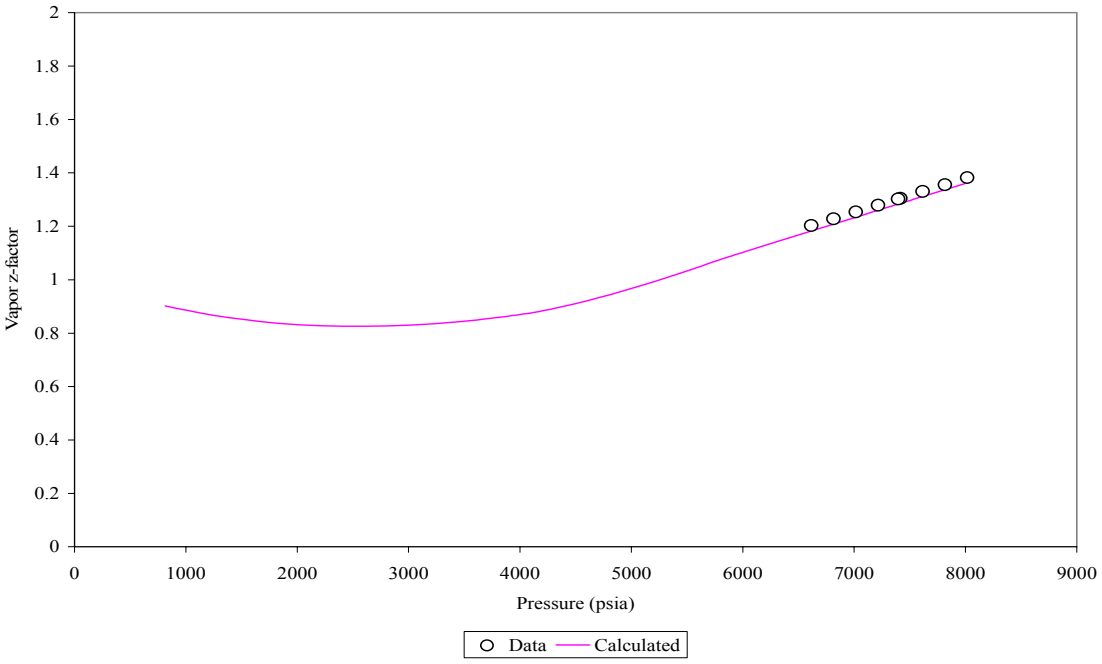

Fig. B.95- Vapor z-factor from CCE experiment for fluid 4 at 150 ºF.

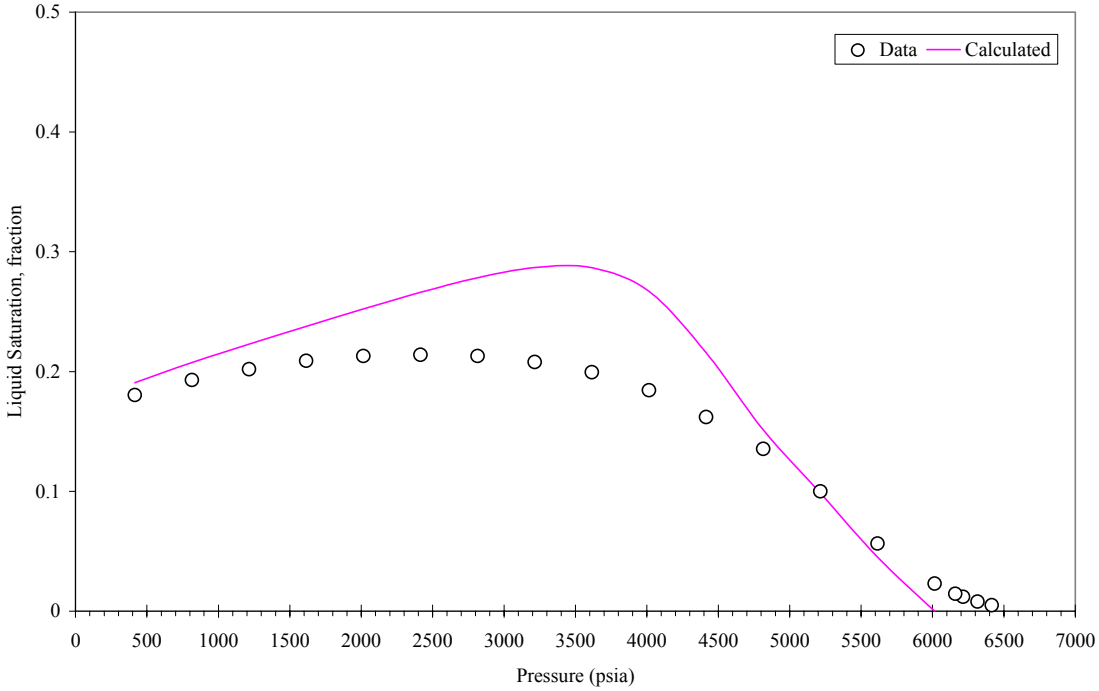

Fig. B.96 - Liquid saturation from CVD experiment for fluid 4 at 150 ºF.

Fluid 4 (matching at temperature of 100 ºF)

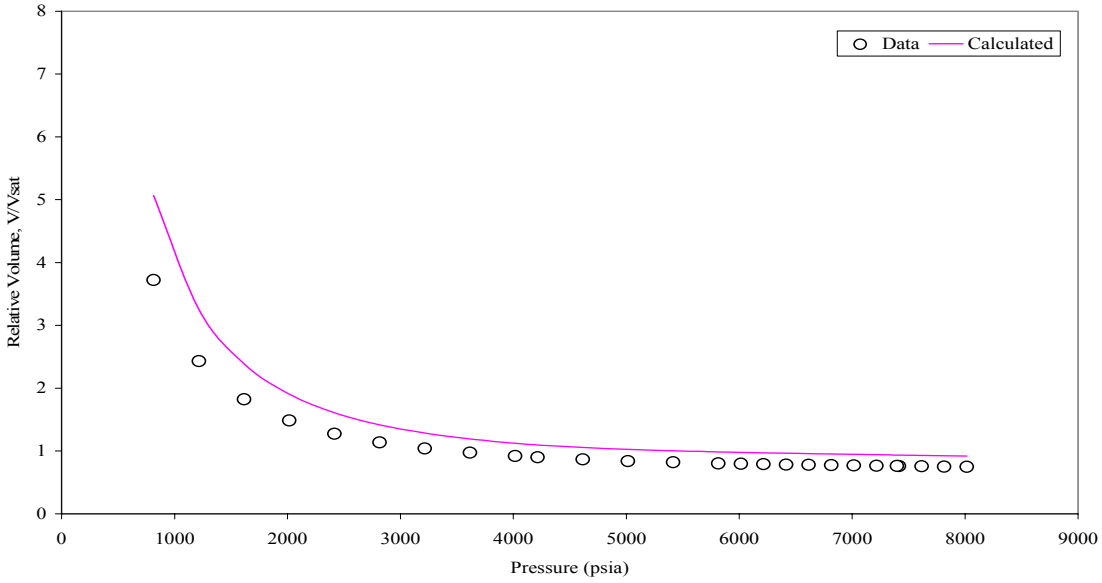

Fig. B.97 - Relative volume from CCE experiment for fluid 4 at 100 ºF.

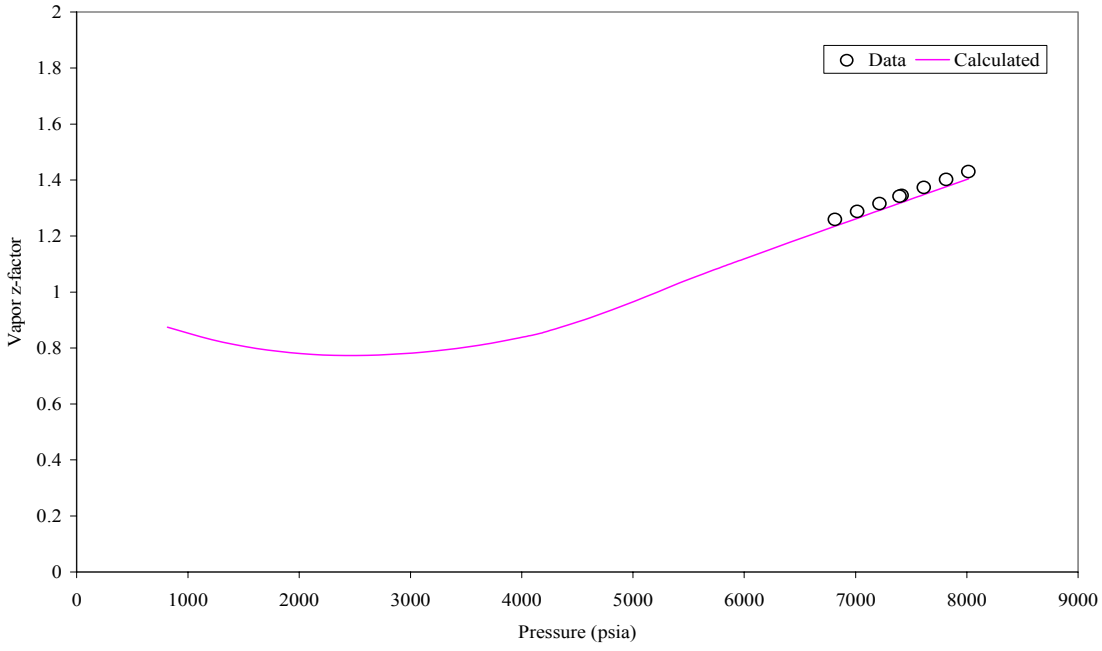

Fig. B.98- Vapor z-factor from CCE experiment for fluid 4 at 100 ºF.

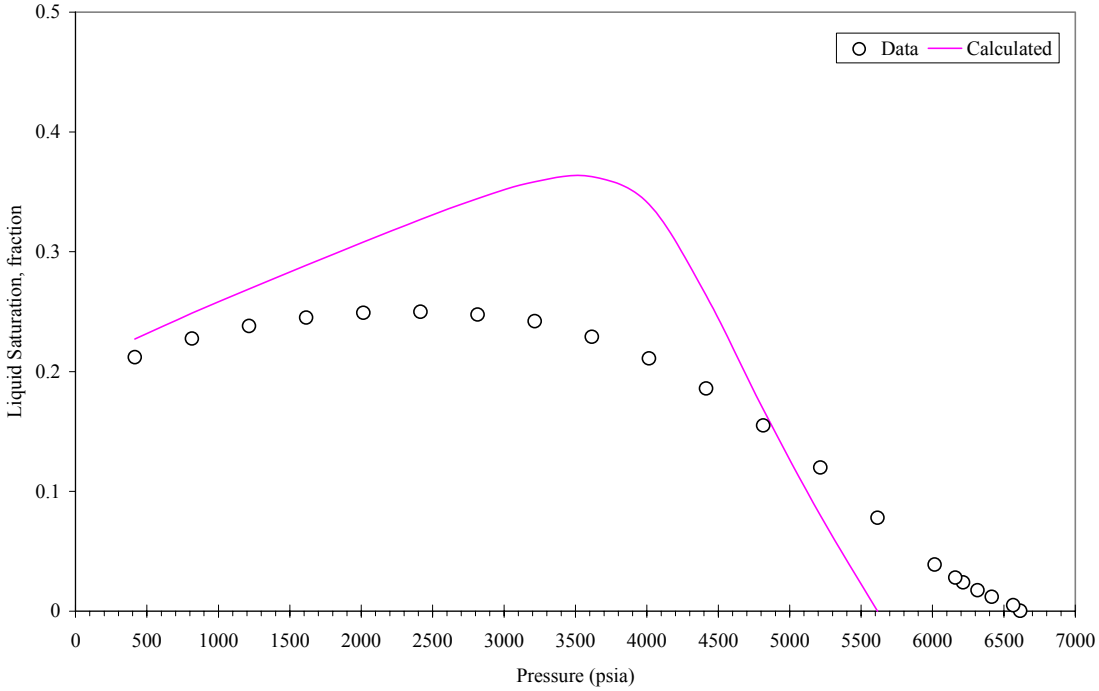

Fig. B.99- Liquid saturation from CVD experiment for fluid 4 at 100 ºF.

Fluid 11 (Matching at reservoir temperature of 275 ºF)

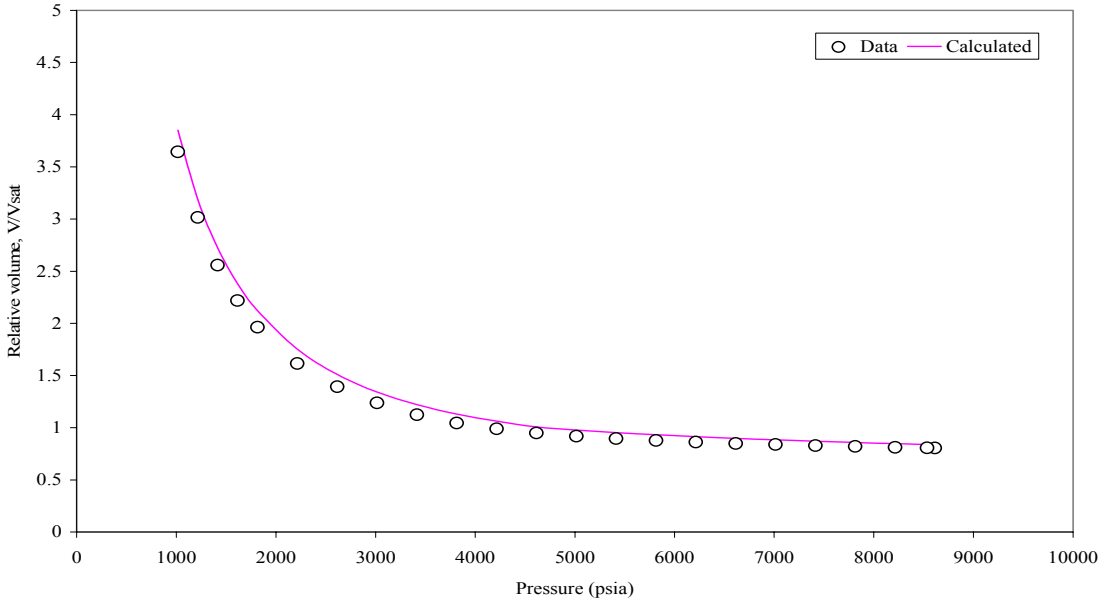

Fig. B.100- Relative volume from CCE experiment for fluid 11 at 275 ºF.

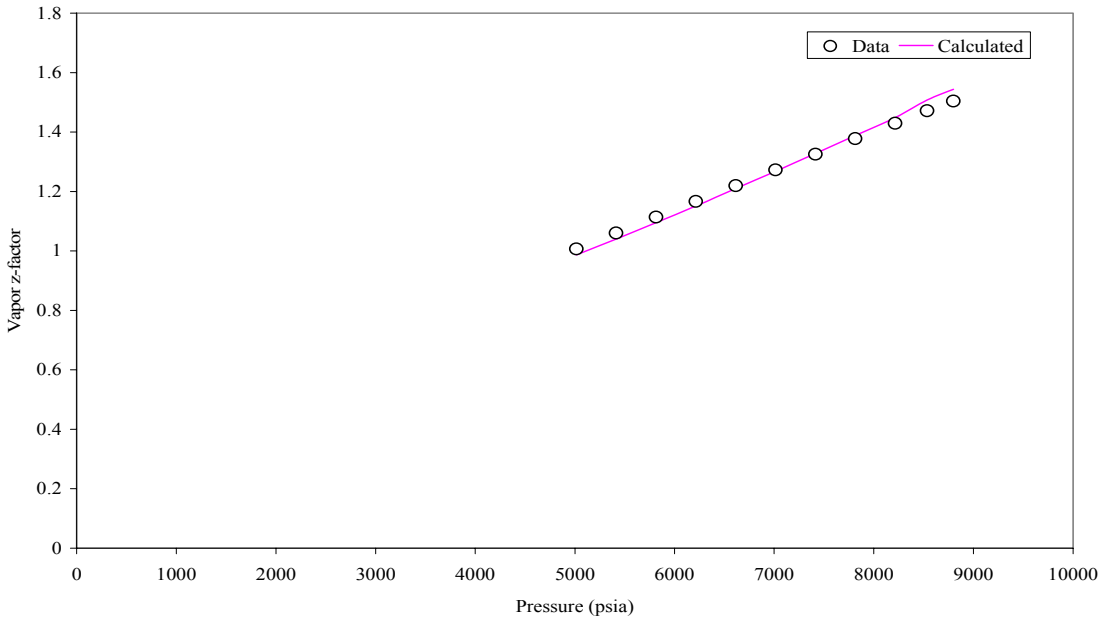

Fig. B.101- Vapor z-factor from CCE experiment for fluid 11 at 275 ºF.

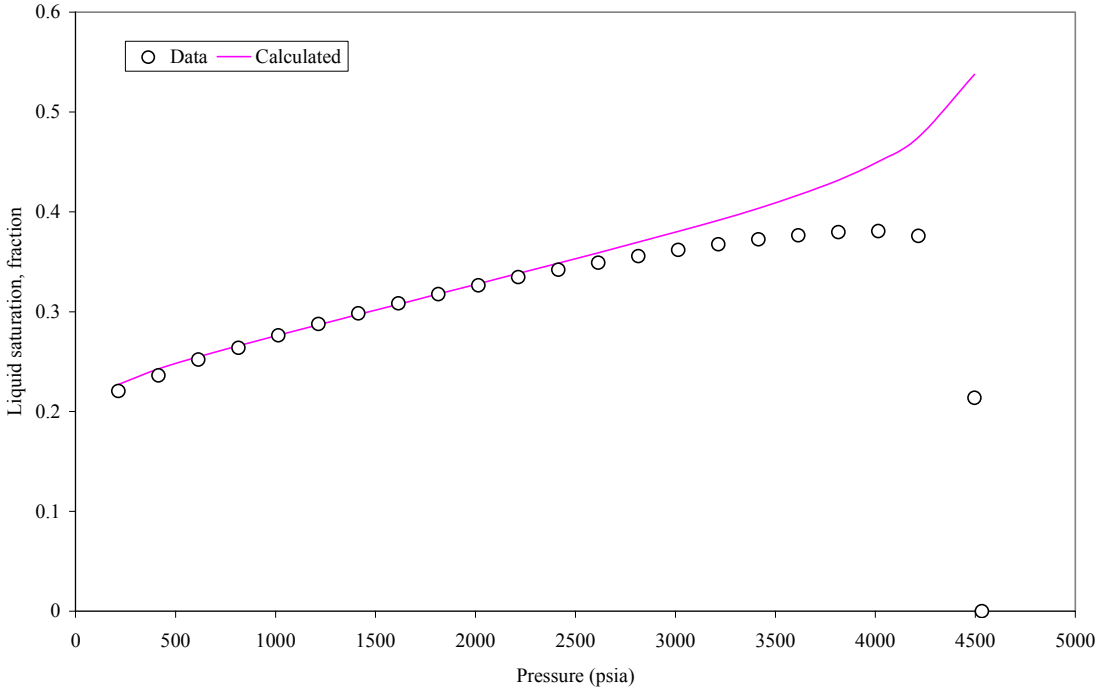

Fig. B.102- Liquid saturation from CVD experiment for fluid 11 at 275 ºF.

Fluid 11 (Matching at reservoir temperature of 250 ºF)

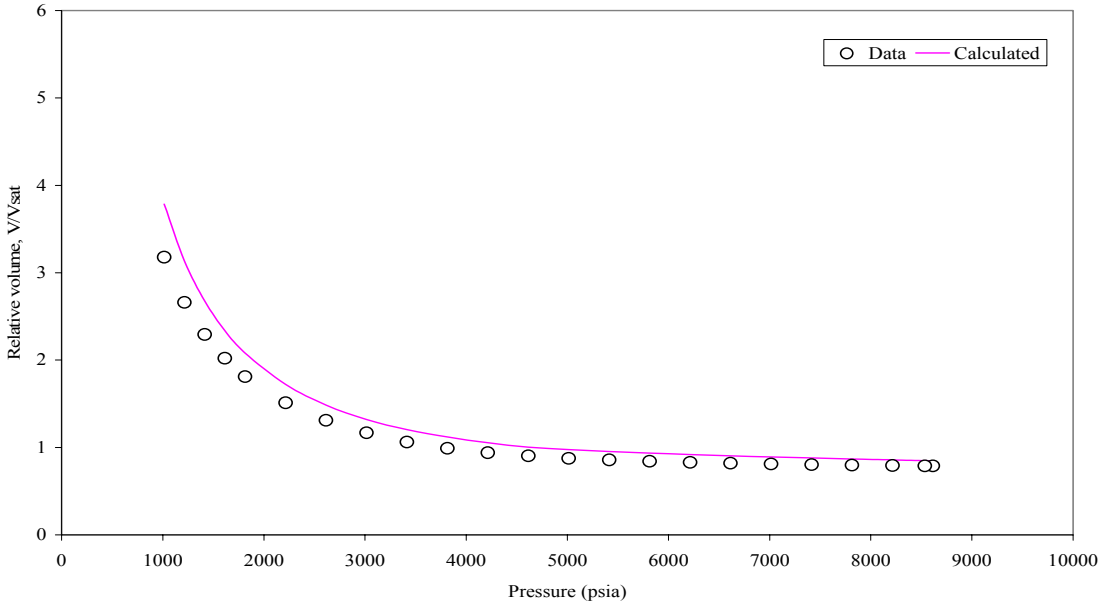

Fig. B.103- Relative volume from CCE experiment for fluid 11 at 250 ºF.

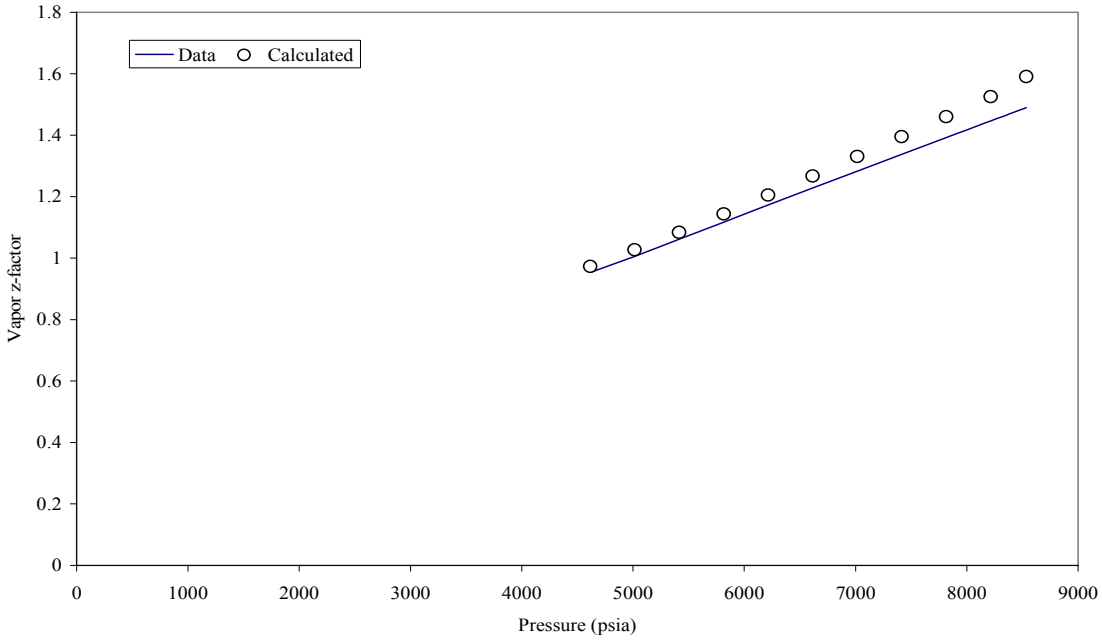

Fig. B.104- Vapor z-factor from CCE experiment for fluid 11 at 250 ºF.

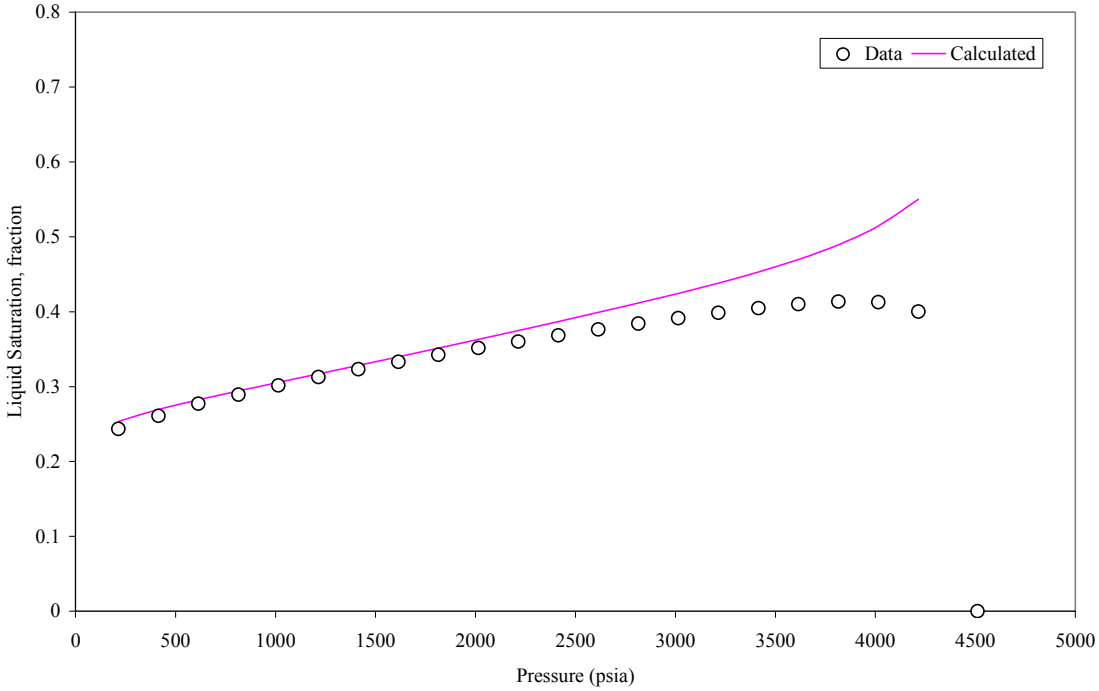

Fig. B.105- Liquid saturation from CVD experiment for fluid 11 at 250 ºF.

APPENDIX C

PVT DATA FOR GAS CONDENSATE SAMPLES

VOLUMETRIC DATA FOR FLUID – 1

Table C-1- Well stream analysis for Fluid 1

Component	Mole fraction
H_2S	0.0394
N_2	0.1086
CO_2	0.0238
C_1	0.6643
C_2	0.065
C_3	0.0281
IC_4	0.0052
NC_4	0.0103
IC_5	0.0032
NC_5	0.0034
C_6	0.0057
C_7	0.0086
C_8	0.009
C_9	0.0068
C_{10}	0.0045
C_{11}	0.002
C_{12}^+	0.0121
Sp. Gr. C_{12}^+	0.8438
MW C_{12}^+	226

Table C-2- Relative volume from Constant Composition Expansion experiment at three different temperatures (reservoir temperature is 262 ºF) for Fluid 1

	150 ºF	**200 ºF**	**262 ºF**
Pressure (psia)	**Relative Volume, V/V_{sat}**		
8000	0.743	0.7935	0.8539
7800	0.7483	0.8002	0.8624
7600	0.7561	0.8101	0.8749
7525	0.7539	0.8073	0.8714
7400	0.7599	0.8149	0.881
7200	0.7663	0.823	0.8913
7000	0.7731	0.8317	0.9022
6800	0.7805	0.8409	0.9139
6600	0.7883	0.8509	0.9265
6400	0.7968	0.8616	0.9401
6200	0.806	0.8732	0.9547
6000	0.8159	0.8858	0.9706
5800	0.8267	0.8992	0.9878
5600	0.8385	0.9143	1.0066
5400	0.8514	0.9307	1.0271
5200	0.8657	0.9486	1.0497
4800	0.899	0.9907	1.1024
4600	0.9186	1.0154	1.1333
4400	0.9408	1.0433	1.1679
4200	0.966	1.0749	1.2071
4000	0.9949	1.1111	1.2516
3800	1.0283	1.1527	1.3025
3600	1.0674	1.2011	1.3611
3400	1.1134	1.2578	1.4289
3200	1.1682	1.3246	1.5076
Dew Points			
5668			1
5928		0.8906	
6091	0.8113		

Table C-3- Deviation factor from Constant Composition Expansion experiment at three different temperatures (reservoir temperature is 262 ºF) for Fluid 1			
	150 ºF	**200 ºF**	**262 ºF**
Pressure (psia)	**z-factor**		
8000	1.351	1.334	1.312
7600	1.303	1.289	1.272
7525	1.294	1.281	1.265
7200	1.255	1.245	1.233
6800	1.207	1.202	1.194
6400	1.16	1.159	1.156
6200	1.136	1.138	1.137
6000	1.113	1.117	1.119
5800	1.09	1.096	1.101
Dew Points			
5668			1.089
5928		1.109	
6091	1.124		

Table C-4- Deviation factor for equilibrium gas and two phases from Constant Volume Depletion experiment at reservoir temperature, 262 ºF, for Fluid 1		
	z-factor	
Pressure (psig)	**Equilibrium Gas**	**Two Phase**
5653	1.089	1.089
4800	1.025	1.018
4000	0.98	0.965
3200	0.949	0.935
2400	0.935	0.92
1600	0.937	0.925
800	0.96	0.952

Table C-5- Retrograde Liquid Volume from Constant Volume Depletion experiment at three different temperatures (reservoir temperature is 262 ºF), for Fluid 1

	150 ºF	**200 ºF**	**262 ºF**
Pressure (psig)	**% of hydrocarbon pore space**		
6076	Dew P.	-----	-----
5913	0.23	Dew P.	-----
5653	1.09	0.19	Dew P.
4800	6.38	4.11	1.69
4600	7.65	5.34	2.46
4400	8.81	6.45	3.25
4200	9.85	7.39	4.02
4000	10.76	8.16	4.72
3800	11.54	8.78	5.34
3600	12.21	9.29	5.89
3200	13.22	10.04	6.76
2800	13.86	10.54	7.36
2400	14.18	10.81	7.73
2000	14.22	10.84	7.86
1600	14.02	10.66	7.77
1200	13.59	10.28	7.49
800	12.93	9.7	7.07
400	12.06	8.92	6.52
0	11	7.91	5.9

VOLUMETRIC DATA FOR FLUID – 2

Table C-6- Well stream analysis for Fluid 2	
Component	**Mole fraction**
H_2S	0.0265
N_2	0.1007
CO_2	0.0201
C_1	0.6689
C_2	0.0685
C_3	0.0305
IC_4	0.0059
NC_4	0.0125
IC_5	0.0046
NC_5	0.005
C_6	0.0068
C_7	0.0079
C_8	0.008
C_9	0.0067
C_{10}	0.0053
C_{11}	0.0038
C_{12}^+	0.0183
Sp. Gr. C_{12}^+	0.8294
MW C_{12}^+	226

Table C-7- Relative volume and deviation factor from Constant Composition Expansion experiment at 275 °F, for Fluid 2		
Pressure (psia)	**Relative Volume, V/V_{sat}**	**z-factor**
8015	0.8617	1.375
7815	0.87	1.354
7615	0.8788	1.332
7415	0.8882	1.311
7341	0.8918	1.303
7215	0.8982	1.29
7015	0.9089	1.269
6815	0.9203	1.248
6615	0.9326	1.228
6415	0.9459	1.208
6215	0.9602	1.188
6015	0.9758	1.168
5815	0.9926	1.148
5733	1	1.141
5615	1.011	1.129
5415	1.0312	
5215	1.0533	
5015	1.0778	
4815	1.1049	
4615	1.1352	
4415	1.1691	
4215	1.2075	
4015	1.2511	
3815	1.3012	
3615	1.3592	
3415	1.4271	
3215	1.5076	

Table C-8- Deviation factor for equilibrium gas and two phases from Constant Volume Depletion experiment at reservoir temperature, 275 ºF, for Fluid 2		
	z-factor	
Pressure (psia)	**Equilibrium Gas**	**Two Phase**
5732.7	1.141	1.141
4814.7	1.058	1.054
4014.7	0.997	0.988
3214.7	0.952	0.935
2414.7	0.927	0.902
1614.7	0.925	0.897
814.7	0.95	0.924

Table C-9- Retrograde Liquid Volume from Constant Volume Depletion experiment at reservoir temperature, 275 ºF, for Fluid 2	
Pressure (psia)	**% of hydrocarbon pore space**
5732.7	0
5614.7	0.18
5414.7	0.64
5214.7	1.47
5014.7	2.64
4814.7	4
4614.7	5.35
4414.7	6.51
4014.7	8.07
3814.7	8.53
3614.7	8.85
3414.7	9.07
3014.7	9.32
2814.7	9.4
2614.7	9.45
2214.7	9.5
2014.7	9.5
1614.7	9.44
1214.7	9.3
814.7	9.05
414.7	8.68
14.7	8.18

VOLUMETRIC DATA FOR FLUID – 3

Table C-10- Well stream analysis for Fluid 3	
Component	**Mole fraction**
H_2S	0
N_2	0.0312
CO_2	0.0323
C_1	0.6976
C_2	0.0903
C_3	0.0402
IC_4	0.0081
NC_4	0.0144
IC_5	0.006
NC_5	0.0055
C_6	0.0096
C_7	0.011
C_8	0.0127
C_9	0.0086
C_{10}	0.0061
C_{11}	0.0029
C_{12}^+	0.0234
Sp. Gr. C_{12}^+	0.8463
MW C_{12}^+	252

Table C-11- Relative volume and deviation factor from Constant Composition Expansion experiment at 305 °F, for Fluid 3		
Pressure (psia)	**Relative Volume, V/V_{sat}**	**z-factor**
9015	0.839	1.406
8815	0.8458	1.386
8015	0.877	1.307
7815	0.8859	1.287
7615	0.8951	1.267
7415	0.9054	1.248
7215	0.9161	1.228
7015	0.927	1.209
6815	0.9396	1.19
6615	0.9526	1.171
6415	0.9666	1.152
6215	0.9815	1.133
6015	0.9977	1.115
5988	1	1.112
5815	1.0152	
5615	1.0342	
5415	1.0549	
5215	1.0775	
5015	1.1024	
4815	1.1298	
4615	1.1602	
4415	1.1941	
4215	1.2332	
4015	1.2753	
3815	1.3243	
3615	1.3808	
3415	1.4463	
3215	1.5233	

Table C-12- Deviation factor for equilibrium gas and two phases from Constant Volume Depletion experiment at reservoir temperature, 275 ºF, for Fluid 3		
	z-factor	
Pressure (psia)	**Equilibrium Gas**	**Two Phase**
5988	1.112	1.112
4815	1.018	1.01
4015	0.973	0.96
4015	0.934	0.918
3215	0.917	0.892
2415	0.919	0.893
1615	0.945	0.925

Table C-13- Retrograde Liquid Volume from Constant Volume Depletion experiment at reservoir temperature, 305 ºF, for Fluid 3	
Pressure (psia)	**% of hydrocarbon pore space**
5988	0
5915	0.01
5815	0.08
5615	0.65
5415	1.55
5215	2.64
5015	3.83
4815	5.02
4615	6.16
4415	7.22
4215	8.16
4015	8.98
3615	10.24
3215	11.05
2815	11.52
2415	11.73
2015	11.74
1615	11.57
1215	11.2
815	10.6
415	9.78
15	8.87

VOLUMETRIC DATA FOR FLUID – 4

Table C-14- Well stream analysis for Fluid 4	
Component	**Mole fraction**
H_2S	0
N_2	0.0679
CO_2	0.0135
C_1	0.6869
C_2	0.0812
C_3	0.0376
IC_4	0.007
NC_4	0.0149
IC_5	0.0058
NC_5	0.0066
C_6	0.0099
C_7	0.0125
C_8	0.0129
C_9	0.0085
C_{10}	0.0064
C_{11}	0.0029
C_{12}^+	0.0255
Sp. Gr. C_{12}^+	0.8453
MW C_{12}^+	232

Table C-15- Relative volume from Constant Composition Expansion experiment at four different temperatures (reservoir temperature is 266 ºF), for Fluid 4

	Relative Volume, V/V_{sat}			
Pressure (psia)	**100 ºF**	**150 ºF**	**225 ºF**	**266 ºF**
8015	0.7479	0.7869	0.8575	0.8999
7815	0.7518	0.7922	0.8652	0.9087
7615	0.7559	0.7976	0.8729	0.9177
7415	0.7601	0.8034	0.8808	0.927
7396	0.7606	0.8038	0.8817	0.9276
7215	0.7646	0.8095	0.8892	0.9365
7015	0.7693	0.816	0.8979	0.9466
6815	0.7743	0.8228	0.9071	0.9574
6615	0.7794	0.83	0.9168	0.969
6415	0.7844	0.837	0.9271	0.9816
6215	0.79	0.8449	0.9392	0.9955
6015	0.7962	0.8536	0.9519	1.0111
5815	0.8031	0.8632	0.9661	1.0278
5415	0.8195	0.886	0.9991	1.0665
5015	0.8401	0.9145	1.0399	1.1142
4615	0.8663	0.9505	1.091	1.1733
4215	0.9001	0.9965	1.1557	1.2476
4015	0.9207	1.0244	1.1946	1.292
3615	0.9717	1.0933	1.2894	1.3996
3215	1.0408	1.1857	1.415	1.5408
2815	1.137	1.313	1.5856	1.7309
2415	1.2756	1.4943	1.8251	1.9955
2015	1.4854	1.7656	2.1774	2.3808
1615	1.8242	2.1987	2.7298	2.9794
1215	2.4308	2.9625	3.6868	4.0066
815	3.7215	4.5608	5.6561	6.1016

Table C-16- Deviation factor from Constant Composition Expansion experiment at four different temperatures (reservoir temperature is 266 ºF), for Fluid 4

	z-factor			
Pressure (psia)	**100 ºF**	**150 ºF**	**225 ºF**	**266 ºF**
8015	1.43	1.382	1.341	1.327
7815	1.402	1.356	1.319	1.307
7615	1.373	1.331	1.297	1.286
7415	1.345	1.305	1.274	1.265
7396	1.342	1.302	1.272	1.263
7215	1.316	1.279	1.251	1.244
7015	1.288	1.254	1.229	1.222
6815	1.259	1.228	1.206	1.201
6615		1.203	1.183	1.18
6415			1.16	1.159
6215				1.139

Table C-17- Retrograde Liquid Volume from Constant Volume Depletion experiment at four different temperatures (reservoir temperature is 266 ºF), for Fluid 4				
	% of Hydrocarbon Pore Space			
Pressure (psia)	**100 ºF**	**150 ºF**	**225 ºF**	**266 ºF**
6729.7	0			
6614.7	0.04			
6564.7	0.5	0		
6414.7	1.2	0.5		
6314.7	1.75	0.8	0	
6214.7	2.4	1.2	0.25	
6159.7	2.8	1.45	0.4	0
6014.7	3.9	2.3	0.9	0.35
5614.7	7.8	5.65	2.9	1.8
5214.7	12	10	6.2	4
4814.7	15.5	13.55	9.3	6.9
4414.7	18.6	16.2	11.8	9.2
4014.7	21.1	18.45	13.75	10.95
3614.7	22.9	19.95	14.9	11.9
3214.7	24.2	20.8	15.6	12.5
2814.7	24.75	21.3	15.9	12.8
2414.7	25	21.4	15.95	12.95
2014.7	24.9	21.3	15.75	13
1614.7	24.5	20.9	15.35	12.8
1214.7	23.8	20.2	14.7	12.4
814.7	22.75	19.3	13.9	11.75
414.7	21.2	18.05	12.8	10.6
14.7	19.2	16.45	11.5	9.1

VOLUMETRIC DATA FOR FLUID – 5

Table C-18- Well stream analysis for Fluid 5	
Component	**Mole fraction**
H_2S	0
N_2	0.002
CO_2	0.0077
C_1	0.7209
C_2	0.0636
C_3	0.0623
IC_4	0.0185
NC_4	0.0222
IC_5	0.0096
NC_5	0.0081
C_6	0.0128
C_7	0.0177
C_8	0.0085
C_9	0.0078
C_{10}^+	0.0383
Sp. Gr. C_{10}^+	0.8416
MW C_{10}^+	195.7

Table C-19- Relative volume, z-factor and liquid saturation from Constant Composition Expansion experiment at reservoir temperature, 229 ºF, for Fluid 5

Pressure, psia	Relative volume, V/Vsat	z-factor	Liquid saturation
9000	0.831095	1.4648	
8500	0.842845	1.4029	
8000	0.85689	1.3424	
7500	0.87182	1.2805	
7157	0.883392	1.2398	
7000	0.889929	1.2199	
6500	0.909187	1.1573	
6000	0.933216	1.0965	
5500	0.961484	1.0356	
5054	1	0.987	0
4900	1.006272	0.9656	1.07
4200	1.086219	0.8934	8.02
3500	1.225177	0.8397	18.43
2800	1.466961	0.8043	22.8
2100	1.933569	0.7952	23.36
1400	2.957774	0.8109	22.38
1000	4.238428	0.83	21.67

Table C-20- Retrograde Liquid Volume, vapor z-factor and 2-phase z-factor from Constant Volume Depletion experiment at reservoir temperature, 229 ºF, for Fluid 5

Pressure, psia	Liquid saturation %	z-factor	2phase z-factor
7167	0	1.24	
5050	0	0.987	0.987
4000	10.2	0.892	0.872
3000	17.59	0.846	0.803
2000	18.01	0.835	0.764
1000	15.9	0.897	0.782

VOLUMETRIC DATA FOR FLUID – 6

Table C-21- Well stream analysis for Fluid 6

Component	Mole fraction
H_2S	0.0017
N_2	0.0752
CO_2	0.0131
C_1	0.6565
C_2	0.0819
C_3	0.0414
IC_4	0.0075
NC_4	0.018
IC_5	0.0065
NC_5	0.0078
C_6	0.01
C_7	0.0117
C_8	0.012
C_9	0.0138
C_{10}	0.0105
C_{11}	0.0062
C_{12}^+	0.0262
Sp. Gr. C_{12}^+	0.8403
MW C_{12}^+	228

Table C-22- Relative volume and z-factor from Constant Composition Expansion experiment at reservoir temperature, 291 ºF, for Fluid 6		
Pressure, psia	**Relative volume, V/Vsat**	**z-factor**
8014.7	0.8711	1.405
7814.7	0.8786	1.382
7795.7	0.8794	1.38
7414.7	0.8949	1.335
7214.7	0.9037	1.312
7014.7	0.9129	1.289
6814.7	0.9228	1.265
6614.7	0.9334	1.242
6414.7	0.9448	1.219
6214.7	0.9571	1.197
6014.7	0.9706	1.174
5814.7	0.9854	1.153
5636.7	1	1.134
5614.7	1.0019	1.131
5414.7	1.0205	
5214.7	1.0415	
5014.7	1.0657	
4814.7	1.0933	
4614.7	1.1247	
4414.7	1.1596	
4214.7	1.1977	
4014.7	1.2388	
3814.7	1.283	
3614.7	1.3315	
3414.7	1.387	
3214.7	1.455	

Table C-23- Deviation factor for equilibrium gas and two phases from Constant Volume Depletion experiment at reservoir temperature, 291 ºF, for Fluid 6

	z-factor	
Pressure (psia)	**Equilibrium Gas**	**Two Phase**
5636.7	1.134	1.134
4814.7	1.058	1.048
4014.7	0.986	0.959
3214.7	0.928	0.896
2414.7	0.894	0.863
1614.7	0.89	0.866
814.7	0.923	0.912

Table C-24- Retrograde Liquid Volume from Constant Volume Depletion experiment at reservoir temperature, 305 ºF, for Fluid 6

Pressure (psia)	**% of hydrocarbon pore space**
5636.7	nil
5614.7	0.17
5414.7	2.6
5214.7	5.59
5014.7	8.7
4814.7	11.47
4614.7	13.67
4414.7	15.27
4214.7	16.37
4014.7	17.1
3814.7	17.57
3614.7	17.87
3414.7	18.05
3214.7	18.14
3014.7	18.17
2614.7	18.06
2214.7	17.75
2014.7	17.53
1814.7	17.25
1614.7	16.92
1214.7	16.13
814.7	15.18
414.7	14.11
14.7	12.98

VOLUMETRIC DATA FOR FLUID – 7

Table C-25- Well stream analysis for Fluid 7	
Component	**Mole fraction**
H_2S	0
N_2	0.0011
CO_2	0.0001
C_1	0.6893
C_2	0.0863
C_3	0.0534
IC_4	0.0115
NC_4	0.0233
IC_5	0.0093
NC_5	0.0085
C_6	0.0173
C_7^+	0.0999
Sp. Gr. C_7^+	0.8299
MW C_7^+	158

Table C-26- Relative volume and z-factor from Constant Composition Expansion experiment at reservoir temperature, 256 ºF, for Fluid 7		
Pressure, psia	**Relative volume, V/Vsat**	**z-factor**
7514.7	0.9341	1.328
7014.7	0.9523	1.264
6514.7	0.9727	1.199
6314.7	0.9834	1.175
6214.7	0.9891	1.163
6114.7	0.9942	1.15
6024.7	1	1.14
5964.7	1.0034	
5914.7	1.0076	
5814.7	1.0138	
5614.7	1.0267	
5314.7	1.0481	
5014.7	1.0749	
4514.7	1.1268	
4014.7	1.2024	
3514.7	1.3096	
3014.7	1.4689	
2514.7	1.7169	
2114.7	2.091	
1874.7	2.2747	
1697.7	2.515	
1474.7	2.9087	
1304.7	3.3173	
1174.7	3.7153	
1064.7	4.1342	

Table C-27- Retrograde Liquid Volume, z-factor and 2-phase z-factor from Constant Volume Depletion experiment at reservoir temperature, 256 ºF, for Fluid 7

Pressure, psia	Liquid Saturation, %	z-factor	2-phase z-factor
6024.7	0	1.14	1.14
5014.7	7.8	1.015	1.016
4014.7	21.3	0.897	0.921
3014.7	25	0.853	0.851
2114.7	24.4	0.865	0.799
1214.7	22.5	0.902	0.722
714.7	21	0.938	0.612
14.7	17.6		

VOLUMETRIC DATA FOR FLUID – 8

Table C-28- Well stream analysis for Fluid 8

Component	Mole fraction
H_2S	0
N_2	0.003
CO_2	0.0435
C_1	0.6255
C_2	0.0999
C_3	0.05
IC_4	0.0131
NC_4	0.022
IC_5	0.0103
NC_5	0.0093
C_6	0.0147
C_7^+	0.1087
Sp. Gr. C_7^+	0.8095
MW C_7^+	173

Table C-29- Relative volume and z-factor from Constant Composition Expansion experiment at reservoir temperature, 305 ºF, for Fluid 8		
Pressure, psia	**Relative Volume, V/Vsat**	**z-factor**
8014.7	0.8588	1.41
7514.7	0.876	1.348
7014.7	0.8949	1.286
6514.7	0.9169	1.224
6014.7	0.9433	1.162
5714.7	0.962	1.126
5614.7	0.9688	1.114
5514.7	0.9759	1.102
5414.7	0.9835	1.091
5314.7	0.9917	1.08
5224.7	1	1.07
5214.7	1.0009	
5194.7	1.0028	
5164.7	1.0057	
5114.7	1.0106	
5014.7	1.0209	
4914.7	1.0318	
4764.7	1.0496	
4614.7	1.0691	
4414.7	1.0982	
4214.7	1.1314	
3964.7	1.1796	
3714.7	1.2369	
3414.7	1.3207	
3114.7	1.4257	
2814.7	1.559	
2514.7	1.7312	
2214.7	1.9584	
1914.7	2.2668	
1614.7	2.7018	
1329.7	3.3104	
1109.7	4.004	
989.7	4.516	

Table C-30- z-factor and 2-phase z-factor from Constant Volume Depletion experiment at reservoir temperature, 305 ºF, for Fluid 8		
	z-factor	
Pressure, psia	**Equilibrium Gas**	**Two Phase**
5224.7	1.07	1.07
4614.7	1.01	1.008
4014.7	0.965	0.962
3314.7	0.927	0.913
2614.7	0.905	0.866
1914.7	0.901	0.813
1214.7	0.917	0.739
614.7	0.948	0.616

Table C-31- Retrograde Liquid Volume from Constant Volume Depletion experiment at reservoir temperature, 305 ºF, for Fluid 8	
Pressure, psia	**% of hydrocarbon pore space**
5224.7	0
4614.7	27.76
4014.7	30.38
3314.7	29.8
2614.7	28.81
1914.7	27.61
1214.7	26.09
614.7	24.25
14.7	17.54

VOLUMETRIC DATA FOR FLUID – 9

Table C-32- Well stream analysis for Fluid 9	
Component	**Mole fraction**
H_2S	0.0004
N_2	0
CO_2	0.0069
C_1	0.5832
C_2	0.1355
C_3	0.0761
IC_4	0
NC_4	0.0403
IC_5	0
NC_5	0.0241
C_6	0.019
C_7^+	0.1145
Sp. Gr. C_7^+	0.8135
MW C_7^+	193

Table C-33- Relative volume and Liquid saturation from Constant Composition Expansion experiment at reservoir temperature, 190 ºF, for Fluid 9		
Pressure, psia	**Relative Volume, V/V_{sat}**	**Liquid saturation, V/V_{tot}**
5594.7	0.9525	
5414.7	0.9589	
5014.7	0.9737	
4814.7	0.9819	
4614.7	0.9916	
4514.7	0.9972	
4464.7	1	0
4454.7	1.0005	4.35
4434.7	1.0018	47.38
4402.7	1.0037	50.82
4353.7	1.0068	51.64
4314.7	1.0093	51.94
4194.7	1.018	51.95
4007.7	1.0372	51.32
3794.7	1.0605	50.07
3504.7	1.1032	47.86
3012.7	1.2053	42.96
2519.7	1.3722	36.75
2014.7	1.6683	28.88
1499.7	2.2378	20.2
1072.7	3.1813	13.06

Table C-34- Liquid saturation and z-factor from Constant Volume Depletion experiment at reservoir temperature, 190 ºF, for Fluid 9		
Pressure , psia	**Liquid saturation, V/V_{tot}**	**Vapor z-factor**
5594.7	0	1.1899
4464.7	0	0.9969
3514.7	52.31	0.8402
2714.7	49.4	0.7966
1914.7	45.33	0.814
1114.7	40.51	0.8603
514.7	36.82	0.9108
14.7	30.37	1

VOLUMETRIC DATA FOR FLUID – 10

Table C-35- Well stream analysis for Fluid 10	
Component	**Mole fraction**
H_2S	0
N_2	0.0343
CO_2	0.0275
C_1	0.6783
C_2	0.0449
C_3	0.0267
IC_4	0.0089
NC_4	0.0179
IC_5	0.0085
NC_5	0.01
C_6	0.0203
C_7	0.0241
C_8	0.0255
C_9	0.0176
C_{10}	0.012
C_{11}	0.007
C_{12}^+	0.0365
Sp. Gr. C_{12}^+	0.8324
MW C_{12}^+	251

Table C-36- Relative volume and z-factor from Constant Composition Expansion experiment at reservoir temperature, 301 ºF, for Fluid 10		
Pressure, psia	**Relative Volume, V/Vsat**	**z-factor**
9014.7	0.8183	1.604
8614.7	0.8278	1.55
8520.7	0.8301	1.537
8214.7	0.838	1.496
8014.7	0.8438	1.469
7814.7	0.8491	1.442
7614.7	0.8552	
7414.7	0.8615	1.388
7214.7	0.8682	1.361
7014.7	0.8753	1.334
6814.7	0.8829	1.307
6614.7	0.891	
6414.7	0.8997	1.254
6214.7	0.9091	1.227
6014.7	0.9193	1.201
5814.7	0.9306	1.175
5614.7	0.9431	1.15
5414.7	0.957	1.125
5214.7	0.9728	1.101
5014.7	0.9908	1.079
4922.7	1	1.069
4614.7	1.0361	
4414.7	1.0647	
4014.7	1.136	
3614.7	1.2255	
3414.7	1.2788	

Table C-37- z-factor and 2-phase z-factor from Constant Volume Depletion experiment at reservoir temperature, 301 ºF, for Fluid 10

Pressure, psia	Equilibrium Gas z-factor	2-phase z
4922.7	1.069	1.069
4214.7	1.011	1.01
3514.7	0.968	0.951
2814.7	0.94	0.895
2114.7	0.926	0.839
1414.7	0.929	0.758
714.7	0.951	0.598

Table C-38- Liquid saturation from Constant Volume Depletion experiment at reservoir temperature, 301 ºF, for Fluid 10

Pressure, psia	Liquid Saturation, %
4922.7	0
4214.7	33.6
3814.7	33.23
3614.7	32.91
3414.7	32.53
3214.7	32.1
3014.7	31.62
2614.7	30.56
2214.7	29.37
2014.7	28.72
1814.7	28.04
1614.7	27.33
1214.7	25.81
814.7	24.18
414.7	22.4

VOLUMETRIC DATA FOR FLUID – 11

Table C-39- Well stream analysis for Fluid 11	
Component	**Mole fraction**
H_2S	0
N_2	0.0345
CO_2	0.0273
C_1	0.5771
C_2	0.1072
C_3	0.0599
IC_4	0.0106
NC_4	0.0239
IC_5	0.0087
NC_5	0.0097
C_6	0.0172
C_7	0.0238
C_8	0.0232
C_9	0.0134
C_{10}	0.0083
C_{11}	0.0036
C_{12}^+	0.0516
Sp. Gr. C_{12}^+	0.8463
MW C_{12}^+	224

Table C-40- Relative volume from Constant Composition Expansion experiment at three different temperatures (reservoir temperature is 305 ºF), for Fluid 11			
	Relative Volume, V /Vsat		
Pressure, psia	**250 ºF**	**275 ºF**	**305 ºF**
8614.7	0.7895	0.806	0.8227
8534.7	0.7903	0.8072	0.824
8214.7	0.7938	0.8126	0.8295
7814.7	0.7988	0.8201	0.8375
7414.7	0.8046	0.8285	0.8467
7014.7	0.8115	0.8381	0.8576
6614.7	0.8196	0.8492	0.8705
6214.7	0.8295	0.8621	0.8859
5814.7	0.8417	0.8774	0.9045
5414.7	0.8571	0.8959	0.9274
5014.7	0.8769	0.9189	0.9558
4614.7	0.9032	0.9485	0.9918
4535.7			1
4214.7	0.9392	0.9882	1.0383
3814.7	0.9898	1.0442	1.0996
3414.7	1.0626	1.125	1.1828
3014.7	1.1683	1.2384	1.2994
2614.7	1.3106	1.3937	1.4697
2214.7	1.511	1.616	1.7311
1814.7	1.8105	1.9632	2.1585
1614.7	2.0203	2.2178	2.479
1414.7	2.2933	2.557	2.914
1214.7	2.6606	3.0159	3.5179
1014.7	3.1782	3.6435	4.3743

Table C-41- Deviation factor from Constant Composition Expansion experiment at three different temperatures (reservoir temperature is 305 ºF), for Fluid 11			
	Vapor z-factor		
Pressure, psia	**250 ºF**	**275 ºF**	**305 ºF**
8614.7	1.591	1.508	1.538
8214.7	1.525	1.448	1.479
7814.7	1.46	1.388	1.42
7414.7	1.395	1.328	1.36
7014.7	1.331	1.268	1.305
6614.7	1.267	1.21	1.249
6214.7	1.205	1.151	1.194
5814.7	1.144	1.095	1.141
5414.7	1.084	1.04	1.089
5014.7	1.027	0.987	1.039
4614.7	0.973		0.992
4535.7			0.983

Table C-42- Retrograde Liquid Volume from Constant Volume Depletion experiment at three different temperatures (reservoir temperature is 305 ºF), for Fluid 11			
	% of hydrocarbon pore space		
Pressure, psia	**250 ºF**	**275 ºF**	**305 ºF**
4520.7			Nil
4517.7			1.17
4495.7		21.36	7.91
4214.7	40.01	37.59	28.83
4014.7	41.28	38.06	31.22
3814.7	41.35	37.96	32.02
3614.7	41.01	37.65	32.18
3414.7	40.47	37.24	32.04
3214.7	39.84	36.74	31.73
3014.7	39.14	36.18	31.31
2814.7	38.4	35.57	30.83
2614.7	37.63	34.91	30.3
2414.7	36.83	34.2	29.74
2214.7	36	33.45	29.15
2014.7	35.14	32.63	28.53
1814.7	34.24	31.76	27.89
1614.7	33.31	30.84	27.21
1414.7	32.32	29.83	26.49
1214.7	31.27	28.77	25.72
1014.7	30.15	27.62	24.88
814.7	28.93	26.39	23.95
614.7	27.73	25.2	22.99
414.7	26.08	23.62	21.59
214.7	24.35	22.06	19.97
14.7	22.32	20.36	17.76

APPENDIX D

PVT DATA FOR VOLATILE OIL SAMPLES

VOLUMETRIC DATA FOR FLUID – 12

Table D-1- Well stream analysis for Fluid 12

Component	Mole fraction
H_2S	0
N_2	0.0088
CO_2	0.0018
C_1	0.6801
C_2	0.074
C_3	0.0475
IC_4	0.0071
NC_4	0.0205
IC_5	0.0066
NC_5	0.0109
C_6	0.0135
C_7^+	0.1292
Sp. Gr. C_7^+	0.837
MW C_7^+	205

Table D-2- Relative volume from Constant Composition Expansion experiment at reservoir temperature, 179 ºF, for Fluid 12	
Pressure, psia	**Relative Volume, V/Vsat**
7014.7	0.9884
6814.7	0.9937
6714.7	0.9965
6614.7	0.9997
6604.7	1
6550.7	1.0021
6502.7	1.004
6399.7	1.0081
6305.7	1.0117
6069.7	1.0214
5642.7	1.0425
5214.7	1.0673
4714.7	1.1047
4214.7	1.1571
3714.7	1.2296
3214.7	1.3368
2714.7	1.5009
2214.7	1.763
1714.7	2.219
1261.7	2.9802
1014.7	3.7167
812.7	4.6693

Table D-3- Vapor z-factor from Constant Composition Expansion experiment at reservoir temperature, 179 ºF, for Fluid 12	
Pressure, psia	**z-factor**
6604.7	
5814.7	1.194
4814.7	1.013
3814.7	0.912
2814.7	0.867
1814.7	0.866
1014.7	0.897
514.7	0.934

Table D-4- Liquid saturation from Constant Volume Depletion experiment at reservoir temperature, 179 ºF, for Fluid 12

Pressure, psia	**Liquid saturation, %**
6604.7	100
6550.7	64.2
6502.7	60.7
6399.7	57.8
6305.7	56.1
5814.7	53.8
4814.7	53.2
3814.7	52.2
2814.7	50.4
1814.7	47.7
1014.7	44.5
514.7	41.6
14.7	38.2

VOLUMETRIC DATA FOR FLUID – 13

Table D-5- Well stream analysis for Fluid 13

Component	Mole fraction
H_2S	0
N_2	0
CO_2	0.0034
C_1	0.7247
C_2	0.0457
C_3	0.0279
IC_4	0.0067
NC_4	0.0133
IC_5	0.0069
NC_5	0.0082
C_6	0.0152
C_7	0.016
C_8	0.0131
C_9	0.0131
C_{10}^+	0.1058
Sp. Gr. C_{10}^+	0.8939
MW C_{10}^+	317.6

Table D-6- Relative volume from Constant Composition Expansion experiment at reservoir temperature, 197 ºF, for Fluid 13	
Pressure, psia	**Relative Volume, V/V_{sat}**
14000	0.9396
13668	0.9427
13000	0.9493
12000	0.9604
11000	0.9728
10000	0.9866
9120	1.0000
8500	1.0101
8000	1.0203
7500	1.0327
7000	1.0479
6000	1.0908
5000	1.1605
4000	1.2819
3000	1.5167
2000	2.0595
1000	3.9325

Table D-7- Solution gas-oil ratio, oil density and formation volume factor from Differential Liberation experiment at reservoir temperature, 197 ºF, for Fluid 13

Pressure	**Solution GOR**	**Oil density**	**Oil FVF**
psia	Mscf/bbl	lb/ft^3	RBbl/STB
14000	2.89	36.91368	2.5346
13668	2.89	36.79506	2.5429
13000	2.89	36.53911	2.5609
12000	2.89	35.98974	2.5908
11000	2.89	35.65887	2.6242
10000	2.89	35.15321	2.6615
9120	2.89	34.685	2.6976
8500	2.071	40.60941	2.0305
8000	1.691	42.75069	1.8094
7500	1.432	43.80573	1.6873
7000	1.192	44.26145	1.5985
6000	0.986	46.07811	1.4778
5000	0.81	47.43904	1.3884
4000	0.622	48.34424	1.3176
3000	0.481	49.18078	1.256
2000	0.333	49.87997	1.2021
1000	0.192	49.81754	1.1681
500	0.116	50.24205	1.1382
15	0	51.39073	1.0657

Table D-8- Z-factor and gas formation volume factor from Gas Differential Liberation experiment at reservoir temperature, 197 ºF, for Fluid 13

Pressure	**z-factor**	**Gas FVF**
psia		bbl/Mscf
8500	2.148	0.854
8000	1.916	0.81
7500	1.723	0.777
7000	1.554	0.751
6000	1.269	0.715
5000	1.058	0.715
4000	0.918	0.776
3000	0.88	0.992
2000	0.88	1.488
1000	0.916	3.097
500	0.947	6.404
15	1	225.038

Table D-9- 2-phase z-factor from Constant Volume Depletion experiment at reservoir temperature, 197 ºF, for Fluid 13

Pressure, psia	**2-phase z-factor**
9074	1.698
8500	1.669
8000	1.537
7500	1.467
7000	1.396
6000	1.264
4000	1.013
2000	0.777

VOLUMETRIC DATA FOR FLUID – 14

Table D-10- Well stream analysis for Fluid 14

Component	Mole fraction
H_2S	0
N_2	0.0016
CO_2	0.001
C_1	0.6984
C_2	0.0537
C_3	0.0322
IC_4	0.0087
NC_4	0.017
IC_5	0.0079
NC_5	0.0088
C_6	0.0141
C_7^+	0.1566
Sp. Gr. C_7^+	0.8601
MW C_7^+	232

Table D-11- Relative volume and liquid density from Constant Composition Expansion experiment at reservoir temperature, 190 ºF, for Fluid 14		
Pressure, psia	**Relative Volume, V/V_{sat}**	**Liquid Density, lb/ft^3**
14014.7	0.9018	39.25473
13500.7	0.907	39.02999
13014.7	0.9123	38.80524
12514.7	0.918	38.56178
12014.7	0.9241	38.31206
11514.7	0.9305	38.04362
11014.7	0.9374	37.76894
10514.7	0.9446	37.47553
10014.7	0.9523	37.17587
9514.7	0.9604	36.85749
9014.7	0.9691	36.53287
8514.7	0.9783	36.18951
8014.7	0.9881	35.82743
7814.7	0.9922	35.6776
7714.7	0.9943	35.60269
7614.7	0.9964	35.52777
7514.7	0.9986	35.45286
7451.7	1	35.40292
7433.7	1.0005	
7408.7	1.0013	
7384.7	1.0019	
7359.7	1.0026	
7336.7	1.0032	
7217.7	1.0062	

Table D-12- Oil relative volume, oil density, and z-factor and gas formation volume factor from Differential Liberation experiment at reservoir temperature, 190 º F, for Fluid 14

Pressure	**Oil relative volume**	**Oil density**	**z- factor**	**Gas FVF**
psia	V @ P and 190 F/Residual V	lb/ft^3		RB/Mscf
7451.7	2.69	35.40292	1.246	
7014.7	2.146	37.94998	1.132	0.8182264
6514.7	1.904	39.59184	1.049	0.7986281
6014.7	1.767	40.67184	0.988	0.8035277
5514.7	1.665	41.53959	0.944	0.8255757
5014.7	1.584	42.32618	0.913	0.867222
4514.7	1.518	43.06908	0.893	0.9309162
4014.7	1.463	43.787	0.881	1.0240078
3514.7	1.416	44.48619	0.878	1.1538462
3014.7	1.374	45.16666	0.883	1.3400294
2514.7	1.335	45.82839	0.895	1.6144047
2014.7	1.297	46.47765	0.913	2.0431161
1514.7	1.258	47.1269	0.937	2.7731504
1014.7	1.216	47.79488	0.966	4.2479177
514.7	1.167	48.55026	0.992	8.633023
129.7	1.116	49.44922		
14.7	1.088	50.71651		

VOLUMETRIC DATA FOR FLUID – 15

Table D-13- Well stream analysis for Fluid 15

Component	Mole fraction
H_2S	0
N_2	0.003
CO_2	0.009
C_1	0.5347
C_2	0.1146
C_3	0.0879
IC_4	0
NC_4	0.0456
IC_5	0
NC_5	0.0209
C_6	0.0151
C_7^+	0.1692
Sp. Gr. C_7^+	0.8364
MW C_7^+	173

Table D-14- Relative volume from Constant Composition Expansion experiment at reservoir temperature, 176 ºF, for Fluid 15	
Pressure, psia	**Relative Volume, V/V_{sat}**
6014.7	0.9589
5514.7	0.97
5014.7	0.9827
4914.7	0.9856
4814.7	0.9883
4714.7	0.9919
4614.7	0.9951
4514.7	0.9984
4474.7	1
4457.7	1.0009
4319.7	1.0097
3914.7	1.0412
3545.7	1.0812
3146.7	1.1425
2783.7	1.2232
2436.7	1.3356
2142.7	1.4738
1894.7	1.6384
1674.7	1.8415
1365.7	2.2768
1075.7	2.9892

Table D-15- Oil relative volume, oil density, z-factor, gas-oil ratio, and gas gravity from Differential Liberation experiment at reservoir temperature, 176 º F, for Fluid 15

Pressure	**Oil Relative volume**	**Oil density**	**z- factor**	**GOR**	**Gas gravity**
psia	Vol. @ P and 176 F/ Residual Vol.	lb/ft^3		Mcf/STB	
4474.7	2.921	33.0868		3.377	
4014.7	2.343	35.1594	0.825	2.351	1.025
3506.7	2.059	36.7264	0.788	1.814	0.932
3017.7	1.886	37.9687	0.772	1.471	0.858
2528.7	1.756	39.0924	0.773	1.205	0.821
2018.7	1.645	40.1849	0.79	0.97	0.799
1548.7	1.555	41.1401	0.816	0.775	0.806
1015.7	1.464	42.1514	0.856	0.573	0.826
519.7	1.372	43.3250	0.912	0.383	0.888
223.7	1.298	44.2302	0.958	0.245	1.067
14.7	1.057	48.7750	0.995	0	1.767

VOLUMETRIC DATA FOR FLUID – 16

Table D-16- Well stream analysis for Fluid 16	
Component	**Mole fraction**
H_2S	0
N_2	0.0065
CO_2	0.0019
C_1	0.5318
C_2	0.1156
C_3	0.0762
IC_4	0.0181
NC_4	0.0319
IC_5	0.0121
NC_5	0.0139
C_6	0.0199
C_7^+	0.172
Sp. Gr. C_7^+	0.8294
MW C_7^+	218

Table D-17- Relative volume and oil density from Constant Composition Expansion experiment at reservoir temperature, 307 ºF, for Fluid 16

Pressure, psia	Relative Volume, V/V_{sat}	Oil Density, lb/ft^3
5514.7	0.9612	31.83204
5277.7	0.9694	31.5636
5014.7	0.9789	31.2577
4914.7	0.9831	31.12036
4814.7	0.9874	30.98926
4714.7	0.9923	30.83319
4614.7	0.9977	30.66463
4577.7	1	30.59596
4544.7	1.0029	
4514.7	1.0057	
4484.7	1.0085	
4454.7	1.0113	
4414.7	1.0152	
4364.7	1.0202	
4314.7	1.0225	
4214.7	1.0362	
4014.7	1.0602	
3714.7	1.1032	
3314.7	1.1778	
2914.7	1.2799	
2514.7	1.4246	
2114.7	1.6378	
1714.7	1.9711	
1314.7	2.5431	
1179.7	2.8365	
979.7	3.4379	
891.7	3.7921	
742.7	4.612	
662.7	5.2186	
597.7	5.8228	
464.7	7.6655	

Table D-18- Oil relative volume, Gas z-factor and Liquid saturation from Constant Volume Depletion experiment at reservoir temperature, 307 ºF, for Fluid 16			
Pressure	**Oil Relative volume**	**Eq. gas z-factor**	**Liquid Volume**
psia	Bbl @ P and 307 ºF/Residual Bbl		% of HC pore space
4577.7	3.215		100
4544.7	3.113		96.8
4514.7	3.042		94.6
4454.7	2.926		91
4364.7	2.762		85.9
4214.7	2.563		79.7
4014.7	2.357	0.949	73.3
3114.7	1.92	0.895	59.7
2114.7	1.691	0.898	52.6
1214.7	1.521	0.93	47.3
714.7	1.431	0.956	44.5
414.7	1.354	0.975	42.1
14.7	1.135		35.3

VOLUMETRIC DATA FOR FLUID – 17

Table D-19- Well stream analysis for Fluid 17

Component	Mole fraction
H_2S	0
N_2	0.0014
CO_2	0.0378
C_1	0.5846
C_2	0.0753
C_3	0.0458
IC_4	0.0113
NC_4	0.0202
IC_5	0.0092
NC_5	0.0086
C_6	0.0156
C_7^+	0.19
Sp. Gr. C_7^+	0.8549
MW C_7^+	250

Table D-20- Relative volume and oil density from Constant Composition Expansion experiment at reservoir temperature, 287 ºF, for Fluid 17		
Pressure, psia	**Relative Volume, V/V_{sat}**	**Density, lb/ft^3**
8014.7	0.9574	37.72524
7514.7	0.9621	37.5442
7014.7	0.97	37.2383
6514.7	0.9863	36.62026
6214.7	1	36.12084
6074.7	1.0064	
6014.7	1.0093	
5964.7	1.0117	
5914.7	1.0142	
5814.7	1.0194	
5714.7	1.0248	
5614.7	1.0304	
5464.7	1.0396	
5314.7	1.0493	
5114.7	1.0634	
4914.7	1.0791	
4714.7	1.0966	
4514.7	1.1162	
4314.7	1.1384	
4014.7	1.1771	
3614.7	1.2419	
3214.7	1.3278	
2814.7	1.4436	
2414.7	1.6054	
2014.7	1.8461	
1614.7	2.2236	
1149.7	3.0171	
934.7	3.6682	
789.7	4.3139	
687.7	4.9604	
609.7	5.3943	
544.7	6.2149	
494.7	6.842	

Table D-21- z-factor, liquid volume, oil relative volume, and oil density from Differential Liberation experiment at reservoir temperature, 287 º F, for Fluid 17				
Pressure	**Gas z-factor**	**Liquid Volume**	**Oil relative volume**	**Oil density**
psia		% HC pore space	Vol. @ P and 287 F/ Residual Vol.	lb/ft^3
6214.7		100	2.127	36.121
6014.7		87.1	1.853	
5814.7		83.45	1.775	
5614.7		80.06	1.703	
5414.7	1.061	78.45	1.669	39.230
4614.7	1.015	72.4	1.54	41.590
3814.7	0.971	68.35	1.454	43.138
3014.7	0.941	65.25	1.388	44.062
2214.7	0.927	62.9	1.338	44.555
1414.7	0.935	60.01	1.277	45.254
714.7	0.961	56.8	1.208	46.247
14.7		51.9	1.104	50.061

VOLUMETRIC DATA FOR FLUID – 18

Table D-22- Well stream analysis for Fluid 18

Component	Mole fraction
H_2S	0
N_2	0.0078
CO_2	0.0148
C_1	0.5047
C_2	0.1111
C_3	0.0679
IC_4	0.0128
NC_4	0.0325
IC_5	0.0091
NC_5	0.0151
C_6	0.0189
C_7^+	0.2053
Sp. Gr. C_7^+	0.8275
MW C_7^+	188

Table D-23- Relative volume and oil density from Constant Composition Expansion experiment at reservoir temperature, 302 ºF, for Fluid 18

Pressure, psia	Relative Volume, V/V_{sat}	Density, lb/ft^3
12014.7	0.8239	37.9250
11514.7	0.8312	37.5879
11014.7	0.8382	37.2758
10514.7	0.8457	36.9449
10014.7	0.8533	36.6140
9514.7	0.8612	36.2832
9014.7	0.8691	35.9523
8514.7	0.8772	35.6214
8014.7	0.8858	35.2718
7514.7	0.895	34.9097
7014.7	0.9048	34.5352
6514.7	0.9154	34.1356
6014.7	0.9272	33.6986
5514.7	0.9407	33.2179
5014.7	0.9561	32.6811
4514.7	0.9746	32.0568
4214.7	0.9881	31.6198
4114.7	0.9931	31.4637
4014.7	0.9983	31.3014
3981.7	1	31.2452
3824.7	1.019	
3789.7	1.0235	
3754.7	1.0282	
3724.7	1.0323	
3580.7	1.0532	
3326.7	1.0963	
2934.7	1.1831	
2523.7	1.3149	
2142.7	1.4916	
1820.7	1.7137	
1550.7	1.9812	
1301.7	2.3385	
1108.7	2.7414	
965.7	3.1451	
763.7	4.0102	
576.7	5.3571	
413.7	7.5696	

Table D-24- z-factor, liquid volume, oil relative volume, gas-oil ratio and oil density from Differential Liberation experiment at reservoir temperature, 302 º F, for Fluid 18					
Pressure	**Gas z-factor**	**Liquid Volume**	**Oil relative volume**	**GOR**	**Oil density**
psia		% HC pore space	Vol. @ P and 287 F/ Residual Vol.	Mscf/STB	Lb/ft^3
3981.7		100	2.951	2.664	31.24521
3914.7		92.8	2.739		
3814.7		86.6	2.556		
3714.7		82.2	2.426		
3614.7		78.9	2.329		
3514.7		76.5	2.258		
3414.7	0.882	74	2.184	1.653	35.31552
2814.7	0.861	65.8	1.942	1.256	38.22466
2214.7	0.864	60.3	1.78	0.969	40.4471
1714.7	0.879	56.4	1.665	0.766	42.11393
1214.7	0.905	53.5	1.58	0.585	42.97544
714.7	0.941	50.3	1.484	0.4401	43.2626
14.7		38.1	1.124	0	46.25291

VOLUMETRIC DATA FOR FLUID – 19

Table D-25- Well stream analysis for Fluid 19

Component	Mole fraction
H_2S	0
N_2	0.0395
CO_2	0.0005
C_1	0.3745
C_2	0.1052
C_3	0.0778
IC_4	0.0273
NC_4	0.057
IC_5	0.0241
NC_5	0.035
C_6	0.0461
C_7^+	0.213
Sp. Gr. C_7^+	0.8067
MW C_7^+	168

Table D-26- Relative volume and oil density from Constant Composition Expansion experiment at reservoir temperature, 220 ºF, for Fluid 19

Pressure, psia	**Relative Volume, V/V_{sat}**	**Density, lb/ft^3**
6014.7	0.9036	36.8825
5514.7	0.913	36.5017
5014.7	0.9234	36.0896
4514.7	0.9352	35.6339
4014.7	0.9486	35.1345
3514.7	0.9642	34.5664
3114.7	0.979	34.0420
3014.7	0.9832	33.8984
2914.7	0.9876	33.7423
2814.7	0.9923	33.5863
2714.7	0.9974	33.4115
2666.7	1	33.3241
2653.7	1.0025	
2642.7	1.0046	
2631.7	1.0068	
2624.7	1.0082	
2614.7	1.0098	
2573.7	1.0188	
2504.7	1.0347	
2384.7	1.0662	
2184.7	1.1308	
1949.7	1.2305	
1714.7	1.3646	
1404.7	1.6253	
1063.7	2.1241	
839.7	2.7118	
709.7	3.2462	
574.7	4.0845	

Table D-27- z-factor, oil density, solution gas-oil ratio, oil relative volume, and gas formation volume factor from Differential Liberation experiment at reservoir temperature, 220 º F, for Fluid 19

Pressure	**Gas z-factor**	**Oil Density**	**Solution GOR**	**Oil relative volume**	**Gas FVF**
psia		lb/ft^3	Mscf/STB	Vol. @ P and 287 F/ Residual Vol.	RBbl/Mscf
2666.7		33.3241	2.759	3.08	
2514.7	0.811	33.9733	2.525	2.92	1.543361
2314.7	0.812	34.7599	2.256	2.742	1.687898
2014.7	0.818	35.8337	1.925	2.531	1.954924
1714.7	0.83	36.7701	1.658	2.368	2.32974
1414.7	0.846	37.6753	1.434	2.234	2.878491
1114.7	0.868	38.5118	1.235	2.115	3.748163
814.7	,896	39.3484	1.042	1.996	5.289074
514.7	0.928	40.2536	0.833	1.862	8.677119
272.7	0.959	41.1650	0.628	1.72	16.91328
166.7	0.974	41.6957	0.515	1.631	28.07937
120.7	0.981	41.9891	0.457	1.581	39.02499
14.7		44.6173	0	1.1	

VOLUMETRIC DATA FOR FLUID – 20

Table D-28- Well stream analysis for Fluid 20	
Component	**Mole fraction**
H_2S	0
N_2	0.0349
CO_2	0.0016
C_1	0.3909
C_2	0.1206
C_3	0.0806
IC_4	0.0199
NC_4	0.042
IC_5	0.0215
NC_5	0.0244
C_6	0.0363
C_7^+	0.2273
Sp. Gr. C_7^+	0.8137
MW C_7^+	177

Table D-29- Relative volume from Constant Composition Expansion experiment at reservoir temperature, 315 ºF, for Fluid 20	
Pressure, psia	**Relative Volume, V/V_{sat}**
4600	0.9685
4400	0.9724
4200	0.9765
4000	0.9807
3800	0.985
3600	0.9895
3400	0.9941
3200	0.9988
3150	1
3000	1.019
2800	1.0493
2600	1.0868
2400	1.1335
2200	1.1927
2000	1.2682
1800	1.3667
1600	1.4976
1400	1.6764
1200	1.9286
1000	2.3015
800	2.8903
600	3.919
400	6.0663

Table D-30- Solution gas-oil ratio and oil relative volume from Differential Liberation experiment at reservoir temperature, 220 º F, for Fluid 20		
Pressure, psia	**GOR, scf/Residual Bbl**	**Oil relative volume, Bbl @ P and 315 ºF/ Residual Bbl**
3150	1811	
2665	1499	1.936
2215	1254	1.7994
1765	1027	1.6842
1315	821	1.5804
865	629	1.4828
415	426	1.3762
215	308	1.3096
90	190	1.227
14.7	0	1.086

VOLUMETRIC DATA FOR FLUID – 21

Table D-31- Well stream analysis for Fluid 21

Component	Mole fraction
H_2S	0
N_2	0.0282
CO_2	0.0005
C_1	0.3768
C_2	0.1409
C_3	0.0873
IC_4	0.021
NC_4	0.041
IC_5	0.0171
NC_5	0.0183
C_6	0.0319
C_7^+	0.237
Sp. Gr. C_7^+	0.8017
MW C_7^+	172

Table D-32- Relative volume from Constant Composition Expansion experiment at reservoir temperature, 185 ºF, for Fluid 21	
Pressure, psia	**Relative Volume, V/V_{sat}**
4200	0.9614
4000	0.9654
3800	0.9695
3600	0.9739
3400	0.9785
3200	0.9835
3000	0.9888
2800	0.9946
2632	1
2600	1.0006
2400	1.0467
2200	1.0991
2000	1.1669
1800	1.2561
1600	1.3757
1400	1.5402
1200	1.7744
1000	2.1232
800	2.6777
600	3.652
400	5.693
200	12.044

Table D-33- Solution gas-oil ratio and oil relative volume from Differential Liberation experiment at reservoir temperature, 185 º F, for Fluid 21		
Pressure, psia	**GOR, scf/Residual Bbl**	**Oil relative volume, Bbl @ P and 315 ºF/ Residual Bbl**
2632	1784	
2115	1411	1.9597
1615	1086	1.7804
1115	822	1.645
615	564	1.5058
145	228	1.2863
55	118	1.1932
14.7	0	1.0685

VOLUMETRIC DATA FOR FLUID – 22

Table D-34- Well stream analysis for Fluid 22

Component	Mole fraction
H_2S	0.0499
N_2	0.0011
CO_2	0.0367
C_1	0.3821
C_2	0.1325
C_3	0.0822
IC_4	0.0089
NC_4	0.0209
IC_5	0.0092
NC_5	0.0169
C_6	0.0128
C_7^+	0.2468
Sp. Gr. C_7^+	0.8586
MW C_7^+	240

Table D-35- Relative volume from Constant Composition Expansion experiment at reservoir temperature, 235 ºF, for Fluid 22	
Pressure, psia	**Relative Volume, V/V_{sat}**
4400	0.9717
4000	0.979
3600	0.9867
3200	0.9952
2996	1
2800	1.0269
2600	1.0609
2400	1.1034
2200	1.1572
2000	1.2264
1800	1.3166
1600	1.4367
1400	1.6013
1200	1.8338
1000	2.1783
800	2.7232
600	3.677
400	5.67
200	11.8

Table D-36- Solution gas-oil ratio and oil relative volume from Differential Liberation experiment at reservoir temperature, 235 º F, for Fluid 22		
Pressure, psia	**GOR, scf/Residual Bbl**	**Oil relative volume, Bbl @ P and 315 ºF/ Residual Bbl**
2996	1197	
2570	992	1.685
2088	835	1.578
1578	643	1.479
1028	476	1.38
520	325	1.288
290	237	1.236
137	154	1.182
14.7	0	1.08

VITA

Ali Abdallah Al-Meshari
P. O. Box 11436
Dhahran 31311
Saudi Arabia

Education

Doctor of Philosophy. Petroleum Engineering. Texas A&M University. December 2004

Master of Science. Petroleum Engineering. The University of Texas at Austin. December 2001

Bachelor of Science. Chemical Engineering. King Fahd University of Petroleum and Minerals. July 1996

Experience

Saudi Aramco (August 1996 – July 2000)

Lab. Scientist (August 1996 – December 1997), Research and Development Center.

Engineer-Special studies (January 1998 – January 2000), Gas Facilities and Projects Division, E&P Facilities and Technology Department.

Lab. Scientist (February 2000 – July 2000), Research and Development Center.